EPIDEMIC DYNAMICS MODELS ON SOCIAL VULNERABILITY AND PUBLIC HEALTH MEASURE

感染症流行に対する社会的脆弱性および公衆衛生対策に関する数理モデル

ZHIQIONG FU
c2id1501

Thesis submitted in fulfillment of the requirements for the degree of
Doctor of Philosophy (Information Sciences): Mathematical Biology,
Department of Computer and Mathematical Sciences,
Graduate School of Information Sciences,
Tohoku University, Sendai, Japan

September 2025

CANDIDATE
Zhiqiong Fu

CANDIDATE ID
C2ID1501

THESIS
Epidemic dynamics models on social vulnerability and public health measure
感染症流行に対する社会的脆弱性および公衆衛生対策に関する数理モデル

DEGREE AWARDED
Doctor of Philosophy (Information Sciences): Mathematical Biology

SUPERVISOR
Professor Hiromi Seno

AFFILIATION
Department of Computer and Mathematical Sciences
Graduate School of Information Sciences
Tohoku University, Sendai, Japan

DISSERTATION REFEREES
Professor Tatsuhito Kono
Associate Professor Naoya Fujiwara

DECLARATION

I, Zhiqiong Fu, declare that this thesis titled, "Epidemic dynamics models on social vulnerability and public health measure" and the work presented in it are my own. I confirm that:

- This work was done wholly or mainly while in candidature for a research degree at this University.
- Where any part of this thesis has previously been submitted for a degree or any other qualification at this University or any other institution, this has been clearly stated.
- Where I have consulted the published work of others, this is always clearly attributed.
- Where I have quoted from the work of others, the source is always given. With the exception of such quotations, this thesis is entirely my own work.
- I have acknowledged all main sources of help.
- Where the thesis is based on work done by myself jointly with others, I have made clear exactly what was done by others and what I have contributed myself.

Zhiqiong Fu
Sendai, September 2025

SUMMARY

The COVID-19 pandemic has revealed the significance of understanding how social vulnerability influences epidemic progression and the effectiveness of public health measures. This work presents three mathematical studies that incorporate different aspects of social vulnerability and public health strategies to investigate their impact on epidemic outcomes. We first investigate the effects of regional lockdown policies in a community composed of two areas with unequal medical treatment levels. By comparing the endemic sizes under different lockdown strategies with different levels of mobility restriction, our mathematical results indicate that stricter restriction of mobility leads to smaller endemic sizes, although it may cause inconvenience to people's daily life. When considering weak lockdowns with partial restrictions, the most effective policy is to prohibit the movement of susceptible individuals from high density area to low density area. Next, we investigated how limited isolation capacity affects epidemic consequences. We identify critical thresholds beyond which isolation strategy breaks down due to the limited capacity. For both non-reinfectious and reinfectious diseases, a sufficiently large isolation capacity is essential to prevent the breakdown of isolation. When incorporating a discharge mechanism into the isolation strategy, maintaining a higher discharge rate and a lower isolation rate helps preserve system functionality and avoid saturation. Furthermore, we propose a structured SIR model to investigate the relation between the distribution of preventive behavior and epidemic consequence. We find that a high proportion of low-caution individuals in the community accelerates transmission and increases social damage. These studies could provide a deeper understanding of the complex interplay between social vulnerability, public health measures, and disease transmission.

Keywords: Epidemic dynamics, Social vulnerability, Public health, Lockdown policy, Isolation capacity, Behavioral heterogeneity, Ordinary differential equations

ACKNOWLEDGE

I would like to express my sincere appreciation to all those who supported and encouraged me throughout the course of my doctoral research and the writing of this thesis.

First and foremost, I would like to express my deepest gratitude to my supervisor, Professor Hiromi Seno, for his constant encouragement, insightful guidance, and generous support throughout my doctoral studies. I have greatly benefited from his mentorship, both academically and personally.

I would also like to extend my heartfelt gratitude to Professor Tatsuhito Kono and Professor Naoya Fujiwara for serving as my dissertation referees.

I gratefully acknowledge the support of the Japan Science and Technology Agency (JST) Pioneering Research Support Project, which enabled me to dedicate myself wholeheartedly to my doctoral studies.

My sincere thanks go to the Department of Computer and Mathematical Sciences, Graduate School of Information Sciences, Tohoku University for fostering a stimulating academic environment. I am especially thankful to all the staff for their professional assistance and kind support.

I am deeply indebted to all members of our laboratory: Xie Ying, Xiao Yang, Goyal Akshat, Victor Schneider, Hattori Haruyuki, Nao Otsuki, Elza Firdiani Sofia, Ishfaq Ahmad, and ThankGod Ikpe.

I owe special thanks to my husband, Dr. Zhang Zhang, whose constant patience and understanding have been my greatest source of strength. His support has sustained me through the most challenging moments.

Finally, I would like to express my deepest appreciation to my family for their unconditional love, continued support, and encouragement.

CONTENTS

1 INTRODUCTION 1
1.1 Epidemics in human history . . . 1
1.1.1 Historical outbreaks . . . 1
1.1.2 Social vulnerability and social damage . . . 2
1.2 Epidemiological background for modeling . . . 3
1.2.1 Classification of infectious diseases . . . 3
1.2.2 Transmission mechanisms of infectious diseases . . . 4
1.2.3 Basic reproduction number . . . 5
1.2.4 Control strategies for infectious diseases . . . 5
1.3 Basic epidemic models . . . 6
1.3.1 Kermack–McKendrick SIR model . . . 6
1.3.2 SIS model . . . 7
1.3.3 SIRS model . . . 8
1.3.4 SIRI model . . . 8
1.3.5 Effect of the quarantine/isolation . . . 9

2 REGIONAL LOCKDOWN 11
2.1 Introduction . . . 11
2.2 Assumptions . . . 12
2.3 Model . . . 12
2.4 Basic Reproduction Numbers . . . 14
2.5 Different Policies of lockdown . . . 14
2.6 Disease-free equilibrium . . . 15
2.7 Endemic equilibrium . . . 16
2.8 Endemic size . . . 16
2.9 Discussion . . . 18
Appendix for Chapter 2 . . . 19
2.A.1 Derivation of the basic reproduction numbers . . . 19
2.A.2 Proof of Theorem 2.1 . . . 20
2.A.3 Proof of Lemma 2.1 . . . 21
2.A.4 Proof of Theorem 2.2 . . . 22

3 ISOLATION CAPACITY 26
3.1 Introduction . . . 26
3.2 Modeling . . . 27
3.2.1 Assumptions . . . 27
3.2.2 Infection and reinfection forces . . . 28
3.2.3 Isolation well-functioning phase . . . 29
3.2.4 Isolation malfunctioning phase . . . 30
3.2.5 SIRI+Q model . . . 31
3.3 For non-reinfectious disease . . . 34
3.3.1 Assumptions and model . . . 34
3.3.2 Conserved quantities . . . 36
3.3.3 Isolation incapable phase . . . 37
3.3.4 Final epidemic size . . . 39
3.3.5 Discussion . . . 41
3.4 For reinfectious disease . . . 42
3.4.1 Assumptions and model . . . 42
3.4.2 Conserved quantities . . . 46

3.4.3 Isolation well-functioning phase . . . 47
3.4.4 Isolation incapable phase . . . 48
3.4.5 Revival of outbreak . . . 51
3.4.6 Endemic size . . . 52
3.4.7 Final epidemic size . . . 52
3.4.8 Discussion . . . 57
3.5 Influence of isolation discharge . . . 58
3.5.1 Endemic equilibria . . . 58
3.5.2 Bistability . . . 64
3.5.3 Epidemic consequence . . . 66
3.5.4 Discussion . . . 72
Appendix for Chapter 3 . . . 74
3.A.1 Proof of Lemma 3.1 . . . 74
3.A.2 Proof of Lemma 3.2 . . . 74
3.A.3 Proof of Theorem 3.1 . . . 76
3.A.4 Derivation of the conserved quantities . . . 78
3.A.5 Proof of Theorem 3.2 and Corollaries 3.2.1 and 3.2.2 . . . 79
3.A.6 Proof of Corollary 3.2.3 . . . 80
3.A.7 Derivation of the final size equation . . . 81
3.A.8 Proof of the unique existence of the final epidemic size . . . 82
3.A.9 Proof of Theorem 3.4 . . . 83
3.A.10 Proof of Lemma 3.3 . . . 85
3.A.11 Derivation of conserved quantities . . . 85
3.A.12 Proof of Lemma 3.5 and 3.6 . . . 86
3.A.13 Proof of Theorem 3.5, and Lemma 3.7 . . . 87
3.A.14 Proof of Theorem 3.6 . . . 88
3.A.15 Proof of Corollaries 3.6.1, 3.6.2, and Lemma 3.8 . . . 88
3.A.16 Proof of Lemma 3.9 and Theorem 3.7 . . . 89
3.A.17 Proof of Theorem 3.8 . . . 91
3.A.18 Proof of Lemma 3.10 . . . 91
3.A.19 Proof of Theorem 3.9 . . . 93
3.A.20 Proof of Theorem 3.11 and Lemma 3.12 . . . 95
3.A.21 Proof of Corollary 3.11.2 . . . 96
3.A.22 Proof of Corollary 3.16.1 . . . 97
3.A.23 Proof of Theorem 3.17 . . . 97

4 BEHAVIORAL HETEROGENEITY IN PEOPLE 99
4.1 Introduction . . . 99
4.2 Assumptions and model . . . 100
4.3 Class-specific basic reproduction number . . . 102
4.4 System basic reproduction number . . . 103
4.5 Conserved quantities . . . 103
4.6 Final epidemic size . . . 104
4.7 Dependence of behavioral heterogeneity . . . 106
4.7.1 Initial behavior of disease spread . . . 106
4.7.2 Final epidemic size . . . 108
4.8 Model with specific behavioral heterogeneity . . . 110
4.8.1 A modified binomial class size distribution . . . 110
4.8.2 Two class model . . . 111
4.8.3 Comparison of two communities . . . 112
4.9 Discussion . . . 114
Appendix for Chapter 4 . . . 116
4.A.1 Proof of Lemma 4.1 . . . 116

4.A.2 Derivation of reproduction numbers 116
4.A.3 Derivation of system reproduction number 117
4.A.4 Proof of Lemma 4.2 118
4.A.5 Derivation of time-independent quantities 118
4.A.6 Proof of Lemma 4.5 and 4.6 119
4.A.7 Proof of Lemma 4.7 120
4.A.8 Proof of Lemma 4.8, 4.9, and Theorem 4.1 120
4.A.9 Proof of Lemma 4.10 121
4.A.10 Proof of Lemma 4.11 124
4.A.11 Derivation of Theorem 4.2 and 4.3 124
4.A.12 Derivation of q_c, θ_c, and $\mathscr{R}_c^{\sup}$ 126
4.A.13 Derivation of conditions for $W^* = 0$ 126
4.A.14 Proof of Lemma 4.12 and 4.13 127

5 CONCLUDING REMARKS 128

BIBLIOGRAPHY 130

1 INTRODUCTION

1.1 EPIDEMICS IN HUMAN HISTORY

1.1.1 *Historical outbreaks*

Infectious diseases have played an important role in shaping human history. One of the earliest well-documented major pandemics in history is the Plague of Athens (430 BCE), which occurred during the Peloponnesian War and was documented by Thucydides[36]. The plague decimated the population and undermined the social order of Athens. While typhoid fever figures prominently as a probable culprit, a recent theory, postulated by Olson and some other epidemiologists and classicists, suggests that the Athenian plague may have been caused by Ebola virus hemorrhagic fever[80,126].

The Antonine Plague (165–180 AD), likely caused by smallpox, spread throughout the Roman Empire and killed millions[140,173]. The epidemic is thought to have weakened Roman military power and contributed to the empire's long-term decline.

The Justinian Plague (541–542 AD), widely considered to be the first pandemic of bubonic plague, originated in the Byzantine Empire[55,90,162]. It spread rapidly through Mediterranean trade routes, killing tens of millions and recurring in waves over two centuries.

A turning point in demographic and social history was the Black Death (1347–1351). Carried from Asia to Europe via the Silk Road and maritime routes, it is estimated to have killed between 75 and 200 million people worldwide, with Europe losing up to 60 percent of its population[16,22,80,90]. This pandemic led to labor shortages, economic restructuring, and shifts in religious authority, setting the stage for the modern era. It also transformed urban planning and burial practices, and triggered waves of scapegoating and social unrest[27]. The black Death underscores the impact of high-mortality pathogens and the potential for nonlinear societal collapse when infection, fear, and misinformation co-evolve.

In the 20th century, the Spanish Flu (1918–1920) infected more than a third of the global population and resulted in an estimated 50 million deaths[84,116,152,157,159]. The unusually high mortality among young adults puzzled researchers and stimulated the development of modern epidemiological surveillance systems. The Spanish Flu demonstrated the importance of early warning systems, the role of asymptomatic transmission, and the need for transparent public health communication in shaping epidemic outcomes[64,157].

The emergence of HIV/AIDS in the 1980s has evolved into one of the longest-lasting pandemics in human history. Originating from cross-species transmission in Central Africa, it has led to over 35 million deaths worldwide and fundamentally transformed approaches to public health[90,147]. The HIV/AIDS is characterized by slow disease progression and primarily behavioral transmission pathways, such as unprotected sex and needle sharing. The early spread was accompanied by misinformation, social stigma, and delayed or inadequate governmental responses[100,108]. In South Africa, long-standing structural inequalities were rooted in the apartheid legacy

and further compounded by delayed political recognition of the crisis. These factors created conditions that facilitated the rapid spread of HIV and obstructed early intervention efforts[108]. Meanwhile, the pandemic galvanized global advocacy and contributed to institutionalized surveillance programs that continue to inform pandemic preparedness[91].

The early 21st century witnessed new challenges posed by emerging infectious diseases. The 2002–2003 SARS outbreak had profound implications for global health governance. It highlighted weaknesses in early warning systems and underscored the importance of transparency and rapid reporting. Consequently, it influenced revisions to the International Health Regulations[10,31,32,73]. Most recently, the COVID-19 pandemic has demonstrated how biological crises can intersect with and amplify pre-existing social vulnerabilities. Since its emergence in late 2019, COVID-19 has caused extensive morbidity and mortality across all world regions[34,156,161]. However, its effects have been unevenly distributed, reflecting disparities in healthcare access, housing, employment, and systemic discrimination. Evidence suggests that marginalized populations have borne a disproportionate burden of infection and death[107]. Furthermore, the pandemic has deepened existing health inequalities both within and between countries, reinforcing the call to integrate equity and social structure into public health planning[13]. The trajectory and impact of historical outbreaks suggest that while the biological features of a pathogen are critical in defining transmission dynamics, the social context plays an important role in shaping epidemic consequences. Factors such as mobility, inequality, and public trust are particularly influential. Therefore, insights from historical pandemics are essential for understanding current outbreaks and for developing effective policies to reduce future risks.

1.1.2 *Social vulnerability and social damage*

Social vulnerability refers to the susceptibility of individuals or communities to harm from external hazards due to underlying social, economic, and environmental disadvantages[61,148,175]. Originally developed in the context of disaster risk and climate change studies, the concept has been increasingly applied in the fields of public health and epidemiology to explain differential outcomes in infectious disease outbreaks[37,123]. Social vulnerability is multidimensional, encompassing indicators such as poverty, education, housing insecurity, access to healthcare, transportation, gender, race, and cultural practices.

The COVID-19 pandemic demonstrated how deeply social vulnerability shapes disease outcomes. In countries across the world, marginalized communities experienced disproportionately high rates of infection, hospitalization, and death due to pre-existing inequities in employment, housing density, and healthcare access[88,89,122,138].

Mathematical modelling has increasingly incorporated social vulnerability through mechanisms such as population distribution, parameter adjustment, and agent-level heterogeneity[39]. For example, McGillen *et al.*[112] developed a compartmental HIV transmission model that incorporates behavioral and geographic heterogeneity across 18 sub-Saharan African countries, and demonstrated that aligning prevention funding with local epidemic patterns and risk profiles can substantially increase the impact and cost-effectiveness of interventions. Munday *et al.*[120] developed a transmission model incorporating social group differences in contact rates and susceptibility, showing that even equal vaccine uptake can amplify infection risk disparities unless

higher coverage is provided to high-risk groups. In the context of COVID-19, Jentsch *et al.*[83] developed a mathematical model that incorporates social behavior and epidemic transmission dynamics to evaluate COVID-19 vaccination strategies. Their results suggest that when vaccination is initiated at a later stage of the pandemic, prioritizing vaccination for individuals who contribute more to transmission can reduce mortality more effectively than targeting vulnerable age groups. The results of Britton *et al.*[23] showed that population heterogeneity in age and social activity can substantially lower the disease-induced herd immunity threshold for COVID-19, and emphasized the importance of incorporating contact structure and individual variation into epidemic models.

Furthermore, the relationship between social vulnerability and infectious disease is bidirectional. While social vulnerability amplifies the risk and severity of disease outcomes, epidemic outbreaks can further reinforce and exacerbate existing social inequalities, functioning as drivers of structural and societal damage. Infectious disease outbreaks frequently intensify existing inequities by disrupting livelihoods, limiting access to education and healthcare, and eroding trust in institutions. For instance, the West African Ebola epidemic devastated health systems and social cohesion in Liberia, Sierra Leone, and Guinea, while also exacerbating stigmatization and fear-based exclusion[79,136,154]. Similarly, COVID-19 deepened poverty, widened gender and racial disparities, and increased exposure to domestic violence and mental health burdens[13,89,121]. Historical pandemics have left similar legacies. In India, the 1918 influenza pandemic is estimated to have killed 17–18 million people, with mortality concentrated in socially disadvantaged regions where famine, malnutrition, and colonial neglect intersected[29,149]. Such examples underline that infectious disease crises are not isolated biomedical phenomena but are shaped by social structures. Naidoo *et al.*[122] argues that models excluding social vulnerability risk underestimate the true burden of disease and may generate policies that inadvertently reinforce inequality. Therefore, understanding social vulnerability is essential for informing equitable and effective public health policy.

1.2 EPIDEMIOLOGICAL BACKGROUND FOR MODELING

1.2.1 *Classification of infectious diseases*

Infectious diseases are transmitted through various routes, depending on the characteristics of the pathogen, the host, and the surrounding environment. The main categories of infectious diseases based on transmission routes are as follows[75,110,169]:

- **Direct-contact transmitted diseases**: Spread through direct contact with an infected individual which includes physical touch or sexual contact, and typically spreading diseases such as herpes, syphilis, and HIV.
- **Respiratory-transmitted diseases**: Transmitted through infectious respiratory particles, either by droplet transmission during close-range interactions or by airborne transmission via particles suspended in the air over long distances. Examples of such diseases are COVID-19, influenza, measles, smallpox, and tuberculosis.

- **Vector-borne diseases**: Transmitted by vectors such as mosquitoes, ticks, or fleas that carry pathogens from one host to another. Examples of vector-borne diseases are malaria, dengue fever, Lyme disease, and Zika virus.
- **Food- and waterborne diseases**: Spread through the ingestion of contaminated food or water. Examples of such diseases are cholera, typhoid fever, and stomach flu.
- **Vertically transmitted diseases**: Passed from mother to child during pregnancy, childbirth, or breastfeeding. Examples of such diseases are HIV, syphilis, rubella, and hepatitis B.

1.2.2 *Transmission mechanisms of infectious diseases*

The classification of infectious diseases by transmission route provides a useful overview of how pathogens move between hosts. However, a deeper understanding of the underlying mechanisms is essential for predicting disease spread and developing effective control strategies. Here, we introduce detailed classification, including the following mechanisms:

- **Direct contact transmission**: This refers to physical transfer of pathogens through close physical contact with an infected individual, such as touching, kissing, or sexual contact.
- **Indirect contact transmission**: In this mechanism, pathogens are transmitted via contaminated surfaces or objects (fomites), such as shared utensils, doorknobs, or medical equipment.
- **Droplet transmission**: Involves the spread of pathogens via large respiratory droplets expelled when an infected person coughs, sneezes, or talks. These droplets typically travel short distances (within one meter) and deposit on the mucous membranes of a nearby host.
- **Airborne transmission**: Occurs when pathogens are carried by fine aerosol particles that remain suspended in the air over long distances and time. Inhalation of these particles can lead to infection even without close contact.
- **Vehicle-borne transmission**: Involves the transmission of pathogens through ingestion, injection, or exposure to contaminated substances such as food, water, blood, or medical instruments.
- **Vector-borne transmission**: Involves transmission by living vectors such as mosquitoes, ticks, or fleas, which carry and transmit the pathogen between hosts.
- **Vertical transmission**: This refers to transmission from mother to child during pregnancy, childbirth, or breastfeeding.
- **Zoonotic transmission**: Describes the spread of infectious agents from animals to humans, either through direct contact (e.g., bites) or indirectly through handling animal products or exposure to animal waste.

These transmission mechanisms may overlap within a single disease. For example, both influenza and COVID-19 involve droplet and airborne transmission mechanisms.

1.2.3 *Basic reproduction number*

The basic reproduction number $\mathscr{R}_0$ is a fundamental epidemiological index that quantifies the transmissibility of an infectious disease in a fully susceptible population. It is defined as the expected number of secondary infections produced by a single infected individual in a community consisting only of susceptible individuals during the entire infectious period[43,47,101,110].

In general, $\mathscr{R}_0$ depends on various factors, including the transmission rate of the pathogen, the duration of infectiousness, and the contact structure of the population. $\mathscr{R}_0 > 1$ indicates that the infection can spread in the population, potentially leading to an outbreak of the epidemic. In contrast, $\mathscr{R}_0 < 1$ indicates that the disease will eventually die out.

In compartmental models such as the SIR or SEIR models, $\mathscr{R}_0$ is derived through the next-generation matrix approach. It serves as a key threshold parameter for assessing outbreak potential and guiding public health interventions.

1.2.4 *Control strategies for infectious diseases*

Effective control of infectious diseases depends on a comprehensive understanding of transmission mechanisms and the implementation of appropriate interventions. Control strategies can be categorized into pharmaceutical and non-pharmaceutical measures[14,71,98,124,168]. These strategies aim to reduce transmission, protect vulnerable populations, and prevent outbreaks.

- **Pharmaceutical interventions**: These include vaccination and medical treatments. Vaccination confers individual immunity and contributes to herd immunity, thereby reducing disease incidence. Antiviral and antimicrobial therapies help lessen the severity and duration of illness.
- **Contact tracing**: This involves identifying and monitoring individuals who have been in close contact with an infected person. It enables early detection of new cases and breaks chains of transmission.
- **Isolation and quarantine**: Isolation involves separating infected individuals from the healthy population, while quarantine restricts the movement of individuals who may have been exposed. These are particularly important for diseases with high transmissibility or no immediate medical treatment.
- **Environmental and behavioral interventions**: These include improving hygiene, sanitation, and ventilation, as well as promoting behaviors such as mask-wearing, handwashing, and physical distancing. Such measures are essential for controlling respiratory and enteric infections.
- **Population-level movement control**: Travel restrictions and community lockdown are used to limit the geographic spread of disease during severe outbreaks. However, such measures may carry significant social and economic consequences and should be implemented with careful consideration.

The selection and combination of these strategies depend on disease characteristics, population vulnerability, and available medical resources.

1.3 BASIC EPIDEMIC MODELS

Mathematical models provide a framework for understanding the progression of infectious diseases and evaluating potential control strategies. In this section, we introduce the fundamental epidemic models, which capture the key mechanisms of disease transmission and serve as a foundation for epidemiological modeling and analysis.

1.3.1 *Kermack–McKendrick SIR model*

The Kermack–McKendrick SIR model, proposed by Kermack and McKendrick[92] in 1927, is widely recognized as one of the foundational contributions to the field of epidemic modeling. The model considered three classes, susceptible, infectious, and recovered. The model is based on the following assumptions[20,144]:

- The total population size of the community is constant, ignoring any demographic change with birth, death, and migration in a given epidemic season.
- The fatality of disease is negligible in the season.
- The recovered individual cannot be infected again.
- The disease transmission follows a mass action, where the infection force is proportional to the infective density in the population.

Based on the above assumptions, we have the following model:

$$\begin{aligned} \frac{dS}{dt} &= -\beta IS; \\ \frac{dI}{dt} &= \beta IS - \rho I; \\ \frac{dR}{dt} &= \rho I. \end{aligned} \tag{1}$$

The variables S, I, R denote the sizes of susceptible, infective, and recovered population. N is the total population size, and it is satisfied that $S(t) + I(t) + R(t) = N$ for any $t \geq 0$. Initial condition is given by $S_0 + I_0 = N$, $I_0 > 0$, and $R_0 = 0$. Every parameter is positive. The parameter ρ denotes the recovery rate of infective individual. Under the mass action assumption, the contact rate is assumed to be proportional to the population density and is given by βN, where β is the corresponding transmission coefficient. Since the probability that a contact by a susceptible is with an infective is I/N, the infection force, defined as the number of new infections per unit time per susceptible individual, is given by $(\beta N)(I/N) = \beta I$. Therefore, the rate of new infections in the population is βIS.

From system (1), the derivative of $S(t)$ is negative for all $t \geq 0$, so that the number of susceptible individuals is monotonically decreasing in terms of time with the positive initial value $S(0) = S_0$. Then, we have

$$\lim_{t\to\infty} S(t) = S_\infty \geq 0.$$

Similarly, the derivative of $R(t)$ is positive for all $t \geq 0$, the number of recovered individuals is monotonically increasing in terms of time and cannot beyond the total population size N. We have

$$\lim_{t\to\infty} R(t) = R_\infty \leq N.$$

On the other hand, the infected population size initially increases and subsequently decreases monotonically to zero if

$$\left.\frac{dI}{dt}\right|_{t=0} = (\beta S_0 - \rho) I_0 > 0,$$

otherwise, it decreases monotonically to zero from the beginning. Therefore, the necessary condition for the initial growth of infectives is the basic reproduction number $\mathscr{R}_0 := \beta N/\rho > 1$.

From $dS/dR = -\beta S/\rho$, the final size of susceptible population at the end of epidemic dynamics is given by

$$S_\infty = S_0 \exp\left(-\frac{\beta R_\infty}{\rho}\right).$$

Then, the final epidemic size defined as the total number of individuals who have experienced the infection until the final stage of the epidemic dynamics is given by $R_\infty := N - S_\infty$.

1.3.2 *SIS model*

The SIS model describes infectious diseases for which recovery does not provide immunity. In this subsection, we introduce a simplest SIS model by Kermack and McKendrick[93]. The assumptions are the same as those in Subsection 1.3.1, except that

- Individuals who recover from infection do not gain immunity and become susceptible again.

The SIS model is given by:

$$\begin{aligned} \frac{dS}{dt} &= -\beta IS + \rho I; \\ \frac{dI}{dt} &= \beta IS - \rho I. \end{aligned} \tag{2}$$

N is the total population size, and it is satisfied that $S(t) + I(t) = N$ for any $t \geq 0$. Initial condition is given by $S_0 + I_0 = N$ with $I_0 > 0$. Every parameter is positive. β is the infection rate and ρ is the recovery rate at which infective individuals return to the susceptible class.The basic reproduction number is given by $\mathscr{R}_0 := \beta N/\rho$.

Since $S(t) + I(t) = N$ for any t, the nature of the epidemic dynamics by (2) can be reduced to one dimensional ordinary differential equation:

$$\frac{dI}{dt} = \beta I(N - I) - \rho I = \beta\left(N - \frac{\rho}{\beta} - I\right) I. \tag{3}$$

When $N - \rho/\beta \leq 0$, that is, $\mathscr{R}_0 \leq 1$, the infective population size is monotonically decreasing to zero with initial value $I_0 > 0$. When $N - \rho/\beta > 0$, that is, $\mathscr{R}_0 > 1$, we can solve the equation (3) explicitly using separation of variables. The expression of the solution is given by

$$I(t) = \frac{K I_0 \exp(rt)}{K - I_0 + I_0 \exp(rt)} = \frac{K}{1 - (1 - K/I_0)\exp(-rt)},$$

where $K = N - \rho/\beta$, $r = \beta N - \rho$. Then, we have

$$\lim_{t\to\infty} I(t) = K$$

for $K > 0$ and $r > 0$. It indicates that the infective population size monotonically approaches the endemic equilibrium K when $\mathscr{R}_0 > 1$. Therefore, if $\mathscr{R}_0 > 1$, the disease remains in the community and the system converges to an endemic equilibrium. In contrast, if $\mathscr{R}_0 \leq 1$, the disease dies out and the system converges to a disease-free equilibrium.

1.3.3 *SIRS model*

The SIRS model assumes that the immunity acquired through recovery is temporary and wanes over time. The assumptions are the same as those in Subsection 1.3.1, except that

- Individuals who recover from infection acquire immunity, but this immunity is eventually lost, and they return to the susceptible class.
- Immunity wanes at a constant rate.

Under these assumptions, the SIRS model is given by:

$$\begin{aligned} \frac{dS}{dt} &= -\beta IS + \delta R; \\ \frac{dI}{dt} &= \beta IS - \rho I; \\ \frac{dR}{dt} &= \rho I - \delta R. \end{aligned} \tag{4}$$

N is the total population size, and it is satisfied that $S(t) + I(t) + R(t) = N$ for any $t \geq 0$. Initial condition is given by $S_0 + I_0 = N$ with $I_0 > 0$. Every parameter is positive. β is the infection rate, ρ is the recovery rate, δ is the rate at which immunity wanes and recovered individuals return to the susceptible class. The basic reproduction number is given by $\mathscr{R}_0 := \beta N / \rho$. This model describes the reinfection mechanism driven by the loss of immunity.

It is easy to obtain that there are at most two equilibria. One is the disease-free equilibrium $E_0(N, 0, 0)$, and the other is endemic equilibrium

$$E_+ \left(S^*, \frac{\delta}{\delta + \rho}(\mathscr{R}_0 - 1)S^*, \frac{\rho}{\delta + \rho}(\mathscr{R}_0 - 1)S^* \right) \quad \text{with} \quad S^* := \frac{\rho}{\beta}.$$

The disease-free equilibrium E_0 is globally asymptotically stable if and only if the basic reproduction number satisfies $\mathscr{R}_0 \leq 1$, implying the disease dies out over time. When $\mathscr{R}_0 > 1$, the endemic equilibrium E_+ exists and becomes globally asymptotically stable, implying the disease persists within the community.

1.3.4 *SIRI model*

The SIRI model assumes that the immunity acquired through recovery is imperfect or partial, and recovered individuals may become infectious again. The assumptions are the same as those in Subsection 1.3.3, except that

- After the recovery from the infection, the individual may get the infection again due to imperfect or partial immunity to against the disease.
- The reinfection after the recovery from the disease generally has a likelihood not beyond that of the infection for the susceptible.

Based on the assumptions, the simple SIRI model is given by :

$$\begin{aligned}\frac{dS}{dt} &= -\beta IS,\\ \frac{dI}{dt} &= \beta IS + \varepsilon\beta IR - \rho I,\\ \frac{dR}{dt} &= \rho I - \varepsilon\beta IR.\end{aligned} \tag{5}$$

N is the total population size, and it is satisfied that $S(t) + I(t) + R(t) = N$ for any $t \geq 0$. The initial condition is given by $S_0 + I_0 = N$ with $I_0 > 0$. Every parameter is positive. β is the infection rate, and the reinfection rate is given by $\varepsilon\beta$, where $0 < \varepsilon < 1$. Here ε is a reduction parameter for the actual infection rate because the recovered individual will have reduced susceptibility due to acquired immunity. In particular, $\varepsilon = 0$ denotes full immunity, corresponding to the SIR model (1) in the Subsection 1.3.1. ρ is the recovery rate. The basic reproduction number is given by $\mathscr{R}_0 := \beta N/\rho$.

This model describes the reinfection mechanism driven by imperfect immunity, and differs from the SIRS model in how reinfection is assumed. In the SIRS model, individuals are assumed to acquire complete immunity after recovery, which subsequently wanes over time. Once immunity is lost, these individuals re-enter the susceptible class. In contrast, the SIRI model assumes that immunity after recovery is inherently partial or imperfect. Recovered individuals do not return to the susceptible class but instead retain partial immunity, which allows for reinfection to primary infection. Furthermore, the reinfection rate in the SIRI model is typically lower than that of primary infection, reflecting partial immune protection rather than a full return to susceptibility. This structural distinction allows the SIRI model to better describe infectious diseases in which reinfection can occur due to imperfect or partial immunity, immune evasion by the pathogen, or latent reactivation. Examples include diseases such as malaria, tuberculosis, and certain viral infections where immunity is not lifelong or pathogen persistence is possible.

1.3.5 *Effect of the quarantine/isolation*

Quarantine and isolation are critical public health interventions aimed at reducing disease transmission by separating infected or potentially infected individuals from the susceptible population. A simple extension of the SIR model that incorporates an isolation compartment Q is given by

$$\begin{aligned}\frac{dS}{dt} &= -\beta\frac{I}{N-Q}S,\\ \frac{dI}{dt} &= \beta\frac{I}{N-Q}S - \sigma I - \rho I,\\ \frac{dQ}{dt} &= \sigma I - \rho Q,\\ \frac{dR}{dt} &= \rho I + \rho Q.\end{aligned} \tag{6}$$

In this model, susceptible individuals (S) become infected through contact with infectious individuals (I). However, only individuals who are not isolated can contribute to the disease transmission. This is reflected in the term $I/(N-Q)$, which assumes that isolated individuals do not contribute to transmission, and susceptible individuals are exposed only to the non-isolated population. Here The denominator $N - Q$ represents the effective

population participating in transmission. Once infected, individuals are either isolated at rate σ, or directly recover at rate ρ. Under the assumption that isolation does not affect the efficiency of recovery, isolated individuals recover at the same rate ρ. Recovered individuals gain lifelong immunity and no longer participate in disease transmission.

To evaluate the potential for epidemic spread under the influence of isolation, we obtain the basic reproduction number $\mathscr{R}_0 := \beta/(\rho + \sigma)$. This expression indicates that basic reproduction number decreases with increasing isolation rate σ or recovery rate ρ. In particular, even if the recovery rate is unchanged, enhancing the isolation rate can reduce the value of $\mathscr{R}_0$, thereby preventing a large-scale outbreak. Thus, isolation contributes to epidemic control not by accelerating recovery, but by reducing the average number of contacts that result in new infections. This result emphasizes the importance of early detection and prompt isolation as non-pharmaceutical interventions, especially for emerging infectious diseases without effective treatments or vaccines.

2 REGIONAL LOCKDOWN

2.1 INTRODUCTION

In addition to vaccination and medical treatment, lockdown can be regarded as a basic strategy for the public health to suppress the spread of a transmissible disease in a community. Especially in some regions with poor medical infrastructure and low emergency response capacity, the lockdown could play a role to give the government and decisionmaker a sufficient time to arrange a strategy for controlling the epidemic[105,115,118]. Many studies have shown that lockdown is effective in reducing the number of new cases in the countries that implement it, compared with those countries that do not (for example, Alfano and Ercolano[6], Lau *et al.*[99], Dechsupa *et al.*[40], Huang *et al.*[78], Milne *et al.*[117], and references therein). The essential role of lockdown is to reduce the frequency and duration of contacts between individuals in the community. Such a strategy includes closing schools and workplaces, preventing from being outside or gathering, restricting the access to public places (e.g., public transportations), and so on[128,129].

Although such a strict restriction has an important role in suppressing the disease transmission in a community, the economic development must tend to face with great challenges due to the decline in the social activities under it, as seen in the COVID-19 pandemic[24,44,125]. At the start of the pandemic, del Rio-Chanona *et al.*[42] estimated that, the immediate impact of COVID-19 in the US could threaten 22 percent of GDP, 24 percent of jobs, and reduce wage income by 17 percent. According to Coccia[35], it is uncertain whether the long-term lockdown can reduce the number of COVID-19 infected individuals and deaths, and the longer lockdown has a negative impact on the economy. Especially, the economy related to tourism has been severely affected[171]. Not only the closure of factories and stores has had a great impact on relevant industries (e.g., retail), but also consumers' spending has declined due to restrictive measures and reduced income[104]. Tonnoir *et al.*[158] considered a mathematical model to investigate the optimal investment strategy under the lockdown situation, and derived that it is difficult to ensure both the reduction of regional disparities and economic growth.

Furthermore, lockdown can cause significant psychological distress by imposing isolation that negatively affects mental well-being[25,86]. Ganesan *et al.*[62] also mentioned that the prolonged lockdown may cause some problems in the physical and mental health. In particular, young people, who are more susceptible to mental health issues than adults, are especially vulnerable to the negative impacts of school closures and reduced opportunities for physical activity and social interaction during lockdowns[41,164]. Hence, it is necessary to consider whether a lockdown could allow a balance between the epidemic control and the social activities.

While previous studies have mainly investigated the economic and psychological impacts of lockdown, emphasizing its social costs, our study mathematically compares different levels of lockdown policies, where each level represents a different degree of restriction on economic and social activities. Within this framework, we aim to investigate whether a lockdown

strategy can be identified that not only suppresses the epidemic but also sustains essential economic and social functions.

In this chapter, we consider a simple mathematical model to investigate the efficiency of different types of lockdown according to the endemic size, that is, the number of infective individuals at the endemic equilibrium. In our modeling, we introduce different restrictions on the mobility of individuals and define four types of lockdown: complete lockdown, strong lockdown, weak lockdown type 1, and type 2. The mathematical analysis on our model shows the existence and stability of possible equilibria and compare those four types of lockdown to discuss which type of the lockdown is better according to the endemic size.

2.2 ASSUMPTIONS

The movement of population must accelerate the spread of an epidemic, which is a fundamental cause of a long-range epidemic transmission. In this work, we consider a simple mathematical model of epidemic dynamics with the following assumptions:

- The disease is not fatal;
- The community is composed of the peripheral area (area 1) and the central area (area 2) with different qualities of the medical treatment for the disease;
- Susceptible individuals of one area can temporarily visit to the other area;
- Some infective individuals of the peripheral area (area 1) can get the medical treatment at the central area (area 2), for example, transported by ambulance;
- Recovered individual becomes susceptible again;
- The population size is constant in each area during the epidemic season. We ignore any demographic change due to the natural birth, death, and migration.

There is no specific assumption about the population sizes of the two areas. The central area represents places where people typically work, go to school, or shop, while the peripheral area consists of residential zones where people return after such activities. Therefore, the central area may have either a higher or lower population density compared to the peripheral area. In Section 2.8, we define ρ as the ratio of the population sizes of the two areas and show how it affects the endemic size for the two types of weak lockdown.

2.3 MODEL

As shown in Figure 1, S_i denotes the population density of healthy individuals in area i who can be infected, I_i that of individuals in area i who have been infected and are able to transmit the disease, and H_{ij} that of individuals belonging to area j who are infective and under the medical treatment in

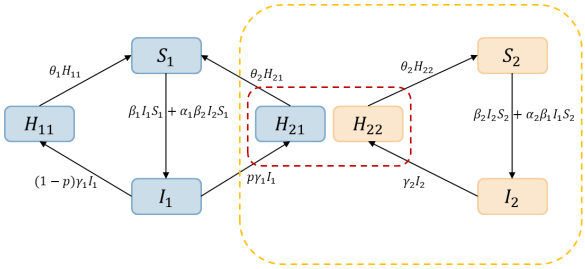

Figure 1: Scheme of the epidemic dynamics in our model (7).

area i. We construct the following mathematical model expressed by the system of ordinary differential equations:

$$\begin{aligned}
\frac{dS_1}{dt} &= -\beta_1 I_1 S_1 - \alpha_1\beta_2 I_2 S_1 + \theta_1 H_{11} + \theta_2 H_{21};\\
\frac{dI_1}{dt} &= \beta_1 I_1 S_1 + \alpha_1\beta_2 I_2 S_1 - \gamma_1 I_1;\\
\frac{dH_{11}}{dt} &= (1-p)\gamma_1 I_1 - \theta_1 H_{11};\\
\frac{dH_{21}}{dt} &= p\gamma_1 I_1 - \theta_2 H_{21};\\
\frac{dS_2}{dt} &= -\beta_2 I_2 S_2 - \alpha_2\beta_1 I_1 S_2 + \theta_2 H_{22};\\
\frac{dI_2}{dt} &= \beta_2 I_2 S_2 + \alpha_2\beta_1 I_1 S_2 - \gamma_2 I_2;\\
\frac{dH_{22}}{dt} &= \gamma_2 I_2 - \theta_2 H_{22},
\end{aligned} \tag{7}$$

where β_i is the infection coefficient in area i, which represents the effective infectivity of the transmissible disease. $\alpha_i\beta_j$ is the infection coefficient during the temporary visit to area j, which is smaller than β_j $(0 < \alpha_i < 1)$. γ_i is the treatment rate of the infective in area i, and θ_i is the recovery rate by the medical treatment in area i. p is the proportion of infectives belonging to the peripheral area, who get the medical treatment in the central area $(0 \le p \le 1)$. From the assumption, it holds that $S_1 + I_1 + H_{11} + H_{21} = N_1$, $S_2 + I_2 + H_{22} = N_2$ for any time t with positive constants N_1 and N_2.

With the frequencies $\phi_i = S_i/N_i$, $\psi_i = I_i/N_i$, $\zeta_{ij} = H_{ij}/N_j$, the area-specified basic reproduction numbers $\mathscr{R}_0^r = \beta_1 N_1/\gamma_1$ for the peripheral area and $\mathscr{R}_0^c = \beta_2 N_2/\gamma_2$ for the central area, we can transform the system (7) to

$$\begin{aligned}
\frac{d\phi_1}{dt} &= -\mathscr{R}_0^r\gamma_1\psi_1\phi_1 - \mathscr{R}_0^c\gamma_2\alpha_1\psi_2\phi_1 + \theta_1\zeta_{11} + \theta_2\zeta_{21};\\
\frac{d\psi_1}{dt} &= \mathscr{R}_0^r\gamma_1\psi_1\phi_1 + \mathscr{R}_0^c\gamma_2\alpha_1\psi_2\phi_1 - \gamma_1\psi_1;\\
\frac{d\zeta_{11}}{dt} &= (1-p)\gamma_1\psi_1 - \theta_1\zeta_{11};\\
\frac{d\zeta_{21}}{dt} &= p\gamma_1\psi_1 - \theta_2\zeta_{21};\\
\frac{d\phi_2}{dt} &= -\mathscr{R}_0^c\gamma_2\psi_2\phi_2 - \mathscr{R}_0^r\gamma_1\alpha_2\psi_1\phi_2 + \theta_2\zeta_{22};\\
\frac{d\psi_2}{dt} &= \mathscr{R}_0^c\gamma_2\psi_2\phi_2 + \mathscr{R}_0^r\gamma_1\alpha_2\psi_1\phi_2 - \gamma_2\psi_2;\\
\frac{d\zeta_{22}}{dt} &= \gamma_2\psi_2 - \theta_2\zeta_{22},
\end{aligned} \tag{8}$$

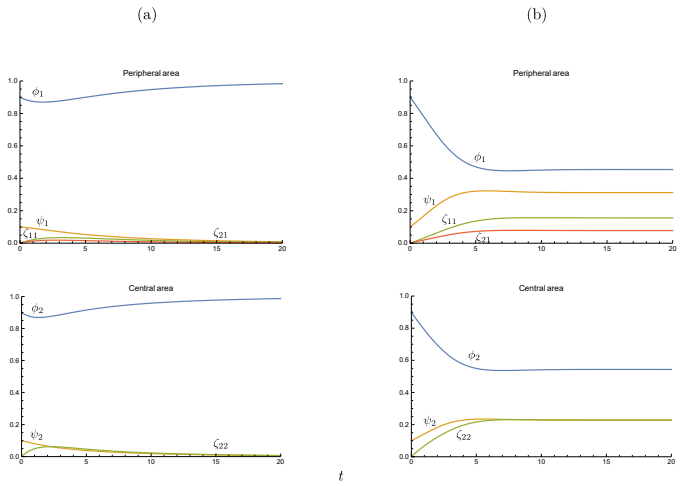

Figure 2: Numerical examples of the temporal variation of the frequencies by the system (8). $(\mathscr{R}_0^r, \mathscr{R}_0^c) =$ (a) $(0.4, 0.7)$; (b) $(1.5, 1.2)$. Commonly, $\alpha_1 = \alpha_2 = 0.5$; $\theta_1 = 0.6$; $\theta_2 = 0.8$; $\gamma_1 = 0.5$; $\gamma_2 = 0.8$; $p = 0.4$.

where $\phi_1 + \psi_1 + \zeta_{11} + \zeta_{21} = 1$, and $\phi_2 + \psi_2 + \zeta_{22} = 1$. As for the area-specified basic reproduction numbers $\mathscr{R}_0^r$ and $\mathscr{R}_0^c$, we will give the detail later in Section 3. Figure 2 shows numerical examples of the temporal variation of the frequencies by the system (8) when the disease is extinct and persistent respectively.

2.4 BASIC REPRODUCTION NUMBERS

The basic reproduction number $\mathscr{R}_0$ is the expected supremum number of secondary cases produced in a totally susceptible population by a single infective individual during the time span of active infectivity [81]. If $\mathscr{R}_0 < 1$, the number of infectives decreases and the disease will disapper after its invasion in the community. Only if $\mathscr{R}_0 > 1$, the disease could persist after its invasion in the community.

As described in Appendix 2.A.1 for the model (7), we can derive the area-specified basic reproduction numbers $\mathscr{R}_0^r = \beta_1 N_1/\gamma_1$ for the peripheral area and $\mathscr{R}_0^c = \beta_2 N_2/\gamma_2$ for the central area respectively. These are the basic reproduction numbers for each area when two areas are fully isolated, that is, the movement of susceptible individuals between them is prohibited. In contrast, the basic reproduction number for the full epidemic dynamics governed by (7) can be mathematically defined as

$$\mathscr{R}_0 = \frac{\mathscr{R}_0^r + \mathscr{R}_0^c + \sqrt{(\mathscr{R}_0^r - \mathscr{R}_0^c)^2 + 4\alpha_1\alpha_2\mathscr{R}_0^r\mathscr{R}_0^c}}{2}, \tag{9}$$

which is the basic reproduction number for the whole community with the mobility of susceptible individuals. We can easily find that $\mathscr{R}_0 > \mathscr{R}_0^r$ and $\mathscr{R}_0 > \mathscr{R}_0^c$. When $\alpha_1\alpha_2 = 0$, that is, under a lockdown introduced in the previous section, we have $\mathscr{R}_0 = \max\{\mathscr{R}_0^r, \mathscr{R}_0^c\}$ from (9).

2.5 DIFFERENT POLICIES OF LOCKDOWN

Depending on the population size, the severity of pandemic, the economic level, the medical condition, and the living customs in each region, it would

be necessary to adopt an appropriate type of lockdown policy. In this work, we consider different levels of restriction on individuals' mobility.

Without the lockdown in our model, the temporary visit of susceptibles is allowed in each area, and infectives of the peripheral area may get the medical treatment in the central area (generally supposing that the central area has a higher quality of the medical treatment than that in the peripheral area). Table 1 shows four different types of the lockdown which we introduce in our model. Under the weak lockdown type 1, only susceptibles of the peripheral area are prohibited to visit the central area. Under the weak lockdown type 2, only susceptibles of the central area are prohibited to visit the peripheral area. Under the strong lockdown, the movement of any susceptibles between two areas is prohibited. For these three types of lockdown, infectives of the peripheral area may get the medical treatment in the central area. In contrast, under the complete lockdown, two areas become fully independent of each other and any movement is prohibited between them, and infectives of the peripheral area cannot get the medical treatment in the central area.

2.6 DISEASE-FREE EQUILIBRIUM

Disease-free equilibrium is defined as an equilibrium state without the disease. For the model (8), it becomes $E_0(1,0,0,0,1,0,0)$. By the eigenvalue analysis on the Jacobian matrix for E_0, we can obtain the following result on the local stability (Appendix 2.A.2):

Theorem 2.1. *Disease-free equilibrium $E_0(1,0,0,0,1,0,0)$ is unstable if one of the following conditions is satisfied:*

(i) $\mathscr{R}_0^r \geq 1$;

(ii) $\mathscr{R}_0^c \geq 1$;

(iii) $\left(\frac{1}{\mathscr{R}_0^r} - 1\right)\left(\frac{1}{\mathscr{R}_0^c} - 1\right) < \alpha_1\alpha_2$.

When the mobility of susceptible individuals is sufficiently large, that is, with sufficiently large $\alpha_1\alpha_2$, E_0 is unstable with the condition $\mathscr{R}_0^r < 1$ and $\mathscr{R}_0^c < 1$. When $\alpha_1\alpha_2 = 0$, that is, the mobility of susceptible individuals is prohibited for any of two areas, E_0 is unstable if and only if the disease persists at least in one of two areas.

Table 1: Different types of lockdown for our model (7).

	α_1	α_2	p
Weak lockdown type 1	0	$+$	$+$
Weak lockdown type 2	$+$	0	$+$
Strong lockdown	0	0	$+$
Complete lockdown	0	0	0

2.7 ENDEMIC EQUILIBRIUM

Endemic equilibrium means an equilibrium state at which the number of infectives keeps a positive value for any time t. As shown in Appendix 2.A.3, we can get the following result on the existence of a unique endemic equilibrium $E^*(\phi_1^*, \psi_1^*, \zeta_{11}^*, \zeta_{21}^*, \phi_2^*, \psi_2^*, \zeta_{22}^*)$:

Lemma 2.1. *Endemic equilibrium E^* uniquely exists if and only if one of the conditions $(i), (ii)$ and (iii) in Theorem 4.1 is satisfied, independently of which type of lockdown is adopted to the community.*

Especially we can show the global stability of E^* under the complete or strong lockdown, making use of the Lyapunov function (Appendix 2.A.4):

Theorem 2.2. *Under the strong lockdown with $\alpha_1 = \alpha_2 = 0$ or the complete lockdown with $\alpha_1 = \alpha_2 = p = 0$, the endemic equilibrium E^* is globally asymptotically stable when it exists.*

We have not obtained any mathematical result on the global stability of E^* under the weak lockdown or no lockdown. Numerical calculations of the system (8), as shown in Figure 2(b), imply that it would be globally asymptotically stable when it exists.

2.8 ENDEMIC SIZE

The proportion of population size in the peripheral area and central area is defined by $\rho := N_1/N_2$. We define here the endemic size as the total number of infective individuals in the community at the endemic equilibrium E^*. For our model (8), we define it by $\Psi^* := (N_1 + N_2 - S_1^* - S_2^*)/(N_1 + N_2) = 1 - (\rho\phi_1^* + \phi_2^*)/(1+\rho)$. We now designate the endemic sizes under the complete, strong, and weak (type 1 and 2) lockdowns respectively by Ψ_c^*, Ψ_s^*, Ψ_{w1}^* and Ψ_{w2}^*. We can get the following formulas of them from (8):

$$\begin{aligned}
\Psi_c^* &= \frac{\rho}{1+\rho}\Big(1 - \frac{1}{\mathscr{R}_0^r}\Big) + \frac{1}{1+\rho}\Big(1 - \frac{1}{\mathscr{R}_0^c}\Big);\\
\Psi_s^* &= \frac{\rho}{1+\rho}\Big(1 - \frac{1}{\mathscr{R}_0^r}\Big) + \frac{1}{1+\rho}\Big(1 - \frac{1}{\mathscr{R}_0^c}\Big);\\
\Psi_{w1}^* &= \frac{\rho}{1+\rho}\Big(1 - \frac{1}{\mathscr{R}_0^r}\Big) + \frac{1}{1+\rho}(1 - \phi_2^*);\\
\Psi_{w2}^* &= \frac{\rho}{1+\rho}(1 - \phi_1^*) + \frac{1}{1+\rho}\Big(1 - \frac{1}{\mathscr{R}_0^c}\Big),
\end{aligned}$$

where ϕ_1^* is the smaller root of the following quadratic equation of x, which is less than $1/\mathscr{R}_0^r$:

$$\mathscr{R}_0^r\gamma_1\theta_1\theta_2 x^2 - \Big\{(\mathscr{R}_0^r + 1)\gamma_1\theta_1\theta_2 + \mathscr{R}_0^c\alpha_1\psi_2^*\gamma_2\big[\theta_1\theta_2 + (1-p)\gamma_1\theta_2 + p\gamma_1\theta_1\big]\Big\}x + \gamma_1\theta_1\theta_2 = 0$$

with $\psi_2^* = \theta_2[1 - (1/\mathscr{R}_0^c)]/(\theta_2 + \gamma_2)$. ϕ_2^* is the smaller root of the following quadratic equation of x, which is less than $1/\mathscr{R}_0^c$:

$$\mathscr{R}_0^c\gamma_2\theta_2 x^2 - \big[(\mathscr{R}_0^c + 1)\gamma_2\theta_2 + \mathscr{R}_0^r\alpha_2\psi_1^*\gamma_1(\gamma_2 + \theta_2)\big]x + \gamma_2\theta_2 = 0$$

with $\psi_1^* = \theta_1\theta_2[1 - (1/\mathscr{R}_0^r)]/[\theta_1\theta_2 + (1-p)\gamma_1\theta_2 + p\gamma_1\theta_1]$.

Since $\phi_1^* < 1/\mathscr{R}_0^r$ and $\phi_2^* < 1/\mathscr{R}_0^c$, we can easily obtain the order of endemic sizes $\Psi_c^* = \Psi_s^* < \Psi_{w\bullet}^*$. The weak lockdown with minimal restrictions has the least effect on preventing the spread of the epidemic.

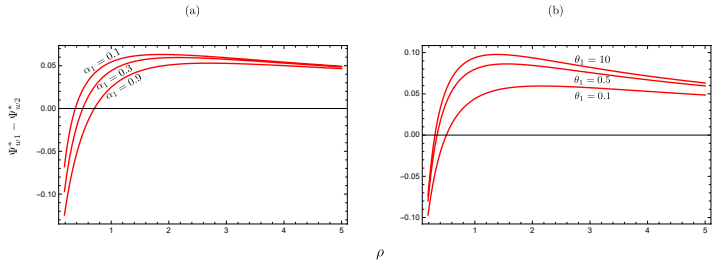

Figure 3: ρ dependence of $\Psi^*_{w1} - \Psi^*_{w2}$. Numerically drawn with different value of (a) $\theta_1 = 0.1$; (b) $\alpha_1 = 0.3$. Commonly, $N_2 = 2.0 \times 10^5$; $\beta_1 = 8.0 \times 10^{-4}$; $\beta_2 = 9.0 \times 10^{-4}$; $\gamma_1 = 0.3$; $\gamma_2 = 0.9$; $\alpha_2 = 0.3$; $p = 0.4$; $\theta_2 = 0.5$.

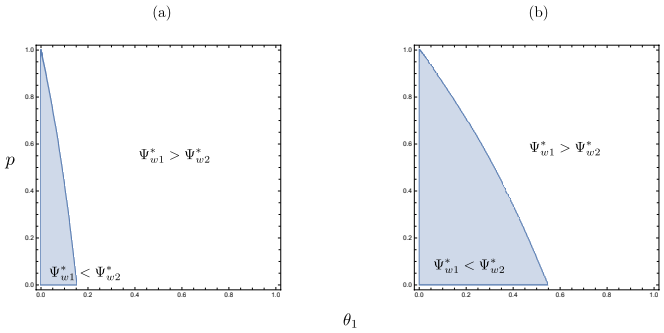

Figure 4: Parameter dependence of the order of epidemic sizes for the two types weak lockdown. Numerically drawn with (a) $\theta_2 = 0.5$; (b) $\theta_2 = 2$. Commonly, $N_1 = 1.0 \times 10^5$; $N_2 = 2.0 \times 10^5$; $\beta_1 = 8.0 \times 10^{-4}$; $\beta_2 = 9.0 \times 10^{-4}$; $\gamma_1 = 0.3$; $\gamma_2 = 0.9$; $\alpha_1 = \alpha_2 = 0.3$; $\theta_2 = 0.5$.

Population distribution

The efficiency of two types of weak lockdown is dependent on the parameter ρ, the population distribution of the whole community. ρ is sufficiently small if the population density of the central area is sufficiently larger than that of the peripheral area. In this case, the endemic size is primarily influenced by the endemic size of the central area, we can get that the weak lockdown type 2 is better than type 1 as shown in Figure 3. Inversely, if we consider the sufficient large population size of the peripheral area, we can get the opposite result. Therefore, a more efficient weak lockdown is the prohibition of mobility for susceptible individuals from an area of high population density to that of low population density.

Hospitalization period

In our model, hospitalization period is given by $1/\theta_\bullet$. The extended hospitalization period aims to reduce the pool of susceptible individuals and slow the spread of the epidemic. Referring to Figure 4, when hospitalization period of the peripheral area is longer than that of central area, raising the proportion of infected individuals from the peripheral area to get medical treatment in the central area could result in an increase in the endemic size of the peripheral area. Furthermore, for a specific value of p, an extended hospitalization period in the central area requires a longer hospitalization period in the peripheral area to ensure that weak lockdown type 1 is better than type 2.

2.9 DISCUSSION

We consider an $SIS + H$ model, where H represents the isolated state in the community. In our model, we assume the community is composed by two areas. The basic reproduction of the whole epidemic system is larger than that of each area, which implies that individuals' mobility could accelerate the spread of transmissible disease. This result is consistent with previous findings that human mobility can substantially accelerate epidemic spread and increase the risk of infection. Lockdown is therefore a strategy to restrict mobility, which could play a significant role in reducing epidemic spread at an early stage, and has indeed been implemented in many countries and regions during recent outbreaks.

Our purpose was to investigate whether different levels of lockdown can achieve a balance between epidemic control and individuals' activities. For this reason, we introduced four types of lockdown by imposing different restrictions on mobility. The mathematical results comparing the endemic sizes under these four types indicate that complete and strong lockdowns have the same endemic size, which is smaller than those under weak lockdown. Allowing peripheral infected individuals to get medical treatment in the central area does not have an effect on the endemic size. The weak lockdown with minimal restriction on mobility has the lowest efficiency in suppressing the spread of an epidemic. When the hospital in the central area has a sufficiently longer isolation period than the peripheral area, free infectives under the strong lockdown are less than those under the complete lockdown. Furthermore, our results reveal that the population distribution between the two areas plays an important role in comparing the endemic sizes of the two weak lockdowns. For the weak lockdown, more efficient is the prohibition of mobility for susceptible individuals from an area of high population density to that of low population density. This finding provides a mathematical explanation for why restrictions on flows connecting highly populated areas can be more impactful in practice.

In summary, our analysis shows that the efficiency of lockdown depends not only on the strictness of mobility restrictions but also on the population distribution. These findings contribute a mathematical perspective on how different lockdown levels shape epidemic consequence.

APPENDIX FOR CHAPTER 2

APPENDIX 2.A.1: DERIVATION OF THE BASIC REPRODUCTION NUMBERS

First, we define the area-specific basic reproduction number $\mathscr{R}_0^r$ for the peripheral area. Let we consider the initial stage of the disease invasion in the peripheral area, at $t = 0$. The number of infective individuals in the peripheral area is sufficiently small. If the disease invasion is successful, the number of infective individuals in the peripheral area increases after it, that is,

$$\left.\frac{dI_1}{dt}\right|_{t=0} = \big(\beta_1 S_1(0) - \gamma_1\big) I_1(0) > 0.$$

This occurs if and only if

$$\frac{\beta_1 S_1(0)}{\gamma_1} > 1. \tag{10}$$

If the inequality of (10) is inverse, the disease invasion fails, and the number of infective individuals decreases in the peripheral area.

From the biological definition of the basic reproduction number, the disease invasion is successful only if $\mathscr{R}_0^r > 1$, while it fails if $\mathscr{R}_0^r < 1$. Since the basic reproduction number is conceptually defined as the expected number of secondary cases by a single infective individual in a totally susceptible population during the infection, we can define $\mathscr{R}_0^r$ as the supremum of the value $\beta_1 S_1(0)/\gamma_1$ from the condition (10) as follows:

$$\mathscr{R}_0^r := \sup_{S_1(0)} \frac{\beta_1 S_1(0)}{\gamma_1} = \frac{\beta_1 N_1}{\gamma_1}.$$

From this definition of $\mathscr{R}_0^r$, we have $dI_1/dt > 0$ only when $\mathscr{R}_0^r > 1$. When $\mathscr{R}_0^r < 1$, we have $dI_1/dt < 0$. The derivation of the area-specified basic reproduction number $\mathscr{R}_0^c$ for the central area is the same as that of $\mathscr{R}_0^r$, and we can define $\mathscr{R}_0^c := \beta_2 N_2/\gamma_2$.

In order to mathematically derive the basic reproduction number $\mathscr{R}_0$ for the community, we use here the method of the next generation matrix[18]. Firstly, we change the order of equations in (8) for a mathematical convenience:

$$\begin{aligned}
\frac{d\psi_1}{dt} &= \mathscr{R}_0^r \gamma_1 \psi_1 \phi_1 + \mathscr{R}_0^c \gamma_2 \alpha_1 \psi_2 \phi_1 - \gamma_1 \psi_1;\\
\frac{d\psi_2}{dt} &= \mathscr{R}_0^c \gamma_2 \psi_2 \phi_2 + \mathscr{R}_0^r \gamma_1 \alpha_2 \psi_1 \phi_2 - \gamma_2 \psi_2;\\
\frac{d\phi_1}{dt} &= -\mathscr{R}_0^r \gamma_1 \psi_1 \phi_1 - \mathscr{R}_0^c \gamma_2 \alpha_1 \psi_2 \phi_1 + \theta_1 \zeta_{11} + \theta_2 \zeta_{21};\\
\frac{d\phi_2}{dt} &= -\mathscr{R}_0^c \gamma_2 \psi_2 \phi_2 - \mathscr{R}_0^r \gamma_1 \alpha_2 \psi_1 \phi_2 + \theta_2 \zeta_{22};\\
\frac{d\zeta_{11}}{dt} &= (1-p)\gamma_1 \psi_1 - \theta_1 \zeta_{11};\\
\frac{d\zeta_{21}}{dt} &= p\gamma_1 \psi_1 - \theta_2 \zeta_{21};\\
\frac{d\zeta_{22}}{dt} &= \gamma_2 \psi_2 - \theta_2 \zeta_{22}.
\end{aligned} \tag{11}$$

Next we decompose the above system as the form

$$\frac{dX}{dt} = F(X) - V(X),$$

where $X = (\psi_1(t), \psi_2(t), \phi_1(t), \phi_2(t), \zeta_{11}(t), \zeta_{21}(t), \zeta_{22}(t))^T$. F contains only the recruitment terms of the infection, and V does the other factors in (11):

$$F := \begin{pmatrix} \mathscr{R}_0^r\gamma_1\psi_1\phi_1+\mathscr{R}_0^c\gamma_2\alpha_1\psi_2\phi_1 \\ \mathscr{R}_0^c\gamma_2\psi_2\phi_2+\mathscr{R}_0^r\gamma_1\alpha_2\psi_1\phi_2 \\ 0 \\ 0 \\ 0 \\ 0 \\ 0 \end{pmatrix}; \quad V := \begin{pmatrix} \gamma_1\psi_1 \\ \gamma_2\psi_2 \\ \mathscr{R}_0^r\gamma_1\psi_1\phi_1+\mathscr{R}_0^c\gamma_2\alpha_1\psi_2\phi_1-\theta_1\zeta_{11}-\theta_2\zeta_{21} \\ \mathscr{R}_0^c\gamma_2\psi_2\phi_2+\mathscr{R}_0^r\gamma_1\alpha_2\psi_1\phi_2-\theta_2\zeta_{22} \\ -(1-p)\gamma_1\psi_1+\theta_1\zeta_{11} \\ -p\gamma_1\psi_1+\theta_2\zeta_{21} \\ -\gamma_2\psi_2+\theta_2\zeta_{22} \end{pmatrix}.$$

The Jacobian matrices of F and V are now obtained as

$$DF(X) := \begin{pmatrix} \mathscr{R}_0^r\gamma_1\phi_1 & \mathscr{R}_0^c\gamma_2\alpha_1\phi_1 & \mathscr{R}_0^r\gamma_1\psi_1+\mathscr{R}_0^c\gamma_2\alpha_1\psi_2 & 0 & 0\,0\,0 \\ \mathscr{R}_0^r\gamma_1\alpha_2\phi_2 & \mathscr{R}_0^c\gamma_2\phi_2 & 0 & \mathscr{R}_0^c\gamma_2\psi_2+\mathscr{R}_0^r\gamma_1\alpha_2\psi_1 & 0\,0\,0 \\ 0 & 0 & 0 & 0 & 0\,0\,0 \\ 0 & 0 & 0 & 0 & 0\,0\,0 \\ 0 & 0 & 0 & 0 & 0\,0\,0 \\ 0 & 0 & 0 & 0 & 0\,0\,0 \\ 0 & 0 & 0 & 0 & 0\,0\,0 \end{pmatrix};$$

$$DV(X) := \begin{pmatrix} \gamma_1 & 0 & 0 & 0 & 0 & 0 & 0 \\ 0 & \gamma_2 & 0 & 0 & 0 & 0 & 0 \\ \mathscr{R}_0^r\gamma_1\phi_1 & \mathscr{R}_0^c\gamma_2\alpha_1\phi_1 & \mathscr{R}_0^r\gamma_1\psi_1+\mathscr{R}_0^c\gamma_2\alpha_2\psi_2 & 0 & -\theta_1 & -\theta_2 & 0 \\ \mathscr{R}_0^r\gamma_1\alpha_2\phi_2 & \mathscr{R}_0^c\gamma_2\phi_2 & 0 & \mathscr{R}_0^c\gamma_2\psi_2+\mathscr{R}_0^r\gamma_1\alpha_2\psi_1 & 0 & 0 & -\theta_2 \\ -(1-p)\gamma_1 & 0 & 0 & 0 & \theta_1 & 0 & 0 \\ -p\gamma_1 & 0 & 0 & 0 & 0 & \theta_2 & 0 \\ 0 & -\gamma_2 & 0 & 0 & 0 & 0 & \theta_2 \end{pmatrix}.$$

For the disease-free equilibrium $X_0 = (0, 0, 1, 1, 0, 0, 0)^T$, we have

$$DF(X_0) := \begin{pmatrix} \mathscr{R}_0^r\gamma_1 & \mathscr{R}_0^c\gamma_2\alpha_1 & 0\,0\,0\,0\,0 \\ \mathscr{R}_0^r\gamma_1\alpha_2 & \mathscr{R}_0^c\gamma_2 & 0\,0\,0\,0\,0 \\ 0 & 0 & 0\,0\,0\,0\,0 \\ 0 & 0 & 0\,0\,0\,0\,0 \\ 0 & 0 & 0\,0\,0\,0\,0 \\ 0 & 0 & 0\,0\,0\,0\,0 \end{pmatrix}; \quad DV(X_0) := \begin{pmatrix} \gamma_1 & 0 & 0\,0 & 0 & 0 & 0 \\ 0 & \gamma_2 & 0\,0 & 0 & 0 & 0 \\ \mathscr{R}_0^r\gamma_1 & \mathscr{R}_0^c\gamma_2\alpha_1 & 0\,0 & -\theta_1 & -\theta_2 & 0 \\ \mathscr{R}_0^r\gamma_1\alpha_2 & \mathscr{R}_0^c\gamma_2 & 0\,0 & 0 & 0 & -\theta_2 \\ -(1-p)\gamma_1 & 0 & 0\,0 & \theta_1 & 0 & 0 \\ -p\gamma_1 & 0 & 0\,0 & 0 & \theta_2 & 0 \\ 0 & -\gamma_2 & 0\,0 & 0 & 0 & \theta_2 \end{pmatrix}.$$

By the upper left 2×2 block matrix for each of $DF(X_0)$ and $DV(X_0)$, we define

$$\mathcal{F} := \begin{pmatrix} \mathscr{R}_0^r\gamma_1 & \mathscr{R}_0^c\gamma_2\alpha_1 \\ \mathscr{R}_0^r\gamma_1\alpha_2 & \mathscr{R}_0^c\gamma_2 \end{pmatrix}; \quad \mathcal{V} := \begin{pmatrix} \gamma_1 & 0 \\ 0 & \gamma_2 \end{pmatrix}.$$

Then we can derive the next generation matrix

$$\mathcal{K} = \mathcal{F}\mathcal{V}^{-1} = \begin{pmatrix} \mathscr{R}_0^r & \mathscr{R}_0^c\alpha_1 \\ \mathscr{R}_0^r\alpha_2 & \mathscr{R}_0^c \end{pmatrix}.$$

Since the basic reproduction number $\mathscr{R}_0$ is given by the maximum absolute value of the eigenvalues of $\mathcal{K}$[18], we can get the basic reproduction number $\mathscr{R}_0$ given by (9).

APPENDIX 2.A.2: PROOF OF THEOREM 2.1

From (8), the Jacobian matrix at the disease-free equilibrium $E_0(1, 0, 0, 0, 1, 0, 0)$ becomes

$$J(1, 0, 0, 0, 1, 0, 0) := \begin{pmatrix} 0 & -\mathscr{R}_0^r\gamma_1 & \theta_1 & \theta_2 & 0 & -\mathscr{R}_0^c\gamma_2\alpha_1 & 0 \\ 0 & (\mathscr{R}_0^r-1)\gamma_1\alpha_2 & 0 & 0 & 0 & \mathscr{R}_0^c\gamma_2 & 0 \\ 0 & (1-p)\gamma_1 & -\theta_1 & 0 & 0 & 0 & 0 \\ 0 & p\gamma_1 & 0 & -\theta_2 & 0 & 0 & 0 \\ 0 & -\mathscr{R}_0^r\gamma_1\alpha_2 & 0 & 0 & 0 & -\mathscr{R}_0^c\gamma_2 & \theta_2 \\ 0 & \mathscr{R}_0^r\gamma_1\alpha_2 & 0 & 0 & 0 & (\mathscr{R}_0^c-1)\gamma_2 & 0 \\ 0 & 0 & 0 & 0 & 0 & \gamma_2 & -\theta_2 \end{pmatrix}.$$

The characteristic equation of this Jacobian matrix can be obtained as

$$\lambda^2(\lambda+\theta_2)^2(\lambda+\theta_1)\Big\{\big[\lambda-(\mathscr{R}_0^r-1)\gamma_1\big]\big[\lambda-(\mathscr{R}_0^c-1)\gamma_2\big]-\alpha_1\alpha_2\gamma_1\gamma_2\mathscr{R}_0^r\mathscr{R}_0^c\Big\}=0.$$

Then we find $-\theta_1$, and degenerated 0, $-\theta_2$ as the eigenvalues. Besides, we have a quadratic equation given by the last factor in the left side, which determines the other two eigenvalues λ_1 and λ_2. Since the discriminant of the quadratic equation is always positive, λ_1 and λ_2 are necessarily real. We can easily find that both λ_1 and λ_2 are non-positive if and only if

$$\begin{cases} (\mathscr{R}_0^r-1)\gamma_1<0; \\ (\mathscr{R}_0^c-1)\gamma_2<0; \\ (\mathscr{R}_0^r-1)(\mathscr{R}_0^c-1)\geq\alpha_1\alpha_2\mathscr{R}_0^r\mathscr{R}_0^c. \end{cases}$$

If one of the above three conditions is unsatisfied, λ_1 or λ_2 is positive. In such a case, the disease-free equilibrium is unstable. The result leads to Theorem 2.1.

APPENDIX 2.A.3: PROOF OF LEMMA 2.1

Consider the existence of an endemic equilibrium $E^*(\phi_1^*,\psi_1^*,\zeta_{11}^*,\zeta_{21}^*,\phi_2^*,\psi_2^*,\zeta_{22}^*)$ with $\psi_1^*>0$ or $\psi_2^*>0$. From (8), we can derive the following relations of ψ_1^* and ψ_2^*:

$$\begin{aligned}\frac{\theta_1\theta_2+(1-p)\gamma_1\theta_2+p\gamma_1\theta_1}{\theta_1\theta_2}\psi_1^*&=\frac{\mathscr{R}_0^c\gamma_2\alpha_1\psi_2^*+(\mathscr{R}_0^r-1)\gamma_1\psi_1^*}{\mathscr{R}_0^r\gamma_1\psi_1^*+\mathscr{R}_0^c\gamma_2\alpha_1\psi_2^*};\\ \frac{\theta_2+\gamma_2}{\theta_2}\psi_2^*&=\frac{\mathscr{R}_0^r\gamma_1\alpha_2\psi_1^*+(\mathscr{R}_0^c-1)\gamma_2\psi_2^*}{\mathscr{R}_0^c\gamma_2\psi_2^*+\mathscr{R}_0^r\gamma_1\alpha_2\psi_1^*},\end{aligned}$$

that is,

$$\begin{aligned}\psi_2^*&=-\frac{\mathscr{R}_0^r\gamma_1}{\mathscr{R}_0^c\gamma_2\alpha_1}\psi_1^*-\frac{\gamma_1\psi_1^*}{\mathscr{R}_0^c\gamma_2\alpha_1(A\psi_1^*-1)}=f(\psi_1^*);\\ \psi_1^*&=-\frac{\mathscr{R}_0^c\gamma_2}{\mathscr{R}_0^r\gamma_1\alpha_2}\psi_2^*-\frac{\gamma_2\psi_2^*}{\mathscr{R}_0^r\gamma_1\alpha_2(B\psi_2^*-1)}=g(\psi_2^*),\end{aligned}$$

where $A:=\big[\theta_1\theta_2+(1-p)\gamma_1\theta_2+p\gamma_1\theta_1\big]/\big(\theta_1\theta_2\big)$ and $B:=\big(\theta_2+\gamma_2\big)/\theta_2$. The curve of $f(\psi_1)$ has asymptotes $\psi_1=1/A$ and

$$\psi_2=-\frac{\mathscr{R}_0^r\gamma_1}{\mathscr{R}_0^c\gamma_2\alpha_1}\psi_1-\frac{\gamma_1}{A\mathscr{R}_0^c\gamma_2\alpha_1}.$$

The curve of $g(\psi_2)$ has asymptotes $\psi_2=1/B$ and

$$\psi_1=-\frac{\mathscr{R}_0^c\gamma_2}{\mathscr{R}_0^r\gamma_1\alpha_2}\psi_2-\frac{\gamma_2}{B\mathscr{R}_0^r\gamma_1\alpha_2}.$$

We have

$$f'(\psi_1)=\frac{\gamma_1}{\mathscr{R}_0^c\gamma_2\alpha_1}\Big[\frac{1}{(A\psi_1-1)^2}-\mathscr{R}_0^r\Big]>0$$

if and only if

$$\frac{1}{A}\Big(1-\frac{\sqrt{\mathscr{R}_0^r}}{\mathscr{R}_0^r}\Big)<\psi_1<\frac{1}{A},\quad \frac{1}{A}<\psi_1<\frac{1}{A}\Big(1+\frac{\sqrt{\mathscr{R}_0^r}}{\mathscr{R}_0^r}\Big).$$

Further we have

$$f\bigg(\frac{1}{A}\Big(1-\frac{\sqrt{\mathscr{R}_0^r}}{\mathscr{R}_0^r}\Big)\bigg)=-\frac{\gamma_1\big(1-\sqrt{\mathscr{R}_0^r}\big)^2}{A\mathscr{R}_0^c\gamma_2\alpha_1}<0;$$
$$f\bigg(\frac{1}{A}\Big(1+\frac{\sqrt{\mathscr{R}_0^r}}{\mathscr{R}_0^r}\Big)\bigg)=-\frac{\gamma_1\big(1+\sqrt{\mathscr{R}_0^r}\big)^2}{A\mathscr{R}_0^c\gamma_2\alpha_1}<0.$$

When $\psi_1\to(1/A)_{-0}$, $f(\psi_1)\to+\infty$, and when $\psi_1\to(1/A)_{+0}$, $f(\psi_1)\to-\infty$. Similarly,

$$g'(\psi_2)=\frac{\gamma_2}{\mathscr{R}_0^r\gamma_1\alpha_2}\Big[\frac{1}{(B\psi_2-1)^2}-\mathscr{R}_0^c\Big]>0$$

if and only if

$$\frac{1}{B}\Big(1-\frac{\sqrt{\mathscr{R}_0^c}}{\mathscr{R}_0^c}\Big)<\psi_2<\frac{1}{B},\quad \frac{1}{B}<\psi_2<\frac{1}{B}\Big(1+\frac{\sqrt{\mathscr{R}_0^c}}{\mathscr{R}_0^c}\Big).$$

Further we have

$$g\bigg(\frac{1}{B}\Big(1-\frac{\sqrt{\mathscr{R}_0^c}}{\mathscr{R}_0^c}\Big)\bigg)=-\frac{\gamma_2\big(1-\sqrt{\mathscr{R}_0^c}\big)^2}{B\mathscr{R}_0^r\gamma_1\alpha_2}<0;$$
$$g\bigg(\frac{1}{B}\Big(1+\frac{\sqrt{\mathscr{R}_0^c}}{\mathscr{R}_0^c}\Big)\bigg)=-\frac{\gamma_2\big(1+\sqrt{\mathscr{R}_0^c}\big)^2}{B\mathscr{R}_0^r\gamma_1\alpha_2}<0.$$

When $\psi_2\to(1/B)_{-0}$, $g(\psi_2)\to+\infty$, and when $\psi_2\to(1/B)_{+0}$, $g(\psi_2)\to-\infty$. Since $1/A$ and $1/B$ are asymptotes of $f(\psi_1)$ and $g(\psi_2)$ respectively, and both are less than 1, if $\mathscr{R}_0^r>1$ or $\mathscr{R}_0^c>1$, two curves $f(\psi_1)$ and $g(\psi_2)$ must have an intersection in the $(\psi_1,\psi_2)=\big((0,1),(0,1)\big)$-plane. We can directly obtain the conclusion from the (ψ_1,ψ_2)-plane that the endemic equilibrium E^* exists. If $\mathscr{R}_0^r<1$ and $\mathscr{R}_0^c<1$, the endemic equilibrium exists if and only if

$$f'(\psi_1)\big|_{\psi_1=0}<\frac{1}{g'(\psi_2)|_{\psi_2=0}},$$

that is, $\big(1/\mathscr{R}_0^r-1\big)\big(1/\mathscr{R}_0^c-1\big)<\alpha_1\alpha_2$. Hence, the conditions for existence of endemic equilibrium E^* are shown in Lemma 2.1.

APPENDIX 2.A.4: PROOF OF THEOREM 2.2

Under the strong lockdown with $\alpha_1=\alpha_2=0$, we can analyze the dynamics for the peripheral area and central area separately. Supposing the endemic equilibrium of peripheral area $E_1^*(\phi_1^*,\psi_1^*,\zeta_{11}^*)$, the system of the epidemic dynamics for the peripheral area can be described from (8) as follows:

$$\begin{aligned}
\frac{d\phi_1}{dt}&=-\mathscr{R}_0^r\gamma_1(\psi_1-\psi_1^*)(\phi_1-\phi_1^*)-\mathscr{R}_0^r\gamma_1\psi_1^*(\phi_1-\phi_1^*)-\theta_2(\phi_1-\phi_1^*)\\
&\qquad-(\gamma_1+\theta_2)(\psi_1-\psi_1^*)+(\theta_1-\theta_2)(\zeta_{11}-\zeta_{11}^*);\\
\frac{d\psi_1}{dt}&=\mathscr{R}_0^r\gamma_1(\psi_1-\psi_1^*)(\phi_1-\phi_1^*)+\mathscr{R}_0^r\gamma_1\psi_1^*(\phi_1-\phi_1^*);\\
\frac{d\zeta_{11}}{dt}&=(1-p)\gamma_1(\psi_1-\psi_1^*)-\theta_1(\zeta_{11}-\zeta_{11}^*),
\end{aligned}\tag{12}$$

where $\phi_1^* = 1/\mathscr{R}_0^r$;

$\psi_1^* = \dfrac{\theta_1\theta_2}{\theta_1\theta_2 + (1-p)\theta_2\gamma_1 + p\theta_1\gamma_1}(1-\phi_1^*)$; $\zeta_{11}^* = \dfrac{(1-p)\theta_2\gamma_1}{\theta_1\theta_2 + (1-p)\theta_2\gamma_1 + p\theta_1\gamma_1}(1-\phi_1^*)$.

Let us define the set $\Omega_1 = \{(\phi_1, \psi_1, \zeta_{11}) \mid \phi_1 \geq 0, \psi_1 \geq 0, \zeta_{11} \geq 0, \phi_1 + \psi_1 + \zeta_{11} \leq 1\}$.
For the case of $\theta_1 > \theta_2$, we can find the following Lyapunov equation:

$$\begin{aligned} V(\phi_1,\psi_1,\zeta_{11}) = &\Big[(\phi_1-\phi_1^*) + (\psi_1-\psi_1^*) + \frac{\theta_1-\theta_2}{\theta_1+\theta_2}(\zeta_{11}-\zeta_{11}^*)\Big]^2 \\ &+ \frac{(\theta_1-\theta_2)\big[\theta_2(2-p)+\theta_1 p\big]}{(\theta_1+\theta_2)^2(1-p)}(\zeta_{11}-\zeta_{11}^*)^2 \\ &+ 2\frac{\big[\theta_2(2-p)+\theta_1 p\big]\gamma_1 + 2\theta_2(\theta_1+\theta_2)}{(\theta_1+\theta_2)\mathscr{R}_0^r\gamma_1}\Big[(\psi_1-\psi_1^*) - \psi_1^*\log\frac{\psi_1}{\psi_1^*}\Big], \end{aligned} \tag{13}$$

which is positive for any $(\phi_1, \psi_1, \zeta_{11}) \neq (\phi_1^*, \psi_1^*, \zeta_{11}^*)$ in Ω_1, and $V(\phi_1^*, \psi_1^*, \zeta_{11}^*) = 0$. Further,

$$\begin{aligned} \frac{dV(\phi_1,\psi_1,\zeta_{11})}{dt} = &-2\theta_2(\phi_1-\phi_1^*)^2 - 2\Big\{\Big[1-\frac{\theta_1-\theta_2}{\theta_1+\theta_2}(1-p)\Big]\gamma_1 + \theta_2\Big\}(\psi_1-\psi_1^*)^2 \\ &- 2\frac{(\theta_1-\theta_2)\big[\theta_1\theta_2 + \theta_1^2 p + \theta_2^2(1-p)\big]}{(\theta_1+\theta_2)^2(1-p)}(\zeta_{11}-\zeta_{11}^*)^2 \end{aligned}$$

becomes negative for any $(\phi_1, \psi_1, \zeta_{11}) \neq (\phi_1^*, \psi_1^*, \zeta_{11}^*)$ in Ω_1, and zero for $(\phi_1, \psi_1, \zeta_{11}) = (\phi_1^*, \psi_1^*, \zeta_{11}^*)$.
For the case of $\theta_1 = \theta_2$, we can find the following Lyapunov equation:

$$V(\phi_1,\psi_1,\zeta_{11}) = \big[(\phi_1-\phi_1^*) + (\psi_1-\psi_1^*)\big]^2 + \frac{2(2\theta_1+\gamma_1)}{\mathscr{R}_0^r\gamma_1}\Big[(\psi_1-\psi_1^*) - \psi_1^*\log\frac{\psi_1}{\psi_1^*}\Big]$$

which is positive for any $(\phi_1, \psi_1, \zeta_{11}) \neq (\phi_1^*, \psi_1^*, \zeta_{11}^*)$ in Ω_1, and $V(\phi_1^*, \psi_1^*, \zeta_{11}^*) = 0$. Further,

$$\frac{dV(\phi_1,\psi_1,\zeta_{11})}{dt} = -2\theta_1(\phi_1-\phi_1^*)^2 - 2(\gamma_1+\theta_1)(\psi_1-\psi_1^*)^2$$

becomes negative for any $(\phi_1, \psi_1, \zeta_{11}) \neq (\phi_1^*, \psi_1^*, \zeta_{11}^*)$ in Ω_1. When $\phi_1 \to \phi_1^*$ and $\psi_1 \to \psi_1^*$, obtain $\zeta_{11}' \to -\theta_1(\zeta_{11} - \zeta_{11}^*)$. Then, denote $\tilde{\zeta_{11}}' = -\theta_1(\tilde{\zeta_{11}} - \zeta_{11}^*)$, since $\zeta_{11}' - \tilde{\zeta_{11}}' \to 0$, obtain $|\zeta_{11} - \tilde{\zeta_{11}}| \to 0$, that is, $\zeta_{11} \to \tilde{\zeta_{11}}$. With $\tilde{\zeta_{11}} \to \zeta_{11}^*$, we get the result that $\zeta_{11} \to \zeta_{11}^*$ when $\phi_1 \to \phi_1^*$ and $\psi_1 \to \psi_1^*$. Hence $dV(\phi_1, \psi_1, \zeta_{11})/dt$ becomes zero for $(\phi_1, \psi_1, \zeta_{11}) = (\phi_1^*, \psi_1^*, \zeta_{11}^*)$.
For the case of $\theta_1 < \theta_2$, considering the reduced system

$$\begin{aligned} \frac{d\phi_1}{dt} &= -\mathscr{R}_0^r\gamma_1(\psi_1-\psi_1^*)(\phi_1-\phi_1^*) - \mathscr{R}_0^r\gamma_1\psi_1^*(\phi_1-\phi_1^*) - \theta_1(\phi_1-\phi_1^*) \\ &\quad - (\gamma_1+\theta_1)(\psi_1-\psi_1^*) + (\theta_2-\theta_1)(\zeta_{21}-\zeta_{21}^*); \\ \frac{d\psi_1}{dt} &= \mathscr{R}_0^r\gamma_1(\psi_1-\psi_1^*)(\phi_1-\phi_1^*) + \mathscr{R}_0^r\gamma_1\psi_1^*(\phi_1-\phi_1^*); \\ \frac{d\zeta_{21}}{dt} &= p\gamma_1(\psi_1-\psi_1^*) - \theta_2(\zeta_{21}-\zeta_{21}^*), \end{aligned} \tag{14}$$

where $\phi_1^* = 1/\mathscr{R}_0^r$, $\psi_1^* = \theta_2(1-\phi_1^*)/(\theta_2+p\gamma_1)$, $\zeta_{21}^* = p\gamma_1(1-\phi_1^*)/(\theta_2+p\gamma_1)$.

Let us define the set $\Omega_2 = \{(\phi_1, \psi_1, \zeta_{21}) \mid \phi_1 \geq 0, \psi_1 \geq 0, \zeta_{21} \geq 0, \phi_1 + \psi_1 + \zeta_{21} \leq 1\}$, we can find the following Lyapunov equation:

$$\begin{aligned} V(\phi_1, \psi_1, \zeta_{21}) = &\Big[(\phi_1 - \phi_1^*) + (\psi_1 - \psi_1^*) + \frac{\theta_2 - \theta_1}{\theta_1 + \theta_2}(\zeta_{21} - \zeta_{21}^*)\Big]^2 \\ &+ \frac{(\theta_2 - \theta_1)\big[\theta_2(1-p) + \theta_1(1+p)\big]}{(\theta_1 + \theta_2)^2 p}(\zeta_{21} - \zeta_{21}^*)^2 \\ &+ 2\frac{\big[\theta_2(1-p) + \theta_1(1+p)\big]\gamma_1 + 2\theta_1(\theta_1 + \theta_2)}{(\theta_1 + \theta_2)\mathscr{R}_0^r \gamma_1}\Big[(\psi_1 - \psi_1^*) - \psi_1^* \log\frac{\psi_1}{\psi_1^*}\Big] \end{aligned}$$

which is positive for any $(\phi_1, \psi_1, \zeta_{21}) \neq (\phi_1^*, \psi_1^*, \zeta_{21}^*)$ in Ω_2, and $V(\phi_1^*, \psi_1^*, \zeta_{21}^*) = 0$. Further,

$$\begin{aligned} \frac{dV(\phi_1, \psi_1, \zeta_{21})}{dt} = &-2\theta_1(\phi_1 - \phi_1^*)^2 - 2\Big\{\Big[1 - \frac{(\theta_2 - \theta_1)p}{\theta_1 + \theta_2}\Big]\gamma_1 + \theta_1\Big\}(\psi_1 - \psi_1^*)^2 \\ &- 2\frac{(\theta_2 - \theta_1)\big[\theta_1\theta_2 + \theta_1^2 p + \theta_2^2(1-p)\big]}{(\theta_1 + \theta_2)^2 p}(\zeta_{21} - \zeta_{21}^*)^2 \end{aligned}$$

becomes negative for any $(\phi_1, \psi_1, \zeta_{21}) \neq (\phi_1^*, \psi_1^*, \zeta_{21}^*)$ in Ω_2, and zero for $(\phi_1, \psi_1, \zeta_{21}) = (\phi_1^*, \psi_1^*, \zeta_{21}^*)$.
Then, supposing the endemic equilibrium of central area $E_2^*(\phi_2^*, \psi_2^*)$, the system of the epidemic dynamics for the central area can be described from (8) as follows:

$$\begin{aligned} \frac{d\phi_2}{dt} = &-\mathscr{R}_0^c \gamma_2(\psi_2 - \psi_2^*)(\phi_2 - \phi_2^*) - \mathscr{R}_0^c \gamma_2 \psi_2^*(\phi_2 - \phi_2^*) - \theta_2(\phi_2 - \phi_2^*) \\ &- (\gamma_2 + \theta_2)(\psi_2 - \psi_2^*); \\ \frac{d\psi_2}{dt} = &\mathscr{R}_0^c \gamma_2(\psi_2 - \psi_2^*)(\phi_2 - \phi_2^*) + \mathscr{R}_0^c \gamma_2 \psi_2^*(\phi_2 - \phi_2^*), \end{aligned} \tag{15}$$

where $\phi_2^* = 1/\mathscr{R}_0^c$, $\psi_2^* = \theta_2(1 - \phi_2^*)/(\gamma_2 + \theta_2)$. Let us define the set $\Omega_2' = \{(\phi_2, \psi_2) | \phi_2 \geq 0, \psi_2 \geq 0, \phi_2 + \psi_2 \leq 1\}$, we can find the following Lyapunov equation:

$$V(\phi_2, \psi_2) = \big[(\phi_2 - \phi_2^*) + (\psi_2 - \psi_2^*)\big]^2 + \frac{2(2\theta_2 + \gamma_2)}{\mathscr{R}_0^c \gamma_2}\Big[(\psi_2 - \psi_2^*) - \psi_2^* \log\frac{\psi_2}{\psi_2^*}\Big]$$

which is positive for any $(\phi_2, \psi_2) \neq (\phi_2^*, \psi_2^*)$ in Ω_2', and $V(\phi_2^*, \psi_2^*) = 0$. Further,

$$\frac{dV(\phi_2, \psi_2)}{dt} = -2\theta_2(\phi_2 - \phi_2^*)^2 - 2(\gamma_2 + \theta_2)(\psi_2 - \psi_2^*)^2$$

becomes negative for any $(\phi_2, \psi_2) \neq (\phi_2^*, \psi_2^*)$ in Ω_2', and zero for $(\phi_2, \psi_2) = (\phi_2^*, \psi_2^*)$. Thus, under the strong lockdown, the endemic equilibrium $E_s^*(\phi_1^*, \psi_1^*, \zeta_{11}^*, \zeta_{21}^*, \phi_2^*, \psi_2^*, \zeta_{22}^*)$ is globally asymptotically stable.

Then, consider the stability of endemic equilibrium under the complete lockdown, the case of $\alpha_1 = \alpha_2 = p = 0$. Supposing the endemic equilibrium of peripheral area $E_{11}^*(\phi_1^*, \psi_1^*)$, the system of the epidemic dynamics for the peripheral area can be described from (8) as follows:

$$\begin{aligned} \frac{d\phi_1}{dt} = &-\mathscr{R}_0^r \gamma_1(\psi_1 - \psi_1^*)(\phi_1 - \phi_1^*) - \mathscr{R}_0^r \gamma_1 \psi_1^*(\phi_1 - \phi_1^*) - \theta_1(\phi_1 - \phi_1^*) \\ &- (\gamma_1 + \theta_1)(\psi_1 - \psi_1^*); \\ \frac{d\psi_1}{dt} = &\mathscr{R}_0^r \gamma_1(\psi_1 - \psi_1^*)(\phi_1 - \phi_1^*) + \mathscr{R}_0^r \gamma_1 \psi_1^*(\phi_1 - \phi_1^*), \end{aligned}$$

where $\phi_1^* = 1/\mathscr{R}_0^r$, $\psi_1^* = \theta_1(1-\phi_1^*)/(\theta_1+\gamma_1)$. Define the set $\Omega_1' = \{(\phi_1,\psi_1)|\phi_1 \geq 0, \psi_1 \geq 0, \phi_1+\psi_1 \leq 1\}$, we can find the following Lyapunov equation:

$$V(\phi_1,\psi_1) = \left[(\phi_1-\phi_1^*)+(\psi_1-\psi_1^*)\right]^2 + \frac{2(2\theta_1+\gamma_1)}{\mathscr{R}_0^r\gamma_1}\left[(\psi_1-\psi_1^*) - \psi_1^*\log\frac{\psi_1}{\psi_1^*}\right]$$

which is positive for any $(\phi_1,\psi_1) \neq (\phi_1^*,\psi_1^*)$ in Ω_1', and $V(\phi_1^*,\psi_1^*) = 0$. Further,

$$\frac{dV(\phi_1,\psi_1)}{dt} = -2\theta_1(\phi_1-\phi_1^*)^2 - 2(\gamma_1+\theta_1)(\psi_1-\psi_1^*)^2$$

becomes negative for any $(\phi_1,\psi_1) \neq (\phi_1^*,\psi_1^*)$ in Ω_1', and zero for $(\phi_1,\psi_1) = (\phi_1^*,\psi_1^*)$.
Then, supposing the endemic equilibrium of central area $E_{22}^*(\phi_2^*,\psi_2^*)$, the system of the epidemic dynamics for the central area can be described from (8) as follows:

$$\begin{aligned}\frac{d\phi_2}{dt} &= -\mathscr{R}_0^c\gamma_2(\psi_2-\psi_2^*)(\phi_2-\phi_2^*) - \mathscr{R}_0^c\gamma_2\psi_2^*(\phi_2-\phi_2^*) - \theta_2(\phi_2-\phi_2^*)\\ &\quad -(\gamma_2+\theta_2)(\psi_2-\psi_2^*);\\ \frac{d\psi_2}{dt} &= \mathscr{R}_0^c\gamma_2(\psi_2-\psi_2^*)(\phi_2-\phi_2^*) + \mathscr{R}_0^c\gamma_2\psi_2^*(\phi_2-\phi_2^*),\end{aligned}$$

where $\phi_2^* = 1/\mathscr{R}_0^c$, $\psi_2^* = \theta_2(1-\phi_2^*)/(\gamma_2+\theta_2)$. Let us define the set $\Omega_{22}' = \{(\phi_2,\psi_2)|\phi_2 \geq 0, \psi_2 \geq 0, \phi_2+\psi_2 \leq 1\}$, we can find the following Lyapunov equation:

$$V(\phi_2,\psi_2) = \left[(\phi_2-\phi_2^*)+(\psi_2-\psi_2^*)\right]^2 + \frac{2(2\theta_2+\gamma_2)}{\mathscr{R}_0^c\gamma_2}\left[(\psi_2-\psi_2^*) - \psi_2^*\log\frac{\psi_2}{\psi_2^*}\right]$$

which is positive for any $(\phi_2,\psi_2) \neq (\phi_2^*,\psi_2^*)$ in Ω_{22}', and $V(\phi_2^*,\psi_2^*) = 0$. Further,

$$\frac{dV(\phi_2,\psi_2)}{dt} = -2\theta_2(\phi_2-\phi_2^*)^2 - 2(\gamma_2+\theta_2)(\psi_2-\psi_2^*)^2$$

becomes negative for any $(\phi_2,\psi_2) \neq (\phi_2^*,\psi_2^*)$ in Ω_{22}', and zero for $(\phi_2,\psi_2) = (\phi_2^*,\psi_2^*)$. Thus, under the complete lockdown, endemic equilibrium E_c^* is globally asymptotically stable.

3

ISOLATION CAPACITY

3.1 INTRODUCTION

To reduce the risk of the spread of an infectious disease in the community, the strategies of quarantine, isolation, vaccination, and treatment are essential[28,54,85,170]. These strategies have been crucial in managing diverse infectious diseases such as severe acute respiratory syndrome (SARS), plague, smallpox, cholera, yellow fever, influenza, and SARS-CoV-2. As summarized by Martcheva[110], the implementation of such control strategies has historically proven effective in mitigating disease spread. In particular, the COVID-19 pandemic underscored the significance of non-pharmaceutical interventions. There have been different policies for the public health from place to place[114,132,160]. Given the importance of isolation and quarantine in the contribution to suppress the spread of diseases, there are a lot of works have been done with mathematical models (for example, Brauer and Castillo-Chavez[18], Chowell *et al.*[33], Feng and Thieme[59] and references therein). However, many countries experienced severe shortages in medical resources during the COVID-19 outbreak[58,87,113,131,137,143,160]. This situation has prompted growing attention in understanding how medical capacity constraints influence epidemic consequence. In recent times, some works using mathematical models considered how the limited medical resources could affect the transmission and management of an infectious disease(for example, Abdelrazec *et al.*[1], Kumar *et al.*[95], Mu *et al.*[119], Qin *et al.*[135], Saha and Samanta[141], Sepulaveda-Salcedo *et al.*[145], Wang *et al.*[163], Wei *et al.*[167], Zhao *et al.*[177] and references therein).

Quarantine/ isolation may be either perfect or imperfect, depending on the nature of the epidemic and the policies adopted by the community. Erdem *et al.*[57] considered imperfect quarantine and found a periodic solution or damped oscillation that indicates recurring outbreaks, depending on the quarantine effectiveness. Since isolation requires a certain space with controlled conditions to keep the infected individuals away from the other community members. If this capacity is too small, the isolation strategy may break down at a finite time on the way of epidemic process. Amador and Gómez-Corral[9] proposed a stochastic SIQS model with two quarantine states in which the quarantine has a limited capacity. Their numerical calculation showed a case where the quarantine compartment may become saturated before the epidemic ends. However, they did not clarify the conditions for this breakdown, as their focus was on the mathematical properties of the model.

In this chapter, we construct and analyze mathematical models to consider the relation of the isolation capacity to the epidemic consequence. In Section 3.2, we consider an SIRI+Q model with the discharge of isolated individuals after the recovery, that is, an epidemic dynamics for a period longer than that for the model in Section 3.4, in which the epidemic dynamics is assumed only for a sufficiently short season, and thus without the discharge from isolation. Since a discharge of recovered individuals from the isolation could serve a supply of potential hosts for the disease spread because of its reinfectivity, the discharge from the isolation must be one of the important factors to

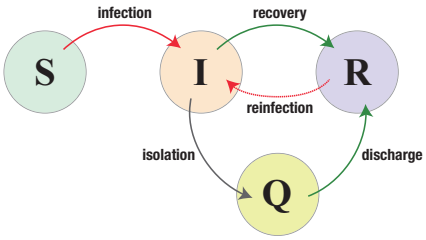

Figure 5: Generic schema of the state transition in the considered epidemic dynamics with the susceptible, infective, isolated (quarantined), and recovered classes: S, I, Q, and R.

determine the effectivity of quarantine/isolation measure for the public health. It is worth considering the model with such a discharge of recovered individuals from the isolation which has a limited capacity. In section 3.3, we introduce a work given by Ahmad and Seno[4], they considered an SIR+Q model with a system of ordinary differential equations, introducing a limited capacity of isolation. In Section 3.4, we focus on the relation of such a limited capacity of isolation to the endemicity and the final epidemic/endemic size for a simplest SIRI+Q model on the epidemic dynamics of a reinfectious disease, expanding the modeling by Ahmad and Seno[4]. The reinfectivity of disease means that the immunity gained by either vaccination or recovery is imperfect, so that the recovered individuals could have a risk of infection again. Actually there are not a few transmissible diseases with a reinfectivity, including chronic lung diseases[174], Ebola virus disease[3,106], hand, foot and mouth disease[176], influenza[38,53,72,134,165], while the reinfectivity has been still requiring further scientific researches to understand its kinetics and other nature. In Section 3.5, we conduct mathematical analysis for the full model given by Section 3.2 and then discuss the epidemic consequences.

3.2 MODELING

3.2.1 *Assumptions*

We consider a modeling on the epidemic dynamics of a reinfectious disease during an epidemic season, which consists of susceptible, infective, isolated, and recovered individuals. We assume the followings for our modeling:

- The demographic change due to the natural birth, death, and migration is negligible.
- The fatality of disease is negligible.
- The infection occurs by the contact of susceptible individual to not only organic but also potentially inorganic subjects contaminated with the pathogen to cause the disease. This assumption indicates that the considered epidemic dynamics would be of a disease, for example, transmitted with aerosols or droplets emitted from the infective individuals. The transmission may not necessarily require person-to-person contacts.
- Even after the recovery from the disease, the individual may get the infection again, that is, the disease is reinfectious.
- The isolation has a capacity beyond which the isolation is impossible. However, even under a situation that the isolation has reached the

capacity, the isolation may be available as the recruitment of isolation-requiring infectives for the vacancy of isolation generated by the discharge of some isolated individuals with their recovery. As long as the recruitment fills the vacancy of isolation by the discharge, the isolation remains deficient, that is, malfunctioning with its saturation. Only after the discharge comes to overcompensate the recruitment, the isolation works below the capacity and with some available vacancy.

- As long as the isolation functions well to work below the capacity, its accessibility is constant independently of how many infectives are isolated.

The "isolation capacity" means here the operational limit of a public health measure to control and make the infectives be away from any occasion to cause the secondary infection. Such an isolation measure requires not only the facilities for the quarantine/isolation but also the workers to serve the operation. Those requirements determine the isolation capacity.

Moreover, since the recovery generates an immunity against the disease, the assumption of possible reinfection means here that the immunity is imperfect or partial against the disease as already mentioned in the introduction section, for example, due to the multiplicity of pathogen types (e.g., mutated variants)[70,165]. As long as we consider a specific pathogen, there may be a immune response as the cross-immunity for the invasion of such similar pathogens by the antigen generated for a specific type of pathogen. The cross-immunity may suppress the reinfection or the effective symptom to reproduce and discharge the pathogen out of the host to cause the disease transmission, while the immunity obtained by the recovery from the disease works only to reduce the risk of reinfection and there is a risk for the recovered individual to get the infection again. For the reasonable modeling, we assume that the reinfection after the recovery from the disease generally has a likelihood not beyond that of the infection for the susceptible.

Since we assume that the reinfection follows the imperfectness of immunity obtained by the recovery from the disease, we will not introduce any specific period or time scale to get reinfected after getting the immunity in our model. Thus the state transition in terms of the disease follows the susceptible–infective–recovered/immunized–infective (SIRI) structure in our modeling, as used for example in Buonomo[26], Georgescu and Zhang[65], Ghosh *et al.*[66], Gomes *et al.*[67,68], Guo *et al.*[69], Gökaydin *et al.*[70], Martins *et al.*[111], Pagliara *et al.*[130], Pinto *et al.*[133], Song *et al.*[151], Srivastava *et al.*[153], Stollenwerk *et al.*[155], Wang[166].

3.2.2 *Infection and reinfection forces*

From the assumption given in the previous subsection, the reinfection force is introduced here not beyond the infection force λ for the susceptible. For the simplest introduction of such a reinfection force, we assume now it as $\varepsilon\lambda$ with a constant $\varepsilon \in [0, 1]$. For the extremal case of $\varepsilon = 1$, the recovery does not work at all to reduce the reinfection risk. For $\varepsilon = 0$, the recovery gives the perfect immunity so that there is no likelihood of reinfection. The parameter ε means the index for the likelihood of reinfection after the recovery.

We introduce the infection force λ for the susceptible as following

$$\lambda = \lambda(I, Q) := \beta \frac{I}{N - Q}, \tag{16}$$

where I and Q are respectively the infective and isolated population sizes (densities), N total population size in the community, and β the infection coefficient. This formula of the infection force is lead from the following idea with the assumption on the transmission route through the subjects contaminated with the pathogen. For the continuous time model, the infection force is generally defined by the probability of infection per susceptible individual in a sufficiently short time interval Δt, which is mathematically given as $\lambda \Delta t + o(\Delta t)$.

We ignore any change/shift in the custom and style of daily life in the community under the epidemic dynamics. This indicates an assumption that the free (non-isolated) individual has a daily life independent of the situation of epidemic dynamics. Then the free individual is assumed to have a probability to contact to the subjects which may be contaminated with the pathogen, given by $c\Delta t + o(\Delta t)$ with a positive constant c in a sufficiently short time interval Δt. The frequency of such contacts to the subjects depends only on the custom and style of daily life, and it is now assumed to be represented by a constant c. The probability of the contact to contagious subjects is assumed to be proportional to the ratio of infective population density I to the free population density $N - Q$, that is given by $I/(N - Q)$. In other words, with the mean-field approximation, the probability that a subject is contaminated by the pathogen is assumed to be proportional to $I/(N - Q)$. The infection by such a contagious contact follows a probability characterizing the infectivity of the pathogen too. The product of these three factors results in the infection probability per susceptible individual in a sufficiently short time interval Δt, given as $\lambda(I, Q)\Delta t + o(\Delta t)$ by the above formula (16) with the infection coefficient β representing the constant parameters determined by those three factors.

3.2.3 *Isolation well-functioning phase*

In our modeling for the epidemic dynamics with a limited capacity of isolation, we need to take account of the epidemic phase determined by the accessibility of isolation: isolation well-functioning phase and isolation malfunctioning phase. In this subsection, we introduce the isolation well-functioning phase, and isolation malfunctioning phase will be discussed in the next subsection.

The isolation well-functioning phase refers to the stage of epidemic dynamics in which the isolated population size Q is less than a given isolation capacity $Q_{\max}$. During this phase, the quarantine/isolation works with a net rate given by σI with the infective population size I and the per capita quarantine rate σ. In our modeling for this phase, the epidemic dynamics is governed by

$$\begin{aligned}
\frac{dS}{dt} &= -\beta \frac{I}{N-Q} S; \\
\frac{dI}{dt} &= \beta \frac{I}{N-Q} S + \varepsilon\beta \frac{I}{N-Q} R - \rho I - \sigma I; \\
\frac{dQ}{dt} &= \sigma I - \alpha Q; \\
\frac{dR}{dt} &= \rho I + \alpha Q - \varepsilon\beta \frac{I}{N-Q} R.
\end{aligned} \tag{17}$$

Variables S and R are the susceptible and recovered population sizes (densities) respectively. The total population size is given by a constant $N =$

$S + I + Q + R$. Parameter ρ and α are the recovery rate for the non-isolated infective individual and the discharge rate for the isolated individual after the recovery respectively.

As introduced in the Subsection 3.2.2, the infection force for the susceptible is given by $\beta I/(N-Q)$ with a positive positive parameter β. The reinfection force for the recovered individual is given by $\varepsilon\beta I/(N-Q)$ with a constant $\varepsilon \in [0,1]$.

3.2.4 *Isolation malfunctioning phase*

The isolation malfunctioning phase refers to the stage of epidemic dynamics in which the isolated population size Q has reached the capacity $Q_{\max} < N$. However, as mentioned in Subsection 3.2.1, the isolation keeps working even in such a situation since there are always some individuals discharged from the isolation, and then the isolation becomes capable only for the vacancy generated by the discharge.

Let us suppose that the system reaches the isolation malfunctioning phase first at $t = t^\star$. Then we can regard $t = t^\star$ as the moment that the epidemic dynamics transfers from the isolation well-functioning phase to the isolation malfunctioning phase. At the isolation malfunctioning phase, the following system governs the epidemic dynamics:

$$\begin{aligned}
\frac{dS}{dt} &= -\beta\frac{I}{N-Q_{\max}}S;\\
\frac{dI}{dt} &= \beta\frac{I}{N-Q_{\max}}S + \varepsilon\beta\frac{I}{N-Q_{\max}}R - \rho I - \min\left[\sigma I,\, \alpha Q_{\max}\right];\\
\frac{dQ}{dt} &= \min\left[\sigma I,\, \alpha Q_{\max}\right] - \alpha Q_{\max};\\
\frac{dR}{dt} &= \rho I + \alpha Q_{\max} - \varepsilon\beta\frac{I}{N-Q_{\max}}R.
\end{aligned} \tag{18}$$

The isolation is available only for the vacancy generated by the discharge of some isolated individuals. At the isolation malfunctioning phase, the net discharge rate is given by $\alpha Q_{\max}$, since the isolated population size is then $Q = Q_{\max}$. Thus, when the isolation remains malfunctioning at the capacity, the number of individuals discharged from the isolation in $[t, t+\Delta t)$ is given by $\alpha Q_{\max}\Delta t$. Since the epidemic dynamics proceeds even at the isolation malfunctioning phase, only the vacancy is available for the isolation of the infectives in $[t, t+\Delta t)$. As given by (17) at the isolation well-functioning phase, the number of detected infectives in $[t, t+\Delta t)$ is given by $\sigma I\Delta t + o(\Delta t)$. However, if the newly detected and isolation-requiring infectives $\sigma I\Delta t + o(\Delta t)$ is beyond the discharge of isolated individuals $\alpha Q_{\max}\Delta t$, that is, if $\sigma I > \alpha Q_{\max}$, then the newly isolated infectives in $[t, t+\Delta t)$ must be equal to the vacancy by the discharge of isolated individuals $\alpha Q_{\max}\Delta t$, because the isolation is not available beyond its capacity. Thus, we mathematically assumed that the isolated population size keeps being the limit $Q_{\max}$ at the isolation malfunctioning phase where $\sigma I > \alpha Q_{\max}$: $dQ/dt = \min\left[\sigma I,\, \alpha Q_{\max}\right] - \alpha Q_{\max} = \alpha Q_{\max} - \alpha Q_{\max} = 0$.

The epidemic dynamics could return to the isolation well-functioning phase from the isolation malfunctioning phase if the isolated population size becomes smaller than the capacity $Q_{\max}$ by the discharge of isolated individuals that overcompensates the recruitment of newly isolation-requiring infectives. Such a transition from the isolation malfunctioning phase to the isolation well-functioning phase occurs if the epidemic dynamics at the isola-

tion malfunctioning phase leads to $\sigma I < \alpha Q_{\max}$. Remark that the situation with $\sigma I = \alpha Q_{\max}$ is regarded here as being at the isolation malfunctioning phase, because it is a situation that the isolation operation is tight even though the isolation can available for all recruitment of newly isolation-requiring infectives.

3.2.5 *SIRI+Q model*

From the arguments for our modeling of epidemic phases in the previous subsection, we shall consider the following mathematical model of epidemic dynamics:

$$\begin{aligned}
\frac{dS}{dt} &= -\beta \frac{I}{N-Q} S; \\
\frac{dI}{dt} &= \beta \frac{I}{N-Q} S + \varepsilon\beta \frac{I}{N-Q} R - \rho I - \Phi(Q, I); \\
\frac{dQ}{dt} &= \Phi(Q, I) - \alpha Q; \\
\frac{dR}{dt} &= \rho I + \alpha Q - \varepsilon\beta \frac{I}{N-Q} R
\end{aligned} \tag{19}$$

with

$$\Phi(Q, I) := \begin{cases} \sigma I & \text{for } Q < Q_{\max}; \\ \min\left[\sigma I,\, \alpha Q_{\max}\right] & \text{for } Q = Q_{\max} \end{cases}$$

and the initial condition $(S(0), I(0), Q(0), R(0)) = (S_0, I_0, 0, 0)$ where $I_0 > 0$ and $S_0 = N - I_0 > 0$. The term $\Phi(Q, I)$ gives the net isolation rate which depends on the accessibility of isolation.

Our model (19) can be regarded as a piecewise smooth system (PSS), especially what is sometimes called Filippov system or switching system [11,15,45,46,60,97].

As a preliminary nature of the system (19) for our model, we have the following boundedness of the solution (Appendix 3.A.1):

Lemma 3.1. *For the initial condition* $(S(0), I(0), Q(0), R(0)) = (S_0, I_0, 0, 0)$ *with* $I_0 > 0$ *and* $S_0 = N - I_0 > 0$, *the solution of* (19) *belongs to the set* $\Omega_N := \{(S, I, Q, R) \in \mathbb{R}^4_+ \mid S + I + Q + R = N\}$ *for* $t > 0$.

From the definitions of isolation well-functioning and malfunctioning phases described in Subsection 3.2.3 and 3.2.4, the solution of the system (19) belonging to $\Omega_N^{\mathrm{w}} := \{(S, I, Q, R) \in \Omega_N \mid Q < Q_{\max}\}$ at the isolation well-functioning phase, while it belongs to $\Omega_N^{\mathrm{m}} := \{(S, I, Q_{\max}, R) \in \Omega_N \mid \sigma I \geq \alpha Q_{\max}\}$ at the isolation malfunctioning phase.

By the transformation of variables and parameters,

$$\begin{aligned}
&\tau := (\rho + \sigma)t; \quad u := \frac{S}{N}; \quad v := \frac{I}{N}; \quad q := \frac{Q}{N}; \quad w := \frac{R}{N}; \\
&\mathscr{R}_0 := \frac{\beta}{\rho + \sigma}; \quad a := \frac{\alpha}{\rho + \sigma}; \quad \gamma := \frac{\sigma}{\rho + \sigma}; \quad q_{\max} := \frac{Q_{\max}}{N},
\end{aligned}$$

with the basic reproduction number $\mathscr{R}_0 := \beta/(\rho+\sigma)$ for the model (19), we can derive the following non-dimensionalized system mathematically equivalent to the system (19):

$$\begin{aligned}
\frac{du}{d\tau} &= -\mathscr{R}_0 \frac{v}{1-q} u; \\
\frac{dv}{d\tau} &= \mathscr{R}_0 \frac{v}{1-q} u + \varepsilon \mathscr{R}_0 \frac{v}{1-q} w - (1-\gamma) v - \phi(q, v); \\
\frac{dq}{d\tau} &= \phi(q, v) - aq; \\
\frac{dw}{d\tau} &= (1-\gamma) v + aq - \varepsilon \mathscr{R}_0 \frac{v}{1-q} w
\end{aligned} \tag{20}$$

with

$$\phi(q, v) := \begin{cases} \gamma v & \text{for } q < q_{\max}; \\ \min\left[\gamma v,\, a q_{\max}\right] & \text{for } q = q_{\max}, \end{cases}$$

and the initial condition $(u(0), v(0), q(0), w(0)) = (u_0, v_0, 0, 0)$ where $v_0 = 1 - u_0 > 0$.

From Lemma 3.1, the solution of (20) belongs to the set $\Omega_1 := \{(u, v, q, w) \in \mathbb{R}^4_+ \mid u + v + q + w = 1\}$ for $\tau > 0$. Further the solution of the system (20) belonging to $\Omega_1^{\mathrm{w}} := \{(u, v, q, w) \in \Omega_1 \mid q < q_{\max}\}$ at the isolation well-functioning phase, while it belongs to $\Omega_1^{\mathrm{m}} := \{(u, v, q_{\max}, w) \in \Omega_1 \mid \gamma v \geq a q_{\max}\}$ at the isolation malfunctioning phase. Remark that variables u, v, q, w, and parameters γ, $q_{\max}$ are less than 1.

Model with no isolation

First we consider an extreme case of the system (20) with $\gamma = 0$, that is, the model (19) with $\sigma = 0$ when the isolation is always unavailable as a measure for the public health. Then we have $Q(t) \equiv 0$ for any $t \geq 0$ for the model (19), that is, $q(\tau) \equiv 0$ for any $\tau \geq 0$ for the system (20):

$$\begin{aligned}
\frac{du}{d\tau} &= -\mathscr{R}_{00} v u; \\
\frac{dv}{d\tau} &= \mathscr{R}_{00} v u + \varepsilon \mathscr{R}_{00} v w - v; \\
\frac{dw}{d\tau} &= v - \varepsilon \mathscr{R}_{00} v w,
\end{aligned} \tag{21}$$

where $\tau = \rho t$, and $\mathscr{R}_0 = \mathscr{R}_{00} := \beta/\rho$ is the basic reproduction number according to (21).

For the system (21), we find the following dynamical nature (Appendix 3.A.2):

Lemma 3.2. *If and only if $\varepsilon \mathscr{R}_{00} \leq 1$, the system (21) approaches a disease-eliminated equilibrium $(u, v, w) = (u^*, 0, w^*)$ with $u^* \in [0, 1)$ and $w^* = 1 - u^* \in (0, 1]$ as $\tau \to \infty$. Otherwise with $\varepsilon \mathscr{R}_{00} > 1$, it approaches the endemic equilibrium*

$$(u, v, w) = \left(0, 1 - \frac{1}{\varepsilon \mathscr{R}_{00}}, \frac{1}{\varepsilon \mathscr{R}_{00}}\right) \tag{22}$$

as $\tau \to \infty$.

Lemma 3.2 mathematically indicates that the endemic equilibrium (22) is globally asymptotically stable for the system (21) when and only when $\varepsilon\mathscr{R}_{00} > 1$. Otherwise, the epidemic dynamics converges to a disease-eliminated equilibrium which is then globally asymptotically stable. The equilibrium value of w^* represents the final epidemic size at the disease-eliminated equilibrium, which depends on the initial condition given by u_0 or v_0 $(= 1 - u_0)$ as indicated in Appendix 3.A.2. The final epidemic size w^* means the proportion of individuals who experienced the disease in the community after the disease has become eliminated.

Model with unlimited isolation

We analyze here the system (20) with $q_{\max} \geq 1$, that is, the system (19) with $Q_{\max} \geq N$. This corresponds to the case where the isolation does not have any capacity to limit the accessibility, and therefore $\phi(q, v) = \gamma v$ for any q in (20). In other words, the epidemic dynamics always stays at the isolation well-functioning phase, and is governed by (17). The system considered here becomes

$$\begin{aligned}
\frac{du}{d\tau} &= -\mathscr{R}_0 \frac{v}{1-q} u; \\
\frac{dv}{d\tau} &= \mathscr{R}_0 \frac{v}{1-q} u + \varepsilon\mathscr{R}_0 \frac{v}{1-q} w - v; \\
\frac{dq}{d\tau} &= \gamma v - aq; \\
\frac{dw}{d\tau} &= (1-\gamma)v + aq - \varepsilon\mathscr{R}_0 \frac{v}{1-q} w,
\end{aligned} \tag{23}$$

corresponding to (17) with the variable and parameter transformation for the non-dimensionalization given in Section 3.2.5.

We can find the following result on the condition that the system (23) approaches a disease-eliminated equilibrium (Appendix 3.A.3):

Theorem 3.1. *If and only if $\varepsilon\mathscr{R}_0 \leq 1$, the system (23) approaches a disease-eliminated equilibrium as $\tau \to \infty$. Otherwise with $\varepsilon\mathscr{R}_0 > 1$, it approaches the endemic equilibrium*

$$(u, v, q, w) = E^*_{\mathrm{w}}\Big(0,\ \frac{a}{\gamma} q^*_{\mathrm{w}},\ q^*_{\mathrm{w}},\ \frac{1}{\varepsilon\mathscr{R}_0}(1 - q^*_{\mathrm{w}})\Big), \tag{24}$$

where

$$q^*_{\mathrm{w}} = \frac{1}{1 + B^*_{\mathrm{w}}} \tag{25}$$

with

$$B^*_{\mathrm{w}} := \frac{a}{\gamma}\Big(1 - \frac{1}{\varepsilon\mathscr{R}_0}\Big)^{-1}. \tag{26}$$

This theorem indicates that the endemic equilibrium E^*_{w} for the system (23) with $\varepsilon\mathscr{R}_0 > 1$ is globally asymptotically stable, as shown by Lemma 3.16 in Appendix 3.A.3.

Since the susceptible subpopulation size is zero at the endemic equilibrium state E^*_{w}, it is sustained by the infective recruitment with the reinfection of recovered individuals. In other words, the endemicity of disease in the

community is established with a sufficiently high likelihood of reinfection, which is now expressed as $\varepsilon\mathscr{R}_0 > 1$. Such the endemic equilibrium can exist only with the discharge of isolated individual, that is, with $a > 0$. No endemic equilibrium exists under unlimited isolation capacity if no discharge occurs, as will be shown in Section 3.4.

According to the mathematical consistency of the results in Theorem 3.1 and Lemma 3.2 of Subsection 3.2.5, we can find the following result:

Corollary 3.1.1. *As $\gamma \to +0$ with $\varepsilon\mathscr{R}_0 > 1$, the endemic equilibrium E^*_{w} given by (24) converges to the endemic equilibrium (22) for the system (20) with $\gamma = 0$, that is, for the model (19) with $\sigma = 0$ when the isolation is not taken as a measure for the public health.*

It can be easily shown that $B^*_{\mathrm{w}} \to \infty$ as $\gamma \to +0$, so that $q^*_{\mathrm{w}} \to 0$ as $\gamma \to +0$ by (25), and then $v^*_{\mathrm{w}} = (a/\gamma)q^*_{\mathrm{w}} \to 1 - 1/(\varepsilon\mathscr{R}_{00})$ as $\gamma \to +0$.

3.3 FOR NON-REINFECTIOUS DISEASE

3.3.1 *Assumptions and model*

We present a framework by Ahmad and Seno[4], which considered an SIR+Q model with a system of ordinary differential equations and incorporated a limited capacity of isolation. They assumed the epidemic dynamics only for a sufficiently short season, and thus without the discharge from isolation. The model is developed under the following assumptions:

- The total population size of the community is constant, ignoring any demographic change with birth, death, and migration in a given epidemic season.
- The fatality of disease is negligible in the season.
- Isolated individuals cannot contact any other in the community.
- Any isolated individual is not discharged in the season.
- The isolation capacity is limited. When the isolation reaches the capacity, it breaks down and becomes incapable.

Based on the above assumptions, the epidemic dynamics may contain two phases: isolation well-functioning phase and isolation incapable phase. The definition of isolation well-functioning phase here is the same as in Subsection 3.2.3, indicating that the isolated population size Q is less than a given isolation capacity $Q_{\max}$. In contrast to the isolation malfunctioning phase introduced in Subsection 3.2.4, isolation incapable phase refers to the situation where the isolated population size Q has reached the capacity $Q_{\max} < N$, and there is no discharge from isolation. The isolation is available at the isolation well-functioning phase, while it is ceased at the isolation incapable phase since it has reached the capacity.

Since the model does not consider reinfectious diseases or the discharge mechanism from isolation, which corresponds to the case of $\varepsilon = 0$ and $\alpha = 0$ for system (19) described in Section 3.2. The epidemic dynamics model is given by:

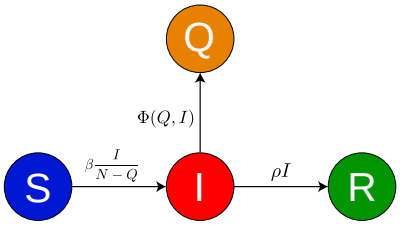

Figure 6: Scheme for the epidemic dynamics model (27).

$$\begin{aligned}
\frac{dS}{dt} &= -\beta\frac{I}{N-Q}S;\\
\frac{dI}{dt} &= \beta\frac{I}{N-Q}S - \rho I - \Phi(Q,I);\\
\frac{dQ}{dt} &= \Phi(Q,I);\\
\frac{dR}{dt} &= \rho I
\end{aligned} \tag{27}$$

with

$$\Phi(Q,I) := \begin{cases} \sigma I & \text{for } Q < Q_{\max};\\ 0 & \text{for } Q = Q_{\max} \end{cases}$$

and the initial condition $(S(0), I(0), Q(0), R(0)) = (S_0, I_0, 0, 0)$. The variables S, I, Q, and R denote the sizes of susceptible, infective, isolated, and recovered subpopulations respectively. The total population size of the community is denoted by a positive constant N, and it is satisfied that $S(t) + I(t) + Q(t) + R(t) = N$ for any $t \geq 0$. Hence it holds that $S_0 + I_0 = N$. The individual state transition according to the epidemic dynamics is schematically shown in Figure 6. Every parameter is positive. The parameter ρ denotes the recovery rate of infective individual. The infection force for the susceptible is given by $\beta I/(N-Q)$ with a positive positive parameter β.

The piece-wise function $\Phi(Q,I)$ denotes the isolation rate of infected individual. Parameter σ is the isolation rate at the isolation well-functioning phase, which represents the efficiency of quarantine operation to detect and isolate an infective. The parameter $Q_{\max}$ denotes the capacity of isolation, which is assumed to satisfy $Q_{\max} < N$. As long as the isolated subpopulation size Q is less than the capacity $Q_{\max}$, the isolation is available, and the epidemic dynamics is at the isolation well-functioning phase with $\Phi(Q,I) = \sigma$. Once Q reaches $Q_{\max}$, the isolation becomes ceased after it. Then the epidemic dynamics enters in the isolation incapable phase with $\Phi(Q,I) = 0$, as numerically exemplified by Figure 7(b). As the above assumption, the isolated subpopulation size Q remains $Q_{\max}$ at the isolation incapable phase since any isolated individual is not discharged from the isolation. In contrast, as numerically exemplified by Figure 7(a), for a sufficiently large capacity $Q_{\max}$, the epidemic dynamics always remains at the isolation well-functioning phase with $\Phi(Q,I) = \sigma$, since the isolation never reaches the capacity.

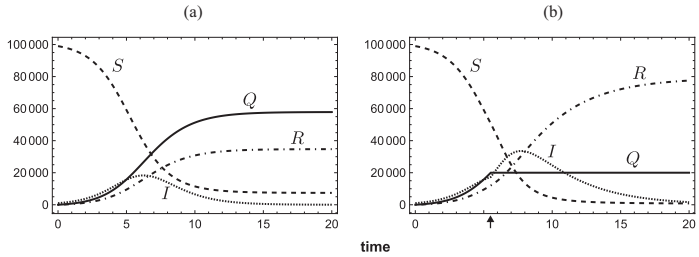

Figure 7: Numerical examples for the temporal variation of the SIR+Q model (27). (a) $Q_{\max} = 70000$; (b) $Q_{\max} = 20000$, $\beta = 1.5$; $\rho = 0.3$; $\sigma = 0.5$; $N = 100000$; $(S_0, I_0, Q_0, R_0) = (99000, 1000, 0, 0)$. In (a), the isolation never reaches the capacity, while it reaches the capacity at a moment indicated by an arrow in (b). At the moment, the epidemic dynamics switches from the isolation well-functioning phase to the isolation incapable phase.

By the transformation of variables and parameters,

$$\tau := (\rho + \sigma)t; \quad u := \frac{S}{N}; \quad v := \frac{I}{N}; \quad q := \frac{Q}{N}; \quad w := \frac{R}{N};$$
$$\mathscr{R}_0 := \frac{\beta}{\rho + \sigma}; \quad \gamma := \frac{\sigma}{\rho + \sigma}; \quad q_{\max} := \frac{Q_{\max}}{N},$$

with the basic reproduction number $\mathscr{R}_0 := \beta/(\rho + \sigma)$ for the model (27), we can derive the following non-dimensionalized system mathematically equivalent to the system (27):

$$\begin{aligned} \frac{du}{d\tau} &= -\mathscr{R}_0 \frac{v}{1-q} u; \\ \frac{dv}{d\tau} &= \mathscr{R}_0 \frac{v}{1-q} u - (1-\gamma)v - \phi(q, v); \\ \frac{dq}{d\tau} &= \phi(q, v); \\ \frac{dw}{d\tau} &= (1-\gamma)v \end{aligned} \tag{28}$$

with

$$\phi(q, v) := \begin{cases} \gamma v & \text{for } q < q_{\max}; \\ 0 & \text{for } q = q_{\max}, \end{cases}$$

and the initial condition $(u(0), v(0), q(0), w(0)) = (u_0, v_0, 0, 0)$ where $v_0 = 1 - u_0 > 0$. It is satisfied that $u(\tau) + v(\tau) + q(\tau) + w(\tau) = 1$ for any $\tau > 0$.

Aside from the isolated state with a limited capacity, the epidemic dynamics is fundamentally governed by the one-way state transition as an SIR model, so that necessarily $I(t) \to 0$ as $t \to \infty$, that is, $v(t) \to 0$ as $\tau \to \infty$ as well as the simple Kermack-McKendrick SIR model[18,19,110].

3.3.2 *Conserved quantities*

We can find the conserved quantity for the epidemic dynamics at the isolation well-functioning and incapable phases, respectively (Appendix 3.A.4)

At the isolation well-functioning phase:

$$u(\tau)+v(\tau)=\left(1+\frac{\rho}{\sigma}\right)\left(\frac{u(\tau)}{u_0}\right)^{\sigma/\beta}-\frac{\rho}{\sigma} \tag{29}$$

Equation (29) gives a relation satisfied by the solution of (28) with $\phi(q,v)=\gamma v$ for any $\hat{t}\geq 0$ at the isolation well-functioning phase.

At the isolation incapable phase:

$$u(\tau)+v(\tau)=u(\tau^\star)+v(\tau^\star)+\frac{\rho}{\beta}(1-q_{\max})\ln\frac{u(\tau)}{u(\tau^\star)} \qquad (\tau>\tau^\star), \tag{30}$$

where $\tau>\tau^\star$ is supposed as the moment at which the isolation reaches the capacity, that is, when the isolation strategy breaks down due to an insufficient isolation capacity, and then the dynamics switches from the isolation well-functioning phase to the isolation incapable phase. Equation (30) is satisfied by the solution of (28) with $\phi(q,v)=0$ for any $\tau>\tau^\star$ at the isolation incapable phase. Remark that, supposed that the isolation reaches the capacity at $\tau=\tau^\star$, the equation (29) holds for $\tau\leq\tau^\star$ about the system (28) with $\phi(q,v)=\gamma v$.

3.3.3 *Isolation incapable phase*

In this subsection, we can obtain the following theorem and corollaries about the condition that the isolation reaches the capacity in a finite time on the way of epidemic process (Appendix 3.A.5):

Theorem 3.2. *The isolation reaches the capacity in a finite time on the way of epidemic process if and only if*

$$1-q_{\max}\left(1+\frac{\rho}{\sigma}\right)>u_0(1-q_{\max})^{\beta/\sigma}. \tag{31}$$

Corollary 3.2.1. *The isolation reaches the capacity in a finite time on the way of epidemic process if and only if $q_{\max}<q_c$, where q_c is the critical value of the isolation capacity and uniquely determined by the positive root of the following equation:*

$$1-q_c\left(1+\frac{\rho}{\sigma}\right)=u_0(1-q_c)^{\beta/\sigma}. \tag{32}$$

If $q_{\max}\geq q_c$, the isolation never reaches the capacity, and is always available.

Corollary 3.2.2. *The isolation reaches the capacity in a finite time on the way of epidemic process only if $q_{\max}<1/(1+\rho/\sigma)$.*

Corollary 3.2.2 indicates that the isolation never reaches the capacity for $q_{\max}\geq 1/(1+\rho/\sigma)$. Hence, from Corollary 3.2.1, it is necessary that $q_c<1/(1+\rho/\sigma)$. From the equation (32), the critical value of the isolation capacity q_c is monotonically increasing in terms of the infection coefficient β. The higher likelihood of infection leads to the demand of a larger capacity of isolation to avoid its breakdown in the epidemic dynamics. In contrast, q_c is

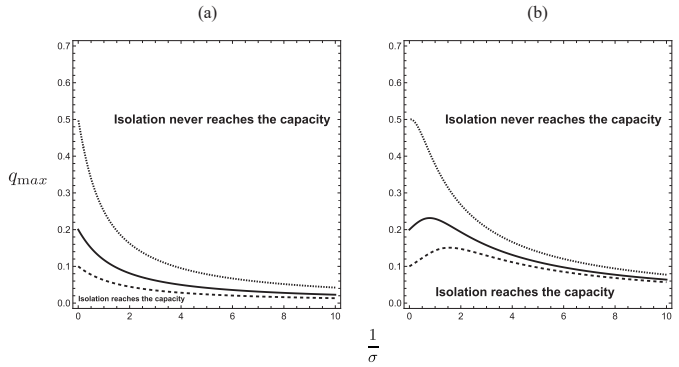

Figure 8: $(1/\sigma)$-dependence of the critical value of the isolation capacity q_c determined by (32) in Corollary 3.2.1. The curves are numerically drawn q_c for $u_0 = 0.5$ (dotted), 0.8 (solid), 0.9 (dashed) with (a) $\beta = 1.0$ and $\rho = 1.5$; (b) $\beta = 1.5$ and $\rho = 1.0$. If and only if $q_{\max} < q_c$, the isolation reaches the capacity in a finite time on the way of epidemic process. Refer to Corollary 3.2.3 too. From (32), we can easily find that $q_c \to 1 - u_0$ as $1/\sigma \to +0$.

monotonically decreasing in terms of the initial susceptible size u_0 and the recovery rate ρ.

The smaller u_0 means the larger initial infective size v_0. Hence this result indicates that the larger isolation capacity is required for the larger initial infective size in order to avoid its saturation, that is, its breakdown. This is because the larger initial infective size must lead to a larger number of secondary cases which is more likely to cause the saturation of isolation.

As the patient can recover after a shorter expected duration of infectivity, defined by $1/\rho$, the isolation capacity to avoid its saturation is smaller. Since the shorter duration of infectivity leads to the smaller infective subpopulation size, the increase of isolated subpopulation must be slower, so that the isolation capacity could be smaller to avoid its saturation. These results may match our intuitive expectation.

Further, the critical value of the isolation capacity q_c may have a non-monotonic relation to the value of $1/\sigma$ which is indicated by the numerical results in Figure 8. The following corollary shows the dependence of q_c on $1/\sigma$ (Appendix 3.A.6):

Corollary 3.2.3. *If $\beta/\rho \leq 1$, the critical value of the isolation capacity q_c is monotonically decreasing in terms of $1/\sigma$. On the other hand, there exists a finite value of $1/\sigma$ to maximize q_c if*

$$\frac{\beta}{\rho} > \frac{u_0 - 1}{u_0 \ln u_0}. \tag{33}$$

It is easily seen that the right side of (33) is greater than 1 for any $u_0 \in (0, 1)$.

Sufficiently low efficiency of quarantine operation corresponds to sufficiently large value of $1/\sigma$, which means much slow quarantine operation to isolate the infectives in the community. In such a case, the isolated subpopulation size Q increases much slow, so that it is less likely to reach the capacity $Q_{\max}$ on the way of epidemic process. Such a dependence of q_c on $1/\sigma$ appears as the decreasing monotonicity of q_c for sufficiently large value of $1/\sigma$.

The public health policy must require a high efficiency of quarantine operation. The higher efficiency of quarantine operation leads to a faster increase of Q, and eventually it could become more likely that the isolation reaches the capacity, whereas such an efficient quarantine operation could make the final epidemic size smaller as we will see in the later.

3.3.4 *Final epidemic size*

The final epidemic size for the system (28) is defined here as the proportion of recovered or isolated individuals in the community at the end of epidemic dynamics. In this subsection, we show the equation to determine the final epidemic size respectively when the isolation never reaches the capacity and when the isolation reaches the capacity on the way of epidemic process, which can be derived from the conserved quantities obtained in Subsection 3.3.2.

Final size equation for $q_{\max} \geq q_c$

When the isolation never reaches the capacity in any time, the final epidemic size is determined only by the isolation well-functioning phase. In this case, the final epidemic size $z_\infty^- = q_\infty^- + w_\infty^-$ satisfies (Appendix 3.A.7):

$$\left(1 - z_\infty^-\right)^{-\sigma/\beta} \left(1 + \frac{\rho}{\sigma} - z_\infty^-\right) = (u_0)^{-\sigma/\beta} \left(1 + \frac{\rho}{\sigma}\right). \tag{34}$$

It is proved that the equation (34) determines a unique final epidemic size $z_\infty^- \in (1 - u_0, 1)$.

Final size equation for $q_{\max} < q_c$

When the isolation reaches the capacity in a finite time due to its insufficient capacity, the final epidemic size $z_\infty^+ = q_{\max} + w_\infty^+$ satisfies (Appendix 3.A.7):

$$\frac{\beta}{\sigma}\left\{\frac{q_{\max}\,(1 + \sigma/\rho)}{1 - q_{\max}} + \ln\left(1 - q_{\max}\right)\right\} = \ln(1 - z_\infty^+) - \ln u_0 + \frac{(\beta/\rho) z_\infty^+}{1 - q_{\max}}. \tag{35}$$

It is proved in Appendix 3.A.8 that the equation (35) determines a unique final epidemic size $z_\infty^+ \in (1 - u(\tau^\star), 1)$, where $u(\tau^\star) = (1 - q_{\max})^{\beta/\sigma} u_0$, and $1 - u(\tau^\star) > q_{\max}(1 + \rho/\sigma) > q_{\max}$. As a result, the following theorem is obtained:

Theorem 3.3. *The final epidemic size for the system* (28) *is uniquely determined by the equations* (34) *or* (35) *for given initial condition, which is $z_\infty^- \in (1 - u_0, 1)$ for $q_{\max} \geq q_c$, and $z_\infty^+ \in (1 - u(\tau^\star), 1)$ for $q_{\max} < q_c$ with $u(\tau^\star) = (1 - q_{\max})^{\beta/\sigma} u_0$.*

The final epidemic size depends on $q_{\max}$ only when the isolation reaches the capacity in a finite time: z_∞^+ depends on $q_{\max}$ while z_∞^- does not. From the equation (35), we can find that the final epidemic size z_∞^+ is monotonically decreasing in terms of $q_{\max}$, since $\partial z_\infty^+ / \partial q_{\max}$ is shown to be negative. Figure 9 numerically shows the $q_{\max}$-dependence of the final epidemic size. It is seen that increasing the isolation capacity makes the final epidemic size smaller. This result indicates that the sufficient capacity of isolation could work as an effective factor to suppress a disease spread.

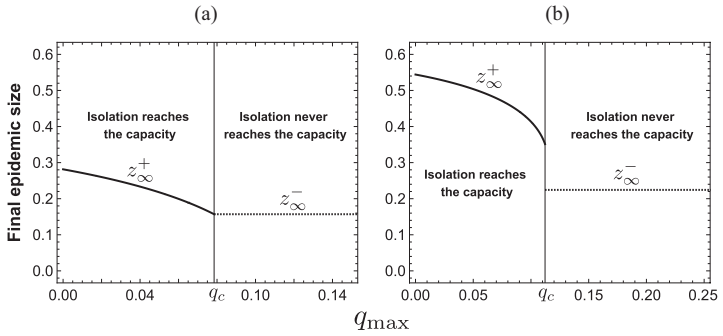

Figure 9: $q_{\max}$-dependence of the final epidemic size. Numerically drawn for (a) $\beta/\sigma = 0.8$ ($\rho/\beta = 1.25$); (b) $\beta/\sigma = 1.25$ ($\rho/\beta = 0.8$), $u_0 = 0.9$ and $\rho/\sigma = 1$.

Figure 9(b) shows a case where the final epidemic size becomes drastically large if the isolation reaches the capacity in a finite time. We obtain the following analytical result on the $q_{\max}$-dependence of the final epidemic size for our model (Appendix 3.A.9):

Theorem 3.4. *The final epidemic size has a discontinuous change at the critical value of the isolation capacity: $q_{\max} = q_c$ such that*

$$z_\infty^\dagger := \lim_{q_{\max} \to q_c - 0} z_\infty^+ > z_\infty^-$$

if and only if

$$\frac{\beta}{\rho} > 1 \quad \textit{and} \quad u_0 > \frac{\rho}{\beta}\left(1 + \frac{1-\rho/\beta}{\rho/\sigma}\right)^{\beta/\sigma - 1}. \tag{36}$$

Otherwise it holds that $z_\infty^\dagger = z_\infty^-$.

When the condition (36) is not satisfied, the final epidemic size has no discontinuous change at $q_{\max} = q_c$, as numerically illustrated by Figure 9(a). In this case, although the final epidemic size increases as the isolation capacity less than the critical value q_c, the change is gradual, that is, a slight shortage isolation capacity leads to a relatively small increase in the final epidemic size. When the condition (36) is satisfied, the final epidemic size has a discontinuous change at $q_{\max} = q_c$, as numerically illustrated by Figure 9(b). In this case, even a slight shortage of isolation capacity can cause a sudden and large jump in the final epidemic size, resulting in disproportionately severe social damage. Inversely, ensuring that the isolation capacity is even slightly above the critical level q_c can drastically reduce the total number of infected individuals. This means that there is an epidemic situation in which the isolation capacity would be the more important factor for the suppression of disease spread. In such a situation, the insufficiency of isolation capacity could cause a drastically severe consequence of the epidemic dynamics.

Figure 10(a) shows the parameter region $(\rho/\sigma, \beta/\sigma)$ with respect to the discontinuous change of the final epidemic size at $q_{\max} = q_c$. It is seen that for sufficiently small $\beta/\sigma > \rho/\sigma$, such a discontinuous change of the final epidemic size is likely to occur at $q_{\max} = q_c$. It is the case where the disease spread is very slow and the recovery from the disease takes sufficiently long time. Thus the severity of insufficient isolation capacity appears especially

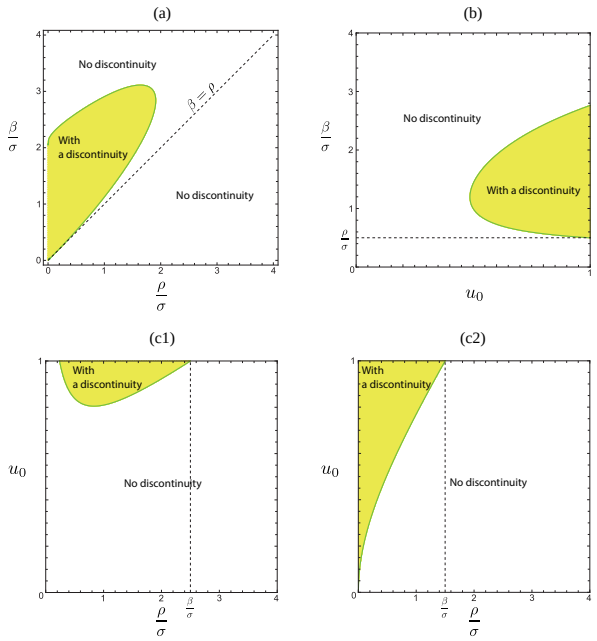

Figure 10: Parameter region with respect to the discontinuous change of the final epidemic size at $q = q_c$. Numerically drawn with the condition (36) in Theorem 3.4 for (a) $u_0 = 0.9$; (b) $\rho/\sigma = 0.5$; (c1) $\beta/\sigma = 2.5$; (c2) $\beta/\sigma = 1.5$.

for the epidemic dynamics of an infectious disease such that the infectivity is weak while the disease is hardly treated to the recovery. On the other hand, when $\beta > \rho$, such a discontinuous change may occur for σ large enough that β/σ becomes sufficiently small.

Figures 10(b, c) indicate moreover that such a discontinuous change may occur only for sufficiently large u_0, that is, for sufficiently small v_0. This can be regarded as a typical situation as the initial condition about the epidemic dynamics which starts with the invasion of an infectious disease in a community.

3.3.5 *Discussion*

This section discusses the epidemiological implications of the SIR+Q model incorporating a limited capacity of isolation. The results show that an increase in the isolation capacity generally leads to a smaller final epidemic size. However, once the isolation reaches its capacity and becomes incapable, the final epidemic size may become significantly larger. This drastic increase is more likely to occur when the disease spreads slowly and recovery takes a sufficiently long time. In such cases, the severity of insufficient isolation capacity becomes especially notable, particularly for infectious diseases with low infectivity and limited treatability. In contrast, for diseases that have high infectivity or are easily treated, the increase in isolation capacity tends to result in only a modest change in the final epidemic size. Nonetheless, it still contributes to epidemic suppression.

From a public health management perspective, a smaller critical value for the isolation capacity is preferable, as it allows the policy to avoid breakdown with limited available resources. In contrast, a larger critical value implies a

more difficult situation for public health policy, since a much higher capacity is required to maintain the isolation function and keep the epidemic size low.

In summary, the study highlights that a breakdown in isolation due to limited capacity can lead to an unexpectedly large epidemic size. Although a sufficiently large isolation capacity can help suppress the epidemic, its effectiveness depends on the characteristics of the disease. While isolation may not be the principal control measure, it remains an important component of public health strategies. It contributes significantly to epidemic control when combined with other policies. Furthermore, the findings point to the essential need for satisfactory public health infrastructure and sufficient social investment to support the effective operation of isolation policies under resource-limited conditions.

3.4 FOR REINFECTIOUS DISEASE

3.4.1 *Assumptions and model*

In this section, we consider a modeling on the epidemic dynamics of a reinfectious disease during a short-term period, satisfying the following assumptions on the epidemic dynamics, most of which are the same as those in Subsection 3.2.1 except for that about the discharge from isolation:

- The demographic change due to the natural birth, death, and migration is negligible in the season.
- The fatality of disease is negligible in the season.
- The infection occurs by the contact of susceptible individual to not only organic but also potentially inorganic subjects contaminated with the pathogen to cause the disease.
- The quarantine/isolation has a capacity beyond which the isolation is impossible.
- As long as the isolation has not reached the capacity, the accessibility of the isolation is constant independently of how many infectives are isolated.
- The isolated individuals cannot contact others or be discharged in the epidemic season. Hence the infectives come to make no contribution to the epidemic dynamics once they enters the isolated state.
- Once the isolation reaches the capacity, its function breaks down to become incapable onward in the season. Then the epidemic dynamics continues without the quarantine/isolation.
- Even after the recovery from the infection, the individual may get the infection again, that is, the disease is reinfectious.

From the assumptions of the availability of isolation, we need to take account of two different epidemic phases in our modeling, which are the same as in 3.3: isolation well-functioning phase and isolation incapable phase.

Isolation well-functioning phase

The isolation well-functioning phase refers to the epidemic phase at which the isolated subpopulation size Q is less than the capacity, a given positive

constant $Q_{\max}$, when the isolation works with quarantine/isolation rate σ. The epidemic dynamics at this phase is governed by

$$\begin{aligned}
\frac{dS}{dt} &= -\beta \frac{I}{N-Q} S; \\
\frac{dI}{dt} &= \beta \frac{I}{N-Q} S + \varepsilon\beta \frac{I}{N-Q} R - \rho I - \sigma I; \\
\frac{dQ}{dt} &= \sigma I; \\
\frac{dR}{dt} &= \rho I - \varepsilon\beta \frac{I}{N-Q} R.
\end{aligned} \tag{37}$$

The variables S, I, and R denote the sizes of susceptible, infective, and recovered subpopulations respectively. The total population size of the community is denoted by a positive constant N, and it is satisfied that $S(t) + I(t) + Q(t) + R(t) = N$ for any $t \geq 0$. The parameter ρ denotes the natural recovery rate of infective individual. The reinfection coefficient is given by $\varepsilon\beta$, where $0 < \varepsilon < 1$. The quarantine/isolation rate of infective individual at this phase σ represents the efficiency of quarantine operation to detect and isolate an infective.

Isolation incapable phase

The isolation incapable phase refers to the epidemic phase at which the isolated subpopulation size Q has reached the capacity $Q_{\max}$, and then the isolation breaks down to become incapable. The epidemic dynamics at this phase is governed by

$$\begin{aligned}
\frac{dS}{dt} &= -\beta \frac{I}{N-Q_{\max}} S; \\
\frac{dI}{dt} &= \beta \frac{I}{N-Q_{\max}} S + \varepsilon\beta \frac{I}{N-Q_{\max}} R - \rho I; \\
\frac{dQ}{dt} &= 0; \\
\frac{dR}{dt} &= \rho I - \varepsilon\beta \frac{I}{N-Q_{\max}} R.
\end{aligned} \tag{38}$$

Once the isolation reaches the capacity, the system switches to the isolation incapable phase. Since we assume no discharge of isolated infectives from the isolation state, the subpopulation size of free individuals is $N - Q_{\max}$ at this phase. The extremal case with $Q_{\max} \geq N$ corresponds to the situation where the isolation never reaches the capacity, that is, it always works in the epidemic dynamics. Only if $Q_{\max} < N$, the isolation could reach the capacity to cease functioning. Therefore, we consider hereafter only the case of $Q_{\max} < N$ as a reasonable setup for our model.

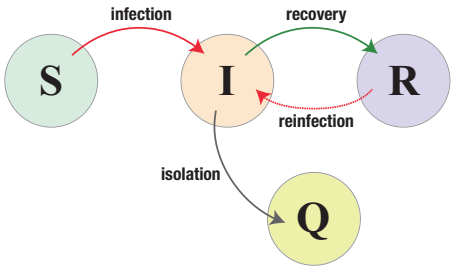

Figure 11: The individual state transition according to the epidemic dynamics of our model (39).

Full system for epidemic dynamics

With the above modeling of the epidemic dynamics at two different epidemic phases, we shall consider the following system as our mathematical model:

$$\begin{aligned}
\frac{dS}{dt} &= -\beta\frac{I}{N-Q}S;\\
\frac{dI}{dt} &= \beta\frac{I}{N-Q}S + \varepsilon\beta\frac{I}{N-Q}R - \rho I - \Phi(Q,I);\\
\frac{dQ}{dt} &= \Phi(Q,I);\\
\frac{dR}{dt} &= \rho I - \varepsilon\beta\frac{I}{N-Q}R
\end{aligned} \tag{39}$$

with

$$\Phi(Q,I) = \begin{cases} \sigma I & \text{for } Q < Q_{\max};\\ 0 & \text{for } Q = Q_{\max}, \end{cases}$$

and the initial condition $(S(0), I(0), Q(0), R(0)) = (S_0, I_0, 0, 0)$ where $S_0 > 0$, $I_0 > 0$, and $S_0 + I_0 = N$. The individual state transition according to the epidemic dynamics is schematically shown in Figure 11. This model with $\varepsilon = 0$ coincides with the SIR+Q model in Section 3.3.

The piecewise function $\Phi(Q, I)$ denotes the net quarantine/isolation rate of infected individuals. As long as the isolated subpopulation size Q is less than the capacity $Q_{\max}$, the isolation is available, and the epidemic dynamics is at the isolation effective phase with $\Phi(Q, I) = \sigma I$. Once Q reaches $Q_{\max}$, the isolation becomes ceased after it. Then the epidemic dynamics switches to the isolation incapable phase with $\Phi(Q, I) = 0$.

With the transformation of variables and parameters,

$$\tau := (\rho+\sigma)t; \quad u := \frac{S}{N}; \quad v := \frac{I}{N}; \quad q := \frac{Q}{N}; \quad w := \frac{R}{N};$$
$$\gamma := \frac{\sigma}{\rho+\sigma}; \quad q_{\max} := \frac{Q_{\max}}{N}; \quad \mathscr{R}_0 := \frac{\beta}{\rho+\sigma},$$

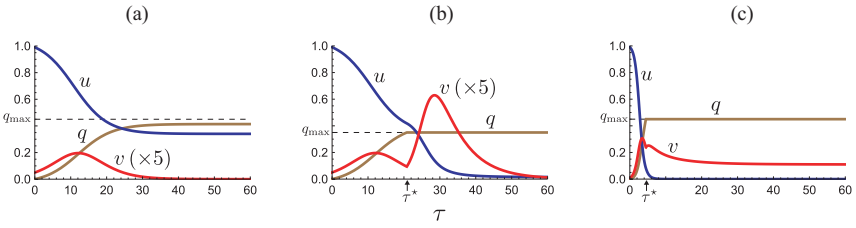

Figure 12: Numerical examples for the temporal variation of the model (40). (a) $q_{\max} = 0.45$, $\mathscr{R}_0 = 1.2$ ($\varepsilon\mathscr{R}_0 = 0.24$); (b) $q_{\max} = 0.35$, $\mathscr{R}_0 = 1.2$ ($\varepsilon\mathscr{R}_0 = 0.24$); (c) $q_{\max} = 0.45$, $\mathscr{R}_0 = 2.5$ ($\varepsilon\mathscr{R}_0 = 0.50$). Commonly, $u_0 = 0.99$; $\varepsilon = 0.2$; $\gamma = 0.6$. In (a), the isolation never reaches the capacity, while it reaches the capacity and becomes incapable after a moment $\tau = \tau^\star$ in (b) and (c).

and with the basic reproduction number $\mathscr{R}_0 := \beta/(\rho + \sigma)$ for the model (39), we can derive the following non-dimensionalized system mathematically equivalent to the system (39):

$$\begin{aligned}
\frac{du}{d\tau} &= -\mathscr{R}_0 \frac{v}{1-q} u; \\
\frac{dv}{d\tau} &= \mathscr{R}_0 \frac{v}{1-q} u + \varepsilon\mathscr{R}_0 \frac{v}{1-q} w - (1-\gamma)v - \phi(q,v); \\
\frac{dq}{d\tau} &= \phi(q,v); \\
\frac{dw}{d\tau} &= (1-\gamma)v - \varepsilon\mathscr{R}_0 \frac{v}{1-q} w
\end{aligned} \tag{40}$$

with

$$\phi(q,v) = \begin{cases} \gamma v & \text{for } q < q_{\max}; \\ 0 & \text{for } q = q_{\max}, \end{cases}$$

and the initial condition $(u(0), v(0), q(0), w(0)) = (u_0, v_0, 0, 0)$ where $u_0 > 0$ and $v_0 = 1 - u_0 > 0$. In the following analysis, we focus on the case $q_{\max} < 1$, which has been previously mentioned as a reasonable setup. For a mathematical convention, we show here the following mathematical feature about the solution of (40) (Appendix 3.A.10):

Lemma 3.3. *For the initial condition* $(u(0), v(0), q(0), w(0)) = (u_0, v_0, 0, 0)$ *with* $v_0 > 0$ *and* $u_0 = 1 - v_0 > 0$, *the solution of* (40) *belongs to the set* $\{(u, v, q, w) \in \mathbb{R}^4_+ \mid u + v + q + w = 1\}$ *for* $\tau > 0$.

As numerically exemplified by Figure 12(a) for a sufficiently large capacity $q_{\max}$, the epidemic dynamics can always remain at the isolation well-functioning phase with $\phi(q, v) = \gamma v$, when the isolation never reaches the capacity. In contrast, as numerically exemplified by Figure 12(b, c), if the isolation capacity is insufficient, it reaches the capacity, and then the isolated subpopulation size q remains $q_{\max}$ at the isolation incapable phase since any isolated individual is not discharged from the isolation, following the assumption and modeling given in the previous and present sections.

3.4.2 *Conserved quantities*

In addition to the time-independent equality $u+v+q+w=1$, we can find the following time-independent equalities for the variables as the conserved quantities in the epidemic dynamics governed by the system (40) (Appendix 3.A.11).

At the isolation well-functioning phase:

$$1-q=\Big(\frac{u}{u_0}\Big)^{\gamma/\mathscr{R}_0}; \tag{41}$$

$$u+v=F(u):=\begin{cases}\dfrac{1-\varepsilon\mathscr{R}_0}{\gamma-\varepsilon\mathscr{R}_0}\Big(\dfrac{u}{u_0}\Big)^{\gamma/\mathscr{R}_0}-\dfrac{1-\gamma}{\gamma-\varepsilon\mathscr{R}_0}\Big(\dfrac{u}{u_0}\Big)^{\varepsilon} & \text{for } \varepsilon\mathscr{R}_0\neq\gamma;\\[2ex] \Big(1+\varepsilon\dfrac{1-\gamma}{\gamma}\ln\dfrac{u}{u_0}\Big)\Big(\dfrac{u}{u_0}\Big)^{\varepsilon} & \text{for } \varepsilon\mathscr{R}_0=\gamma.\end{cases} \tag{42}$$

At the isolation incapable phase:

$$q=q_{\max};\quad u+v=G(u):=\Big(1-\frac{1-\gamma}{\varepsilon\mathscr{R}_0}\Big)(1-q_{\max})+B\Big(\frac{u}{u_0}\Big)^{\varepsilon} \tag{43}$$

with

$$B:=\begin{cases}\dfrac{1-\gamma}{\varepsilon\mathscr{R}_0(1-\varepsilon\mathscr{R}_0/\gamma)}\Big[(1-q_{\max})^{1-\varepsilon\mathscr{R}_0/\gamma}-\dfrac{\varepsilon\mathscr{R}_0}{\gamma}\Big] & \text{for } \varepsilon\mathscr{R}_0\neq\gamma;\\[2ex] \dfrac{1-\gamma}{\gamma}\big[\ln(1-q_{\max})+1\big] & \text{for } \varepsilon\mathscr{R}_0=\gamma.\end{cases} \tag{44}$$

The equations for $\varepsilon\mathscr{R}_0=\gamma$ in (42) and (44) can be mathematically derived also by taking the limit as $\varepsilon\mathscr{R}_0\to\gamma$ for those for $\varepsilon\mathscr{R}_0\neq\gamma$. Hence we may use only the equations for $\varepsilon\mathscr{R}_0\neq\gamma$ without distinguishing the case of $\varepsilon\mathscr{R}_0=\gamma$ unless it would be necessary in the mathematical argument. That is, we may use the equations for $\varepsilon\mathscr{R}_0\neq\gamma$ as those mathematically including the specific case of $\varepsilon\mathscr{R}_0=\gamma$.

As described about the derivation of (43) in Appendix 3.A.11, we used the continuity of the temporal variation of the variables in the system (40) at the moment that the isolation reaches the capacity and the system (40) switches to the isolation incapable phase. Then we have noted the following feature of the system (40), which will be useful for our subsequent mathematical analysis on the model:

Lemma 3.4. *If the system enters the isolation incapable phase at a finite time $\tau=\tau^\star$, then the susceptible subpopulation size at the moment becomes*

$$u(\tau^\star)=u^\star:=u_0(1-q_{\max})^{\mathscr{R}_0/\gamma}. \tag{45}$$

Note that, from the continuity of variables u and v at $\tau = \tau^\star$, the equalities (41), (42), and (43) simultaneously holds at $\tau = \tau^\star$, so that we have $F(u^\star) = G(u^\star)$.

3.4.3 *Isolation well-functioning phase*

In this section, suppose that the system (40) always remains at the isolation well-functioning phase, when it never reaches its capacity at finite time along the path of the epidemic process. Then with the arguments given in Appendix 3.A.12, we can obtain the following results on the consequence of the epidemic dynamics when the system (40) always remains at the isolation well-functioning phase.

First, we find the following result implying that a sufficiently large isolation capacity could lead the system to a disease-eliminated equilibrium E_0^-, even though the disease is reinfectious for the recovered individuals (Appendix 3.A.12):

Lemma 3.5. *If the system always remains at the isolation well-functioning phase, the disease is eventually eliminated.*

Next, we can obtain the following important feature of the epidemic dynamics by the system (40):

Lemma 3.6. *If the system (40) can always remains at the isolation well-functioning phase, there are necessarily some susceptibles who can escape from the infection at the end of the epidemic dynamics.*

The existence of such susceptibles at the end of the epidemic dynamics is well known for the Kermack-McKendrick SIR model , while the above lemma indicates such a case even for the epidemic dynamics with a reinfectious disease in our model.

Consequently with these lemmas, we can obtain the following result (Appendix 3.A.13):

Theorem 3.5. *If the system always remains at the isolation well-functioning phase, it eventually approaches a disease-eliminated equilibrium E_0^- given by*

$$E_0^-(u_\infty^-, v_\infty^-, q_\infty^-, w_\infty^-) = \left(u_\infty^-, 0, 1 - \left(\frac{u_\infty^-}{u_0}\right)^{\gamma/\mathscr{R}_0}, \left(\frac{u_\infty^-}{u_0}\right)^{\gamma/\mathscr{R}_0} - u_\infty^-\right), \quad (46)$$

with a positive susceptible subpopulation size $u_\infty^- \in (0, u_0)$, which is determined by the unique positive root of the equation

$$u_\infty^- = F(u_\infty^-). \quad (47)$$

The equation (47) is derived by taking $\tau \to \infty$ for the equality (42) with $v \to 0$. The disease-eliminated equilibrium E_0^- is uniquely determined for each given initial condition with $u_0 > 0$. In other words, the disease-eliminated equilibrium E_0^- depends on the initial condition given by the initial infective subpopulation size v_0 (alternatively u_0).

In the next subsection, we will show the necessary and sufficient condition that the system (40) always remains at the isolation well-functioning phase, and alternatively the condition that the isolation reaches the capacity at finite time along the path of the epidemic process. As an important preliminary found by the arguments in Appendix 3.A.13 for Theorem 3.5, we obtain the following lemma too:

Lemma 3.7. *The system (40) can always remains at the isolation well-functioning phase only if $\varepsilon\mathscr{R}_0 < 1$. Otherwise, if $\varepsilon\mathscr{R}_0 \geq 1$, then the isolation reaches the capacity, and the system enters the isolation incapable phase at finite time.*

This result shows a sufficient condition that the isolation reaches the capacity at finite time. Even when $\varepsilon\mathscr{R}_0 < 1$, there could be such a case as shown in the next subsection.

3.4.4 *Isolation incapable phase*

Taking account of the results shown in the previous section, we can prove the following theorem to show the necessary and sufficient condition that the isolation reaches the capacity at finite time along the path of the epidemic process (Appendix 3.A.14):

Theorem 3.6. *Isolation reaches the capacity and becomes incapable at finite time along the path of the epidemic process if and only if one of the following conditions is satisfied:*

(i) $\varepsilon\mathscr{R}_0 \geq 1$*;*

(ii) $\varepsilon\mathscr{R}_0 < 1$ *and*

$$u_0(1-q_{\max})^{\mathscr{R}_0/\gamma} < F\big(u_0(1-q_{\max})^{\mathscr{R}_0/\gamma}\big). \tag{48}$$

Otherwise, if both conditions (i) and (ii) are not satisfied, the isolation never reaches the capacity in the epidemic dynamics.

In other words, the system always remains at the isolation well-functioning phase when and only when both conditions (i) and (ii) are not satisfied. The inequality (48) for $\varepsilon = 0$ matches the condition (32) obtained in Corollary 3.2.1 on the SIR+Q model without reinfection.

This result of Theorem 3.6 can be translated in the following way with the critical value q_c for the isolation capacity $q_{\max}$ (Appendix 3.A.15):

Corollary 3.6.1. *Isolation reaches the capacity and becomes incapable at finite time if and only if $q_{\max} < q_c$, where q_c is defined as the smallest positive root of the equation*

$$u_0(1-q_c)^{\mathscr{R}_0/\gamma} = F\big(u_0(1-q_c)^{\mathscr{R}_0/\gamma}\big). \tag{49}$$

If and only if $q_{\max} \geq q_c$, the system always remains at the isolation well-functioning phase, where the isolation never reaches the capacity.

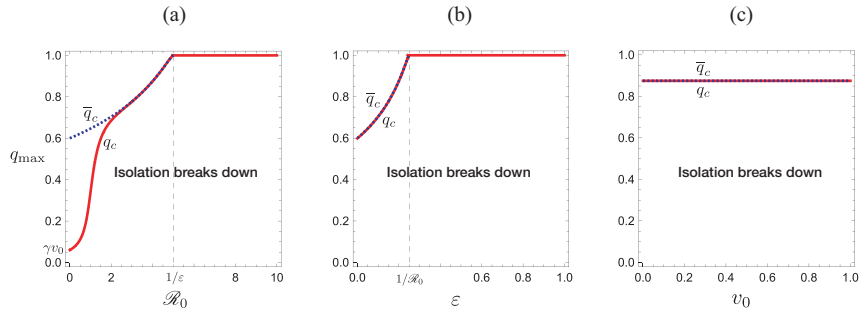

Figure 13: (a) $\mathscr{R}_0$-dependence; (b) ε-dependence; (c) v_0-dependence of the critical value q_c of the isolation capacity $q_{\max}$. Numerically drawn by Theorem 3.6, Corollaries 3.6.1 and 3.6.2 with (a) $\varepsilon = 0.2$, $u_0 = 0.9$; (b) $\mathscr{R}_0 = 4$, $u_0 = 0.9$, (c) $\varepsilon = 0.2$, $\mathscr{R}_0 = 4$, and commonly $\gamma = 0.6$. The boundary q_c is given by (49), and the dotted curve of $\overline{q}_c$ is by (50). The difference between q_c and $\overline{q}_c$ appears rather slight in (b) and (c). In (c), $\overline{q}_c = 0.875$ independently of v_0 while q_c depends on $v_0 = 1 - u_0$.

As shown in Appendix 3.A.15 and Figure 13, the critical value q_c defined in Corollary 3.6.1 becomes less than 1 for $\varepsilon\mathscr{R}_0 < 1$, while it becomes 1 for $\varepsilon\mathscr{R}_0 \geq 1$. Since $q_{\max} < 1$ from our assumption, it is impossible to satisfy that $q_{\max} \geq q_c$ when $\varepsilon\mathscr{R}_0 \geq 1$. That is, the system necessarily enters the isolation incapable phase at finite time, in accordance with the result shown in Theorem 3.6.

From the equation (49), we can easily find that the critical value q_c for the isolation capacity $q_{\max}$ is monotonically increasing in terms of the basic reproduction number $\mathscr{R}_0$, the index for the reinfection ε, and the initial infective subpopulation size v_0. The stronger infectivity, the higher likelihood of reinfection, or the larger number of the initial infected individuals leads to the demand of a larger isolation capacity to avoid its breakdown in the epidemic dynamics, as numerically illustrated in Figure 13.

Moreover, we note that $q_c \to \gamma v_0 = \gamma(1 - u_0)$ as $\mathscr{R}_0 \to 0$ with (49) (see Figure 13(a)). We can easily find that the condition (48) becomes $q_{\max} < \gamma(1 - u_0)$ as $\mathscr{R}_0 \to 0$. This is a reasonable mathematical feature about our model (40). When no disease transmission occurs with $\mathscr{R}_0 = 0$, every initial infective belonging to v_0 alternatively recovers or is isolated, and the system eventually approaches the equilibrium $(u, v, q, w) = (u_0, 0, \gamma v_0, (1 - \gamma)v_0)$, if the isolation capacity is not below γv_0, which can be easily found by considering the system (40) with $\mathscr{R}_0 = 0$. Otherwise, if $q_{\max} < \gamma v_0$, the isolation reaches the capacity on the way of the infective elimination, and it becomes incapable.

As clearly indicated by Theorem 3.6, the isolation reaches the capacity at finite time if $q_{\max} < q_c$ even when $\varepsilon\mathscr{R}_0 < 1$. It has been already shown in Lemma 3.7 that the system can always remain at the isolation well-functioning phase only when $\varepsilon\mathscr{R}_0 < 1$, and now we can find the following subsidiary result too (Appendix 3.A.15):

Corollary 3.6.2. *When $\varepsilon\mathscr{R}_0 < 1$, if*

$$q_{\max} \geq \overline{q}_c := \begin{cases} 1 - \left(\dfrac{1-\varepsilon\mathscr{R}_0}{1-\gamma}\right)^{\gamma/(\varepsilon\mathscr{R}_0-\gamma)} & \text{for } \varepsilon\mathscr{R}_0 \neq \gamma; \\ 1 - \mathrm{e}^{-\gamma/(1-\gamma)} & \text{for } \varepsilon\mathscr{R}_0 = \gamma, \end{cases} \tag{50}$$

the system always remains at the isolation well-functioning phase and the isolation never reaches the capacity.

This corollary gives a sufficient condition that the system always remains at the isolation well-functioning phase when $\varepsilon\mathscr{R}_0 < 1$, that is, the right side of (50) gives a sufficient isolation capacity for it, independently of the initial condition given by the value u_0. The sufficient isolation capacity $\overline{q}_c$ is the supremum of q_c in terms of u_0: It holds that $\overline{q}_c > q_c$, so that we have $q_{\max} > q_c$ if $q_{\max} \geq \overline{q}_c$ (see Figure 13). Only if the condition (50) is unsatisfied, the system enters the isolation incapable phase at finite time along the path of the epidemic process.

As the other important subsidiary result obtained in the proof for Corollary 3.6.1 in Appendix 3.A.15, we can find

Lemma 3.8. $u_\infty^- = u_0(1-q_c)^{\mathscr{R}_0/\gamma}$.

This result will be useful in the subsequent analysis. Note that the equilibrium value u_∞^- is independent of the isolation capacity $q_{\max}$ because it is for the equilibrium at the isolation well-functioning phase when the isolation never reaches the capacity.

We obtain the following lemma and theorem about the feasible equilibria at the isolation incapable phase (Appendix 3.A.16):

Lemma 3.9. *At the isolation incapable phase, $u \to u_\infty^+ \in (0, u^\star)$ as $\tau \to \infty$, if and only if $\varepsilon\mathscr{R}_0 < 1-\gamma$. The equilibrium value u_∞^+ is determined by the unique positive root in $(0, u^\star)$ of the equation*

$$u_\infty^+ = G(u_\infty^+), \tag{51}$$

where G is defined by (43) and (44). If $\varepsilon\mathscr{R}_0 \geq 1-\gamma$, then $u \to 0$ as $\tau \to \infty$.

Theorem 3.7. *At the isolation incapable phase, if and only if $\varepsilon\mathscr{R}_0 < 1-\gamma$, the system (40) approaches a disease-eliminated equilibrium E_0^+:*

$$E_0^+(u_\infty^+, v_\infty^+, q_\infty^+, w_\infty^+) = \big(u_\infty^+, 0, q_{\max}, 1-u_\infty^+-q_{\max}\big), \tag{52}$$

where u_∞^+ is determined by the unique positive root in $(0, u^\star)$ of the equation (51). If $\varepsilon\mathscr{R}_0 = 1-\gamma$ at the isolation incapable phase, it approaches the disease-eliminated equilibrium E_0^+ given as $(0, 0, q_{\max}, 1-q_{\max})$. Otherwise, if $\varepsilon\mathscr{R}_0 > 1-\gamma$ at the isolation incapable phase, it approaches the endemic equilibrium E_*^+:

$$E_*^+(u_\infty^+, v_\infty^+, q_\infty^+, w_\infty^+) = \left(0, \left(1-\frac{1-\gamma}{\varepsilon\mathscr{R}_0}\right)(1-q_{\max}), q_{\max}, \frac{1-\gamma}{\varepsilon\mathscr{R}_0}(1-q_{\max})\right). \tag{53}$$

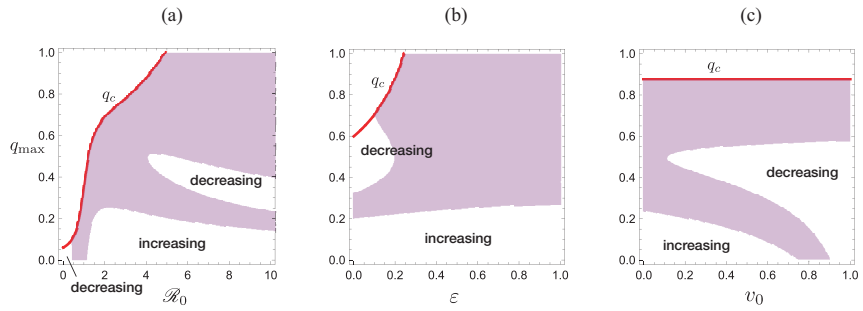

Figure 14: Parameter region for the revival of outbreak, numerically drawn by Theorem 3.8 with the parameter values used in Figure 13: (a) $\mathscr{R}_0$-dependence; (b) ε-dependence; (c) v_0-dependence. The revival of outbreak occurs for the filled region. For the other region, the infective subpopulation size keeps decreasing or increasing even at the moment that the isolation reaches the capacity and the system enters the isolation incapable phase.

As a result, the system approaches an endemic equilibrium if and only if $\varepsilon\mathscr{R}_0 > 1-\gamma$ at the isolation incapable phase. Otherwise, it approaches a disease-eliminated equilibrium, independently of whether it enters the isolation incapable phase or not.

Figure 12(b, c) numerically exemplify the cases in which the system approaches an disease-eliminated equilibrium E_0^+ and the endemic equilibrium E_*^+ respectively after it enters the isolation incapable phase. The endemic state arises in the community necessarily after the isolation reaches the capacity. The endemic state is sustained by the reinfection for the recovered individuals, since there is no susceptible who has not experienced the disease in the community (i.e., $u_\infty^+ = 0$). From Theorems 3.5 and 3.7, even after the isolation reaches the capacity, the elimination of the disease may occur if the reinfectivity is weak enough to satisfy that $\varepsilon\mathscr{R}_0 \le 1-\gamma$.

3.4.5 *Revival of outbreak*

As already seen in Figure 12(b, c), there could be a case where the infective subpopulation size turns from decreasing to increasing at the moment that the isolation reaches the capacity and the system enters the isolation incapable phase. Such a case appears as a revival of outbreak of the disease spread in the community. We can get the following condition that such a revival of outbreak occurs (Appendix 3.A.17):

Theorem 3.8. *When the isolation reaches the capacity at finite time, a revival of outbreak occurs if*

$$\frac{\varepsilon\mathscr{R}_0 - 1}{\mathscr{R}_0}(1-q_{\max}) < \varepsilon F(u^\star) - u^\star < \frac{\varepsilon\mathscr{R}_0 - (1-\gamma)}{\mathscr{R}_0}(1-q_{\max}),$$

where $u^\star$ is defined by (45).

Figure 14 shows numerically obtained parameter regions for the revival of outbreak. It is implied that the parameter dependence is not simple. Roughly the larger isolation capacity or the larger infectivity is more likely to cause the revival of outbreak, while the sufficiently small isolation capacity is less likely. We may expect that the breakdown of the isolation operation along the path of the epidemic process could lead to the revival of outbreak.

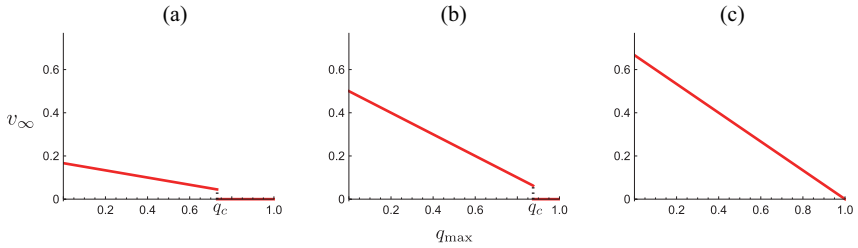

Figure 15: $q_{\max}$-dependence of the endemic size v_∞. Numerically drawn with (a) $\varepsilon = 0.12$ ($\varepsilon\mathscr{R}_0 = 0.48$; $q_c = 0.7305$); (b) $\varepsilon = 0.2$ ($\varepsilon\mathscr{R}_0 = 0.8$; $q_c = 0.8750$); (c) $\varepsilon = 0.3$ ($\varepsilon\mathscr{R}_0 = 1.2$; $q_c = 1$), and commonly $u_0 = 0.9$; $\gamma = 0.6$; $\mathscr{R}_0 = 4.0$. Note that $v_\infty = 0$ independently of $q_{\max}$ if $\varepsilon\mathscr{R}_0 \leq 1 - \gamma$, as indicated in Theorem 3.7.

3.4.6 *Endemic size*

The endemic size is defined here as the equilibrium value of the infective subpopulation size v_∞, which is hence zero if the system approaches a disease-eliminated equilibrium. From Theorem 3.7, it can become positive only at the isolation incapable phase, and given as $v_\infty^+ = \{1 - (1-\gamma)/(\varepsilon\mathscr{R}_0)\}(1 - q_{\max})$ from E_*^+ given by (53).

From Theorem 3.6, Corollary 3.6.1, and Theorem 3.7, we have noted that, when $\varepsilon\mathscr{R}_0 \geq 1$, the system necessarily approaches an endemic equilibrium at the isolation incapable phase. Then the endemic size v_∞^+ is monotonically decreasing in terms of the isolation capacity $q_{\max}$ as shown by (53). See the numerical example in Figure 15(c).

In contrast, especially when the disease spreads with $\varepsilon\mathscr{R}_0 \in (1-\gamma, 1)$, the disease becomes eliminated if $q_{\max} \geq q_c \in (0,1)$, while it becomes endemic if $q_{\max} < q_c$, as seen in the numerical examples of Figure 15(a, b). Then the endemic size shows a discontinuity at $q_{\max} = q_c$, where it is continuous and positive in terms of $q_{\max} < q_c$, and zero for $q_{\max} > q_c$. Thus, in such a case, the isolation capacity is a crucial factor for the endemicity of the spreading disease.

3.4.7 *Final epidemic size*

The final epidemic size z_∞ is defined here as the proportion of individuals in the community who have experienced the infection until the final stage of the epidemic dynamics. Hence it is given by $z_\infty := 1 - u_\infty$ for the system (40). From this definition of the final epidemic size, when the system (40) approaches an endemic equilibrium, we have $z_\infty = 1$, because every individual in the community has experienced the infection at the end of the epidemic dynamics with $u_\infty = 0$.

First, as shown by Theorems 3.6, 3.7, and Corollary 3.6.1, when the isolation never reaches the capacity in the epidemic dynamics with $\varepsilon\mathscr{R}_0 < 1$ and $q_{\max} \geq q_c$, the system (40) approaches a disease-eliminated equilibrium, and then the final epidemic size z_∞ is given by $z_\infty^- := 1 - u_\infty^-$ with u_∞^- given by Lemma 3.8. That is, we have $z_\infty^- = 1 - u_0(1-q_c)^{\mathscr{R}_0/\gamma} \in (0,1)$.

Next, from those results obtained in the previous subsections, when the isolation reaches the capacity at finite time with $q_{\max} < q_c$, we have the following results on the final epidemic size z_∞:

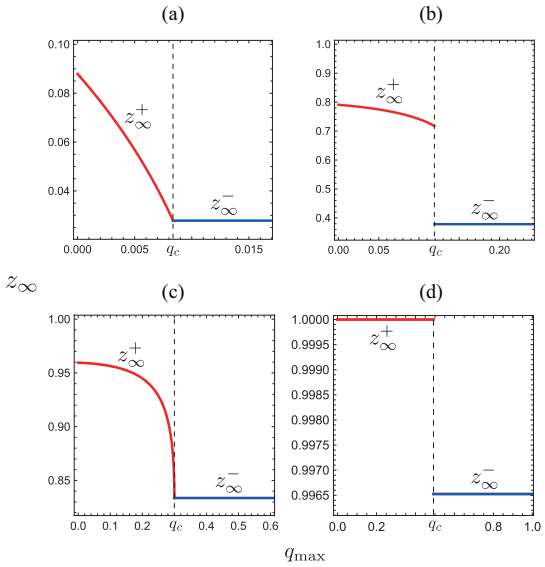

Figure 16: $q_{\max}$-dependence of the final epidemic size z_∞. Numerically drawn for (a) $\mathscr{R}_0 = 0.65$ ($\varepsilon\mathscr{R}_0 = 0.195$; $q_c = 0.0084$); (b) $\mathscr{R}_0 = 1.1$ ($\varepsilon\mathscr{R}_0 = 0.33$; $q_c = 0.1192$); (c) $\mathscr{R}_0 = 1.5$ ($\varepsilon\mathscr{R}_0 = 0.45$; $q_c = 0.3000$); (d) $\mathscr{R}_0 = 2.5$ ($\varepsilon\mathscr{R}_0 = 0.75$; $q_c = 0.4925$), and commonly $u_0 = 0.99$; $\varepsilon = 0.3$; $\gamma = 0.3$. In (d), $z_\infty^+ = 1$ because the system approaches an endemic equilibrium with $\varepsilon\mathscr{R}_0 > 1 - \gamma$ as indicated in Theorem 3.7.

- If $\varepsilon\mathscr{R}_0 < 1 - \gamma$, the system (40) approaches a disease-eliminated equilibrium as shown by Theorem 3.7. Then the final epidemic size z_∞ is given by $z_\infty^+ := 1 - u_\infty^+$ with the unique positive root u_∞^+ of the equation (51).

- If $\varepsilon\mathscr{R}_0 = 1 - \gamma$, the system (40) approaches a disease-eliminated equilibrium accompanied with $u \to 0$ as $\tau \to \infty$, as shown by Theorem 3.7. Then the final epidemic size z_∞ is given by $z_\infty^+ = 1$.

- If $\varepsilon\mathscr{R}_0 > 1 - \gamma$, the system (40) approaches the endemic equilibrium (53) as shown by Theorem 3.7. Then the final epidemic size becomes $z_\infty = 1$ accompanied with $u \to 0$ as $\tau \to \infty$.

Especially as for the final epidemic size at the isolation incapable phase $z_\infty = z_\infty^+$ with $\varepsilon\mathscr{R}_0 < 1 - \gamma$ and $q_{\max} < q_c$, we can find the following feature (Appendix 3.A.18):

Lemma 3.10. *The final epidemic size $z_\infty = z_\infty^+$ is monotonically decreasing in terms of $q_{\max} \in (0, q_c)$ at the isolation incapable phase with $\varepsilon\mathscr{R}_0 < 1 - \gamma$.*

Figure 16 numerically shows the $q_{\max}$-dependence of the final epidemic size z_∞. It is seen that the larger isolation capacity makes the final epidemic size smaller. Figure 16(b) shows a case where the final epidemic size z_∞ becomes drastically large if the isolation reaches the capacity at finite time. The same tendency is seen also in Figure 16(d) whereas the difference between z_∞^- (around 0.9965) and $z_\infty^+ = 1$ is rather small. In contrast, the final epidemic

size z_∞ can be continuous in terms of the isolation capacity $q_{\max}$ as shown in Figure 16(a, c).

We can obtain the following analytical result on such the discontinuity in the $q_{\max}$-dependence of the final epidemic size z_∞ (Appendix 3.A.19):

Theorem 3.9. *When $\varepsilon\mathscr{R}_0 < 1$, the final epidemic size z_∞ has a discontinuity at $q_{\max} = q_c$ such that*

$$z_\infty^\dagger := \lim_{q_{\max}\to q_c - 0} z_\infty^+ > z_\infty^-$$

if and only if one of the following conditions is satisfied:

(i) $1-\gamma \le \varepsilon\mathscr{R}_0 < 1$;

(ii) $\varepsilon(1-\gamma) < \varepsilon\mathscr{R}_0 < 1-\gamma$ *and*

$$u_0(1-q_c)^{\mathscr{R}_0/\gamma - 1} > \frac{\varepsilon}{1-\varepsilon}\Big(\frac{1-\gamma}{\varepsilon\mathscr{R}_0} - 1\Big). \tag{54}$$

If the condition (54) is unsatisfied for $\varepsilon\mathscr{R}_0 \in (\varepsilon(1-\gamma), 1-\gamma)$, then it holds that $z_\infty^\dagger = z_\infty^-$.

The condition (ii) for $\varepsilon = 0$ becomes coincident with the condition obtained in Ahmad and Seno[4] for such a discontinuity about the SIR+Q model without reinfection. The numerical example Figure 16(d) shows the case (i) in Theorem 3.9, and Figure 16(b) does the case (ii). Figure 16(c) shows the case where the condition (54) is unsatisfied with $\varepsilon\mathscr{R}_0 \in (\varepsilon(1-\gamma), 1-\gamma)$. In contrast, Figure 16(a) corresponds to the case of $\mathscr{R}_0 < 1-\gamma$.

In Figure 17, we numerically show the $(\varepsilon, \mathscr{R}_0)$-dependence of the discontinuity of the final epidemic size z_∞ at $q_{\max} = q_c$. For the region corresponding to the case (i) in Theorem 3.9, that is, for the region between two solid boundary curves $\varepsilon\mathscr{R}_0 = 1$ and $\varepsilon\mathscr{R}_0 = 1-\gamma$, we have an endemic equilibrium (53) with $z_\infty^+ = 1$ for $q_{\max} < q_c$, when we can observe the discontinuity at $q_{\max} = q_c$ as Figure 16(d). For the filled region below the solid boundary curve $\varepsilon\mathscr{R}_0 = 1-\gamma$, corresponding to the case (ii) in Theorem 3.9, we have a disease-eliminated equilibrium (52) with $z_\infty^+ < 1$ for $q_{\max} > q_c$, when we can observe the discontinuity at $q_{\max} = q_c$ as Figure 16(b). For the blank region below the solid boundary curve $\varepsilon\mathscr{R}_0 = 1-\gamma$ in Figure 17, we have $z_\infty^+ \to z_\infty^-$ as $q_{\max} \to q_c - 0$, when the final epidemic size z_∞ is continuous even at $q_{\max} = q_c$ as Figure 16(a). For the blank region beyond the solid boundary curve $\varepsilon\mathscr{R}_0 = 1$ in Figure 17, we have an endemic equilibrium (53) at the isolation incapable phase for any $q_{\max} \in [0, 1)$, and there is no case of $q_{\max} \ge q_c = 1$. As indicated by Figure 17, although not simple is the dependence of the discontinuity of the final epidemic size z_∞ on the nature of spreading disease, represented by the parameters $\mathscr{R}_0$ and ε, it is implied that the higher risk of reinfection (i.e., with the larger ε) is more likely to cause such the discontinuity. Moreover, the faster isolation (i.e., with the larger γ) is more like to do so too. The faster isolation means the more effective quarantine, which could be regarded as a better feature in the isolation operation for the public health measure. Therefore, sufficiently effective quarantine and fast isolation would be highly important to suppress

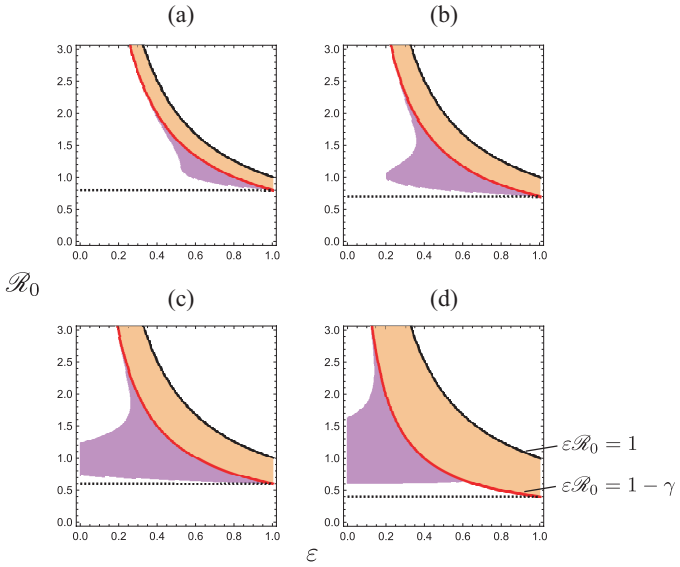

Figure 17: $(\varepsilon, \mathscr{R}_0)$-dependence of the discontinuity of the final epidemic size z_∞ at $q_{\max} = q_c$. For the filled region, we have $z_\infty^\dagger > z_\infty^-$ as shown in Theorem 3.9. Numerically drawn with (a) $\gamma = 0.2$; (b) $\gamma = 0.3$; (c) $\gamma = 0.4$; (d) $\gamma = 0.6$, and commonly $u_0 = 0.9$. The upper solid boundary curve is of $\varepsilon\mathscr{R}_0 = 1$, and the lower is of $\varepsilon\mathscr{R}_0 = 1-\gamma$. The horizontal dotted line is of $\mathscr{R}_0 = 1-\gamma$. The detail is in the main text.

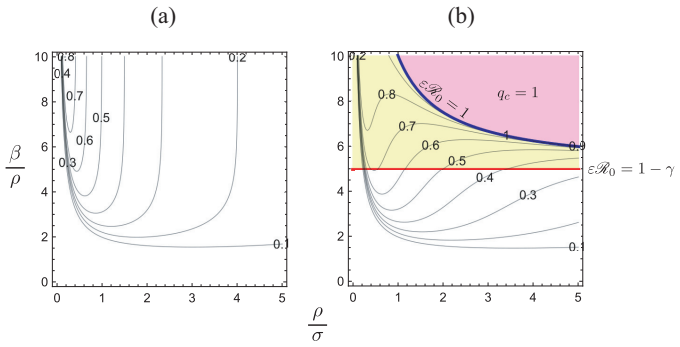

Figure 18: Numerically drawn contour plots of q_c in terms of $(\rho/\sigma, \beta/\rho)$, making use of Theorem 3.6, Corollary 3.6.1, and Theorem 3.7: (a) $\varepsilon = 0$; (b) $\varepsilon = 0.2$. Commonly, $u_0 = 0.99$. In (b), the endemic equilibrium may appear only for $\varepsilon\mathscr{R}_0 > 1-\gamma$, that is, for $\beta/\rho > 1/\varepsilon$. For $\varepsilon\mathscr{R}_0 \geq 1$, that is, for $\varepsilon\beta/\rho \geq 1+\sigma/\rho$, the system (40) necessarily enters the isolation incapable phase for any isolation capacity $q_{\max}$, corresponding to $q_c = 1$.

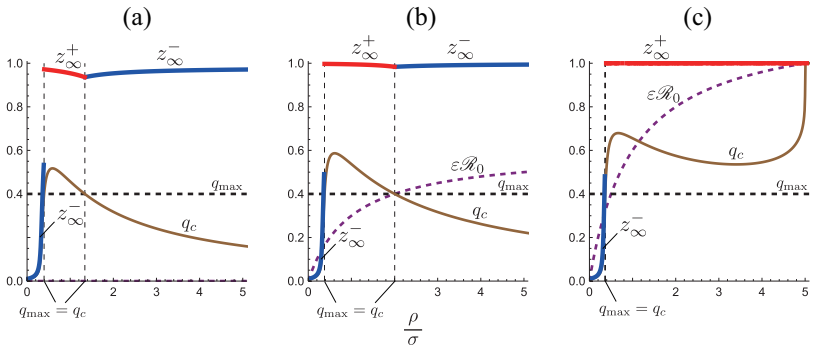

Figure 19: ρ/σ-dependence of the critical isolation capacity q_c and the final epidemic size z_∞. Numerically drawn for (a) $\varepsilon = 0.0$; (b) $\varepsilon = 0.15$; (c) $\varepsilon = 0.30$, and commonly $u_0 = 0.99$; $q_{\max} = 0.4$; $\beta/\rho = 4.0$.

the endemic size or the final epidemic size, because the sufficient capacity of isolation may drastically reduce such sizes as the consequence of the epidemic dynamics.

Figure 18 shows the numerical calculation of the $(\rho/\sigma, \beta/\rho)$-dependence of q_c for our model (40), where we used q_c determined by (49) in Corollary 3.6.1, which can be expressed by only four parameters u_0, ε, β/ρ, and ρ/σ with the original parameters in our model (39). The parameter β/ρ corresponds in fact to the basic reproduction number of the epidemic dynamics by (39) without isolation. Hence, in contrast to $\mathscr{R}_0$ with isolation, we may call β/ρ the *primitive* basic reproduction number at the stage of the disease invasion in the community when the quarantine measure has not yet been applied.

Numerical results in Figure 18 clearly demonstrate that the severe epidemic with the larger primitive basic reproduction number requires the larger isolation capacity to avoid its breakdown, which matches our intuitive expectation as seen in the $\mathscr{R}_0$-dependence of q_c in Subsection 3.4.4 (refer to Figure 13). On the whole, a sufficiently high efficiency of the quarantine could make the isolation capacity smaller to avoid its breakdown, and a sufficiently low efficiency could induce the breakdown, as mentioned also at the end of the previous section. On the other hand, the critical isolation capacity q_c appears to have a non-trivial relation to the efficiency of quarantine operation, represented by the parameter σ. There are some cases where q_c becomes relatively large in an intermediate range of σ, while q_c gets smaller for sufficiently small or large σ. Such a non-trivial dependence of the q_c on the quarantine efficiency was found and discussed also in Ahmad and Seno[4] on the SIR+Q model without reinfection (refer to Figure 18(a)). Our numerical calculations in Figure 18 imply that such a feature appears remarkably for $\varepsilon = 0$, that is, for the model without reinfection, and it becomes more complicated for the model with reinfection.

Actually as for the dependence of the final epidemic size z_∞ on the quarantine efficiency, it can result in an unexpected feature as shown in Figure 19. As Ahmad and Seno[4] investigated for the model without reinfection, the final epidemic size z_∞ could have a non-monotone relation to σ, and then z_∞ could take a local maximum for an intermediate value of σ. Sufficiently high quarantine efficiency (i.e., sufficiently large σ) can make the critical isolation capacity q_c rather small, and thus it can significantly reduce the final epidemic size z_∞. As indicated by Figure 19, it is necessary for the quarantine to have

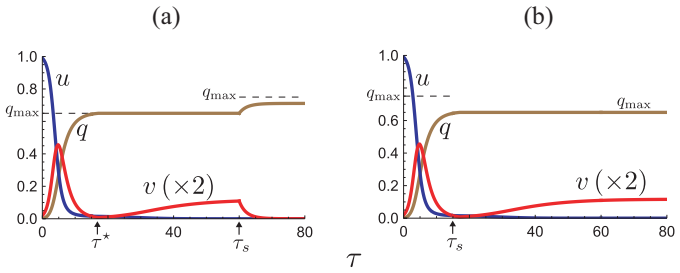

Figure 20: Numerical examples for the temporal variation of the model (40) with a change of the isolation capacity at $\tau = \tau_s$: (a) $q_{\max} = 0.65$ to 0.75, $\tau_s = 60$; (b) $q_{\max} = 0.75$ to 0.65, $\tau_s = 15$. Commonly, $\gamma = 0.5$; $\mathscr{R}_0 = 2.0$; $\varepsilon = 0.3$ ($\varepsilon\mathscr{R}_0 = 0.6$); $u_0 = 0.99$; $q_c = 0.6554$. In (a), the isolation reaches the capacity and becomes incapable at a moment $\tau = \tau^\star$, and then the disease tends to become endemic until $\tau = \tau_s$, whereas it turns to be eliminated after the raise of isolation capacity at $\tau = \tau_s$. In (b), the disease tends to be eliminated until $\tau = \tau_s$, whereas it revives after the reduction of isolation capacity after it.

a sufficiently high efficiency in order to avoid the breakdown of isolation and to successfully suppress the final epidemic size. However, as shown by the numerical calculations in Figures 18 and 19, the reinfection could make complicated the relation of the quarantine efficiency to the critical isolation capacity, and such a complicatedness implies a difficulty to prepare an appropriate measure of the quarantine and isolation for the public health in a community.

From the definition of parameters ρ and σ for the epidemic dynamics by (39), the expected duration of the infectivity (i.e., the transmissibility of the disease by an infective) is given by $1/\rho$, and the expected duration of the detection of an infective until it gets isolated is given by $1/\sigma$ at the isolation effective phase. In a sense, it would be reasonable to assume that $1/\sigma < 1/\rho$, that is, $\rho/\sigma < 1$, because the detection of an infective is possible only when the individual has the infectivity. However, the quarantine efficiency must depend on the availability of medical services and the voluntary access of infectives to such a service. Therefore, with the dependence on such factors, poor quarantine efficiency could make $\rho/\sigma \geq 1$.

3.4.8 *Discussion*

In this section, we analyzed an SIRI+Q model that incorporates both reinfection and limited isolation capacity. The results indicate that the increase of the isolation capacity makes the endemic size and the final epidemic size smaller as implied by the mathematical results on the SIR+Q model in Section 3.3, while mathematical arguments required to show important features because of the reinfection introduced.

More significantly, it is implied that the breakdown of isolation due to its limited capacity could induce a considerable change of the epidemic severity accompanied with the revival of outbreak, the emergence of endemicity, or a staggeringly wide spread of the disease, for example. In other words, the isolation capacity could be a crucial factor for the public health policy not only to reduce the epidemic size but also to suppress the endemicity.

The higher risk of reinfection leads to the larger critical capacity of isolation: The larger isolation capacity is necessary to avoid the severe con-

sequence of the epidemic dynamics with a reinfectious disease. In general, the reinfectivity of spreading disease must induce the higher importance of the isolation capacity for the effective public health measure, because the recovered individual may get infected again and further become a spreader of the disease. Actually, since the existence of reinfectivity could induce the endemicity of the disease, the isolation capacity must be rather important to control the disease spread. Figure 20 gives numerical examples with our model (40) to indicate the importance. An increase of the isolation capacity may result in the effective suppression of the endemicity and drive the disease to its elimination as in Figure 20(a). In contrast, a careless reduction of the isolation capacity, as in Figure 20(b), for example, because of the low prevalence monitored in the epidemic dynamics, may induce the revival of the disease spread by the released endemicity with the reinfectivity.

In our results as illustrated by Figure 17, when the isolation capacity is insufficient, the higher risk of reinfection is more likely to not only induce an endemic state but also lead to a discontinuously larger epidemic size even though the disease finally gets eliminated. Further, as was shown in our mathematical results, the highly effective quarantine with a sufficient capacity of isolation could result in a successful suppression of the endemic size or the final epidemic size to an unexpectedly distinct extent. This implies the importance of the isolation capacity as a measure for the public health, while such a sufficient capacity of the isolation or an effective quarantine must be ready before the outbreak of a disease spread because it would generally become hard to prepare after it.

The smaller critical value of the isolation capacity q_c is better for the management of the epidemic dynamics. That is, the smaller critical value for the isolation capacity makes an isolation policy with a feasible capacity more likely to be invulnerable to avoid its breakdown. The larger critical value for the isolation capacity indicates a harder situation for the public health policy since a large capacity of isolation is necessary to avoid its breakdown and to suppress the endemicity or make the final epidemic size at a low level. As the factors to determine the effectiveness of a public health policy against a spreading disease, the isolation capacity and the quarantine efficiency could be independently improved. Our results clearly indicate their relevance, and it is implied that the improvement about one of them could make that about the other more feasible, as discussed in Shahverdi *et al.*[146]. Inversely, when one of them could not be sufficiently improved, the improvement of the other becomes less effective.

3.5 INFLUENCE OF ISOLATION DISCHARGE

In this section, we analyze the system (20) introduced in Subsection 3.2.5, which incorporates both reinfection and discharge from isolation.

3.5.1 *Endemic equilibria*

Endemic equilibrium at the isolation well-functioning phase

As numerically exemplified by Figure 21(b), there is a case where the system (20) with a limited isolation capacity may approach an endemic equilibrium E^*_{w} given by (24) in Subsection 3.2.5 at the isolation well-functioning phase, even if there is a finite period in which it temporally stays at the isolation malfunctioning phase. In this subsection, we consider the condition that such

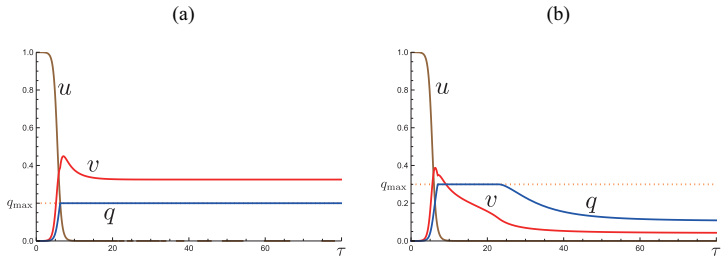

Figure 21: Numerical examples of the convergence to an endemic state for the system (20). (a) $q_{\max} = 0.2$; (b) $q_{\max} = 0.3$, commonly with $(u(0), v(0), q(0), w(0)) = (0.99999, 0.00001, 0.0, 0.0)$; $\mathscr{R}_0 = 3.0$; $\varepsilon = 0.35$; $\varepsilon\mathscr{R}_0 = 1.05$; $\gamma = 0.5$; $a = 0.2$; $q^*_{\mathrm{w}} = 0.106383$. In (a), the system approaches an endemic equilibrium E^*_{m} at the isolation malfunctioning phase, while, in (b), it approaches an endemic equilibrium E^*_{w} at the isolation well-functioning phase.

an endemic equilibrium E^*_{w} exists as an asymptotically stable state at the isolation well-functioning phase for the system (20) with a limited isolation capacity.

If such an equilibrium E^*_{w} exists for the system (17) at the isolation well-functioning phase, that is, for (23), then it is locally asymptotically stable if and only if $\varepsilon\mathscr{R}_0 > 1$, as shown by Theorem 3.1. To have it as a feasible equilibrium at the isolation well-functioning phase for the system (20), it must belong to Ω^{w}_1 defined in Subsection 3.2.5. In other words, it is necessary that $q^*_{\mathrm{w}} < q_{\max}$, because otherwise E^*_{w} given by (24) cannot exist for the system (20) at the isolation well-functioning phase where the value of q must be less than $q_{\max}$. Hence, from (25) and Theorem 3.1, we have the following result:

Theorem 3.10. *For the system (20), the endemic equilibrium E^*_{w} with the endemic size v^*_{w} given by (24) exists at the isolation well-functioning phase if and only if*

$$\varepsilon\mathscr{R}_0 > 1 \quad \textit{and} \quad q_{\max} > q^*_{\mathrm{w}}, \tag{55}$$

where q^*_{w} is given by (25) and (26) in Subection 3.2.5. Then E^*_{w} is locally asymptotically stable.

Furthermore from (24) and (55), we note that the endemic size v^*_{w} at E^*_{w} necessarily has the following feature:

Corollary 3.10.1. *At the endemic equilibrium E^*_{w} for the system (20), the endemic size v^*_{w} satisfies that $\gamma v^*_{\mathrm{w}} < a q_{\max}$.*

Remark that the system (20) approaches a disease-eliminated equilibrium only if $\varepsilon\mathscr{R}_0 \leq 1$, as shown by Theorem 3.1. Then we have $q \to 0$ as $\tau \to \infty$ because of the discharge of isolated individuals from the isolation. However, we will show in the following part that the condition $\varepsilon\mathscr{R}_0 \leq 1$ is not sufficient for the system (20) to approach a disease-eliminated equilibrium. On the other hand, Lemma 3.15 in Appendix 3.A.3 for the proof of Theorem 3.1 indicates that the system (20) never approaches any disease-eliminated equilibrium if $\varepsilon\mathscr{R}_0 > 1$, and then it approaches an endemic state.

Endemic equilibrium at the isolation malfunctioning phase

As numerically exemplified in Figure 21(a), there is a case where the system approaches an endemic equilibrium

$$(u, v, q, w) = E_{\mathrm{m}}^{*}\Big(0,\, v_{\mathrm{m}}^{*},\, q_{\max},\, 1 - q_{\max} - v_{\mathrm{m}}^{*}\Big), \tag{56}$$

with $v_{\mathrm{m}}^{*} > 0$ at the isolation malfunctioning phase. Here we consider the condition that such an endemic equilibrium E_{m}^{*} exists as an asymptotically stable state.

When the system (20) stays at the isolation malfunctioning phase, that is, when the solution of (20) belongs to Ω_1^{m} defined in Subsection 3.2.5, the epidemic dynamics is governed by the following system corresponding to (18) with the variable and parameter transformation for the non-dimensionalization given in Subsection 3.2.5:

$$\begin{aligned}
\frac{du}{d\tau} &= -\mathscr{R}_0 \frac{v}{1 - q_{\max}} u; \\
\frac{dv}{d\tau} &= \mathscr{R}_0 \frac{v}{1 - q_{\max}} u + \varepsilon \mathscr{R}_0 \frac{v}{1 - q_{\max}} w - (1 - \gamma) v - a q_{\max}; \\
\frac{dq}{d\tau} &= 0; \\
\frac{dw}{d\tau} &= (1 - \gamma) v + a q_{\max} - \varepsilon \mathscr{R}_0 \frac{v}{1 - q_{\max}} w.
\end{aligned} \tag{57}$$

Since it holds that $u + v + q_{\max} + w = 1$ for any τ at the isolation malfunctioning phase, the dynamics governed by the system (57) can be regarded as mathematically equivalent to the dynamics with the following two dimensional closed system:

$$\begin{aligned}
\frac{du}{d\tau} &= -\mathscr{R}_0 \frac{v}{1 - q_{\max}} u; \\
\frac{dv}{d\tau} &= (1 - \varepsilon) \mathscr{R}_0 \frac{v}{1 - q_{\max}} u - \Psi(v),
\end{aligned} \tag{58}$$

where

$$\Psi(v) := \frac{\varepsilon \mathscr{R}_0}{1 - q_{\max}} v^2 - \big\{\varepsilon \mathscr{R}_0 - (1 - \gamma)\big\} v + a q_{\max}. \tag{59}$$

From the former equation of (58), we have $u \to 0$ when $v \to v_{\mathrm{m}}^{*} > 0$ as $\tau \to \infty$. Hence, from the latter equation of (58), to have the system (20) approaching an endemic equilibrium E_{m}^{*} given by (56), it is necessary that the equation $\Psi(v) = 0$ has a root such that $v = v_{\mathrm{m}}^{*} \in [a q_{\max}/\gamma,\, 1 - q_{\max})$. This is because $\gamma v_{\mathrm{m}}^{*} \geq a q_{\max}$ is necessary to have the system (20) at the isolation malfunctioning phase as described in Subsection 3.2.5. Further, since such an endemic state of E_{m}^{*} must be sustained with the reinfection for the recovered population after the susceptible individuals disappear, it is necessary that $w_{\mathrm{s}}^{*} = 1 - v_{\mathrm{m}}^{*} - q_{\max} > 0$, that is, $v_{\mathrm{m}}^{*} < 1 - q_{\max}$. These conditions about v_{m}^{*} show it necessary that $a q_{\max}/\gamma < 1 - q_{\max}$:

Lemma 3.11. *If the endemic equilibrium E_{m}^{*} given by (56) exists at the isolation malfunctioning phase for the system (20), then it is necessary that*

$$\mathcal{A} := \frac{a q_{\max}}{1 - q_{\max}} < \gamma. \tag{60}$$

Here the parameter $\mathcal{A}$ represents the nature of isolation, which is positively correlated to $q_{\max}$ and a, that is, to the capacity $Q_{\max}$ and the discharge rate α.

Now taking account of Lemma 3.11, we can obtain the following result about the existence and stability of the endemic equilibrium E^*_{m} for the system (20) at the isolation malfunctioning phase (Appendix 3.A.20):

Theorem 3.11. *Once the system* (20) *enters the isolation malfunctioning phase at a moment, it necessarily approaches the unique endemic equilibrium* E^*_{m} *given by* (56) *with the endemic size*

$$v^*_{\mathrm{m}} = \frac{1-q_{\max}}{2}\left\{1 - \frac{1-\gamma}{\varepsilon\mathscr{R}_0} + \sqrt{\left(1-\frac{1-\gamma}{\varepsilon\mathscr{R}_0}\right)^2 - \frac{4\mathcal{A}}{\varepsilon\mathscr{R}_0}}\right\}, \tag{61}$$

if and only if

$$\varepsilon\mathscr{R}_0 > 1-\gamma \quad \textit{and} \quad \mathcal{A} \le \mathcal{A}_c \tag{62}$$

with

$$\mathcal{A}_c := \begin{cases} \mathcal{A}_1 := \dfrac{\varepsilon\mathscr{R}_0}{4}\left(1-\dfrac{1-\gamma}{\varepsilon\mathscr{R}_0}\right)^2 & \textit{for } \varepsilon\mathscr{R}_0 \in (1-\gamma,\, 1+\gamma\,]; \\ \mathcal{A}_2 := \gamma\left(1-\dfrac{1}{\varepsilon\mathscr{R}_0}\right) \quad (= a/B^*_{\mathrm{w}}) & \textit{for } \varepsilon\mathscr{R}_0 \in (1+\gamma,\, \infty). \end{cases} \tag{63}$$

We can easily find that $\mathcal{A}_c \le \gamma$ for any $\gamma \in (0,1)$ and $\varepsilon\mathscr{R}_0 > 1-\gamma$, in logical accordance with Lemma 3.11. In addition, it holds that $\mathcal{A}_1 \ge \mathcal{A}_2$ for $\varepsilon\mathscr{R}_0 > 1-\gamma$, and $\mathcal{A}_1 = \mathcal{A}_2$ only for $\varepsilon\mathscr{R}_0 = 1+\gamma$.

Remark that the condition $\mathcal{A} \le \mathcal{A}_2$ is equivalent to $q_{\max} \le q^*_{\mathrm{w}}$ that is the complement to the latter condition of (55) in Theorem 3.10. Therefore, under the condition that $\varepsilon\mathscr{R}_0 > 1+\gamma$ and $\mathcal{A} \le \mathcal{A}_2$, no endemic state exists at the isolation well-functioning phase. Thus, taking account of Theorem 3.1, we find the following result:

Corollary 3.11.1. *If* $\varepsilon\mathscr{R}_0 > 1+\gamma$ *and* $\mathcal{A} \le \mathcal{A}_2$, *the system* (20) *enters the isolation malfunctioning phase at a moment, and it necessarily approaches the endemic equilibrium* E^*_{m} *given by* (56).

We note that the result of Theorem 3.11 as $a \to 0$, that is, $\mathcal{A} \to 0$ agrees with the result (53) of Theorem 3.7 in Subsection 3.4.4, where the endemic equilibrium E^*_{m} given by (56) with (61) agrees with the endemic equilibrium E^+_* at "the isolation incapable phase", and the condition (62) becomes only the former as shown therein.

According to a mathematical consistency of the results in Theorem 3.11 and Lemma 3.2 of Subsection 3.2.5, we can obtain the following corollary too (Appendix 3.A.21):

Corollary 3.11.2. *As* $\gamma \to +0$ *with* $\varepsilon\mathscr{R}_0 > 1$, *the endemic equilibrium* E^*_{m} *given by* (56) *converges to the endemic equilibrium* (22) *for the system* (20) *with* $\gamma = 0$, *that is, for the model* (19) *with* $\sigma = 0$ *when the isolation is not taken as a measure for the public health.*

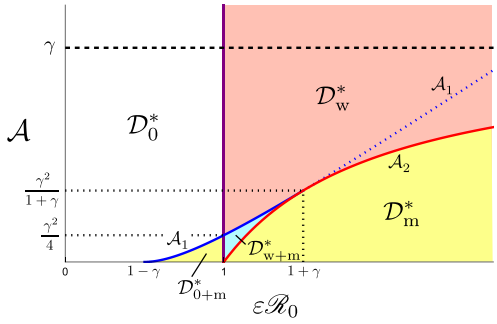

Figure 22: $(\varepsilon\mathscr{R}_0, \mathcal{A})$-dependence of the existence of feasible endemic equilibria, E_{w}^* at the isolation well-functioning phase and E_{m}^* at the isolation malfunctioning phase. For the regions $\mathcal{D}_0^*$, $\mathcal{D}_{0+\mathrm{m}}^*$, $\mathcal{D}_{\mathrm{w}}^*$, $\mathcal{D}_{\mathrm{w+m}}^*$, and $\mathcal{D}_{\mathrm{m}}^*$.

From the arguments in Appendix 3.A.20 for the proof of Theorem 3.11, we can obtain the following important result on the behavior of the system (20) at the isolation malfunctioning phase:

Lemma 3.12. *When the condition* (62) *is unsatisfied, the system* (20) *never enters the isolation malfunctioning phase, or it eventually returns to the isolation well-functioning phase from the isolation malfunctioning phase at a certain moment.*

Accordingly, from Lemma 3.12 with Theorems 3.1 and 3.10, we can find the following result:

Theorem 3.12. *When the condition* (62) *is unsatisfied, the system* (20) *approaches the endemic equilibrium E_{w}^* given by* (24) *at the isolation well-functioning phase if $\varepsilon\mathscr{R}_0 > 1$, or alternatively a disease-eliminated equilibrium if $\varepsilon\mathscr{R}_0 \leq 1$.*

With those results of Theorems 3.10–3.12, Lemma 3.11, and Corollary 3.11.1, we can get the $(\varepsilon\mathscr{R}_0, \mathcal{A})$-dependence of the existence of feasible endemic equilibria, E_{w}^* at the isolation well-functioning phase and E_{m}^* at the isolation malfunctioning phase, as shown by Figure 22, where the parameter region can be classified in the following five subregions:

$$
\begin{aligned}
\mathcal{D}_0^* &:= \left\{(\varepsilon\mathscr{R}_0, \mathcal{A}) \,\middle|\, \varepsilon\mathscr{R}_0 \leq 1,\, \mathcal{A} > \mathcal{A}_1\right\};\\
\mathcal{D}_{0+\mathrm{m}}^* &:= \left\{(\varepsilon\mathscr{R}_0, \mathcal{A}) \,\middle|\, 1-\gamma < \varepsilon\mathscr{R}_0 \leq 1,\, 0 < \mathcal{A} \leq \mathcal{A}_1\right\};\\
\mathcal{D}_{\mathrm{w}}^* &:= \left\{(\varepsilon\mathscr{R}_0, \mathcal{A}) \,\middle|\, 1 < \varepsilon\mathscr{R}_0 < 1+\gamma,\, \mathcal{A} > \mathcal{A}_1\right\} \cup \left\{(\varepsilon\mathscr{R}_0, \mathcal{A}) \,\middle|\, \varepsilon\mathscr{R}_0 \geq 1+\gamma,\, \mathcal{A} > \mathcal{A}_2\right\};\\
\mathcal{D}_{\mathrm{w+m}}^* &:= \left\{(\varepsilon\mathscr{R}_0, \mathcal{A}) \,\middle|\, 1 < \varepsilon\mathscr{R}_0 < 1+\gamma,\, \mathcal{A}_2 < \mathcal{A} \leq \mathcal{A}_1\right\};\\
\mathcal{D}_{\mathrm{m}}^* &:= \left\{(\varepsilon\mathscr{R}_0, \mathcal{A}) \,\middle|\, \varepsilon\mathscr{R}_0 > 1,\, \mathcal{A} \leq \mathcal{A}_2\right\}.
\end{aligned}
$$

For the region $\mathcal{D}_{\mathrm{w+m}}^*$, both of E_{w}^* and E_{m}^* exist. For the region $\mathcal{D}_{0+\mathrm{m}}^*$, the endemic equilibrium E_{m}^* exists while a disease-eliminated equilibrium is feasible at the same time. For the regions $\mathcal{D}_{\mathrm{w}}^*$ and $\mathcal{D}_{\mathrm{m}}^*$, the equilibria E_{w}^* and E_{m}^* are globally asymptotically stable respectively. For the region $\mathcal{D}_0^*$, the system eventually approaches a disease-eliminated equilibrium.

Then we find the following result on the sufficient capacity of isolation to avoid its malfunction:

Theorem 3.13. *If $\mathcal{A} \geq \gamma$, that is, if the isolation capacity $q_{\max}$ is large enough to satisfy that*

$$q_{\max} \geq q_{\text{suff}} := \frac{1}{1 + a/\gamma}, \tag{64}$$

then the epidemic dynamics of (20) never results in the saturation of isolation capacity, independently of ε and $\mathscr{R}_0$, that is, of the disease's infectivity.

This result is mathematically consistent to Lemma 3.11: When the condition (64) is satisfied, there is no endemic equilibrium at the isolation malfunctioning phase. Remark that the sufficient capacity q_{suff} is determined only by the ratio $a/\gamma = \alpha/\sigma$, that is, by the ratio of isolation discharge and quarantine rates.

However, even if the condition (64) is satisfied, the disease may become endemic while the isolation is functioning well. Actually we can easily find that necessarily $q_{\text{w}}^* < q_{\text{suff}}$. Such an endemicity arises if $\varepsilon\mathscr{R}_0 > 1$, as already indicated by Theorem 3.12:

Corollary 3.13.1. *Even when the isolation capacity $q_{\max}$ is large enough to satisfy the condition (64), so that the isolation becomes functioning well, the system (20) approaches the endemic equilibrium E_{w}^* defined by (24) if $\varepsilon\mathscr{R}_0 > 1$.*

Consequently, for the disease with a sufficiently high likelihood of reinfection as $\varepsilon\mathscr{R}_0 > 1$, the disease eventually becomes endemic, independently of whether the isolation becomes malfunctioning or not. For such a reinfectious disease, the isolation measure could not suppress its spread even with its satisfactory management, whereas it necessarily serves the reduction of endemic size in the community. Nonetheless, independently of how high likelihood of reinfection the spreading disease has, the community should have an action to avoid the malfunction of isolation, because the malfunction of isolation must show the deficiency in the public health measure to the people, which may causes a social unrest with the exhaustion of medical services about the quarantine/isolation measure. Thus, naturally it is desirable to have a sufficient isolation capacity ready for the public health in a community, even though it could not suppress the endemicity of a disease.

In contrast, for the disease with a low likelihood of reinfection as $\varepsilon\mathscr{R}_0 < 1$, we find the secondary sufficient capacity of isolation to suppress the endemicity as indicated by Figure 22:

Corollary 3.13.2. *If $\mathcal{A} \geq \gamma^2/4$, that is, if the isolation capacity $q_{\max}$ is large enough to satisfy that*

$$q_{\max} \geq q_{\text{secsuff}} := \frac{1}{1 + 4a/\gamma^2}, \tag{65}$$

then the epidemic dynamics of (20) for the disease with $\varepsilon\mathscr{R}_0 < 1$ necessarily results in the elimination of disease.

The inequality $q_{\text{secsuff}} < q_{\text{suff}}$ necessarily holds. We may regard q_{secsuff} as the critical value for the isolation capacity $q_{\max}$ according to the transmissible disease relatively less reinfectious. However, as seen from Figure 22, even

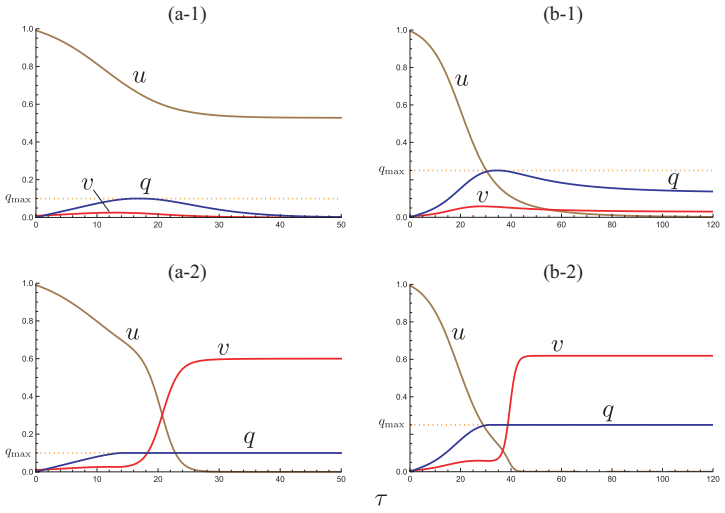

Figure 23: Temporal variations by the system (20) in the bistable situation of (a) $\mathcal{D}^*_{0+\mathrm{m}}$; (b) $\mathcal{D}^*_{\mathrm{w}+\mathrm{m}}$ respectively. Numerically calculated with (a) $(\varepsilon\mathscr{R}_0, \mathcal{A}) = (0.4, 0.02222)$; $q_{\max} = 0.1$; $\mathscr{R}_0 = 1.14286$; $\varepsilon = 0.35$; $\varepsilon\mathscr{R}_0^c = 0.248676$; $v(0) = 0.009$ for (a-1), 0.010 for (a-2). (b) $(\varepsilon\mathscr{R}_0, \mathcal{A}) = (1.035, 0.06667)$; $q_{\max} = 0.25$, $\mathscr{R}_0 = 1.15$; $\varepsilon = 0.9$; $\varepsilon\mathscr{R}_0^{cc} = 1.08$; $v(0) = 0.005$ for (b-1), 0.006 for (b-2). Commonly $\gamma = 0.9$; $a = 0.2$. In (a-1), the system approaches a disease-eliminated equilibrium, and in (b-1), it approaches the endemic equilibrium E^*_{w} at the isolation well-functioning phase. In contrast, it approaches the endemic equilibrium E^*_{m} at the isolation malfunctioning phase in (a-2) and (b-2).

if $q_{\max} \geq q_{\mathrm{secsuff}}$, the emergence of a reinfectious disease with a high reinfectivity as $\varepsilon\mathscr{R}_0 > 1$ leads to its endemicity in the community, and then the isolation may become malfunctioning if $q_{\max} < q_{\mathrm{suff}}$. Since the community should prepare also for the emergence of such a highly reinfectious disease from the viewpoint of well-organized public health policy, it must be desirable to have a sufficient capacity of isolation as $q_{\max} \geq q_{\mathrm{suff}}$. This would be one of lessons drawn from our experience of the recent pandemic with COVID-19.

Incidentally we note that the results of Theorem 3.13 and Corollary 3.13.2 become meaningless as $a \to 0$ when no discharge of the isolation occurs. The conditions (64) and (65) can actually never satisfied for $a = 0$, since the condition $q_{\max} \geq 1$, that is, $Q_{\max} \geq N$, is regarded as unrealizable in general. As seen from Figure 22, for $a = 0$, that is, for $\mathcal{A} = 0$, we have only three regions $\mathcal{D}^*_0$, $\mathcal{D}^*_{\mathrm{m}}$, and $\mathcal{D}^*_{0+\mathrm{m}}$ on the horizontal axis, correspondingly to the results obtained about the model without the discharge from isolation in Subsection 3.4.4.

3.5.2 *Bistability*

From Theorems 3.1 and 3.10–3.12, we find that there are some cases where a bistable situation occurs as indicated in Figure 22:

Theorem 3.14. *The system* (20) *is in a bistable situation to approach either of*

(i) a disease-eliminated equilibrium or the endemic equilibrium E^*_{m} if $(\varepsilon\mathscr{R}_0, \mathcal{A}) \in \mathcal{D}^*_{0+\mathrm{m}}$;

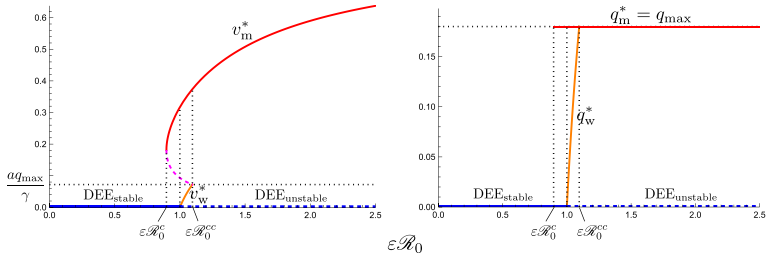

Figure 24: Bifurcation of the equilibrium values v^* and q^* in terms of $\varepsilon\mathscr{R}_0$ for the system (20) with $q_{\max}$ satisfying the condition (66). Numerically drawn with (24), (25), and (61) for $\mathcal{A} = 0.04390$; $a = 0.2$; $q_{\max} = 0.18$; $\gamma = 0.5$, taking account of the results given by Theorems 3.1–3.11, and Lemma 3.12. Refer to Figure 22. In the figures, $(v^*_{\rm w}, q^*_{\rm w})$ is of the endemic equilibrium $E^*_{\rm w}$ at the isolation well-functioning phase, and $(v^*_{\rm m}, q^*_{\rm s})$ is of the endemic equilibrium $E^*_{\rm m}$ at the isolation malfunctioning phase. DEE indicates a disease-eliminated equilibrium with $v^* = q^* = 0$. Two critical values $\varepsilon\mathscr{R}_0^c$ and $\varepsilon\mathscr{R}_0^{cc}$ for $\varepsilon\mathscr{R}_0$ are given by (67) and (68), 0.896859 and 1.09626 respectively in this numerical calculation. Remark that $\varepsilon\mathscr{R}_0^c \in (1-\gamma, 1)$ and $\varepsilon\mathscr{R}_0^{cc} \in (1, 1+\gamma)$.

(ii) endemic equilibria $E^*_{\rm w}$ or $E^*_{\rm m}$ if $(\varepsilon\mathscr{R}_0, \mathcal{A}) \in \mathcal{D}^*_{\rm w+m}$.

As mentioned in the previous subsection, the system (20) with $a \to 0$, that is, the model (40) without the discharge from isolation considered in Section 3.4 does not have any bistable situation with different asymptotically stable endemic equilibria. It has only a bistable situation with a disease-eliminated equilibrium and an endemic one, where the endemic equilibrium is at "the isolation incapable phase" where the isolation breaks down by the saturation of its capacity. Such a bistable situation corresponds to the region $\mathcal{D}^*_{0+\rm m}$ in Figure 22 for the system (20) with the discharge from isolation. As a distinct nature of the system (20) with the discharge from isolation, it can be in a bistable situation with different two asymptotically stable endemic equilibria $E^*_{\rm w}$ and $E^*_{\rm m}$, which corresponds to the region $\mathcal{D}^*_{\rm w+m}$ in Figure 22. As in the model (40) in Section 3.4, the final state of the system (20) depends on whether the system enters the isolation malfunctioning phase or not in such a bistable situation.

Figure 23(a) gives numerical examples for $(\varepsilon\mathscr{R}_0, \mathcal{A}) \in \mathcal{D}^*_{0+\rm m}$ such that the system approaches either of a disease-eliminated equilibrium or the endemic equilibrium $E^*_{\rm m}$, depending on the initial condition. Numerical examples for $(\varepsilon\mathscr{R}_0, \mathcal{A}) \in \mathcal{D}^*_{\rm w+m}$ are given as Figure 23(b) too. As seen from Figure 22, such a bistable situation occurs only for sufficiently small $\mathcal{A}$ and a limited range of $\varepsilon\mathscr{R}_0$:

Corollary 3.14.1. *A bistable situation occurs only if $\varepsilon\mathscr{R}_0 \in (1-\gamma, 1+\gamma)$ and $\mathcal{A} < \gamma^2/(1+\gamma)$, that is,*

$$q_{\max} < \frac{1}{1 + a/\gamma + a/\gamma^2} \in (q_{\rm secsuff}, q_{\rm suff}). \tag{66}$$

We remark that the range $(1-\gamma, 1+\gamma)$ of $\varepsilon\mathscr{R}_0$ for the bistable situation is bounded above by 2 because of $\gamma \in (0, 1)$. Thus, if $\varepsilon\mathscr{R}_0 \geq 2$, such a bistable situation does not occur, and the epidemic dynamics leads to an endemic state, as already seen by Figure 22 in Subsection 3.5.1.

The bifurcation diagram given in Figure 24 clearly indicates the existence of bistability according to two equilibria for the system (20) with $q_{\max}$ sat-

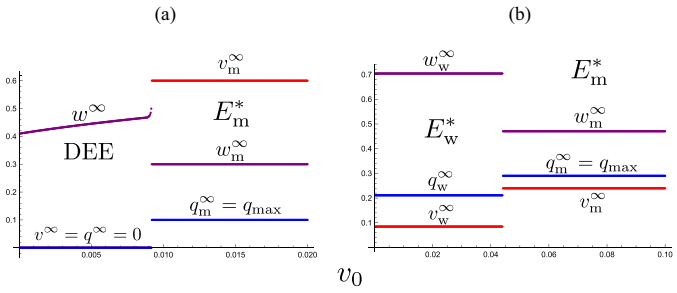

Figure 25: Dependence of the values v^{∞}, q^{∞}, and w^{∞} at the final state on the initial infective population size v_0 for the system (20) in a bistable situation: (a) $\mathcal{D}_{0+\mathrm{m}}^{*}$; (b) $\mathcal{D}_{\mathrm{w}+\mathrm{m}}^{*}$. The system converges to an equilibrium with v_{∞} and q_{∞} which are numerically calculated with (a) $(\varepsilon\mathscr{R}_0, \mathcal{A}) = (0.4, 0.02222)$; $q_{\max} = 0.10$; $\mathscr{R}_0 = 1.14286$; $\varepsilon = 0.35$; $\gamma = 0.9$; (b) $(\varepsilon\mathscr{R}_0, \mathcal{A}) = (1.12, 0.08169)$; $q_{\max} = 0.29$; $\mathscr{R}_0 = 1.4$; $\varepsilon = 0.8$; $\gamma = 0.5$, and commonly $a = 0.2$; $v(0) = 0.00001$.

isfying the condition (66). As shown in Figure 24, we have critical values $\varepsilon\mathscr{R}_0^{c}$ and $\varepsilon\mathscr{R}_0^{cc}$ for $\varepsilon\mathscr{R}_0$ according to the bifurcation, where the critical value $\varepsilon\mathscr{R}_0^{c} \in (1-\gamma, 1)$ is determined by the root of equation $\mathcal{A}_1 = \mathcal{A}$:

$$\varepsilon\mathscr{R}_0^{c} := 1 - \gamma + 2\mathcal{A} + 2\sqrt{\mathcal{A}(1-\gamma+\mathcal{A})}, \tag{67}$$

and the other critical value $\varepsilon\mathscr{R}_0^{cc} \in (1, 1+\gamma)$ is by the root of equation $\mathcal{A}_2 = \mathcal{A}$:

$$\varepsilon\mathscr{R}_0^{cc} := \left(1 - \frac{\mathcal{A}}{\gamma}\right)^{-1} \tag{68}$$

with the condition (60). We have a bistable situation only for $\varepsilon\mathscr{R}_0 \in (\varepsilon\mathscr{R}_0^{c}, \varepsilon\mathscr{R}_0^{cc})$.

In such a bistable situation, once the system (20) enters the isolation malfunctioning phase, it approaches E_{m}^{*}, as indicated by Corollary 3.11.1. We could not find the mathematical condition that the system (20) enters the isolation malfunctioning phase at a certain moment. Like the analytical result obtained for the model without the discharge from isolation in Section 3.4, the condition must depend on the initial value v_0 (alternatively $u_0 = 1 - v_0$) and the other parameters, as already implied by Figures 23 and 24. Indeed Figure 25 shows numerical results according to the dependence of the final state on the initial infective population size v_0.

As expected, Figure 25 implies that the larger value of initial infective population size v_0 is more likely to induce the convergence of the system (20) to a severer endemic equilibrium with malfunctioning isolation. Besides, we remark that, even when the system (20) converges to a disease-eliminated equilibrium, the larger v_0 results in the larger final epidemic size w^{*} defined in Lemma 3.2, since it means the number of individuals who have experienced the infection until the elimination of disease.

3.5.3 *Epidemic consequence*

While the epidemic consequence would depend also on the initial condition as shown in the previous section, we find that the higher reinfectivity (the larger $\varepsilon\mathscr{R}_0$) is more likely to cause the convergence to the severer endemic equilibrium E_{m}^{*} with malfunctioning isolation, as indicated by Figure 26. Such an epidemic consequence with the endemic equilibrium E_{m}^{*} with

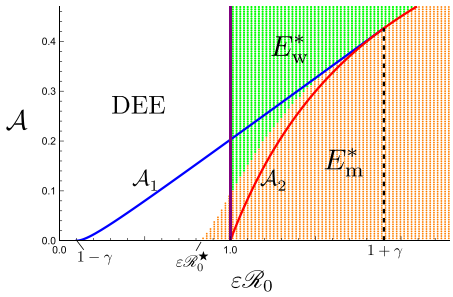

Figure 26: $(\varepsilon\mathscr{R}_0, \mathcal{A})$-dependence of the final state for the system (20). Numerically calculated with $q_{\max} = 0.3$; $\gamma = 0.9$; $v(0) = 0.00001$. Refer to Figure 22. The definition of $\varepsilon\mathscr{R}_0^\bigstar$ is given in Subsection 3.5.3.

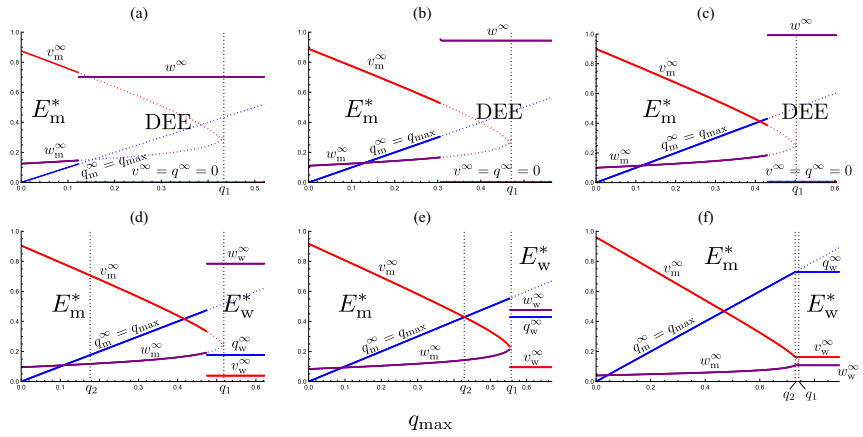

Figure 27: $q_{\max}$-dependence of the values v^∞, q^∞, and w^∞ to which v, q, and w of the system (20) converge. Numerically drawn with $(\mathscr{R}_0, \varepsilon\mathscr{R}_0) =$ (a) $(1.143, 0.8)$; (b) $(1.286, 0.9)$; (c) $(1.429, 1.0)$; (d) $(1.5, 1.05)$; (e) $(1.714, 1.2)$; (f) $(3.571, 2.5)$, and commonly $\varepsilon = 0.7$; $\gamma = 0.9$; $a = 0.2$; $v(0) = 0.00001$. Here q_i is defined as (69).

malfunctioning isolation requires a small value of $\mathcal{A}$, which corresponds to a small isolation capacity $Q_{\max}$ or/and a small discharge rate α. Inversely, a sufficiently large isolation capacity or/and a large discharge rate could make the epidemic consequence less severe without the malfunction of isolation or lead to the elimination of disease.

For further detail, Figure 26 clearly illustrates that the system may approach the endemic equilibrium E^*_{m} even when $\varepsilon\mathscr{R}_0 \leq 1$, which depends on the initial condition and the parameter values including $q_{\max}$ as shown by Figures 23(a) and 27(a–c): For $(\varepsilon\mathscr{R}_0, \mathcal{A}) \in \mathcal{D}^*_{0+\mathrm{m}}$, there is a critical value $\mathcal{A}_c < \mathcal{A}_1$ for $\mathcal{A}$ below which the system (20) could enter the isolation malfunctioning phase and approaches the endemic equilibrium E^*_{m}. As seen by Figures 26 and 27(a–c), the critical value $\mathcal{A}_c$ depends on $\varepsilon\mathscr{R}_0 \in (1-\gamma, 1)$. If $\mathcal{A} > \mathcal{A}_c$ when $\varepsilon\mathscr{R}_0 \leq 1$, the system (20) approaches a disease-eliminated equilibrium.

This result indicates the existence of a critical capacity q_c for the isolation, which depends on the reinfectivity $\varepsilon\mathscr{R}_0$. As $\varepsilon\mathscr{R}_0$ gets greater, it is larger. Such the critical capacity q_c could be regarded as corresponding to the result for the model with no discharge from isolation of (50) in Subsection 3.4.4, whereas the parameter region $\mathcal{D}^*_{0+\mathrm{m}}$ significantly narrows down for the model (20) with the discharge from isolation.

Actually the case for the model with no discharge from isolation in Section 3.4 appears on the horizontal axis (i.e., $\mathcal{A} = 0$) in Figure 26. From the result given in Section 3.4, the critical value for $\varepsilon\mathscr{R}_0 < 1$ on the horizontal axis is given as $\varepsilon\mathscr{R}_0 = \varepsilon\mathscr{R}_0^\bigstar$ with $\mathscr{R}_0^\bigstar \in (0, 1/\varepsilon)$ which is uniquely determined by the root of the following equation in terms of $\mathscr{R}_0$:

$$u_0(1-q_{\max})^{\mathscr{R}_0/\gamma} = F\big(u_0(1-q_{\max})^{\mathscr{R}_0/\gamma}\big)$$

with

$$F(u) := \begin{cases} \dfrac{1-\varepsilon\mathscr{R}_0}{\gamma-\varepsilon\mathscr{R}_0}\Big(\dfrac{u}{u_0}\Big)^{\gamma/\mathscr{R}_0} - \dfrac{1-\gamma}{\gamma-\varepsilon\mathscr{R}_0}\Big(\dfrac{u}{u_0}\Big)^{\varepsilon} & \text{for } \varepsilon\mathscr{R}_0 \neq \gamma; \\ \Big(1+\varepsilon\dfrac{1-\gamma}{\gamma}\ln\dfrac{u}{u_0}\Big)\Big(\dfrac{u}{u_0}\Big)^{\varepsilon} & \text{for } \varepsilon\mathscr{R}_0 = \gamma. \end{cases}$$

It is clear that $\mathscr{R}_0^\bigstar$ depends on the initial condition, that is, on the initial value $u_0 = 1 - v_0$.

In contrast to Section 3.4, where explicit conditions for determining the critical capacity q_c and the threshold $\varepsilon\mathscr{R}_0^\bigstar$ were obtained, it is difficult to derive analytical results when discharge from isolation is considered.

Nevertheless, when $\varepsilon\mathscr{R}_0 \leq 1$, Figures 26 and 27(a–c) clearly indicate the existence of the critical capacity $q_c < q_1$, where

$$q_i := \frac{1}{1 + a/\mathcal{A}_i} \quad (i = 1, 2) \tag{69}$$

from the definition of $\mathcal{A}$ in (60) and that of $\mathcal{A}_i$ by (63), and thus $q_{\max} = q_i$ corresponds to $\mathcal{A} = \mathcal{A}_i$. We have $q_1 \geq q_2$ for $\varepsilon\mathscr{R}_0 \geq 1 - \gamma$, and $q_1 = q_2$ only for $\varepsilon\mathscr{R}_0 = 1 + \gamma$.

Next, when $\varepsilon\mathscr{R}_0 > 1$, the epidemic dynamics by the model (20) leads to the endemic equilibrium E^*_{w} even when the isolation is functioning well without the saturation of its capacity. As indicated by Figures 26 and 27(d–f), when $\varepsilon\mathscr{R}_0 > 1$, there is a critical value $\mathcal{A}_c \in [\mathcal{A}_2, \mathcal{A}_1]$ for $\mathcal{A}$ below which the system (20) enters the isolation malfunctioning phase and approaches the endemic equilibrium E^*_{m}. If $\mathcal{A} > \mathcal{A}_c$ when $\varepsilon\mathscr{R}_0 > 1$, the system (20) approaches the endemic equilibrium E^*_{w}, where the epidemic consequence could be regarded as less severe in terms of the infective population size at the endemic state. In accordance with such the criticality when $\varepsilon\mathscr{R}_0 > 1$, the system (20) approaches E^*_{w} if $q_{\max} > q_c \in [q_2, q_1)$, while it does E^*_{m} if $q_{\max} \leq q_c$. We could not analytically identify the critical value $\mathcal{A}_c$ or q_c for $\varepsilon\mathscr{R}_0 \in (1, 1+\gamma)$, while we find $\mathcal{A}_c = \mathcal{A}_2$, that is, $q_c = q_2$ for $\varepsilon\mathscr{R}_0 \geq 1 + \gamma$, as seen from Figures 22, 26, and 27(f).

As shown in Subsection 3.5.2, the critical values A_c and q_c depend on the initial condition only at the bistable situation. That is, they depend on the initial condition for $\varepsilon\mathscr{R}_0 \in (1-\gamma, 1+\gamma)$, while it is given by $\mathcal{A}_c = \mathcal{A}_2$ and $q_c = q_2$ independently of the initial condition for $\varepsilon\mathscr{R}_0 \geq 1 + \gamma$. Remark that the critical value $\mathcal{A}_c$ or q_c indicates the criticality not for the endemicity but for the function of isolation, whereas it can do the criticality also for the endemicity when $\varepsilon\mathscr{R}_0 \leq 1$.

Finally, for the criticality of isolation function and endemicity, we obtain the following result:

Theorem 3.15. *There exists a unique critical value q_c for the isolation capacity $q_{\max}$ such that the endemic size becomes minimal or the disease is eliminated with*

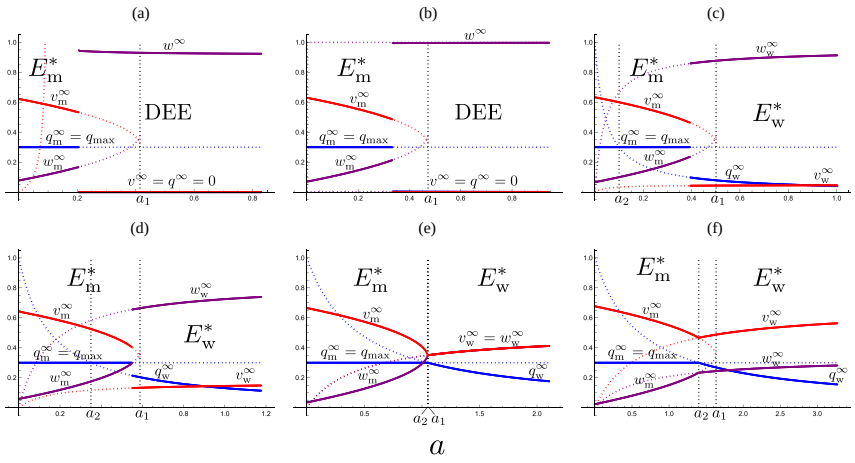

Figure 28: a-dependence of of the values v^∞, q^∞, and w^∞ to which v, q, and w of the system (20) converge. Numerically drawn with $(\mathscr{R}_0, \varepsilon\mathscr{R}_0) =$ (a) $(1.286, 0.9)$; (b) $(1.429, 1.0)$; (c) $(1.5, 1.05)$; (d) $(1.714, 1.2)$; (e) $(2.857, 2.0)$; (f) $(4.286, 3.0)$, and commonly $\varepsilon = 0.7$; $\gamma = 0.9$; $q_{\max} = 0.3$; $v(0) = 0.00001$. We have $v^*_{\mathrm{w}} = w^*_{\mathrm{w}}$ for $\varepsilon\mathscr{R}_0 = 2$ from (24). Here $a = a_i$ is defined as (70), and $a_1 = a_2$ only for $\varepsilon\mathscr{R}_0 = 1 + \gamma$.

well-functioning isolation if $q_{\max} > q_c$, while the isolation capacity $q_{\max} < q_c$ induces the larger endemic size with malfunctioning isolation.

It is easily found from (61) that the endemic size v^*_{m} at the equilibrium E^*_{m} is monotonically decreasing in terms of $q_{\max}$, as shown by Figure 27.

In the same way, we can find the criticality according to the parameter a as seen in Figure 28. A critical value a_c exists in the range $[a_2, a_1)$ with

$$a_i := \frac{1 - q_{\max}}{q_{\max}} \mathcal{A}_i \quad (i = 1, 2), \tag{70}$$

where $a = a_i$ corresponds to $\mathcal{A} = \mathcal{A}_i$. Both of a_1 and a_2 are monotonically decreasing in terms of $q_{\max}$. We have $a_1 \geq a_2$ for $\varepsilon\mathscr{R}_0 \geq 1 - \gamma$, and $a_1 = a_2$ only for $\varepsilon\mathscr{R}_0 = 1 + \gamma$. When $\varepsilon\mathscr{R}_0 \in (1 - \gamma, 1]$, the disease becomes eliminated if $a \geq a_c \in (0, a_1)$, and it becomes endemic at E^*_{m} with malfunctioning isolation if $a < a_c$. When $\varepsilon\mathscr{R}_0 > 1$, the disease becomes endemic at E^*_{w} with well-functioning isolation if $a \geq a_c \in [a_2, a_1)$, and it becomes endemic at E^*_{m} with malfunctioning isolation if $a < a_c$. Although we could not analytically obtain the expression of a_c for $\varepsilon\mathscr{R}_0 \in (1 - \gamma, 1 + \gamma)$, the same as $\mathcal{A}_c$ about $\mathcal{A}$, we find that $a_c = a_2$ for $\varepsilon\mathscr{R}_0 \geq 1 + \gamma$. As well as the critical capacity q_c for the isolation capacity $q_{\max}$, the critical value a_c indicates the criticality for the function of isolation.

While the larger a must work to avoid the malfunction of isolation because it means the faster discharge from isolation, it does not necessarily suppress the endemicity or reduce the endemic size as seen in Figures 28 and 29. If the system approaches the endemic equilibrium E^*_{w} with well-functioning isolation for a sufficiently large $a \geq a_c$ when $\varepsilon\mathscr{R}_0 > 1$, the larger a makes the endemic size v^*_{w} bigger. Indeed, v^*_{w} is monotonically increasing in terms of a, since we have

$$v^*_{\mathrm{w}} = \frac{a/\gamma}{1 + a/\mathcal{A}_2},$$

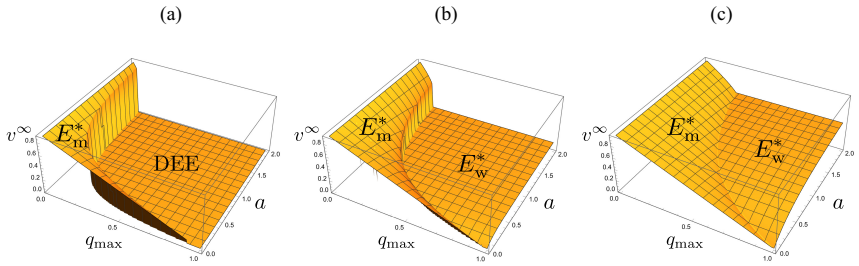

Figure 29: $(q_{\max}, a)$-dependence of the value v^∞ to which v of the system (20) converges. Numerically drawn with $(\mathscr{R}_0, \varepsilon\mathscr{R}_0) =$ (a) $(1.286, 0.9)$; (b) $(1.714, 1.2)$; (c) $(4.286, 3.0)$, and commonly $\varepsilon = 0.7$; $\gamma = 0.9$; $v(0) = 0.00001$.

from (24–26). In contrast, it can be easily seen from (61) that the endemic size v^*_{m} at the endemic equilibrium E^*_{m} with malfunctioning isolation is monotonically decreasing in terms of a.

As a result for the criticality about the isolation function and endemicity, we obtain the following result:

Theorem 3.16. *There exists a unique critical value a_c for the parameter a to minimize the endemic size or make the disease eliminated: When $\varepsilon\mathscr{R}_0 \in (1-\gamma, 1]$, the disease becomes eliminated if and only if $a > a_c$. When $\varepsilon\mathscr{R}_0 > 1$, the endemic size takes the infimum for $a \to a_c + 0$.*

Especially when $\varepsilon\mathscr{R}_0 \geq 1 + \gamma$, we have the infimum endemic size as

$$\lim_{a \to a_2 + 0} v^*_{\mathrm{w}} = (1 - q_{\max})\Big(1 - \frac{1}{\varepsilon\mathscr{R}_0}\Big)$$

from (24–26), (63), and (70), because $a_c = a_2$ in this case as mentioned before. We could not find the explicit formula for the infimum endemic size as well as a_c for $\varepsilon\mathscr{R}_0 \in (1-\gamma, 1+\gamma)$.

The critical value a_c leads to the critical value for the discharge rate α. Theorem 3.16 implies that the faster discharge from isolation does not necessarily favor the better epidemic consequence. For the disease with a weak reinfectivity as $\varepsilon\mathscr{R}_0 \leq 1$, the faster discharge can work to eliminate it, while the faster discharge may induce the higher endemicity for the disease with a strong reinfectivity as $\varepsilon\mathscr{R}_0 > 1$. Since the faster discharge leads to the more efficient recruitment of (recovered) individuals susceptible for the reinfection, too fast discharge could result in an overcompensating increase in the endemic size.

From the further investigation in Appendix 3.A.22 about the endemic size v^* when $\varepsilon\mathscr{R}_0 > 1 - \gamma$, we can find the following result about its supremum in terms of a too:

Corollary 3.16.1. *When $\varepsilon\mathscr{R}_0 > 1 - \gamma$, if*

$$q_{\max} \leq \frac{\gamma}{\varepsilon\mathscr{R}_0 - 1 + \gamma}, \tag{71}$$

then the endemic size v^* takes the supremum

$$(1 - q_{\max})\Big(1 - \frac{1-\gamma}{\varepsilon\mathscr{R}_0}\Big)$$

for $a \to +0$, that is, when no isolated individual is discharged. Otherwise, if

$$q_{\max} > \frac{\gamma}{\varepsilon\mathscr{R}_0 - 1 + \gamma}, \tag{72}$$

the endemic size for

$$a > a^\dagger := \gamma(1 - q_{\max})\Big(q_{\max} - \frac{\gamma}{\varepsilon\mathscr{R}_0 - 1 + \gamma}\Big)^{-1}\Big(1 - \frac{1}{\varepsilon\mathscr{R}_0}\Big) \tag{73}$$

becomes bigger than any endemic size for $a \le a^\dagger$, and the supremum is given as its upper bound $1 - 1/(\varepsilon\mathscr{R}_0)$.

Remark that the condition (72) can be satisfied only for $\varepsilon\mathscr{R}_0 > 1$, and the condition (71) is necessarily satisfied for $\varepsilon\mathscr{R}_0 \in (1-\gamma, 1)$. Especially when the condition (72) is satisfied for $\varepsilon\mathscr{R}_0 > 1$, too large a could make the epidemic consequence the worst.

Although the larger isolation capacity and the faster discharge from isolation would be preferable from the viewpoint of public health measure, Theorem 3.16 and Corollary 3.16.1 imply a difficulty to make a better policy for the public health, because the optimal policy could depend on the nature of spreading disease. To appropriately manage the public health measure for a spreading disease, it must be important to monitor the epidemic situation and adjust the measure, following the accumulating scientific knowledge about the disease.

As we have already seen in Figures 21 and 27–29, the final infective population size v^∞ may become discontinuously larger if the system enters the isolation malfunctioning phase and approaches an endemic equilibrium at the phase. Numerical results in Figures 27–29 clearly show the existence of such a discontinuous shift of the endemic size in terms of the isolation capacity $q_{\max}$ and the parameter a. It is indicated that the endemicity arises to make the endemic size discontinuously large for $q_{\max}$ and a below their critical values.

Although we could not obtain the analytical result on the critical values for $q_{\max}$ and a with which such a discontinuous shift of the endemic size v^* occurs, we can obtain the following result about it (Appendix 3.A.23):

Theorem 3.17. *Only in the bistable situation of $\mathcal{D}^*_{0+\mathrm{m}}$ and $\mathcal{D}^*_{\mathrm{w}+\mathrm{m}}$, the endemic size v^* has a discontinuous shift at $q_{\max} = q_c$ or $a = a_c$ where the approached equilibrium switches between those at the isolation well-functioning and malfunctioning phases. In other cases, the endemic size v^* continuously depends on $q_{\max}$ and a, that is, v^* is continuous even at either $q_{\max} = q_c = q_2$ and $a = a_c = a_2$.*

Hence such a discontinuous shift of endemic size occurs only for $\varepsilon\mathscr{R}_0 \in (1-\gamma, 1+\gamma)$.

Numerical results show the existence of such a discontinuous shift of the endemic size v^* for $q_{\max} = q_c$ in Figure 27(a–c) and for $a = a_c$ in Figure 28(a, b) with respect to $\mathcal{D}^*_{0+\mathrm{m}}$. So do those for $q_{\max} = q_c$ in Figure 27(d, e) and for $a = a_c$ in Figure 28(c–e) with respect to $\mathcal{D}^*_{\mathrm{w}+\mathrm{m}}$. In contrast, Figures 27(f) and 28(f) show numerical examples such that the endemic size v^* continuously depends on $q_{\max}$ and a when $\varepsilon\mathscr{R}_0 \ge 1+\gamma$ out of $\mathcal{D}^*_{0+\mathrm{m}}$ and $\mathcal{D}^*_{\mathrm{w}+\mathrm{m}}$. The endemic size v^* continuously varies between v^*_{m} and v^*_{w} at the critical value either $q_{\max} = q_2$ and $a = a_2$, that is, at the boundary between $\mathcal{D}^*_{\mathrm{w}}$ and $\mathcal{D}^*_{\mathrm{m}}$ for $\varepsilon\mathscr{R}_0 \ge 1+\gamma$ in Figure 22. See also numerical results in Figure 29.

3.5.4 *Discussion*

In this section, we analyzed an SIRI+Q model that incorporates both reinfection and limited isolation capacity with the discharge mechanism. The results highlight the significant role of both isolation capacity and isolation period in determining the epidemic consequences of a reinfectious disease. There could be a critical value for the isolation capacity $Q_{\max}$ below which the isolation becomes malfunction to induce the endemicity. For a highly reinfectious disease, such a situation with malfunctioning isolation may induce a significantly large endemic size. Further, there could exist a critical value for the isolation period ($1/\alpha$ in our model) such that the endemic size becomes significantly large if the isolation period is longer than the critical.

For the disease with a weak reinfectivity, which is given by the case of $\varepsilon\mathscr{R}_0 < 1$ in our model, the isolation measure could be the key factor in achieving disease elimination. In this case, elimination can be possible through a sufficiently large isolation capacity and efficient discharge of patient. Inversely, the disease could become endemic if the capacity is rather small or the isolation takes much long period before the discharge of patient. Such endemicity is necessarily accompanied by the malfunction of isolation measure. In our model, when the isolation reaches its capacity and becomes malfunctioning, the epidemic dynamics leads to an endemic equilibrium with a significantly large endemic size. This result clearly demonstrates the importance of well-functioning isolation measure to suppress the endemic size.

When the isolation remains malfunctioning with the saturation of its capacity, the epidemic dynamics could be qualitatively different from when the isolation functions well. Such a qualitative shift in the epidemic dynamics could cause a drastic deterioration of the social damage for the community. Once isolation reaches its capacity, it can place growing strain on medical services and potentially lead to a progressive worsening of the epidemic situation, as public health measures fail to function effectively. A sufficient isolation capacity is also essential for maintaining the quality of medical services during an epidemic.

Moreover, our results indicate that a higher discharge rate and a lower quarantine rate tend to reduce the occupancy of isolation facilities, thereby decreasing the likelihood of reaching the isolation capacity. However, from a public health perspective, quarantine measures are generally promoted to suppress disease transmission, whereas the discharge rate is inherently constrained by the nature of the disease and the limitations of medical resources. Hence, the discharge rate is generally cannot be easily increased as we would prefer. Even though a sufficient isolation capacity may theoretically prevent the malfunction of isolation, ensuring such capacity is often difficult due to limited medical resources and societal pressure to extend the isolation period. These factors increase the likelihood of saturation, thereby requiring the sufficient isolation capacity to remain effective.

Furthermore, our results of Theorems 3.15 and 3.16 imply that a certain intermediate value of isolation discharge rate would be optimal to make the epidemic consequence as minor as possible. As shown in Figure 29, the critical value a_c is monotonically decreasing in terms of the isolation capacity $q_{\max}$, whereas we could not analytically prove it for the case where $\varepsilon\mathscr{R}_0 \in (1-\gamma, 1+\gamma)$. Hence, such an optimal value of the isolation discharge rate α would become smaller for the larger isolation capacity $Q_{\max}$. Therefore,

a larger isolation capacity enables more flexible and effective management of quarantine and isolation to reduce social damage.

APPENDIX FOR CHAPTER 3

APPENDIX 3.A.1: PROOF OF LEMMA 3.1

The isolated population size Q never becomes greater than $Q_{\max}$ in the epidemic dynamics governed by (19) with the initial value $Q(0) = 0$. From (19), we have $dQ/dt \leq 0$ for $Q = Q_{\max}$. Thus the isolated population size Q never becomes greater than $Q_{\max} < N$ for any $t \geq 0$.

Then from (19), we formally have

$$I(t) = I(0) \exp\Big[\int_0^t \beta \frac{S(\nu)}{N - Q(\nu)} + \varepsilon\beta \frac{R(\nu)}{N - Q(\nu)} - \rho - \sigma \, d\nu \Big] > 0$$

with $I(0) > 0$ for any t such that $Q(\nu) < Q_{\max}$ for any $\nu < t$. If the system gets in the isolation malfunctioning phase at $t = t^\star$ and stays there for $t \in [t^\star, t^\dagger]$, we have $I(t^\star) > 0$ from the above argument, and

$$I(t) = I(t^\star) \exp\Big[\int_{t^\star}^t \beta \frac{S(\nu)}{N - Q_{\max}} + \varepsilon\beta \frac{R(\nu)}{N - Q_{\max}} - \rho - \frac{\alpha Q_{\max}}{I(\nu)} \, d\nu \Big] > 0$$

for any $t \in [t^\star, t^\dagger]$ when the system remains at the isolation malfunctioning phase. If the system returns to the isolation well-functioning phase after $t = t^\dagger < \infty$ and stays there for $t \in (t^\dagger, t^\ddagger)$, then we have

$$I(t) = I(t^\dagger) \exp\Big[\int_{t^\dagger}^t \beta \frac{S(\nu)}{N - Q(\nu)} + \varepsilon\beta \frac{R(\nu)}{N - Q(\nu)} - \rho - \sigma \, d\nu \Big] > 0$$

with $I(t^\dagger) > 0$ for any $t \in (t^\dagger, t^\ddagger)$. From these arguments, we have $I(t) > 0$ for any $t \geq 0$ according to the system (19). Thus, we have $dQ/dt\big|_{Q=0} > 0$ for any $t \geq 0$. Since $dQ/dt > 0$ at $t = 0$, we finally find that $Q \in (0, Q_{\max})$ for any $t > 0$.

Then with the same arguments, we can have $S > 0$ and $R > 0$ for any $t > 0$. Lastly, since it must hold that $S + I + Q + R = N$ (a given positive constant) for any $t \geq 0$ from the equations of (19), we obtain the lemma.

APPENDIX 3.A.2: PROOF OF LEMMA 3.2

In the case of $\varepsilon = 0$ where no reinfection occurs, the system (21) becomes one of the well-known Kermack-McKendrick SIR model, and we know that the system approaches a disease-eliminated equilibrium $(u, v, w) = (u^*, 0, w^*)$ where u^* is given by the unique positive root in $(0, 1)$ satisfying the equation

$$u^* - \frac{1}{\mathscr{R}_{00}} \log u^* = 1 - \frac{1}{\mathscr{R}_{00}} \log u_0,$$

and $w^* = 1 - u^*$ (for example, see Martcheva [110], Seno [144]).

To prove Lemma 3.2, we consider the other two cases about the value of ε: $\varepsilon = 1$ and $\varepsilon \in (0, 1)$, where the reinfection occurs. The former is the case where the reinfection is possible with the same infection force as that for the initial infection.

1) CASE OF $\varepsilon = 1$ In this case, the second equation of (21) becomes

$$\frac{dv}{d\tau} = \{\mathscr{R}_{00}(u + w) - 1\} = \{\mathscr{R}_{00}(1 - v) - 1\} = \mathscr{R}_{00}\Big(1 - \frac{1}{\mathscr{R}_{00}} - v\Big)v.$$

Hence, as known well for the logistic equation, we find that v is monotonically decreasing toward zero as time passes if $\mathscr{R}_{00} \leq 1$, while v monotonically approaches $1 - 1/\mathscr{R}_{00} > 0$ as time passes if $\mathscr{R}_{00} > 1$. Therefore, for the system (21) with $\varepsilon = 1$, the system approaches a disease-eliminated equilibrium if $\mathscr{R}_{00} \leq 1$, while it does an endemic equilibrium if $\mathscr{R}_{00} > 1$.

From the first and third equations in (21) with $\varepsilon = 1$, we can derive

$$\frac{dw}{du} = -\frac{1 - \mathscr{R}_{00} w}{\mathscr{R}_{00} u}.$$

Then, from this equation, we can find the following equality that holds for any $\tau \geq 0$:

$$\mathscr{R}_{00} w(\tau) = 1 - \frac{u(\tau)}{u_0}, \tag{74}$$

where we used the initial condition that $u(0) = u_0 \in (0, 1)$ and $w(0) = 0$. When $\mathscr{R}_{00} \leq 1$, since $u + w = 1 - v$ for any $\tau \geq 0$ and $v \to 0$ as $\tau \to \infty$, we can get the equilibrium values u^* and w^* as $\tau \to \infty$ from (74):

$$u^* = \frac{1 - \mathscr{R}_{00}}{1 - u_0 \mathscr{R}_{00}} u_0; \quad w^* = \frac{1 - u_0}{1 - u_0 \mathscr{R}_{00}}.$$

In the same way, when $\mathscr{R}_{00} > 1$, since $v \to 1 - 1/\mathscr{R}_{00}$ as $\tau \to \infty$, we can get

$$u \to 0; \quad w \to \frac{1}{\mathscr{R}_{00}}$$

as $\tau \to \infty$. Note that $du/d\tau < 0$ for any positive u and v. Since v converges to a positive value as $\tau \to \infty$ when $\mathscr{R}_{00} > 1$, we have $du/d\tau < 0$ as long as $u > 0$.

II) CASE OF $\varepsilon \in (0, 1)$ When $\varepsilon \mathscr{R}_{00} \leq 1$, from the third equation of (21), we have

$$\frac{dw}{d\tau} = v - \varepsilon \mathscr{R}_{00} v w \geq (1 - w) v. \tag{75}$$

Since we have $dw/d\tau\big|_{\tau=0} > 0$ with $w(0) = 0$ and $v(0) > 0$, w becomes and remains positive for $\tau > 0$ (refer to Lemma 3.1). Besides, from the second equation of (21), we formally have

$$v(\tau) = v(0) \exp\left[\int_0^\tau \mathscr{R}_{00} u(s) + \varepsilon \mathscr{R}_{00} w(s) - 1 \, ds \right] > 0$$

for any $\tau \geq 0$. Thus v remains positive for $\tau \geq 0$. Hence, we further find that $w = 1 - u - v < 1$ for $\tau \geq 0$ (refer to Lemma 3.1). With these arguments, we have $(1 - w)v > 0$ for $\tau > 0$. Therefore, from (75), we find that $dw/d\tau > 0$ for any $\tau > 0$, that is, w is monotonically increasing when $\varepsilon \mathscr{R}_{00} \leq 1$. Since $w \in (0, 1)$ for any $\tau > 0$, this result indicates that $w \to w^* \in (0, 1]$ as $\tau \to \infty$. At the same time, it is necessary that $dw/d\tau \to 0$ as $\tau \to \infty$. Then, from (75), it is necessary that $(1 - w)v \to 0$ as $\tau \to \infty$, that is, $w \to w^* = 1$ or $v \to 0$ as $\tau \to \infty$. Since $v \to 0$ even when $w \to 1$ as $\tau \to \infty$ because of the equality $v = 1 - u - v \in (0, 1)$ for $\tau \geq 0$, we conclude that $v \to 0$ as $\tau \to \infty$ when $\varepsilon \mathscr{R}_{00} \leq 1$. This is the case where the system approaches a disease-eliminated equilibrium.

From the first and third equations of (21), we can derive

$$\frac{dw}{du} = -\frac{1 - \varepsilon \mathscr{R}_{00} w}{\mathscr{R}_{00} u}.$$

With this equation, we can find the following equality that holds for any $\tau \geq 0$:

$$\varepsilon \mathscr{R}_{00} w(\tau) = 1 - \left\{ \frac{u(\tau)}{u_0} \right\}^{\varepsilon}, \tag{76}$$

where we used the initial condition that $u(0) = u_0 \in (0,1)$ and $w(0) = 0$. Since $v \to 0$ as $\tau \to \infty$ when $\varepsilon \mathscr{R}_{00} \leq 1$, we find from (76) that $(u, w) \to (u^*, w^*) \in (0,1) \times (0,1)$ as $\tau \to \infty$ when $\varepsilon \mathscr{R}_{00} \leq 1$, where u^* is uniquely determined by the equation

$$\varepsilon \mathscr{R}_{00}(1 - u^*) = 1 - \left(\frac{u^*}{u_0} \right)^{\varepsilon},$$

and $w^* = 1 - u^*$.

Next let us consider the case where $\varepsilon \mathscr{R}_{00} > 1$. From (76), we formally have

$$v(\tau) = 1 - w(\tau) - u(\tau) = 1 - \frac{1}{\varepsilon \mathscr{R}_{00}} \left[1 - \left\{ \frac{u(\tau)}{u_0} \right\}^{\varepsilon} \right] - u(\tau). \tag{77}$$

Then, substituting (76) and (77) for the first equation of (21), we can get the following closed ordinary differential equation of u:

$$\frac{du}{d\tau} = -\frac{u}{\varepsilon} \left\{ \varepsilon \mathscr{R}_{00}(1 - u) + \left(\frac{u}{u_0} \right)^{\varepsilon} \right\}. \tag{78}$$

Since the right side of (78) is necessarily negative for any $u \in (0,1)$ and becomes zero for $u = 0$, we find that $u \to 0$ as $\tau \to \infty$. Lastly, from (76) and (77), we can get the result that $v \to 1 - 1/(\varepsilon \mathscr{R}_{00})$ and $w \to 1/(\varepsilon \mathscr{R}_{00})$ as $\tau \to \infty$ when $\varepsilon \mathscr{R}_{00} > 1$.

APPENDIX 3.A.3: PROOF OF THEOREM 3.1

Lemma 3.13. *If $\varepsilon \mathscr{R}_0 < 1$, the system (23) approaches a disease-eliminated equilibrium as $\tau \to \infty$.*

Proof. Taking account of $u + v + q + w = 1$ for any $\tau \geq 0$, the system (23) is mathematically equivalent to the following three dimensional one:

$$\begin{aligned} \frac{du}{d\tau} &= -\mathscr{R}_0 \frac{v}{1-q} u; \\ \frac{dv}{d\tau} &= \mathscr{R}_0 \frac{v}{1-q} u + \varepsilon \mathscr{R}_0 \frac{v}{1-q}(1 - u - v - q) - v; \\ \frac{dq}{d\tau} &= \gamma v - a q. \end{aligned} \tag{79}$$

From (79), we have

$$\frac{d(u+v)}{d\tau} = -\varepsilon \mathscr{R}_0 \frac{v}{1-q}(u+v) - (1 - \varepsilon \mathscr{R}_0) v < 0 \tag{80}$$

for any $v > 0$ when $\varepsilon \mathscr{R}_0 < 1$. Besides u is monotonically decreasing for any $\tau > 0$ since u, v, and q are positive and less than 1 for any $\tau > 0$ with $v(0) \in (0,1)$ and $u(0) = 1 - v(0)$ (refer to Lemma 3.1). If $v \to v^* > 0$ as $\tau \to \infty$, then $u \to 0$ and $u + v \to 0$ since the right side of (80) is always negative. Thus, v would have to converge to zero. This is contradictory. Hence we find that $v \to 0$ as $\tau \to \infty$ when $\varepsilon \mathscr{R}_0 < 1$. This proves the lemma. □

Lemma 3.14. *For the system* (23) *with* $\varepsilon\mathscr{R}_0 = 1$, *we have* $(u, v, q, w) \to (0, 0, 0, 1)$ *as* $\tau \to \infty$.

Proof. For the special case of $\varepsilon\mathscr{R}_0 = 1$, the system (79) becomes

$$\begin{aligned} \frac{du}{d\tau} &= -\mathscr{R}_0 \frac{v}{1-q} u; \\ \frac{dv}{d\tau} &= \{(\mathscr{R}_0 - 1)u - v\} \frac{v}{1-q}; \\ \frac{dq}{d\tau} &= \gamma v - aq. \end{aligned} \tag{81}$$

Suppose that $\mathscr{R}_0 > 1$ for $\varepsilon < 1$ because of $\varepsilon\mathscr{R}_0 = 1$. From (81), we can obtain

$$\frac{d}{d\tau} \ln(u + v) = -\frac{v}{1-q}; \quad \frac{d}{d\tau} \ln u = -\mathscr{R}_0 \frac{v}{1-q},$$

and subsequently

$$(u + v)^{\mathscr{R}_0} = \frac{u}{u_0}, \tag{82}$$

making use of $u_0 + v_0 = 1$ for the initial condition $(u(0), v(0), q(0), w(0)) = (u_0, v_0, 0, 0)$ with $v(0) \in (0, 1)$. Then, from the first equation of (81) and the relation (82), we can get the following closed ordinary differential equation of u:

$$\frac{du}{d\tau} = -\mathscr{R}_0 \frac{u_0}{1-q} \left\{ \left(\frac{u}{u_0} \right)^{1+1/\mathscr{R}_0} - u_0 \left(\frac{u}{u_0} \right)^2 \right\}, \tag{83}$$

where $u/u_0 < 1$ for any $\tau > 0$ because the first equation of (81) indicates that u is monotonically decreasing with $du/d\tau < 0$ for any $\tau > 0$. Thus, we find from (83) that $du/d\tau\big|_{u>0} < 0$ with $\mathscr{R}_0 \geq 1$ and $du/d\tau\big|_{u=0} = 0$. Hence we have $u \to 0$ as $\tau \to \infty$. Therefore, from (82), we have $v \to 0$ as $\tau \to \infty$ at the same time. Finally, from the third equation of (81), we have $q \to 0$ as $\tau \to \infty$, and subsequently $w = 1 - u - v - q \to 0$ as $\tau \to \infty$. These arguments are valid even for the case of $\mathscr{R}_0 = 1$ with $\varepsilon = 1$. As a result, we have this lemma. □

Consequently, from Lemmas 3.13 and 3.14, we find that the system (23) approaches a disease-eliminated equilibrium as $\tau \to \infty$ if $\varepsilon\mathscr{R}_0 \leq 1$. Those lemmas indicate also that the convergence to a disease-eliminated equilibrium is independent of the initial condition.

Lemma 3.15. *If* $\varepsilon\mathscr{R}_0 > 1$, *the disease-eliminated equilibrium* $(u, v, q, w) = (u^*, 0, 0, 1 - u^*)$ *with any* $u^* \in [0, 1)$ *for the system* (23) *is unstable.*

Proof. The Jacobi matrix at the equilibrium $(u, v, q) = (u^*, 0, 0)$ for the system (79) becomes

$$J_0 = \begin{pmatrix} 0 & -\mathscr{R}_0 u^* & 0 \\ 0 & (1-\varepsilon)\varepsilon\mathscr{R}_0 u^* + \varepsilon\mathscr{R}_0 - 1 & 0 \\ 0 & \gamma & -a \end{pmatrix}.$$

The eigenvalues for J_0 are 0, $(1-\varepsilon)\varepsilon\mathscr{R}_0 u^* + \varepsilon\mathscr{R}_0 - 1$, and $-a$. The second eigenvalue is positive for any $u^* \in [0, 1)$ with $\varepsilon\mathscr{R}_0 > 1$. Therefore the lemma is proved. □

Lemma 3.15 indicates that the system (23) does not approach any disease-eliminated equilibrium when $\varepsilon\mathscr{R}_0 > 1$. That is, the system (23) can approach a disease-eliminated equilibrium only when $\varepsilon\mathscr{R}_0 \leq 1$. As a result from Lemmas 3.13, 3.14, and 3.15, we can get the former part of Theorem 3.1. The latter part of Theorem 3.1 is proved by the following lemma on the existence and stability of the endemic equilibrium E_{w}^* given by (24):

Lemma 3.16. *The unique endemic equilibrium E_{w}^* given by (24) exists for the system (23) if and only if $\varepsilon\mathscr{R}_0 > 1$, and then it is globally asymptotically stable.*

Proof. It is easy to see that the condition $\varepsilon\mathscr{R}_0 > 1$ is necessary and sufficient for the existence of the endemic equilibrium E_{w}^* given by (24) with (25) and (26). When E_{w}^* exists with $\varepsilon\mathscr{R}_0 > 1$, the global asymptotic stability can be proved with a Lyapunov function for E_{w}^* as follows: With $\varepsilon\mathscr{R}_0 > 1$, we define the following function in $\widehat{\Omega}_1 := \{(u, v, q) \mid u \geq 0,\, v > 0,\, q \geq 0,\, u + v + q < 1\}$:

$$V(u,v,q) := \frac{1}{\varepsilon\mathscr{R}_0 - 1}\Big\{u + (v - v_{\mathrm{w}}^*) - v_{\mathrm{w}}^* \ln\frac{v}{v_{\mathrm{w}}^*}\Big\} + \frac{1}{\gamma}\Big\{(1-q) - (1-q_{\mathrm{w}}^*) - (1-q_{\mathrm{w}}^*)\ln\frac{1-q}{1-q_{\mathrm{w}}^*}\Big\},$$

where $v_{\mathrm{w}}^* = (a/\gamma)q_{\mathrm{w}}^*$ with q_{w}^* given by (25). Then, from (79), we can easily derive

$$\frac{dV}{d\tau} = -\frac{\varepsilon\mathscr{R}_0}{\varepsilon\mathscr{R}_0 - 1}\cdot\frac{(v - v_{\mathrm{w}}^*)^2}{1-q} - \frac{a}{\gamma}\cdot\frac{(q - q_{\mathrm{w}}^*)^2}{1-q} - \frac{\mathscr{R}_0}{\varepsilon\mathscr{R}_0 - 1}\cdot\frac{\{\varepsilon v + (1-\varepsilon)v_{\mathrm{w}}^*\}u}{1-q}.$$

From Lemma 3.1, the solution for the system (23), that is, for the mathematically equivalent system (79) with the initial condition that $u(0) = 1 - v(0)$, $v(0) \in (0,1)$, and $q(0) = 0$ stays in $\widehat{\Omega}_1$ for any $\tau \geq 0$, and the endemic equilibrium E_{w}^* belongs to $\widehat{\Omega}_1$. The function V is positive definite for any $(u,v,q) \in \widehat{\Omega}_1\backslash\{(0, v_{\mathrm{w}}^*, q_{\mathrm{w}}^*)\}$, and $V(0, v_{\mathrm{w}}^*, q_{\mathrm{w}}^*) = 0$. The derivative $dV/d\tau$ is negative definite for any $(u,v,q) \in \widehat{\Omega}_1\backslash\{(0, v_{\mathrm{w}}^*, q_{\mathrm{w}}^*)\}$, and $dV/d\tau = 0$ for $(u,v,q) = (0, v_{\mathrm{w}}^*, q_{\mathrm{w}}^*)$.

On the other hand, from Lemma 3.1 and the non-dimensionalization in Subsection 3.2.5, we know that the solution for the system (23) belongs to Ω_1 defined in Subsection 3.2.5. Since $\Omega_1 \subset \widehat{\Omega}_1$ and $E_{\mathrm{w}}^* \in \Omega_1$, we can conclude that the function V is a Lyapunov function for the endemic equilibrium E_{w}^* of the system (79). Therefore the global asymptotic stability of the endemic equilibrium E_{w}^* has been proved by the existence of a Lyapunov function V in Ω_1. □

APPENDIX 3.A.4: DERIVATION OF THE CONSERVED QUANTITIES

The isolation effective phase

When the isolation never reaches the capacity in a finite time due to a sufficient isolation capacity for the epidemic dynamics, the system (28) always follow the isolation well-functioning phase with $\phi(q,v) = \gamma v$. In this case, from the equations in (28), we can derive the following differential equations:

$$\frac{dv}{du} = -1 + \frac{1-q}{\mathscr{R}_0 u}, \tag{84}$$

and

$$\frac{dq}{dw} = \frac{\gamma}{1-\gamma}. \tag{85}$$

From (85), we can obtain the following relation between q and w:

$$q = \frac{\gamma}{1-\gamma} w, \tag{86}$$

where we used $q(0) = w(0) = 0$. Since $u + v + q + w = 1$, the equation (86) becomes

$$1 - q = \gamma(u + v) + 1 - \gamma. \tag{87}$$

Substituting (87) for (84), we can derive the following ordinary differential equation of v in terms of u:

$$\frac{dv}{du} = \frac{\gamma}{\mathscr{R}_0}\frac{v}{u} + \frac{1-\gamma}{\mathscr{R}_0}\frac{1}{u} + \frac{\gamma}{\mathscr{R}_0} - 1.$$

We can easily solve this ordinary differential equation, and get the relation (29), making use of $v(0) = v_0$, $u(0) = u_0$, and $v_0 + u_0 = 1$.

The isolation incapable phase

Once the isolation reaches the capacity in a finite time on the way of the epidemic process with an insufficient isolation capacity, the system (28) comes to follow the isolation incapable phase. In this case, from the first and second equations of (28), we can derive the following differential equation:

$$\frac{dv}{du} = -1 + \frac{(1-\gamma)(1-q_{\max})}{\mathscr{R}_0 u}. \tag{88}$$

We can easily solve (88), and get the relation

$$v(\tau) = -u(\tau) + \frac{\rho(1-q_{\max})}{\beta} \ln u(\tau) + C \tag{89}$$

with an undetermined constant C. For $\tau = \tau^\star$, we have

$$C = u(\tau^\star) + v(\tau^\star) - \frac{\rho(1-q_{\max})}{\beta} \ln u(\tau^\star). \tag{90}$$

Making use of (90) for (89), we can get the equation (30) that gives the conserved quantity at the isolation incapable phase.

APPENDIX 3.A.5: PROOF OF THEOREM 3.2 AND COROLLARIES 3.2.1 AND 3.2.2

From the equation (29), when the isolation never reaches the capacity, we have the equation

$$u_\infty^- = F(u_\infty^-) := -\frac{\rho}{\sigma} + \left(\frac{u_\infty^-}{u_0}\right)^{\gamma/\mathscr{R}_0} \left(1 + \frac{\rho}{\sigma}\right), \tag{91}$$

since $v(\tau) \to 0$ as $\tau \to \infty$. We have $F(0) = -\rho/\gamma$, $F(u_0) = 1$, and $F'(u) > 0$ for $u \in (0, u_0)$. Hence $F(u)$ is a monotonically increasing, continuous and differentiable function of $u \in (0, u_0)$, which satisfies that $F(0) < 0$ and

$F(u_0) > u_0$. Further we can easily find that $F(u)$ is linear if $\sigma/\beta = 1$, and otherwise it is alternatively convex or concave for $u \in (0, u_0)$. Therefore we find that the equation (91) has a unique root $u_\infty^- \in (0, u_0)$, and $F(u) < u$ for $u \in (0, u_\infty^-)$ while $F(u) > u$ for $u \in (u_\infty^-, u_0)$.

On the other hand, from $u_\infty^- + q_\infty^- + w_\infty^- = 1$ and $q_\infty^- = (\sigma/\rho)w_\infty^-$ by (86) in Appendix 3.A.4, we find that $u_\infty^- = 1 - q_\infty^-/\gamma$. Making use of this relation, we find that the equation (91) is equivalent to the following equation:

$$q_\infty^- = 1 - \left(\frac{u_\infty^-}{u_0}\right)^{\gamma/\beta}. \tag{92}$$

It must be satisfied that $q_\infty^- \le q_{\max}$ in the case where $q(\tau)$ never reaches $q_{\max}$ for any $\tau > 0$. Since $q(\tau)$ is monotonically increasing in terms of τ, if $q_\infty^- \le q_{\max}$, the isolation does not reach the capacity for any $\tau > 0$. Therefore, if and only if $q_\infty^- \le q_{\max}$, the isolation does not reach the capacity for any $\tau > 0$.

Consequently we find that, if and only if $q_\infty^- > q_{\max}$, the isolation reaches the capacity at $\tau = \tau^\star < \infty$. From (91) and (92), we can derive the following condition equivalent to $q_\infty^- > q_{\max}$:

$$u_\infty^- < 1 - q_{\max}\left(1 + \frac{\rho}{\sigma}\right). \tag{93}$$

Since $u_\infty^- > 0$, we note that this inequality holds only if $q_{\max} < 1/(1 + \rho/\sigma)$. Hence if $q_{\max} \ge 1/(1 + \rho/\sigma)$, the inequality (93) does not hold and we necessarily have $q_\infty^- \le q_{\max}$, so that the isolation does not reach the capacity for any $\tau > 0$. From the nature of the function $F(u)$ shown in the above, the condition (93) is equivalent to the condition that $F(u) > u$ for $u = 1 - q_{\max}(1 + \rho/\sigma)$. This leads to the condition (31) in Theorem 3.2.

On the other hand, from the condition (93), we can define the critical value for the isolation capacity q_c as $q_c := (1 - u_\infty^-)/(1 + \rho/\sigma)$ such that the condition (93) is satisfied if and only if $q_{\max} < q_c$, which becomes necessary and sufficient for the isolation to reach the capacity in a finite time. Substituting $u_\infty^- = 1 - q_c(1 + \rho/\sigma)$ for the equation $F(u_\infty^-) = u_\infty^-$, we can get the equation (32). Then the uniqueness of q_c follows that of u_∞^- shown in the above.

APPENDIX 3.A.6: PROOF OF COROLLARY 3.2.3

Form (32), we can easily derive the following derivative of q_c in terms of $1/\sigma_0$:

$$\frac{\partial q_c}{\partial(1/\sigma)} = \frac{\sigma^2\rho q_c + \sigma\beta\{\sigma - q_c(\sigma + \rho)\}\ln(1 - q_c)}{-\sigma(\sigma + \rho) + \beta\{\sigma - q_c(\sigma + \rho)\}/(1 - q_c)}. \tag{94}$$

As we can easily find from (32) that $q_c \to 1 - u_0$ as $1/\sigma \to +0$, we have

$$\left.\frac{\partial q_c}{\partial(1/\sigma)}\right|_{(1/\sigma, q_c)\to(+0, 1-u_0)} > 0 \iff \frac{\beta}{\rho} > \frac{u_0 - 1}{u_0 \ln u_0}. \tag{95}$$

Next, to find the sign of (94) for sufficiently large value of $1/\sigma$, we use the Maclaurin expansion in terms of σ and get

$$\frac{\partial q_c}{\partial(1/\sigma)} = (1 - q_c)\ln(1 - q_c)\sigma + o(\sigma).$$

Since $(1-q_c)\ln(1-q_c) < 0$ for $q_c \in (0,1)$, the sign of (94) must be necessarily negative for sufficiently large value of $1/\sigma$. As a consequence, q_c is monotonically decreasing for sufficiently large value of $1/\sigma$.

Since q_c is continuous in terms of $1/\sigma$, q_c is monotonically increasing for a sufficiently small value of $1/\sigma$ if the condition (95) is satisfied. Then, q_c has at least one extremal maximum for a finite value of $1/\sigma$. It is easily seen that $(u_0-1)/(u_0\ln u_0) > 1$ for any $u_0 \in (0,1)$.

On the other hand, the following equation must be satisfied at the extremum that makes the derivative (94) zero:

$$1+\frac{\rho}{\sigma} = \frac{1}{q_c} + \frac{\rho/\beta}{\ln(1-q_c)}. \tag{96}$$

We can easily prove that the right side of (96) is less than 1 for any $q_c \in (0,1)$ if $\beta/\rho \le 1$. Since the left side of (96) is always greater than 1, this means that the equation (96) cannot hold for $\beta/\rho \le 1$. Hence, the derivative (94) cannot become zero if $\beta/\rho \le 1$.

Therefore, $\beta/\rho > 1$ is necessary for the existence of a certain value of $1/\sigma > 0$ to maximize q_c. At the same time, this result means that, when $\beta/\rho \le 1$, the derivative (94) cannot change the sign at any value of $1/\sigma$. Then from the above arguments, it must be negative, so that q_c is monotonically decreasing in terms of $1/\sigma$ when $\beta/\rho \le 1$.

APPENDIX 3.A.7: DERIVATION OF THE FINAL SIZE EQUATION

Final size equation for $q_{\max} \ge q_c$

By applying $\tau \to \infty$ for the equation (29), we get the following equation:

$$(u_\infty^-)^{-\sigma/\beta}\Big(u_\infty^- + \frac{\rho}{\sigma}\Big) = (u_0)^{-\sigma/\beta}\Big(1+\frac{\rho}{\sigma}\Big), \tag{97}$$

where we used $v(\tau) \to 0$ as $\tau \to \infty$. The final epidemic size is given by $z_\infty^- = q_\infty^- + w_\infty^- = 1 - u_\infty^-$. Making use of $u_\infty^- = 1 - z_\infty^-$ for (97), we can get the equation (34) which determines the final epidemic size when the isolation never reaches the capacity.

Final size equation for $q_{\max} < q_c$

By applying $\tau \to \infty$ for the equation (30), we can get the following equation:

$$u_\infty^+ = u(\tau^\star) + v(\tau^\star) + \frac{\rho}{\beta}(1-q_{\max})\ln\frac{u_\infty^+}{u(\tau^\star)}, \tag{98}$$

where we used $v(\tau) \to 0$ as $\tau \to \infty$. Now, from the equality $u(\tau)+v(\tau) = 1-\{q(\tau)+w(\tau)\}$ and (86) derived in Appendix 3.A.4, we have

$$u(\tau)+v(\tau) = 1 - q(\tau)\Big(1+\frac{\rho}{\sigma}\Big). \tag{99}$$

For the continuity of the solution at $\tau = \tau^\star$, we have $u(\tau) = u(\tau^\star)$, $v(\tau) = v(\tau^\star)$, and $q(\tau^\star) = q_{\max}$. Then the equations (29) and (99) become

$$u(\tau^\star)+v(\tau^\star) = -\frac{\rho}{\sigma} + \Big\{\frac{u(\tau^\star)}{u_0}\Big\}^{\sigma/\beta}\Big(1+\frac{\rho}{\sigma}\Big); \tag{100}$$

$$u(\tau^\star)+v(\tau^\star) = 1 - q_{\max}\Big(1+\frac{\rho}{\sigma}\Big). \tag{101}$$

We can solve the parallel equations (100) and (101) in terms of $u(\tau^\star)$ and $v(\tau^\star)$,

$$u(\tau^\star) = (1-q_{\max})^{\beta/\sigma} u_0; \quad v(\tau^\star) = 1 - u(\tau^\star) - q_{\max}\Big(1+\frac{\rho}{\sigma}\Big), \tag{102}$$

and then substitute them for (98). As a result, we can get the equation

$$\frac{\beta/\rho}{1-q_{\max}}\Big\{u_\infty^+ - 1 + q_{\max}\Big(1+\frac{\rho}{\sigma}\Big)\Big\} = \ln u_\infty^+ - \ln u_0 - \frac{\beta}{\sigma}\ln(1-q_{\max}). \tag{103}$$

When the isolation reaches the capacity at any finite time, the final epidemic size is defined by $z_\infty^+ = q_{\max} + w_\infty^+ = 1 - u_\infty^+$. Thus, making use of $u_\infty^+ = 1 - z_\infty^+$ for (103), we can get the equation (35).

APPENDIX 3.A.8: PROOF OF THE UNIQUE EXISTENCE OF THE FINAL EPIDEMIC SIZE

Unique existence of z_∞^-

The left side of equation (34) is a function of z_∞^-, which we denote here by $A(z_\infty^-)$. The right side of (34) is a positive constant B_0 independent of z_∞^-. The function $A(z)$ is continuous and differentiable for $z \in (1-u_0, 1)$, satisfying that

$$A(1-u_0) = (u_0)^{-\sigma/\beta}\left(u_0 + \frac{\rho}{\sigma}\right) < B_0; \quad \lim_{z\to 1-0} A(z) = \infty > B_0.$$

Hence, there exist at least one root of the equation $A(z) = B_0$ for $z \in (1-u_0, 1)$.

We can easily find that the function $A(z)$ is monotonically increasing or has a unique extremal minimum in $(1-u_0, 1)$. When $A(z)$ is monotonically increasing for $z \in (1-u_0, 1)$, it must have a unique intersection with the horizontal line B_0 in $(1-u_0, 1)$. Even when $A(z)$ has a unique extremal minimum for $z \in (1-u_0, 1)$, it has a unique intersection with the horizontal line B_0 since $A(1-u_0) < B_0$. Thus in both cases, the equation $A(z) = B_0$ has a unique root in $(1-u_0, 1)$. As a result, the final epidemic size $z_\infty^- \in (1-u_0, 1)$ is uniquely determined by the equation (34).

Unique existence of z_∞^+

To prove that the final epidemic size z_∞^+ is uniquely determined by the equation (35), let us consider the existence of a root for the equation $G(u) = 0$ where

$$G(u) := u - \big\{u(\tau^\star) + v(\tau^\star)\big\} - \frac{\rho}{\beta}(1-q_{\max})\ln\frac{u}{u(\tau^\star)}. \tag{104}$$

From (30) in Subsection 3.3.2 and (98) in Appendix 3.A.7, the equation $G(1-z_\infty^+) = 0$ is mathematically equivalent to the final size equation (35). Since $u(\tau)$ is monotonically decreasing as time passes, we have $u(\tau) < u(\tau^\star)$ for $\tau > \tau^\star$. Hence we consider $G(u)$ hereafter for $u \in (0, u(\tau^\star))$. The function $G(u)$ is continuous and differentiable for $u \in (0, u(\tau^\star))$. Moreover, it satisfies that $\lim_{u\to+0} G(u) = \infty > 0$, and $G(u(\tau^\star)) = -v(\tau^*) < 0$. From these facts, the equation $G(u) = 0$ has at least one root in $(0, u(\tau^\star))$. Further we can easily find that $G(u)$ is monotonically decreasing or has a unique

extremal minimum in $(0, u(\tau^\star))$. When $G(u)$ is monotonically decreasing for $u \in (0, u(\tau^\star))$, the equation $G(u) = 0$ has a unique root in $(0, u(\tau^\star))$. Even when $G(u)$ has a unique extremal minimum in $(0, u(\tau^\star))$, it has a unique root in $(0, u(\tau^\star))$, because the extremum value of G must be negative since $G(u(\tau^\star)) < 0$. Hence in both cases, the equation $G(u) = 0$ has a unique root $u = u_\infty^+ \in (0, u(\tau^\star))$. Therefore, the equation (35) determines a unique final epidemic size $z_\infty^+ \in (1 - u(\tau^\star), 1)$. This is because $u_\infty^+ = 1 - z_\infty^+$ and $z_\infty^+ = 1 - u_\infty^+ \in (1 - u(\tau^\star), 1)$ where $1 - u(\tau^\star) = v(\tau^\star) + q_{\max}(1 + \rho/\sigma) > q_{\max}(1 + \rho/\sigma) > q_{\max}$ from (101), and $u(\tau^\star)$ is given by (102) in Appendix 3.A.7.

APPENDIX 3.A.9: PROOF OF THEOREM 3.4

In order to prove the Theorem 3.4, we use two lemmas.

Lemma 3.17. *It holds that* $z_\infty^+ \geq q_c\,(1 + \rho/\sigma) \geq z_\infty^-$.

Proof. The proof is given straightforward from the arguments in the proof for Theorem 3.2 and its corollaries, given in Appendix 3.A.5. From (93), the condition $q_\infty^- \leq q_{\max}$ is equivalent to

$$u_\infty^- \geq 1 - q_{\max}\left(1 + \frac{\rho}{\sigma}\right), \tag{105}$$

where u_∞^- is the root of (97), and subsequently q_∞^- is given by (92). Thus, when and only when the condition (105) is satisfied, the isolation never reaches the capacity, so that the epidemic dynamics is always at the isolation well-functioning phase. Inversely, when and only when the condition (105) is unsatisfied, the epidemic dynamics enters in the isolation incapable phase in a finite time.

Thus, for the value $u(\tau^\star)$ at the moment when the isolation incapable phase begins, it must hold that

$$u(\tau^\star) < 1 - q_{\max}\left(1 + \frac{\rho}{\sigma}\right).$$

The value $u(\tau)$ is monotonically decreasing in terms of time since $du/d\tau$ is negative for any $\tau > 0$. Hence we have $u_\infty^+ < u(\tau^\star)$ where u_∞^+ is the root of (103) at the isolation incapable phase. Therefore, we have

$$u_\infty^+ < 1 - q_{\max}\left(1 + \frac{\rho}{\sigma}\right). \tag{106}$$

Since $z_\infty^- = 1 - u_\infty^-$, these arguments indicate that, when and only when the isolation never reaches the capacity, we have $z_\infty^- \leq q_{\max}(1 + \rho/\sigma)$ from (105). Since this condition must hold for any $q_{\max} \geq q_c$ from Corollary 3.2.1, and since z_∞^- is independent of $q_{\max}$, we find that $z_\infty^- \leq q_c(1 + \rho/\sigma)$.

On the other hand, when the isolation reaches the capacity at a finite time with $q_{\max} < q_c$, we have $z_\infty^+ > q_{\max}(1 + \rho/\sigma)$ from (106). Since this condition must hold for any $q_{\max} < q_c$, we have $z_\infty^+ \geq q_c(1 + \rho/\sigma)$. □

Lemma 3.18. *It holds that* $z_\infty^- = q_c\,(1 + \rho/\sigma)$.

Proof. Substituting $z_\infty^- = q_c\,(1 + \rho/\sigma)$ for (34) and taking account of (32) in Corollary 3.2.1, we can easily find that the equation (103) holds. Since z_∞^- is uniquely determined as the root of (34), we can result in this lemma. □

Now, the equation (35) can be rewritten as

$$q_{\max}\left(1+\frac{\rho}{\sigma}\right)-z_\infty^+=\frac{\rho}{\beta}(1-q_{\max})\ln\frac{1-z_\infty^+}{u_0(1-q_{\max})^{\beta/\sigma}}. \tag{107}$$

Taking the limit as $q_{\max}\to q_c$ for (107), we have the following equation with respect to $z_\infty^\dagger$ from Lemma 3.18 and (34):

$$H(z_\infty^\dagger):=z_\infty^- - z_\infty^\dagger-\frac{\rho}{\beta}(1-q_c)\ln\frac{1-z_\infty^\dagger}{1-z_\infty^-}=0.$$

It is easily found that $H(z_\infty^-)=0$ and $\lim_{z\to 1-0}H(z)=\infty$. The derivative of $H(z)$ becomes

$$H'(z)=-1+\frac{\rho}{\beta}\frac{1-q_c}{1-z},$$

which is monotonically increasing in terms of $z\in(z_\infty^-,1)\subset(0,1)$ with $H'(z)\to\infty$ as $z\to 1-0$. If $H'(z_\infty^-)\geq 0$, then $H(z)>0$ for any $z\in(z_\infty^-,1)$. In this case, the root of $H(z)=0$ in $[z_\infty^-,1]$ is only $z=z_\infty^-$. In contrast, if $H'(z_\infty^-)<0$, there exists a unique value $\eta\in(z_\infty^-,1)$ such that $H'(z)<0$ for $z\in(z_\infty^-,\eta)$ and $H'(z)>0$ for $z\in(\eta,1)$. This means that $H(z)<0$ for $z\in(z_\infty^-,\eta)$, and $H(z)$ is monotonically increasing for $z\in(\eta,1)$ with $\lim_{z\to 1-0}H(z)=\infty$. Therefore we have a unique value $\zeta\in(\eta,1)\subset(z_\infty^-,1)$ such that $H(\zeta)=0$, because $H(z)$ is continuous in $(z_\infty^-,1)$.

On the other hand, from (35), we can derive

$$\frac{\partial z_\infty^+}{\partial q_{\max}}=\frac{1+(\rho/\beta)\ln\left[(1-z_\infty^+)/\left\{u_0(1-q_{\max})^{\beta/\sigma}\right\}\right]}{1-(\rho/\beta)(1-q_{\max})/(1-z_\infty^+)}.$$

Then we have

$$\left.\frac{\partial z_\infty^+}{\partial q_{\max}}\right|_{(q_{\max},z_\infty^+)=(q_c,z_\infty^-)}=\frac{1}{1-(\rho/\beta)(1-q_c)/(1-z_\infty^-)}=-\frac{1}{H'(z_\infty^-)}. \tag{108}$$

Hence we find that, if $H'(z_\infty^-)<0$, the derivative (108) becomes positive. Thus, if $z_\infty^\dagger=z_\infty^+$ with $H'(z_\infty^-)<0$, z_∞^+ must be smaller than z_∞^- for $q_{\max}$ less than and sufficiently near q_c because z_∞^+ is continuous and differentiable for $q_{\max}\in(0,q_c)$ and the derivative (108) is positive. This is contradictory to the result of Lemma 3.17. Therefore, if $H'(z_\infty^-)<0$, $z_\infty^\dagger$ must be greater than z_∞^-.

The condition $H'(z_\infty^-)<0$ is equivalent to the following:

$$\frac{\rho}{\beta}<1 \quad\text{and}\quad q_c<q_{cc}:=\frac{1-\rho/\beta}{1-\rho/\beta+\rho/\sigma}. \tag{109}$$

From $q_{\max}<q_c$ and (32), the second inequality of (109) is equivalent to

$$1-q_{cc}\left(1+\frac{\rho}{\sigma}\right)<u_0\left(1-q_{cc}\right)^{\beta/\sigma}.$$

This inequality results in the second condition of (36). If $H'(z_\infty^-)\geq 0$, $z_\infty^\dagger$ must be z_∞^- since the equation $H(z)=0$ has the unique root $z=z_\infty^-$ in $[z_\infty^-,1]$ and the derivative (108) is non-positive with no contradiction. These arguments prove the theorem.

APPENDIX 3.A.10: PROOF OF LEMMA 3.3

Note that the isolated population size q never becomes greater than $q_{\max}$ in the epidemic dynamics governed by (40) with the initial value $q(0) = 0$. From (40), we have $dq/d\tau = 0$ for $q = q_{\max}$. Thus, also in accordance with the modeling assumption, the isolated population size q never becomes greater than $q_{\max} < 1$ for any $\tau \geq 0$.

Then from (40), we formally have

$$v(\tau) = v(0) \exp\Big[\int_0^\tau \mathscr{R}_0 \frac{u(\nu)}{1-q(\nu)} + \varepsilon \mathscr{R}_0 \frac{w(\nu)}{1-q(\nu)}\, d\nu - \tau \Big] > 0$$

with $v(0) > 0$ for any τ such that $q(\nu) < q_{\max}$ for any $\nu < \tau$. If the system gets in the isolation incapable phase after $\tau = \tau^\star > 0$, we have $v(\tau^\star) > 0$ from the above argument, and

$$v(\tau) = v(\tau^\star) \exp\Big[\int_{\tau^\star}^\tau \mathscr{R}_0 \frac{u(\nu)}{1-q(\nu)} + \varepsilon \mathscr{R}_0 \frac{w(\nu)}{1-q(\nu)}\, d\nu - (1-\gamma)(\tau - \tau^\star) \Big] > 0$$

for any $\tau \geq \tau^\star$ because the system remains at the isolation incapable phase once it enters the phase. Therefore from these arguments, we have $v(t) > 0$ for any $\tau \geq 0$ about the system (40) with $v(0) = v_0 > 0$. Thus we have $dq/d\tau > 0$ with $q = 0$ for any $\tau \geq 0$. Since $dq/d\tau > 0$ at $\tau = 0$, we finally find that $q \in (0, q_{\max})$ for any $\tau > 0$.

With the same arguments, we can prove that $u > 0$ and $w > 0$ for any $\tau > 0$. Finally, since it holds from the equations of (40) that $u + v + q + w = 1$ for any $\tau \geq 0$, we obtain the lemma.

APPENDIX 3.A.11: DERIVATION OF CONSERVED QUANTITIES

At the isolation effective phase

This is the phase when the system (40) follows the isolation effective phase with $\phi(q, v) = \gamma v$. First, from the equations of $du/d\tau$ and $dq/d\tau$ in (40), we can derive the following differential equation:

$$\frac{du}{dq} = -\frac{\mathscr{R}_0}{\gamma} \frac{u}{1-q}. \tag{110}$$

We can easily solve the equation (110), and find the equation (41) between u and q, making use of $u(0) = u_0 > 0$, and $q(0) = 0$.

Next, from the equations of $du/d\tau$ and $dv/d\tau$ in (40), we can derive the following differential equation:

$$\frac{dv}{du} = \varepsilon \frac{v}{u} - \varepsilon \Big(1 - \frac{1}{\varepsilon \mathscr{R}_0}\Big) \frac{1-q}{u} - (1-\varepsilon), \tag{111}$$

using the relation $w = 1 - u - v - q$. Then substituting (41) for (111), we can solve it and derive the equation (42), making use of $u(0) = u_0$ and $v(0) = v_0 = 1 - u_0$.

At the isolation incapable phase

Once the isolation reaches the capacity at finite time, the system (40) switches to the isolation incapable phase with $\phi(q, v) = 0$. From the equations of

$du/d\tau$ and $dv/d\tau$ in (40) at the isolation incapable phase, we can obtain the following differential equation:

$$\frac{dv}{du} = \varepsilon\frac{v}{u} - \varepsilon\Big(1 - \frac{1-\gamma}{\varepsilon\mathscr{R}_0}\Big)\frac{1-q_{\max}}{u} - (1-\varepsilon). \tag{112}$$

We can easily solve (112) and get the following equation

$$u(\tau) + v(\tau) = \Big(1 - \frac{1-\gamma}{\varepsilon\mathscr{R}_0}\Big)(1-q_{\max}) + C\{u(\tau)\}^{\varepsilon} \tag{113}$$

from the general solution of (112) with an undetermined constant C.

Since the isolation incapable phase arises only after the isolation reaches the capacity, suppose now that it arises at $\tau = \tau^\star > 0$. From the continuity of the temporal variation of the variables in the system (40), both of the equations (42) and (113) are satisfied at $\tau = \tau^\star$. This is the continuity condition that is satisfied by the system (40) if it switches the isolation effective phase to the isolation incapable phase at $\tau = \tau^\star$.

First, as shown in Lemma 3.4, we find the susceptible subpopulation size $u = u^\star$ defined by (45) at the moment $\tau = \tau^\star$ from (41), because $q(\tau^\star) = q_{\max}$ at the moment when the isolation reaches the capacity. Next, from the continuity condition about the equations (42) and (113), we have the following equality which holds at $\tau = \tau^\star$:

$$\frac{1-\varepsilon\mathscr{R}_0}{\gamma-\varepsilon\mathscr{R}_0}\Big(\frac{u^\star}{u_0}\Big)^{\gamma/\mathscr{R}_0} - \frac{1-\gamma}{\gamma-\varepsilon\mathscr{R}_0}\Big(\frac{u^\star}{u_0}\Big)^{\varepsilon} = \Big(1-\frac{1-\gamma}{\varepsilon\mathscr{R}_0}\Big)(1-q_{\max}) + C(u^\star)^{\varepsilon}$$

when $\gamma \neq \varepsilon\mathscr{R}_0$, and

$$\begin{aligned}\Big[\Big(\frac{1}{\mathscr{R}_0} - \epsilon\Big)\ln\frac{u^\star}{u_0} + 1\Big]\Big(\frac{u^\star}{u_0}\Big)^{\varepsilon} &= \Big(1-\frac{1-\gamma}{\varepsilon\mathscr{R}_0}\Big)(1-q_{\max}) + C(u^\star)^{\varepsilon} \\ &= \Big(2-\frac{1}{\gamma}\Big)(1-q_{\max}) + C(u^\star)^{\varepsilon}\end{aligned}$$

when $\gamma = \varepsilon\mathscr{R}_0$. Hence with (45), we find

$$C = \begin{cases} \dfrac{1-\gamma}{\varepsilon\mathscr{R}_0(1-\varepsilon\mathscr{R}_0/\gamma)}\Big[(1-q_{\max})^{1-\varepsilon\mathscr{R}_0/\gamma} - \dfrac{\varepsilon\mathscr{R}_0}{\gamma}\Big](u_0)^{-\varepsilon} & \text{when } \varepsilon\mathscr{R}_0 \neq \gamma; \\ \dfrac{1-\gamma}{\gamma}\big[\ln(1-q_{\max}) + 1\big](u_0)^{-\varepsilon} & \text{when } \varepsilon\mathscr{R}_0 = \gamma. \end{cases} \tag{114}$$

Finally, substituting (114) for (113), we can derive the equation (43) for the isolation incapable phase.

APPENDIX 3.A.12: PROOF OF LEMMA 3.5 AND 3.6

If the system remains at the isolation effective phase, the isolated subpopulation size q monotonically increases for any $\tau \geq 0$ since the infective subpopulation size $v > 0$ from Lemma 3.3. Since it holds that $q < q_{\max} < 1$ for any $\tau \geq 0$, q must converge to a positive finite value less than or equal to $q_{\max} < 1$ as $\tau \to \infty$, so that we have $dq/d\tau \to 0$ as $\tau \to \infty$. Therefore, it is necessary that $v \to 0$ as $\tau \to \infty$. This proves Lemma 3.5. Then, from the equation in (40), we have $du/d\tau \to 0$ as $\tau \to \infty$ at the same time. Subsequently, from the relations $u + v + q + w = 1$ and (41), we can get the disease-eliminated equilibrium E_0^- given by (46), and find that u_∞^- must be positive. This leads to Lemma 3.6.

APPENDIX 3.A.13: PROOF OF THEOREM 3.5, AND LEMMA 3.7

If $u \to 0$ as $\tau \to \infty$, we have $q \to 1$ as $\tau \to \infty$ because of the conserved quantity (41). This is contradictory to the supposition which means that $q < q_{\max} < 1$ for any $\tau \geq 0$. Hence the convergence such that $u \to u_\infty^- > 0$ as $\tau \to \infty$ is necessary when the system always remains at the isolation effective phase.

By applying the equations (41) and (42) for the equation of $du/d\tau$ in (40), we can reduce the system (40) to the following mathematically equivalent one dimensional system:

$$\frac{du}{d\tau} = -\mathscr{R}_0 u_0 \{F(u) - u\} \Big(\frac{u}{u_0} \Big)^{1-\gamma/\mathscr{R}_0}. \tag{115}$$

From the above arguments to show that $du/d\tau \to 0$ as $\tau \to \infty$ while the value u is positive, we find it necessary that $F(u) - u \to 0$ as $\tau \to \infty$, while $u \to u_\infty^-$ which is given by a positive root in $(0, u_0)$ for the equation (47).

Since u is monotonically decreasing from u_0 as time passes, and $F(u_0) - u_0 = 1 - u_0 > 0$, we have $u \to u_\infty^- > 0$ as $\tau \to \infty$ if and only if the equation (47) has a positive root u_∞^- in $(0, u_0)$. Now the function $F(u)$ is continuous and differentiable in $(0, u_0)$, with $F(u) \to 0$ as $u \to +0$, and $F(u) \to 1$ as $u \to u_0 - 0$. Moreover, from the derivative

$$F'(u) = \begin{cases} \dfrac{\varepsilon}{u_0} \dfrac{1-\gamma}{\gamma - \varepsilon\mathscr{R}_0} \Big(\dfrac{u}{u_0} \Big)^{\gamma/\mathscr{R}_0 - 1} \Big[\dfrac{\gamma}{1-\gamma} \Big(\dfrac{1}{\varepsilon\mathscr{R}_0} - 1 \Big) - \Big(\dfrac{u}{u_0} \Big)^{\varepsilon - \gamma/\mathscr{R}_0} \Big] & \\ & \text{when } \varepsilon\mathscr{R}_0 \neq \gamma; \\ \varepsilon \Big(1 + \varepsilon \dfrac{1-\gamma}{\gamma} \ln \dfrac{u}{u_0} + \dfrac{1-\gamma}{\gamma} \dfrac{1}{u_0} \Big) & \text{when } \varepsilon\mathscr{R}_0 = \gamma, \end{cases} \tag{116}$$

we can easily find that $F'(u) > 0$ and further $F''(u) < 0$ for $u \in (0, u_0)$ when $\varepsilon\mathscr{R}_0 \geq 1$. In contrast, when $\varepsilon\mathscr{R}_0 < 1$, there is a unique critical value $u = u_c \in (0, u_0)$ such that $F'(u_c) = 0$, $F'(u) < 0$ for $u \in (0, u_c)$, and $F'(u) > 0$ for $u \in (u_c, u_0)$, where

$$u_c := \begin{cases} u_0 \Big\{ \dfrac{\gamma}{1-\gamma} \Big(\dfrac{1}{\varepsilon\mathscr{R}_0} - 1 \Big) \Big\}^{\mathscr{R}_0/(\varepsilon\mathscr{R}_0 - \gamma)} & \text{when } \varepsilon\mathscr{R}_0 \neq \gamma; \\ u_0 \exp \Big[-\dfrac{1}{\varepsilon} \Big(\dfrac{\gamma}{1-\gamma} + \dfrac{1}{u_0} \Big) \Big] & \text{when } \varepsilon\mathscr{R}_0 = \gamma. \end{cases} \tag{117}$$

From these features of the function F, we have $F(u) - u > 0$ for any $u \in (0, u_0)$ when and only when $\varepsilon\mathscr{R}_0 \geq 1$. This is the case where the equation (47) has no positive root in $(0, u_0)$. In contrast, there exists a unique positive root $u = u_\infty^-$ in $(0, u_0)$ for the equation (47) when and only when $\varepsilon\mathscr{R}_0 < 1$, proved by the intermediate value theorem for the continuous function $F(u)$ in $[0, u_0]$, because $F(u) - u \to 0$ as $u \to +0$ and $F(u) - u \to 1 - u_0 > 0$ as $u \to u_0 - 0$ while $F(u) - u < 0$ for $u \in (0, u_c)$.

Consequently, the system can always remains at the isolation effective phase only when $\varepsilon\mathscr{R}_0 < 1$, and then $u \to u_\infty^- > 0$ as $\tau \to \infty$, where u_∞^- is determined by the unique positive root in $(0, u_0)$ for the equation (47). This indicates the equilibrium E_0^- given by (46) is uniquely determined, and it is globally asymptotically stable because the temporal variation is determined by the above one dimensional ordinary differential equation (115) when the

system always remains at the isolation effective phase, about which we find from the features of F that $F(u) - u < 0$ for $u \in (0, u_\infty^-)$, and $F(u) - u > 0$ for $u \in (u_\infty^-, u_0)$. Lastly these arguments prove Theorem 3.5.

Further from the above arguments, when $\varepsilon\mathscr{R}_0 \geq 1$, the susceptible subpopulation size u is monotonically decreasing toward zero, and then the isolated subpopulation size q monotonically increasing toward one, which is impossible unless there is no capacity for the isolation, that is, $q_{\max} = 1$. Hence, we can conclude that q reaches $q_{\max} < 1$ when $\varepsilon\mathscr{R}_0 \geq 1$. This proves Lemma 3.7.

APPENDIX 3.A.14: PROOF OF THEOREM 3.6

Since we have the result of Lemma 3.7 for the case of $\varepsilon\mathscr{R}_0 \geq 1$, it is sufficient to consider only the case of $\varepsilon\mathscr{R}_0 < 1$. As shown in (46) by the conserved quantity (41), we have the equation

$$q_\infty^- = 1 - \left(\frac{u_\infty^-}{u_0}\right)^{\gamma/\mathscr{R}_0} \tag{118}$$

for the equilibrium values u_∞^- and q_∞^- at the equilibrium E_0^- if the system always remains at the isolation effective phase. Then it must be satisfied that $q_\infty^- \leq q_{\max}$. Since $q(\tau)$ is monotonically increasing in terms of τ, if $q_\infty^- > q_{\max}$, it means that the system cannot remain at the isolation effective phase, and the isolation reaches the capacity at finite time. Inversely, in a mathematical sense, when the isolation reaches the capacity at finite time, it never holds that $q_\infty^- \leq q_{\max}$, and instead it holds that $q_\infty^- > q_{\max}$. From (118) , the condition that $q_\infty^- > q_{\max}$ is mathematically equivalent to

$$u_\infty^- < u_0(1 - q_{\max})^{\mathscr{R}_0/\gamma}. \tag{119}$$

This can be regarded as the necessary and sufficient condition that the isolation reaches the capacity at finite time. As shown in Appendix 3.A.13 to prove Theorem 3.5 and the related results, we have found that $F(u) - u < 0$ for $u \in (0, u_\infty^-)$, and $F(u) - u > 0$ for $u \in (u_\infty^-, u_0)$ when $\varepsilon\mathscr{R}_0 < 1$. Hence the condition (119) becomes equivalent to (48) of Theorem 3.6.

APPENDIX 3.A.15: PROOF OF COROLLARIES 3.6.1, 3.6.2, AND LEMMA 3.8

The condition (48) cannot hold if the right side

$$F\big(u_0(1 - q_{\max})^{\mathscr{R}_0/\gamma}\big) = \begin{cases} \dfrac{1-\gamma}{\gamma - \varepsilon\mathscr{R}_0}(1 - q_{\max})\Big[\dfrac{1 - \varepsilon\mathscr{R}_0}{1-\gamma} - (1 - q_{\max})^{\varepsilon\mathscr{R}_0/\gamma - 1}\Big] & \text{when } \varepsilon\mathscr{R}_0 \neq \gamma; \\ (1 - q_{\max})\Big[1 + \dfrac{1-\gamma}{\gamma}\ln(1 - q_{\max})\Big] & \text{when } \varepsilon\mathscr{R}_0 = \gamma \end{cases} \tag{120}$$

is not positive, which leads to (50) in Corollary 3.6.2.

The critical value q_c for the isolation capacity $q_{\max}$ must be defined as the upper bound of $q_{\max}$ that satisfies the condition (119) in Appendix 3.A.14. Therefore, it must hold that $u_\infty^- = u_0(1 - q_c)^{\mathscr{R}_0/\gamma}$. This proves Lemma 3.8. Then this is the case that $u = u_0(1 - q_c)^{\mathscr{R}_0/\gamma}$ becomes the unique positive roof of the equation $u = F(u)$ when $\varepsilon\mathscr{R}_0 < 1$, as the definition of u_∞^-. This result shows Corollary 3.6.1.

APPENDIX 3.A.16: PROOF OF LEMMA 3.9 AND THEOREM 3.7

Applying the equation (43) for the equation of $du/d\tau$ in (40), we can obtain the following one dimensional ordinary equation which determines the dynamics by (40) for $\tau \geq \tau^\star$ at the isolation incapable phase:

$$\frac{du}{d\tau} = -\frac{\mathscr{R}_0}{1-q_{\max}}\{G(u)-u\}u. \tag{121}$$

Let us consider the case of $\varepsilon\mathscr{R}_0 < 1$ first. Then, from the condition (ii) of Theorem 3.6, it holds that

$$G(u^\star) > u_0(1-q_{\max})^{\mathscr{R}_0/\gamma} = u^\star = u(\tau^\star), \tag{122}$$

Besides, as already mentioned at the end of Subsection 3.4.2, from the continuity of $u(\tau)$ and $v(\tau)$ at $\tau = \tau^\star$, it holds that $F(u^\star) = G(u^\star)$.

Thus we have $du/d\tau < 0$ at $\tau = \tau^\star$ with $G(u^\star) - u^\star > 0$. Now we consider the function $G(u) - u$ with $B \neq 0$ in order to investigate the sign of $du/d\tau$ in $(0, u^\star)$. From the definition of G and B by (43) and (44), we have

$$G(0) = \Big(1 - \frac{1-\gamma}{\varepsilon\mathscr{R}_0}\Big)(1-q_{\max}) \tag{123}$$

and

$$G'(u) - 1 = \varepsilon B\Big(\frac{u}{u_0}\Big)^{\varepsilon-1} - 1; \quad G''(u) = -\varepsilon(1-\varepsilon)B\Big(\frac{u}{u_0}\Big)^{\varepsilon-2}. \tag{124}$$

If $B < 0$, then the function $G(u) - u$ is convex and monotonically decreasing for $u \in (0, u^\star)$ since $G''(u) > 0$ and $G'(u) - 1 < 0$ from (124) in this case. Hence, there is no positive root of the equation $G(u) - u = 0$ if $B < 0$, because $G(u) - u > 0$ for all $u \in (0, u^\star)$ with $G(u^\star) - u^\star > 0$.

If $B > 0$, then the function $G(u) - u$ is concave for all $u > 0$ and has at most one extremal maximum value in $(0, u^\star)$ since $G''(u) < 0$, and the number of positive root for the equation $G'(u) - 1 = 0$ is only one from (124). The function $G(u) - u$ is unimodal in $(0, u^\star)$ if the extremal maximal value exists there, while it is monotonically increasing in $(0, u^\star)$ if the extremal maximal value exists out of $(0, u^\star)$. Thus, independently of whether the function $G(u) - u$ is unimodal or monotonically increasing, there is no positive root of the equation $G(u) - u = 0$ if $G(0) \geq 0$, because then $G(u) - u > 0$ for all $u \in (0, u^\star)$ with $G(u^\star) - u^\star > 0$. In contrast, if $G(0) < 0$, there is a unique positive root of the equation $G(u) - u = 0$ in $(0, u^\star)$, that is u^+_∞, independently of whether the function $G(u) - u$ is unimodal or monotonically increasing. Then it holds that $G(u) - u > 0$ for $u \in (u^+_\infty, u^\star)$ and $G(u) - u < 0$ for $u \in (0, u^+_\infty)$. Therefore, from the temporally continuous decreasing change of u, we can conclude that u must converge to $u^+_\infty \in (0, u^\star)$ as $\tau \to \infty$ if $B > 0$ and $G(0) < 0$, while it must converge to 0 if $B < 0$ or if $B > 0$ and $G(0) \geq 0$.

When $B = 0$, $G(u)$ becomes constant for all $u \in [0, u^\star]$:

$$G(u) \equiv G(0) = \Big(1 - \frac{1-\gamma}{\varepsilon\mathscr{R}_0}\Big)(1-q_{\max}) = \Big(1 - \frac{1-\gamma}{\varepsilon\mathscr{R}_0}\Big)\Big(\frac{\varepsilon\mathscr{R}_0}{\gamma}\Big)^{\gamma/(\gamma-\varepsilon\mathscr{R}_0)} \tag{125}$$

from (43) and (44). Then the condition (122) results in

$$\Big(1 - \frac{1-\gamma}{\varepsilon\mathscr{R}_0}\Big)\Big(\frac{\varepsilon\mathscr{R}_0}{\gamma}\Big)^{(\gamma-\mathscr{R}_0)/(\gamma-\varepsilon\mathscr{R}_0)} > u_0.$$

Hence, under the condition (122) with which the system enters the isolation incapable phase, we find it necessary that $\varepsilon\mathscr{R}_0 > 1-\gamma$. Thus we find that $G(u) \equiv G(0) \in (0,1)$ in this case. Since u is temporally monotonically decreasing from $u = u^\star$ with $G(u) \equiv G(0) > u^\star$, we have $G(u) - u = G(0) - u > 0$ for any $\tau > \tau^\star$ and any $u \in (0, u^\star)$. Therefore, u must converge to 0 as $\tau \to \infty$ in this case because $du/d\tau < 0$ for any $u \in (0, u^\star)$. Finally, we can conclude that, when $\varepsilon\mathscr{R}_0 < 1$, u converges to $u_\infty^+ \in (0, u^\star)$ as $\tau \to \infty$ if and only if $B > 0$ and $G(0) < 0$, and otherwise it converges to 0.

Next let us consider the case of $\varepsilon\mathscr{R}_0 \geq 1$. Then we have $G(0) > 0$ from (123). Further we necessarily have $G(u^\star) = u^\star + v^\star > u^\star$ in this case, because $v(\tau^\star) = v^\star > 0$ at $\tau = \tau^\star$ from Lemma 3.3. Thus we can apply the same arguments as those for the case of $\varepsilon\mathscr{R}_0 < 1$, and find that u converges to 0 as $\tau \to \infty$ in this case. Consequently we have the following result:

Lemma 3.19. *At the isolation incapable phase, $u \to u_\infty^+ \in (0, u^\star)$ as $\tau \to \infty$ if and only if $\varepsilon\mathscr{R}_0 < 1$, $B > 0$ and $G(0) < 0$. Otherwise, $u \to 0$ as $\tau \to \infty$.*

From the condition $G(0) < 0$, we have $\varepsilon\mathscr{R}_0 < 1-\gamma$. From the condition $B > 0$, we have

$$\begin{cases} \left(1 - \dfrac{\varepsilon\mathscr{R}_0}{\gamma}\right)\left[(1-q_{\max})^{1-\varepsilon\mathscr{R}_0/\gamma} - \dfrac{\varepsilon\mathscr{R}_0}{\gamma}\right] > 0 & \text{when } \varepsilon\mathscr{R}_0 \neq \gamma; \\ \ln(1-q_{\max}) + 1 > 0 & \text{when } \varepsilon\mathscr{R}_0 = \gamma. \end{cases} \tag{126}$$

When $\varepsilon\mathscr{R}_0 < 1-\gamma$ and $\varepsilon\mathscr{R}_0 = \gamma$, the condition $\gamma < 1/2$ must be satisfied. In this case, the condition (ii) of Theorem 3.6 can be written as

$$1 + \ln(1-q_{\max}) > u_0(1-q_{\max})^{1/\varepsilon - 1} - \frac{1-2\gamma}{\gamma}\ln(1-q_{\max}),$$

and we find that the right side of this inequality is necessarily positive. Thus, when $\varepsilon\mathscr{R}_0 < 1-\gamma$ and $\varepsilon\mathscr{R}_0 = \gamma$, the condition (126) for $B > 0$ holds at the isolation incapable phase. Therefore, the condition $\varepsilon\mathscr{R}_0 < 1-\gamma$ is necessary and sufficient to have $u \to u_\infty^+ \in (0, u^\star)$ as $\tau \to \infty$ when $\varepsilon\mathscr{R}_0 = \gamma$.

When $\varepsilon\mathscr{R}_0 < 1-\gamma$ and $\varepsilon\mathscr{R}_0 \neq \gamma$, the condition (126) becomes equivalent to the following:

$$(1-q_{\max})^{1-\varepsilon\mathscr{R}_0/\gamma} > \frac{\varepsilon\mathscr{R}_0}{\gamma} \quad \text{with } \frac{\varepsilon\mathscr{R}_0}{\gamma} < 1 \tag{127}$$

or

$$(1-q_{\max})^{1-\varepsilon\mathscr{R}_0/\gamma} < \frac{\varepsilon\mathscr{R}_0}{\gamma} \quad \text{with } \frac{\varepsilon\mathscr{R}_0}{\gamma} > 1. \tag{128}$$

Now, from Corollary 3.6.2, it is necessary in order to have the isolation incapable phase that the condition (50) is unsatisfied, which we can find equivalent to the following:

$$(1-q_{\max})^{1-\varepsilon\mathscr{R}_0/\gamma} > \frac{1-\gamma}{1-\varepsilon\mathscr{R}_0} \quad \text{for } \frac{\varepsilon\mathscr{R}_0}{\gamma} < 1; \tag{129}$$

$$(1-q_{\max})^{1-\varepsilon\mathscr{R}_0/\gamma} < \frac{1-\gamma}{1-\varepsilon\mathscr{R}_0} \quad \text{for } \frac{\varepsilon\mathscr{R}_0}{\gamma} > 1. \tag{130}$$

On the other hand, we have

$$\frac{1-\gamma}{1-\varepsilon\mathscr{R}_0}-\frac{\varepsilon\mathscr{R}_0}{\gamma}=\frac{(1-\gamma)-\varepsilon\mathscr{R}_0}{1-\varepsilon\mathscr{R}_0}\Big(1-\frac{\varepsilon\mathscr{R}_0}{\gamma}\Big).$$

Hence, when $\varepsilon\mathscr{R}_0<1-\gamma$, we find that the conditions (129) and (130) are sufficient for (127) and (128) respectively. That is, since the condition (127) or (128) necessarily holds when (129) or (130) is satisfied with $\varepsilon\mathscr{R}_0<1-\gamma$, the condition (127) or (128) is satisfied at the isolation incapable phase with $\varepsilon\mathscr{R}_0<1-\gamma$. Therefore, when $\varepsilon\mathscr{R}_0\neq\gamma$, the condition $\varepsilon\mathscr{R}_0<1-\gamma$ is necessary and sufficient to have $u\to u_\infty^+\in(0,u^\star)$ as $\tau\to\infty$. Finally this result and Lemma 3.19 prove Lemma 3.9.

Then, from the conserved quantity (43), we note that $v\to 0$ when $u\to u_\infty^+\in(0,u^\star)$ as $\tau\to\infty$, while $v\to G(0)>0$ when $u\to 0$ as $\tau\to\infty$. Thus, the system (40) approaches a disease-eliminated equilibrium at the isolation incapable phase if $u\to u_\infty^+\in(0,u^\star)$ as $\tau\to\infty$. Besides, exceptionally with $\varepsilon\mathscr{R}_0=1-\gamma$, the disease goes extinct even when $u\to 0$ as $\tau\to\infty$ at the isolation incapable phase. In contrast, the system approaches the endemic equilibrium if $u\to 0$ as $\tau\to\infty$ when $\varepsilon\mathscr{R}_0>1-\gamma$. These results with Lemma 3.9 prove Theorem 3.7.

APPENDIX 3.A.17: PROOF OF THEOREM 3.8

From the equation of $dv/d\tau$ in the system (40) before and after the isolation reaches the capacity at $\tau=\tau^\star$, we can obtain the value of $dv/d\tau$ at $q=q_{\max}$ respectively as follows:

$$\begin{aligned}\frac{dv}{d\tau}\Big|_{\tau\to\tau^\star-0}&=\frac{\mathscr{R}_0v^\star}{1-q_{\max}}\Big\{u^\star-\varepsilon F(u^\star)+\frac{\varepsilon\mathscr{R}_0-1}{\mathscr{R}_0}(1-q_{\max})\Big\};\\ \frac{dv}{d\tau}\Big|_{\tau\to\tau^\star+0}&=\frac{\mathscr{R}_0v^\star}{1-q_{\max}}\Big\{u^\star-\varepsilon G(u^\star)+\frac{\varepsilon\mathscr{R}_0-(1-\gamma)}{\mathscr{R}_0}(1-q_{\max})\Big\},\end{aligned}\tag{131}$$

where $u(\tau^\star)=u^\star$ defined by (45), and we used

$$\lim_{\tau\to\tau^\star-0}v(\tau)=v^\star:=F(u^\star)-u^\star;\qquad\lim_{\tau\to\tau^\star+0}v(\tau)=G(u^\star)-u^\star$$

from the continuity of $u(\tau)$ and $v(\tau)$ at $\tau=\tau^\star$. Besides, as mentioned at the end of Subsection 3.4.2, from the continuity of $u(\tau)$ and $v(\tau)$ at $\tau=\tau^\star$, it holds that $F(u^\star)=G(u^\star)$.

Note that the former of (131) is necessarily less than the latter because

$$\lim_{\tau\to\tau^\star-0}\phi(q,v)=\gamma v^\star>\lim_{\tau\to\tau^\star+0}\phi(q,v)=0.$$

Hence the value v may continuously increase or decrease at $\tau=\tau^\star$ unless the revival does not occur. If the former is negative and the latter is positive, it occur. Thus these arguments result in Theorem 3.8.

APPENDIX 3.A.18: PROOF OF LEMMA 3.10

Taking into account the continuity of u_∞^+ in terms of $q_{\max}\in(0,q_c)$ when $\varepsilon\mathscr{R}_0<1-\gamma$, we prove first its monotonicity:

Lemma 3.20. *z_∞^+ is monotone in terms of $q_{\max}\in(0,q_c)$.*

Proof. Suppose that $\partial z_\infty^+/\partial q_{\max} = -\partial u_\infty^+/\partial q_{\max}$ becomes zero for $q_{\max} = q^\diamond \in (0, q_c)$. First let us consider the case with $\varepsilon\mathscr{R}_0 \neq \gamma$. From the $q_{\max}$-derivative of the equation (51) with (43) and (44), we can find that such $q^\diamond$ must satisfy the following equation:

$$-\frac{1-\gamma-\varepsilon\mathscr{R}_0}{\varepsilon\mathscr{R}_0} + \frac{1-\gamma}{\varepsilon\mathscr{R}_0}(1-q^\diamond)^{-\varepsilon\mathscr{R}_0/\gamma}\left(\frac{u_\infty^+}{u_0}\right)^\varepsilon_{q_{\max}=q^\diamond} = 0,$$

that is,

$$\left(\frac{u_\infty^+}{u_0}\right)^\varepsilon_{q_{\max}=q^\diamond} = \frac{1-\gamma-\varepsilon\mathscr{R}_0}{1-\gamma}(1-q^\diamond)^{\varepsilon\mathscr{R}_0/\gamma}.$$

Then from (43) and (44) again, we have

$$G(u_\infty^+)\big|_{q_{\max}=q^\diamond} = \frac{1-\gamma-\varepsilon\mathscr{R}_0}{\gamma(1-\varepsilon\mathscr{R}_0/\gamma)}(1-q^\diamond)\big[1-(1-q^\diamond)^{\varepsilon\mathscr{R}_0/\gamma-1}\big] < 0.$$

This is contradictory to the existence of $u_\infty^+ > 0$ that satisfies the equation (51) for each $q_{\max} \in (0, q_c)$ as shown by Lemma 3.9. Therefore such $q^\diamond$ cannot exist in $(0, q_c)$. Thus the derivative $\partial z_\infty^+/\partial q_{\max}$ has a constant sign for $q_{\max} \in (0, q_c)$.

For the case with $\varepsilon\mathscr{R}_0 = \gamma$, we can apply the same arguments to have

$$G(u_\infty^+)\big|_{q_{\max}=q^\diamond} = \frac{1-2\gamma}{\gamma}\ln(1-q^\diamond) < 0$$

since $2\gamma < 1$ when $\varepsilon\mathscr{R}_0 = \gamma < 1-\gamma$. Hence from the contradiction again, we find that the derivative $\partial z_\infty^+/\partial q_{\max}$ has a constant sign for $q_{\max} \in (0, q_c)$ also in this case. Lastly these arguments prove the lemma. □

Next to complete the proof for Lemma 3.10, we prove the following feature of the derivative $\partial z_\infty^+/\partial q_{\max}$:

Lemma 3.21. $\left.\dfrac{\partial z_\infty^+}{\partial q_{\max}}\right|_{q_{\max}\to 0+} < 0.$

Proof. As $q_{\max} \to 0+$, the equation (51) becomes

$$1-u_\infty^+ = \frac{1-\gamma}{\varepsilon\mathscr{R}_0}\left[1-\left(\frac{u_\infty^+}{u_0}\right)^\varepsilon\right] \tag{132}$$

for both cases of $\varepsilon\mathscr{R}_0 \neq \gamma$ and $\varepsilon\mathscr{R}_0 = \gamma$. It is easily found that this equation has a unique positive root $u_\infty^+ = u_\infty^{+0} \in (0, u_0)$. From the equation (51) with (43) and (44), we can derive

$$\left.\frac{\partial z_\infty^+}{\partial q_{\max}}\right|_{q_{\max}\to 0+} = -\left.\frac{\partial u_\infty^+}{\partial q_{\max}}\right|_{q_{\max}\to 0+} = \frac{u_\infty^{+0}}{1-G'(u_\infty^{+0})}, \tag{133}$$

making use of (132).

First let us consider the case with $\varepsilon\mathscr{R}_0 \neq \gamma$. Then from (43) and (44) with (132) again, we have

$$\begin{aligned} 1-G'(u_\infty^{+0}) &= 1-\frac{\varepsilon}{u_0}\left(\frac{u_\infty^{+0}}{u_0}\right)^{\varepsilon-1}\left(\frac{1-\gamma}{\varepsilon\mathscr{R}_0}\right) = 1-\frac{\varepsilon}{u_\infty^{+0}}\left(\frac{u_\infty^{+0}}{u_0}\right)^{\varepsilon}\left(\frac{1-\gamma}{\varepsilon\mathscr{R}_0}\right) \\ &= \frac{1-u_\infty^{+0}}{u_\infty^{+0}}\left[\frac{u_\infty^{+0}}{1-u_\infty^{+0}} - \varepsilon\frac{(u_\infty^{+0}/u_0)^\varepsilon}{1-(u_\infty^{+0}/u_0)^\varepsilon}\right]. \end{aligned} \tag{134}$$

Now consider the function $\zeta(\varepsilon) := \varepsilon a^\varepsilon/(1-a^\varepsilon)$ for $\varepsilon \in (0,1)$ with $a \in (0,1)$. We can easily find that

$$\zeta'(\varepsilon) = \frac{a^\varepsilon}{(1-a^\varepsilon)^2}\big(1 - a^\varepsilon + \varepsilon \ln a\big) < 0$$

because the function $h(x) := 1 - x^\varepsilon + \varepsilon \ln x$ is negative for $x \in (0,1)$ about any $\varepsilon \in (0,1)$. Hence the function $\zeta(\varepsilon)$ is monotonically decreasing in terms of ε, so that we have $\zeta(\varepsilon) > \zeta(1) = \xi(a) := a/(1-a)$. Since $\xi(a)$ is monotonically increasing in terms of $a \in (0,1)$, we finally find the following order:

$$\zeta(\varepsilon)\big|_{a=u_\infty^{+0}/u_0} > \zeta(1)\big|_{a=u_\infty^{+0}/u_0} = \xi\big(u_\infty^{+0}/u_0\big) > \xi\big(u_\infty^{+0}\big)$$

because $u_\infty^{+0} < u_0 < 1$. Then, since the equation (134) can be rewritten as

$$1 - G'(u_\infty^{+0}) = \frac{1}{\xi\big(u_\infty^{+0}\big)}\left[\, \xi\big(u_\infty^{+0}\big) - \zeta(\varepsilon)\big|_{a=u_\infty^{+0}/u_0} \,\right],$$

we conclude that $1 - G'(u_\infty^{+0}) < 0$, so that the derivative (133) is negative. These arguments can be simply applied for the case of $\varepsilon\mathscr{R}_0 = \gamma$, and show that the derivative (133) is negative. Consequently we have proved that the derivative (133) is negative. □

From the continuity of u_∞^+ in terms of $q_{\max} \in (0, q_c)$, Lemmas 3.20 and 3.21 prove that the $q_{\max}$-derivative of z_∞^+ is negative for $q_{\max} \in (0, q_c)$. As a result, Theorem 3.10 has been proven.

APPENDIX 3.A.19: PROOF OF THEOREM 3.9

First we show the following lemma:

Lemma 3.22. $z_\infty^\dagger \geq z_\infty^-$.

Proof. If the system (40) enters the isolation incapable phase at time $\tau = \tau^\star$ with $q_{\max} < q_c$, we have $u_\infty^+ < u(\tau^\star) = u^\star$ because $du/d\tau < 0$ even after $\tau = \tau^\star$. Hence $z_\infty^+ := 1 - u_\infty^+ > 1 - u^\star$ for $q_{\max} < q_c$ with $u(\tau^\star) = u^\star$ given by (45). Therefore we find that

$$\lim_{q_{\max}\to q_c - 0} z_\infty^+ = z_\infty^\dagger \geq \lim_{q_{\max}\to q_c - 0}(1 - u^\star) = 1 - u_0(1-q_c)^{\mathscr{R}_0/\gamma}. \tag{135}$$

Then from Lemma 3.8, the right side of (135) is equal to z_∞^-, which proves this lemma. □

As shown in the first part of Subsection 3.4.7 if $\varepsilon\mathscr{R}_0 \geq 1-\gamma$ and $q_{\max} < q_c$, we have the final epidemic size $z_\infty = z_\infty^+ = 1$. From Theorem 3.6 and Corollary 3.6.1, if $\varepsilon\mathscr{R}_0 \geq 1$, we have $q_c = 1$, and thus there is no critical capacity for the isolation. Then we do not have any case of the final epidemic size at the isolation effective phase, that is, z_∞^- does not exist. Only if $\varepsilon\mathscr{R}_0 < 1$, we can have z_∞^- as the final epidemic size at the isolation effective phase. Therefore, we can conclude that, the final epidemic size z_∞ shows a discontinuity at $q_{\max} = q_c$ for $\varepsilon\mathscr{R}_0 \in [\,1-\gamma, 1)$, when $z_\infty^+ = 1 > z_\infty^-$ which is given by Lemma 3.8.

If $\varepsilon\mathscr{R}_0 < 1-\gamma$ and $q_{\max} < q_c$, we have the final epidemic size $z_\infty = z_\infty^+ < 1$ when the system (40) approaches a disease-eliminated equilibrium

E_0^+ given by (52). Then the final epidemic size $z_\infty^+ := 1 - u_\infty^+$ is determined by the unique positive root u_∞^+ of the equation (51) in Lemma 3.9. As argued in Appendix 3.A.16 for the proof of Lemma 3.9, the unique existence of the positive root u_∞^+ of the equation (51) follows the condition that $G(u^\star) - u^\star > 0$ and $G(0) < 0$, where the function $G(u) - u$ with $q_{\max} \in (0, q_c)$ is unimodal or monotonically increasing in $(0, u^\star)$.

Now we can find that

Lemma 3.23. *$u^\star \to u_\infty^-$, $G(u^\star) - u^\star \to G(u_\infty^-) - u_\infty^- = 0$, and $G(0) < 0$ as $q_{\max} \to q_c - 0$ with $\varepsilon\mathscr{R}_0 < 1 - \gamma$.*

This lemma can be easily proved by the straightforward calculation with (42–44), (45), (49), and Lemma 3.8. Hence from the continuity of u_∞^+ in terms of $q_{\max} \in (0, q_c)$, we have $u_\infty^+ \to u_\infty^-$ as $q_{\max} \to q_c - 0$ if the function $G(u) - u$ becomes monotonically increasing in $(0, u^\star)$ as $q_{\max} \to q_c - 0$. This is because there is no root of the equation $G(u) - u = 0$ in $(0, u^\star)$ as $q_{\max} \to q_c - 0$, while u_∞^+ is continuous in terms of $q_{\max} \in (0, q_c)$. In contrast, if the function $G(u) - u$ becomes unimodal with a maximal extremum in $(0, u^\star)$ as $q_{\max} \to q_c - 0$, the equation $G(u) - u = 0$ has a root $u_\infty^{++} \in (0, u^\star)$, and we have $u_\infty^+ \to u_\infty^{++}$ as $q_{\max} \to q_c - 0$ because of the continuity of u_∞^+ in terms of $q_{\max} \in (0, q_c)$.

As shown in Appendix 3.A.16, the continuous function $G(u) - u$ has at most one extremum for $u > 0$, and $G'(u) - 1 = (\varepsilon/u_0)B(u/u_0)^{\varepsilon-1} - 1 \to \infty$ as $u \to +0$ with $\varepsilon\mathscr{R}_0 < 1 - \gamma$. Thus it is monotonically increasing in $(0, u^\star)$ if and only if the derivative of $G(u) - u$, that is, $G'(u) - 1$ is non-negative for $u = u^\star$, while it is unimodal in $(0, u^\star)$ if $G'(u) - 1$ is negative for $u = u^\star$. As a result, taking account of Lemma 3.23 and the above arguments on the limit of u_∞^+ as $q_{\max} \to q_c - 0$, we get

Lemma 3.24. *As $q_{\max} \to q_c - 0$ with $\varepsilon\mathscr{R}_0 < 1 - \gamma$,*

$$u_\infty^+ \to \begin{cases} u_\infty^- & \text{if } G'(u_\infty^-) \geq 1; \\ u_\infty^{++} < u_\infty^- & \text{if } G'(u_\infty^-) < 1. \end{cases}$$

Therefore, if and only if $G'(u_\infty^-) < 1$ with $\varepsilon\mathscr{R}_0 < 1 - \gamma$, we have $z_\infty^\dagger = 1 - u_\infty^{++} > 1 - u_\infty^- = z_\infty^-$. the condition $G'(u_\infty^-) < 1$ with $\varepsilon\mathscr{R}_0 < 1 - \gamma$ becomes (54) in Theorem 3.9 by the straightforward calculation with Lemma 3.8 and (49). The calculation must be carried out respectively for the cases of $\varepsilon\mathscr{R}_0 \neq \gamma$ and $\varepsilon\mathscr{R}_0 = \gamma$, while the final result for $\varepsilon\mathscr{R}_0 = \gamma$ appears to be included in (54).

Making use of (49) in a different way, the condition (54) can be rewritten as

$$\frac{1-\gamma}{\gamma - \varepsilon\mathscr{R}_0}(1 - q_c)^{\varepsilon\mathscr{R}_0 - \gamma} < \frac{1 - \varepsilon\mathscr{R}_0}{\gamma - \varepsilon\mathscr{R}_0} - \frac{\varepsilon}{1-\varepsilon}\left(\frac{1-\gamma}{\varepsilon\mathscr{R}_0} - 1\right) \quad \text{for } \varepsilon\mathscr{R}_0 \neq \gamma; \tag{136}$$

$$\frac{1-\gamma}{\gamma}\ln(1 - q_c) > \frac{\varepsilon}{1-\varepsilon}\frac{1-2\gamma}{\gamma} - 1 \quad \text{for } \varepsilon\mathscr{R}_0 = \gamma. \tag{137}$$

Since $1 - q_c \in (0, 1)$, it is necessary that the right side of (136) is greater than $(1-\gamma)/(\gamma - \varepsilon\mathscr{R}_0)$, and the right side of (137) is negative. Then we can find the following necessary condition:

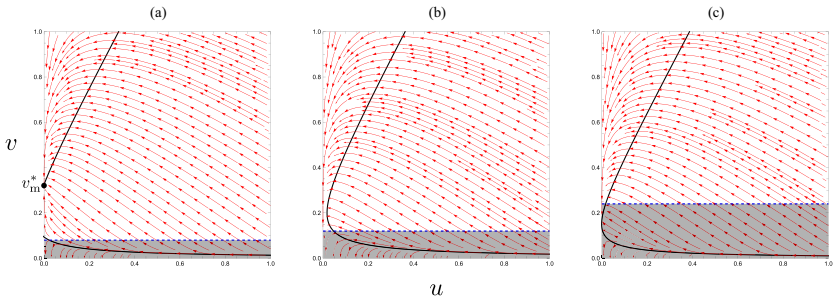

Figure 30: Numerically drawn vector flows for the system (58) with $(\varepsilon\mathscr{R}_0,\, q_{\max})$ = (a) $(1.05, 0.2)$; (b) $(1.05, 0.3)$; (c) $(2.1, 0.6)$, and commonly $\varepsilon = 0.35$; $\gamma = 0.5$; $a = 0.2$. The solid curve indicates the nullcline for v: $dv/d\tau = 0$ in (58), and the dashed horizontal line does $v = aq_{\max}/\gamma$. Vector flows are drawn over $\mathbb{R}^2_+$, though only those above the dashed horizontal line are valid for the arguments on the dynamics governed by (58).

Lemma 3.25. *For $G'(u^-_\infty) < 1$ with $\varepsilon\mathscr{R}_0 < 1-\gamma$, it is necessary that $\mathscr{R}_0 > 1-\gamma$.*

Finally Lemmas 3.24 and 3.25 prove Theorem 3.9.

APPENDIX 3.A.20: PROOF OF THEOREM 3.11 AND LEMMA 3.12

Suppose that there exists an endemic equilibrium E^*_{m} defined by (56) with the endemic size $v^*_{\mathrm{m}} \in [aq_{\max}/\gamma,\, 1-q_{\max})$. It is easy to see that the condition (62) is sufficient to satisfy (60). Since the endemic size v^*_{m} is given by a root of the quadratic equation $\Psi(v) = 0$ with (59), it is necessary that its discriminant is non-negative and the root of $\Psi'(v) = 0$ is positive, because $\Psi(v)$ is a convex parabola with $\Psi(0) = aq_{\max} > 0$. The former condition gives

$$\mathcal{A} \le \mathcal{A}_1 \tag{138}$$

with the latter condition $\varepsilon\mathscr{R}_0 > 1-\gamma$ which is the same as the former of (62). These conditions are necessary for the existence of E^*_{m}.

Under these two conditions, the equation $\Psi(v) = 0$ has one or two positive roots necessarily less than $1-q_{\max}$, since we can easily find that $\Psi(1-q_{\max}) > 0$ and $\Psi'(1-q_{\max}) > 0$. Besides we can prove that the smaller root cannot correspond to v^*_{m} when the equation $\Psi(v) = 0$ has two distinct roots, as shown in the subsequent arguments making use of the isocline method for the two dimensional system (58). Therefore the formula of v^*_{m} is given by (61) as the non-smaller root for the equation $\Psi(v) = 0$ with (59).

As seen in Figure 30(a), the isocline method in the (u, v)-phase plane can show that the smaller root of the equation $\Psi(v) = 0$ corresponds to an unstable equilibrium for the system (58), while the larger root corresponds to an asymptotically stable equilibrium for it. In a specific case where the equation $\Psi(v) = 0$ has only one positive root, the isocline method indicates that the root corresponds to an equilibrium which has a singular stability as follows: There is a subset of points with a positive measure in the neighborhood of the equilibrium such that the trajectory from the point of the subset goes far away (i.e., repelled) from the equilibrium, while the trajectory from the point of the complement in the neighborhood asymptotically approaches the equilibrium. It is easily seen also by the isocline method that the trajectory must asymptotically approach the equilibrium even in such a specific case

once the system enters the isolation malfunctioning phase after the isolation well-functioning phase. Hence, as a possible case where the system (58) approaches an endemic equilibrium at the isolation mulfunctioning phase, we include the case where the discriminant of $\Psi(v) = 0$ is zero, that is, the case of $\mathcal{A} = \mathcal{A}_1$. As a result, we obtain $v_{\rm m}^*$ given by (61) which is the non-smaller root of the equation $\Psi(v) = 0$.

Next, from (61), the condition that $v_{\rm m}^* \geq aq_{\max}/\gamma$ leads to the following condition:

$$\mathcal{A} \leq \mathcal{A}_3 := \frac{\gamma}{2}\left(1 - \frac{1-\gamma}{\varepsilon\mathscr{R}_0}\right) \text{ with } \varepsilon\mathscr{R}_0 > 1-\gamma$$
$$\text{or} \tag{139}$$
$$\mathcal{A}_3 < \mathcal{A} \leq \mathcal{A}_2 \text{ with } \varepsilon\mathscr{R}_0 > 1+\gamma.$$

We can easily prove the followings:

$$\mathcal{A}_3 \geq \mathcal{A}_1 < \gamma \qquad \text{for } \varepsilon\mathscr{R}_0 \in (1-\gamma,\, 1\,];$$
$$\mathcal{A}_3 > \mathcal{A}_1 < \gamma \text{ and } \mathcal{A}_1 \geq \mathcal{A}_2 \qquad \text{for } \varepsilon\mathscr{R}_0 \in (1,\, 1+\gamma\,];$$
$$\mathcal{A}_3 < \mathcal{A}_2 < \mathcal{A}_1 < \gamma \qquad \text{for } \varepsilon\mathscr{R}_0 \in (1+\gamma,\, 1-\gamma+2\sqrt{\gamma}\,];$$
$$\mathcal{A}_3 < \mathcal{A}_2 < \gamma \leq \mathcal{A}_1 \qquad \text{for } \varepsilon\mathscr{R}_0 \in [\,1-\gamma+2\sqrt{\gamma},\, \infty).$$

Finally from these arguments, we can find the condition (62) which is necessary and sufficient to satisfy all of those conditions (60), $\varepsilon\mathscr{R}_0 > 1-\gamma$, (138), and (139).

When the condition (62) is unsatisfied, the isocline method shows that the trajectory for the system (58) in the region of $v > aq_{\max}/\gamma$ eventually enters the region of $v < aq_{\max}/\gamma$ in a finite time, as illustrated by Figure 30(b, c), because there is no asymptotically stable state in the region of $v \geq aq_{\max}/\gamma$. This means that the system (20) cannot keep staying at the isolation malfunctioning phase, and eventually enters the isolation well-functioning phase. This result shows Lemma 3.12. These arguments indicate that the condition (62) is necessary if the system (20) approaches the endemic equilibrium $E_{\rm m}^*$ at the isolation malfunctioning phase. Consequently we have proved Theorem 3.11.

APPENDIX 3.A.21: PROOF OF COROLLARY 3.11.2

As long as we consider the endemic equilibrium $E_{\rm m}^*$, the condition (60) in Lemma 3.11 is necessary to be satisfied. Since the right side of inequality (60) converges to zero as $\gamma \to +0$, we have to take into account that $q_{\max} \to +0$ at the same time as $\gamma \to +0$. This is reasonable for the reasonability of mathematical modeling too, because both limits of $\gamma \to +0$ and $q_{\max} \to +0$ mean that the isolation becomes incapable. Hence we must take the limit as $q_{\max} \to +0$ for $v_{\rm m}^*$ given by (61) when $\gamma \to +0$. Then we find that $v_{\rm m}^* \to 1 - 1/(\varepsilon\mathscr{R}_{00})$ as $\gamma \to +0$ and $q_{\max} \to +0$.

APPENDIX 3.A.22: PROOF OF COROLLARY 3.16.1

We have

$$\overline{v_{\mathrm{m}}^*} := \sup_a v_{\mathrm{m}}^* = \lim_{a\to+0} v_{\mathrm{m}}^* = (1-q_{\max})\Big(1-\frac{1-\gamma}{\varepsilon\mathscr{R}_0}\Big);$$
$$\overline{v_{\mathrm{w}}^*} := \sup_a v_{\mathrm{w}}^* = \lim_{a\to\infty} v_{\mathrm{w}}^* = 1-\frac{1}{\varepsilon\mathscr{R}_0}$$

from the monotonicity of v_{m}^* and v_{w}^* in terms of a. Hence, we find the following result on the a-dependence of endemic size: When $\varepsilon\mathscr{R}_0 > 1$, if $\overline{v_{\mathrm{w}}^*} > \overline{v_{\mathrm{m}}^*}$, that is, if the condition (72) is satisfied, then there exists a specific value $a^\dagger$ for a such that the endemic size v_{w}^* for $a > a^\dagger$ at the isolation well-functioning phase is bigger than any endemic size for $a \le a^\dagger$, where $a^\dagger$ can be obtained as the root of the equation $v_{\mathrm{w}}^* = \overline{v_{\mathrm{m}}^*}$, which leads to the definition of $a^\dagger$ given in (73). In contrast, if $\overline{v_{\mathrm{m}}^*} > \overline{v_{\mathrm{w}}^*}$, that is, if

$$q_{\max} < \frac{\gamma}{\varepsilon\mathscr{R}_0 - 1 + \gamma}, \tag{140}$$

then there exists a specific value $a^\ddagger$ for a such that the endemic size v_{m}^* for $a < a^\ddagger$ at the isolation malfunctioning phase is bigger than any endemic size for $a \ge a^\ddagger$, where

$$a^\ddagger = \frac{\gamma}{1-q_{\max}}\Big(\frac{1}{q_{\max}} - \frac{\varepsilon\mathscr{R}_0 - 1 + \gamma}{\gamma}\Big)\Big(1-\frac{1}{\varepsilon\mathscr{R}_0}\Big),$$

derived by solving the equation $v_{\mathrm{m}}^* = \overline{v_{\mathrm{w}}^*}$. We can easily find that necessarily $a^\dagger > a_2$ and $a^\ddagger < a_2$ when either of them exists for $\varepsilon\mathscr{R}_0 > 1$ under the condition (72) or alternatively (140). If $\overline{v_{\mathrm{m}}^*} = \overline{v_{\mathrm{w}}^*}$, the endemic size v_{w}^* for any finite $a > a_c$ is smaller than $\overline{v_{\mathrm{m}}^*}$. Finally, these arguments prove Corollary 3.16.1.

APPENDIX 3.A.23: PROOF OF THEOREM 3.17

First we can get the following result on the endemic size:

Lemma 3.26. *$v_{\mathrm{m}}^* \to v_{\mathrm{w}}^*$ as $q_{\max} \to q_c - 0$ for $\varepsilon\mathscr{R}_0 \ge 1+\gamma$.*

This lemma can be easily proved by straightforward calculation of the limit for v_{m}^* given by (61). Lemma 3.26 indicates that E_{m}^* converges to E_{w}^* as $q_{\max} \to q_c - 0$ for $\varepsilon\mathscr{R}_0 \ge 1+\gamma$, where $q_c = q_2$ defined by (69) as shown in Subsection 3.5.3. Thus the endemic size v^* continuously depends on $q_{\max}$ for $\varepsilon\mathscr{R}_0 \ge 1+\gamma$ where it switches between v_{w}^* and v_{m}^* (refer to Figures 22 and 26 too).

Next, again by straightforward calculations of the limit for v_{w}^* given by (24–26), we can find

Lemma 3.27. *$v_{\mathrm{w}}^* \to 0$ as $\varepsilon\mathscr{R}_0 \to 1+0$.*

Lemma 3.27 indicates that E_{w}^* converges to a disease-eliminated equilibrium as $\varepsilon\mathscr{R}_0 \to 1+0$. Thus the endemic size v^* continuously depends on $\varepsilon\mathscr{R}_0$ unless the condition in Corollary 3.14.1 is satisfied when v^* switches between

a disease-eliminated equilibrium and the endemic equilibrium E^*_{w} at the isolation well-functioning phase for $\varepsilon\mathscr{R}_0 = 1$ (refer to Figures 22 and 26).

As a result from Lemmas 3.26 and 3.27, there is no discontinuity at the boundaries between $\mathcal{D}^*_{\mathrm{m}}$ and $\mathcal{D}^*_{\mathrm{w}}$, and between $\mathcal{D}^*_0$ and $\mathcal{D}^*_{\mathrm{w}}$ in Figure 22. This means that, if a discontinuity exists, it must be only for the parameter region $\mathcal{D}^*_{0+\mathrm{m}}$ or $\mathcal{D}^*_{\mathrm{w}+\mathrm{m}}$. Therefore, from Lemmas 3.26 and 3.27, we get the result given in the latter half of Theorem 3.17.

To consider the possibility to have a discontinuity for the parameter region $\mathcal{D}^*_{0+\mathrm{m}}$ or $\mathcal{D}^*_{\mathrm{w}+\mathrm{m}}$, we shall use the decreasing monotonicity of v^*_{m} in terms of $q_{\max}$, which has been already mentioned in Subsection 3.5.3. We find the following result on the endemic size v^*_{m} for the parameter region $\mathcal{D}^*_{0+\mathrm{m}}$:

Lemma 3.28. *The endemic size v^*_{m} is definitely positive for the parameter region $\mathcal{D}^*_{0+\mathrm{m}}$.*

This is because we have

$$v^*_{\mathrm{m}} \to \frac{1-q_1}{2}\left(1-\frac{1-\gamma}{\varepsilon\mathscr{R}_0}\right) > 0$$

as $q_{\max} \to q_1 - 0$ for the parameter region $\mathcal{D}^*_{0+\mathrm{m}}$, so that v^*_{m} is necessarily greater than the above limit for the parameter region $\mathcal{D}^*_{0+\mathrm{m}}$ because of its decreasing monotonicity in terms of $q_{\max}$. Therefore, for the parameter region $\mathcal{D}^*_{0+\mathrm{m}}$, we have a discontinuity of the final infective population size v^∞ between v^*_{m} and 0 (i.e., a disease-eliminated state) at the critical value of $q_{\max}$ in $\mathcal{D}^*_{0+\mathrm{m}}$ where the state approached by the system switches between a disease-eliminated equilibrium and the endemic equilibrium E^*_{m}.

Next, since it necessarily holds from Corollary 3.10.1 and arguments in Subsection 3.5.1 that $v^*_{\mathrm{w}} < aq_{\max}/\gamma \le v^*_{\mathrm{m}}$, we would have $v^*_{\mathrm{w}} \to aq_c/\gamma = v^*_{\mathrm{m}}$ with a proper limit $q_{\max} \to q_c$ in the parameter region $\mathcal{D}^*_{\mathrm{w}+\mathrm{m}}$ if v^* is continuous at a critical value of $q_{\max}$. For v^*_{w} given by (24–26), we find that $q_{\max} = 1/(1+B^*_{\mathrm{w}})$ when $v^*_{\mathrm{w}} = aq_{\max}/\gamma$. On the other hand, from (61), we can find that, as $q_{\max} \to 1/(1+B^*_{\mathrm{w}}) + 0$,

$$v^*_{\mathrm{m}} \to \frac{\gamma}{\varepsilon\mathscr{R}_0}\cdot\frac{B^*_{\mathrm{w}}}{1+B^*_{\mathrm{w}}} = \left\{1+\frac{(1+\gamma)/(\varepsilon\mathscr{R}_0)-1}{1-1/(\varepsilon\mathscr{R}_0)}\right\}\frac{a/\gamma}{1+B^*_{\mathrm{w}}} > \frac{a/\gamma}{1+B^*_{\mathrm{w}}} = v^*_{\mathrm{w}}$$

for $\varepsilon\mathscr{R}_0 \in (1, 1+\gamma)$. Therefore, it is impossible that $v^*_{\mathrm{w}} \to aq_{\max}/\gamma = v^*_{\mathrm{m}}$ as $q_{\max} \to 1/(1+B^*_{\mathrm{w}}) + 0$. Consequently we do not have any value of $q_{\max}$ in the parameter region $\mathcal{D}^*_{\mathrm{w}+\mathrm{m}}$ such that $v^*_{\mathrm{w}} \to aq_{\max}/\gamma = v^*_{\mathrm{m}}$ with a proper limit $q_{\max} \to q_c$. That is, it is satisfied that $v^*_{\mathrm{w}} < aq_{\max}/\gamma \le v^*_{\mathrm{m}}$ for any $q_{\max}$ in $\mathcal{D}^*_{\mathrm{w}+\mathrm{m}}$. This means that there is a discontinuity of the endemic size v^* between v^*_{m} and v^*_{w} for the critical value of $q_{\max}$ in $\mathcal{D}^*_{\mathrm{w}+\mathrm{m}}$ where the state approached by the system switches between E^*_{m} and E^*_{w}. The way of these arguments can be applied for the corresponding arguments with respect to the equilibrium switch at the critical value of a in $\mathcal{D}^*_{0+\mathrm{m}}$ and $\mathcal{D}^*_{\mathrm{w}+\mathrm{m}}$. Finally these arguments have proved Theorem 3.17.

4 BEHAVIORAL HETEROGENEITY IN PEOPLE

4.1 INTRODUCTION

The COVID-19 pandemic has resulted in an unprecedented worldwide public health emergency and revealed that population heterogeneity plays a crucial role in the spread of the transmissible disease[5,23,30,49,127]. In contrast to the assumption of homogeneous mixing, considering population heterogeneity, including differences in age, economic status, and individual behavior may help to better understand the transmission dynamics of infectious diseases.

Many studies have extended epidemic models to account for such heterogeneity and have demonstrated the substantial impact on disease spread and control strategies (for example, Sattenspiel and Dietz[142], Garnett and Anderson[63], Dwyer *et al.*[51], Dwyer *et al.*[52], Brauer[21], Hickson and Roberts[76], Izhar and Ben-Ami[82], Bonaccorsi and Ottaviano[17], Acemoglu *et al.*[2], Almeida *et al.*[7]). Acemoglu *et al.*[2] developed a multigroup SIR model dividing the population into three age classes and used numerical optimization to design optimal targeted lockdown policies that balance health outcomes and economic losses. Their study highlighted the importance of population heterogeneity in policy design.

In particular, the heterogeneity in individual susceptibility plays an important role in shaping epidemic outcomes. This is because susceptibility directly determines the likelihood that an individual becomes infected, and thus affects the spread of transmission within the population. Several studies have shown that a small fraction of the population may carry a majority of the total susceptibility, significantly affecting transmission potential (for example, Smith *et al.*[150], King *et al.*[94], Althouse *et al.*[8], Liu *et al.*[102], Wong and Collins[172], Rose *et al.*[139]). This phenomenon implies that individuals with higher susceptibility can disproportionately drive epidemic spread, especially in the early stages of an outbreak. It also suggests that targeted interventions for these highly susceptible groups could substantially reduce overall transmission.

In addition to susceptibility, heterogeneity in infectivity also plays a critical role in epidemic dynamics. The findings by Markwalter *et al.*[109] showed that a small number of highly infectious individuals can disproportionately contribute to the transmission for malaria. Similar patterns have been observed in other diseases, such as SARS-CoV-2, where superspreading events dominate the transmission process[50]. Lloyd-Smith *et al.*[103] showed that individual-level variation in infectiousness can result in superspreading events and significantly shape the dynamics of the outbreak. Kuylen *et al.*[96] further distinguished between heterogeneity in infectiousness and contact behavior, showing that higher infectiousness-related heterogeneity may reduce outbreak resurgence, while contact-related heterogeneity may increase it.

Beyond individual-level differences in susceptibility and infectivity, the structure of social contact patterns also has a crucial influence on epidemic dynamics. Hill *et al.*[77] analyzed a multi-group SIR model incorporating preferential and proportionate mixing and found that contact heterogeneity significantly alters the effective reproduction number and vaccination thresholds. Dimarco *et al.*[48] investigated this aspect using a Boltzmann-type

kinetic model, showing that individuals with a higher contact rate drive transmission disproportionately, and that targeting these individuals may lead to more effective intervention strategies.

Furthermore, some studies have highlighted the importance of structured population heterogeneity in shaping epidemic outcomes. Britton *et al.*[23] demonstrated that incorporating age and social activity levels into epidemic models significantly reduces the estimated herd immunity threshold for SARS-CoV-2. Elbasha and Gumel[56] further showed that in heterogeneous populations, optimal vaccination strategies depend on the underlying contact structure and group-specific transmission rates.

In this chapter, we introduce a population structure defined by heterogeneity in individual preventive behaviors. These behavioral differences are shaped by underlying educational backgrounds and influence both susceptibility and transmissibility. Rather than focusing on variation in contacts between individuals, this study considers heterogeneity in both individual susceptibility and infectivity, which have been considered separately in previous studies, thereby capturing the combined effect of these two factors on epidemic consequence. Moreover, this study provides analytical results that quantify the role of preventive behavior heterogeneity. Our theoretical analysis aims to provide valuable insights for the development of effective public health policies and try to provide a theoretical foundation for understanding epidemic progression.

4.2 ASSUMPTIONS AND MODEL

We assume the following for our modeling:

- The total population size is constant, when any demographic change due to birth, death or migration is assumed to be negligible in the epidemic season.
- The fatality of disease is negligible.
- Disease transmission occurs through contact between pathogens and individuals. For example, the transmission of COVID-19 can be caused by contact with contaminated materials.
- Individuals of the community are categorized into n classes based on their caution level.
- The differences in caution level are caused by the education level. Compared to the spread of disease transmission, improvements in education require a significantly longer period. Hence the transition between different classes during the epidemic season is negligible.
- Caution level affects preventive behavior in both susceptible and infected individuals.
- Susceptible individuals of low caution level are more likely to get infected compared to those with high caution level.
- Infected individuals of low caution level contribute more to disease transmission due to lower-quality preventive behavior, even after infection.
- The recovery rate is the same for infected individuals regardless of their level of caution.

From the assumptions, we obtain the following mathematical model:

$$\begin{aligned}\frac{dS_i}{dt} &= -\varepsilon_i\beta\sum_{k=1}^{n}\gamma_k I_k S_i;\\ \frac{dI_i}{dt} &= \varepsilon_i\beta\sum_{k=1}^{n}\gamma_k I_k S_i - \rho I_i;\\ \frac{dR_i}{dt} &= \rho I_i.\end{aligned} \tag{141}$$

The variables S_i, I_i, and R_i denote the sizes of susceptible, infective, and recovered subpopulation of caution level i respectively. The total population size of the community is given by a positive constant N, the population size of caution level i is given by $N_i := p_i N$, with $p_i \in (0,1)$, and $\sum_{i=1}^{n} p_i = 1$. It is satisfied that $S_i(t) + I_i(t) + R_i(t) = p_i N$ for any $t \geq 0$. Initial condition is given by $S_i(0) + I_i(0) = p_i N$, $I_i(0) \geq 0$, and $R_i(0) = 0$ for all i. The infection coefficient for susceptible individuals of caution level i is given by $\varepsilon_i\beta$. ε_i indicates the efficiency of preventive behavior, where $\varepsilon_i \in (0,1]$, and $1 = \varepsilon_1 > \varepsilon_2 > \ldots > \varepsilon_n$. A small value of ε_k corresponds to a high caution level, indicating that susceptible individuals adopt higher-quality preventive behaviors, such as regular mask-wearing and frequent hand-washing, which reduce the potential route for disease transmission. Conversely, a large value of ε_k corresponds to a low caution level, reflecting less effective preventive behaviors. Within this framework, individuals of class 1 are assumed to have the lowest caution level, while those of class n with the highest caution level. The parameter $\gamma_k \in (0,1]$ represents the contribution of the epidemic by an infected individual of caution level k, which could be regarded as the density of the pathogen produced by an infected individual of caution level k. For example, wearing a mask or reducing the frequency of going out could decrease the contamination of objects and air by pathogens produced by infected individuals. The contribution of slowing down the spread of the epidemic by infected individuals of caution level 1 is the smallest, indicating that $1 = \gamma_1 > \gamma_2 > \ldots > \gamma_n$. The parameter ρ denotes the recovery rate of an infected individual.

With the following transformation of variables and parameters, we can derive the non-dimensionalized system mathematically equivalent to the system (141):

$$\tau := \rho t; \quad u_i := \frac{S_i}{N}; \quad v_i := \frac{I_i}{N}; \quad w_i := \frac{R_i}{N}; \quad \mathscr{R}_{0,i} := \gamma_i\langle\varepsilon\rangle\mathscr{R}_0^{\sup};$$
$$\mathscr{R}_0^{\sup} := \frac{\beta N}{\rho};$$

$$\begin{aligned}\frac{du_i}{d\tau} &= -u_i\frac{\varepsilon_i}{\langle\varepsilon\rangle}\sum_{k=1}^{n}\mathscr{R}_{0,k}v_k;\\ \frac{dv_i}{d\tau} &= u_i\frac{\varepsilon_i}{\langle\varepsilon\rangle}\sum_{k=1}^{n}\mathscr{R}_{0,k}v_k - v_i;\\ \frac{dw_i}{d\tau} &= v_i.\end{aligned} \tag{142}$$

The initial condition is given by $u_i(0) + v_i(0) = p_i$, $v_i(0) > 0$, and $w_i(0) = 0$ for all i. Here $\mathscr{R}_{0,i}$ denotes the class-specific basic reproduction number, which will be formally defined in Section 4.3. $\mathscr{R}_0^{\sup}$ is the upper

bound of the system basic reproduction number $\mathscr{R}_0$ which will be defined in Section 4.4. For the mathematical convention, we show here the following mathematical feature about the solution of (142) (Appendix 4.A.1):

Lemma 4.1. *With the initial condition* $u_i(0) + v_i(0) = p_i$, $v_i(0) \in (0, p_i)$, *and* $w_i(0) = 0$ *for all* i, *the solution of* (142) *belongs to the set* $\{(u_i, v_i, w_i) \in \mathbb{R}^3_+ \mid u_i + v_i + w_i = p_i\}$ *for all* i *and* $\tau \geq 0$.

Then we can get $u_i(\tau) + v_i(\tau) + w_i(\tau) = p_i$ for all i and $\tau \geq 0$.

4.3 CLASS-SPECIFIC BASIC REPRODUCTION NUMBER

In this section, we divide the population into n classes based on the different caution levels. We consider the basic reproduction number in terms of different classes. Here we define the class-specific basic reproduction number $\mathscr{R}_{0,i}$ as the supremum of the expected number of secondary cases generated by an infected individual at caution level i over the entire course of the infectious period.

We can get the class-specific reproduction number as following (Appendix 4.A.2):

$$\mathscr{R}_{0,i} := \sup_{\{S_k\}} \frac{1}{\rho} \sum_{k=1}^{n} \varepsilon_k \beta S_k \gamma_i = \frac{1}{\rho} \sum_{k=1}^{n} \varepsilon_k \beta p_k N \gamma_i = \frac{\gamma_i \langle \varepsilon \rangle \beta N}{\rho}, \tag{143}$$

where $\langle \varepsilon \rangle = \sum_{k=1}^{n} p_k \varepsilon_k$. Here $\langle \varepsilon \rangle$ means the mean efficiency of preventive behavior in the community. A small value of $\langle \varepsilon \rangle$ indicates the overall level of preventive behavior is high, while a large value of $\langle \varepsilon \rangle$ indicates the overall level of preventive behavior is low.

Since $\gamma_1 > \gamma_2 > \cdots > \gamma_n$ is a decreasing sequence, we can derive the following order of the class-specific basic reproduction numbers $\mathscr{R}_{0,i}$ from the definition:

$$\mathscr{R}_{0,1} > \mathscr{R}_{0,2} > \cdots > \mathscr{R}_{0,n}. \tag{144}$$

A larger value of class-specific basic reproduction number $\mathscr{R}_{0,i}$ in class i indicates a higher susceptibility and infectivity of this class, thereby resulting in a greater contribution to the disease transmission.

Then, we define the mean value of the class-specific basic reproduction number $\langle \mathscr{R}_{0,i} \rangle$ as the class-level mean of $\mathscr{R}_{0,i}$, determined by the distribution of individuals across all caution levels. Here we define

$$\langle \mathscr{R}_{0,i} \rangle := \sum_{i=1}^{n} p_i \mathscr{R}_{0,i}, \tag{145}$$

where p_i represents the proportion of individuals in the community at caution level i. By substituting (143) into (145), we can obtain

$$\langle \mathscr{R}_{0,i} \rangle = \sum_{i=1}^{n} p_i \frac{1}{\rho} \sum_{k=1}^{n} \varepsilon_k \beta p_k N \gamma_i = \frac{\langle \varepsilon \rangle \langle \gamma \rangle \beta N}{\rho}. \tag{146}$$

From the order shown in (144), we can obtain the following result:

$$\mathscr{R}_{0,1} > \langle \mathscr{R}_{0,i} \rangle > \mathscr{R}_{0,n}.$$

4.4 SYSTEM BASIC REPRODUCTION NUMBER

Here we consider the basic reproduction number $\mathscr{R}_0$ for the n classes in the community. We define the system basic reproduction number $\mathscr{R}_0$ as the supremum of the expected number of secondary cases generated by an infected individual of the community over the entire course of the infectious period.

We derive the system basic reproduction number by the Next Generation Matrix Method (Appendix 4.A.3):

$$\mathscr{R}_0 := \sup_{\{S_i\}} \frac{1}{\rho} \sum_{i=1}^{n} \varepsilon_i \beta S_i \gamma_i = \frac{1}{\rho} \sum_{i=1}^{n} \varepsilon_i \beta p_i N \gamma_i = \frac{\langle \varepsilon\gamma \rangle \beta N}{\rho}, \tag{147}$$

where $\langle \varepsilon\gamma \rangle = \sum_{k=1}^{n} p_k \varepsilon_k \gamma_k$. Here $\langle \varepsilon\gamma \rangle$ depends on the efficiency of an individual's preventive behavior and the transmission potential of pathogens by infected individuals. The basic reproduction number $\mathscr{R}_0$ is neither the sum nor the mean value of the class-specific basic reproduction number $\mathscr{R}_{0,i}$.

The mathematical property of the reproduction numbers is shown as follows (Appendix 4.A.4):

Lemma 4.2. $\mathscr{R}_{0,1} > \mathscr{R}_0 > \langle \mathscr{R}_{0,i} \rangle$.

$\mathscr{R}_{0,1}$ represents the class with the lowest caution level and minimal preventive behavior against a transmissible disease. $\langle \mathscr{R}_{0,i} \rangle$ reflects the mean individual-level transmission potential, which does not account for behavioral differences across classes. $\mathscr{R}_0$ describes the infection potential at the population level and captures the heterogeneity in population. This order indicates that the overall transmission potential of the population cannot be determined by a simple mean value of individual reproduction numbers, but is instead shaped by the behavioral structure among individuals.

4.5 CONSERVED QUANTITIES

We derive the following time-independent equalities from system (142) (Appendix 4.A.5):

Lemma 4.3.

$$\left\{ \frac{u_1(\tau)}{u_1(0)} \right\}^{1/\varepsilon_1} = \left\{ \frac{u_2(\tau)}{u_2(0)} \right\}^{1/\varepsilon_2} = \cdots = \left\{ \frac{u_n(\tau)}{u_n(0)} \right\}^{1/\varepsilon_n} \tag{148}$$

for any $\tau > 0$.

Lemma 4.4.

$$\log\{U(\tau)\}^{\langle \varepsilon \rangle} + \sum_{k=1}^{n} \mathscr{R}_{0,k} \left[p_k - u_k(0) \{U(\tau)\}^{\varepsilon_k} \right] = X(\tau) \tag{149}$$

for any $\tau > 0$, *where*

$$U(\tau) := \left\{ \frac{u_i(\tau)}{u_i(0)} \right\}^{1/\varepsilon_i}, \quad X(\tau) := \sum_{k=1}^{n} \mathscr{R}_{0,k} v_k(\tau). \tag{150}$$

4.6 FINAL EPIDEMIC SIZE

We find the following results implying that the disease disappears at the final stage of epidemics in the community (Appendix 4.A.6):

Lemma 4.5. *$u_i(\tau) \to u_i^\infty \geq 0$, $v_i(\tau) \to 0$, and $w_i(\tau) \to w_i^\infty > 0$ as $\tau \to \infty$ for any i.*

From Lemma 4.5, we can get $u_i(\tau) + v_i(\tau) + w_i(\tau) \to u_i^\infty + w_i^\infty$, and $X(\tau) \to 0$ as $\tau \to \infty$. Since $u_i(\tau) + v_i(\tau) + w_i(\tau) = p_i$ for all i and $\tau \geq 0$, we can get $u_i^\infty + w_i^\infty = p_i$ as $\tau \to \infty$. Let us define $u_i(\tau) \to u_i^\infty$ as $\tau \to \infty$, from (150), U_∞ can be defined by

$$U_\infty := \left\{ \frac{u_i^\infty}{u_i(0)} \right\}^{1/\varepsilon_i} = \left\{ \frac{u_j^\infty}{u_j(0)} \right\}^{1/\varepsilon_j} \tag{151}$$

for any i, j as $\tau \to \infty$. From equation (149) and Lemma 4.5, we can get the following result to show the unique root of equality (149) as $\tau \to \infty$ (Appendix 4.A.6):

Lemma 4.6. *$U_\infty \in (0, 1)$ is the unique root of equation $F(U) = 0$, where*

$$F(U) := \log U^{\langle \varepsilon \rangle} + \sum_{k=1}^{n} \mathscr{R}_{0,k} \left[p_k - u_k(0) U^{\varepsilon_k} \right]. \tag{152}$$

From (151), u_i^∞ is uniquely defined by

$$u_i^\infty = u_i(0) U_\infty^{\varepsilon_i}. \tag{153}$$

Then, we can find the following results implying the relation of the initial size of infective population on the final size of the susceptibles (Appendix 4.A.7):

Lemma 4.7. $\dfrac{\partial u_i^\infty}{\partial v_j(0)} < 0$ *for any j.*

Lemma 4.7 indicates that a larger initial value $u_j(0)$ (a smaller $v_j(0)$) could lead to a greater u_i^∞. Since p_i is the upper bound of the initial value $u_j(0)$ for any j, we can define the supreme of u_i^∞ which is given by

$$u_i^* := \sup_{\{u_i(0)\}} u_i^\infty = u_i^\infty \big|_{u_j(0) \to p_j - 0}$$

for all j.

Next, we define the final epidemic size W_∞ as the proportion of individuals in the community who have experienced the infection until the final stage of the epidemic dynamics. We can obtain

$$W_\infty := \sum_{i=1}^{n} w_i^\infty = \sum_{i=1}^{n} (p_i - u_i^\infty) = \sum_{i=1}^{n} p_i - \sum_{i=1}^{n} u_i^\infty = 1 - \sum_{i=1}^{n} u_i^\infty. \tag{154}$$

Using (153) for (154), we can obtain

$$W_\infty = 1 - \sum_{i=1}^{n} u_i(0) U_\infty^{\varepsilon_i}. \tag{155}$$

It is easy to derive $\partial w_i^\infty / \partial v_j(0) > 0$, indicating a large initial size of the infective population could result in a larger final epidemic size.

Since the initial values of each class are independent, we obtain the following result (Appendix 4.A.8):

Lemma 4.8. $\dfrac{\partial}{\partial u_j(0)} \left(\dfrac{u_i^\infty}{u_i(0)} \right) > 0$ *for any* j.

Following the Lemma 4.8, we define the supreme of U_∞ from (151), which is given by

$$U^* := \sup_{\{u_i(0)\}} \left\{ \frac{u_i^\infty}{u_i(0)} \right\}^{1/\varepsilon_i} = \sup_{\{u_i(0)\}} U_\infty = U_\infty \big|_{u_i(0) \to p_i - 0}. \tag{156}$$

Further, U^* is a root of

$$\lim_{u_i(0) \to p_i - 0} F(U) = 0, \tag{157}$$

where

$$\lim_{u_i(0) \to p_i - 0} F(U) = \mathscr{F}(U) := \log U^{\langle \varepsilon \rangle} + \sum_{k=1}^{n} \mathscr{R}_{0,k} p_k \left(1 - U^{\varepsilon_k} \right).$$

It is easy to find that equation (157) always has a root $U = 1$. Then, we show the following mathematical result about the solution of (157) (Appendix 4.A.8):

Lemma 4.9. *As* $u_i(0) \to p_i$ *for all* i, *we have*

$$U_\infty \to \begin{cases} 1, & \text{if } \mathscr{R}_0 \le 1, \\ U^* \in (0,1), & \text{if } \mathscr{R}_0 > 1. \end{cases}$$

Therefore, equation (157) has a unique root $U = 1$ if $\mathscr{R}_0 \le 1$, and a unique root U^* in $(0,1)$ if $\mathscr{R}_0 > 1$. From (156), taking the limit of $u_i(0) \to p_i$ for all i, we can get

$$U^* = \left\{ \frac{u_i^\infty}{u_i(0)} \right\}_{u_i(0) \to p_i - 0}^{1/\varepsilon_i} = \left(\frac{u_i^*}{p_i} \right)^{1/\varepsilon_i} = \left(\frac{u_j^*}{p_j} \right)^{1/\varepsilon_j} \tag{158}$$

for any i, j. Then, we define the infimum of w_i^∞ which is given by

$$w_i^* := \inf_{\{u_i(0)\}} w_i^\infty = \inf_{\{u_i(0)\}} (p_i - u_i^\infty) = p_i - \sup_{\{u_i(0)\}} u_i^\infty = p_i - u_i^*. \tag{159}$$

From (154), the infimum of the final epidemic size W^* is given by

$$W^* := \inf_{\{u_i(0)\}} W_\infty = \inf_{\{u_i(0)\}} \sum_{k=1}^{n} w_i^\infty = \sum_{i=1}^{n} \inf_{\{u_i(0)\}} w_i^\infty = \sum_{k=1}^{n} w_i^*. \tag{160}$$

Making use of (158) and (159) to (160), we can get

$$W^* = 1 - \sum_{i=1}^{n} (U^*)^{\varepsilon_i} p_i. \tag{161}$$

The following Theorem illustrates the dependence of the system basic reproduction number on the infimum of final epidemic size (Appendix 4.A.8):

Theorem 4.1. *$W^* = 0$ if $\mathscr{R}_0 \leq 1$, $W^* > 0$ if $\mathscr{R}_0 > 1$. In particular, when $\mathscr{R}_0 = 1$, U_∞ approaches 1 and the infimum of the final epidemic size satisfies $W^* = 0$.*

The above Theorem states that the infimum of the final epidemic size is zero when the system basic reproduction number does not exceed 1, however, this does not imply that the final epidemic size W_∞ is zero. W^* represents the minimal outcome or lower bound of final epidemic size. A larger W^* implies that even under the most optimistic circumstances, the epidemic cannot be avoided and will inevitably result in a social damage. Thus, W^* could be considered as an indicator to quantify the minimal unavoidable damage the epidemic may cause to the community.

4.7 DEPENDENCE OF BEHAVIORAL HETEROGENEITY

4.7.1 *Initial behavior of disease spread*

The initial behavior of a disease within a community is a critical aspect of understanding the progress of the spread of the epidemic. The early-stage dynamics of the disease are not only determined by whether the system basic reproduction number $\mathscr{R}_0$ is greater than or less than 1. Instead, specific conditions related to the dynamics of the disease and the characteristics of the population play a significant role. To characterize the initial trend of the epidemic, let us denote the proportion of the total infective population size in the community as

$$V(\tau) := \frac{\sum_{i=1}^{n} I_i(\tau)}{N} = \sum_{i=1}^{n} v_i(\tau).$$

Then, we can derive the following result about the initial variation of the total infective population size (Appendix 4.A.9):

Lemma 4.10. *Suppose that the disease initially emerges in class ℓ, which means $v_\ell(0) = v_0$ is positive and sufficiently small, while $v_k(0) = 0$ for all $k \neq \ell$. Then, V initially decreases if*

$$\mathscr{R}_{0,\ell} < \frac{\langle \varepsilon \rangle}{\langle \varepsilon \rangle - v_0 \varepsilon_\ell};$$

V initially increases if

$$\mathscr{R}_{0,\ell} > \frac{\langle \varepsilon \rangle}{\langle \varepsilon \rangle - v_0 \varepsilon_\ell}.$$

Since the inequality $\langle \varepsilon \rangle (\mathscr{R}_{0,\ell} - 1) \leq v_0 \varepsilon_\ell \mathscr{R}_{0,\ell}$ holds when $\mathscr{R}_{0,\ell} \leq 1$, we can get V initially decreases when $\mathscr{R}_{0,\ell} \leq 1$. When $\mathscr{R}_{0,\ell} > 1$, we observe that the inequality $\langle \varepsilon \rangle > (\varepsilon_\ell / (1 - 1/\mathscr{R}_\ell)) v_0$ is more easily satisfied than its

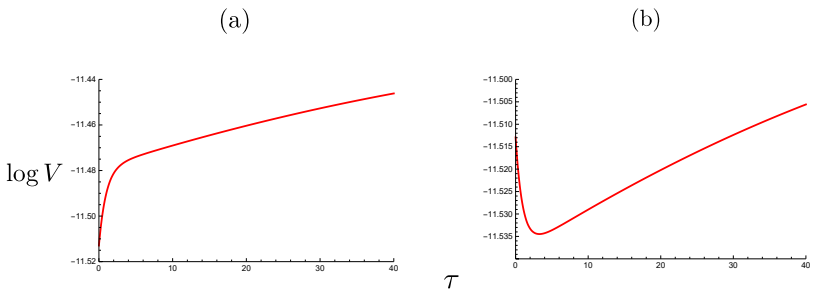

Figure 31: Temporal variation of the total infective population size where the initial infection appears at the class ℓ. Numerically drawn with (a) $\ell = 50$, $v_0 = 1.0 \times 10^{-5}$, $v_i(0) = 0.0$ for $i \neq \ell$; (b) $\ell = 80$, $v_0 = 1.0 \times 10^{-5}$, $v_i(0) = 0.0$ for $i \neq \ell$. Commonly, $N = 1.0 \times 10^5$; $n = 100$; $p_k = [{}_n\mathrm{C}_k q^k (1-q)^{n-k}]/[1-(1-q)^n]$; $\varepsilon_k = 0.99^{k-1}$; $\gamma_k = 0.998^{k-1}$; $\beta = 2.0 \times 10^{-5}$; $\rho = 0.9$; $q = 0.673$; $\langle\varepsilon\rangle = 0.514$. In (a), $(\mathscr{R}_{0,1}, \mathscr{R}_{0,50}, \mathscr{R}_0, \langle\mathscr{R}_{0,i}\rangle, \mathscr{R}_{0,100}) = (1.143, 1.036, 1.001, 1.001, 0.937)$; $\varepsilon_{50} = 0.611$. In (b), $(\mathscr{R}_{0,1}, \mathscr{R}_0, \langle\mathscr{R}_{0,i}\rangle, \mathscr{R}_{0,80}, \mathscr{R}_{0,100}) = (1.143, 1.001, 1.001, 0.975, 0.937)$; $\varepsilon_{80} = 0.452$.

reverse inequality, since v_0 is assumed to be sufficiently small and $\langle\varepsilon\rangle$ is a finite positive value. Hence, We may approximate that V initially increases when $\mathscr{R}_{0,\ell} > 1$. On the other hand, since $\mathscr{R}_{0,i}$ follows a decreasing order $\mathscr{R}_{0,1} > \cdots > \mathscr{R}_{0,n}$, we can get V initially decreases when $\mathscr{R}_{0,1} < 1$ and increases when $\mathscr{R}_{0,n} > 1$.

Furthermore, if the first derivative of the total infected population size is zero at the initial moment, that is, $dV(\tau)/d\tau|_{\tau=0} = 0$, the initial variation of the total infected population is determined by the system basic reproduction number $\mathscr{R}_0$. V initially decreases if $\mathscr{R}_0 \leq 1$, and initially increases if $\mathscr{R}_0 > 1$ (Appendix 4.A.9).

Figure 31 illustrates the impact of initial disease emergence in a different class on the initial variation of the total infected population size. When the disease emerges within a class with high cautiousness, the total number of infectives initially declines. However, when the disease appears in a class with low cautiousness, the higher transmission risk leads to an initial increase in the total number of infectives. The rapid increase in the total infected population inevitably leads to social damage, which emphasizes the importance of enhancing individuals' cautiousness in reducing the social damage of infectious diseases. Figure 32 illustrates how the class size distribution affects the initial variation of the total infected population size. In particular, as shown in Figure 32(b), there could be a case where the total infective subpopulation size turns from decreasing to increasing at the moment. Such a case appears as a revival of outbreak of the disease spread in the community.

The following lemma shows a sufficient condition for the monotonic decrease of the total infective population size(Appendix 4.A.10):

Lemma 4.11. *If $\mathscr{R}_{0,1} \leq 1$, then V decreases monotonically over time.*

The result of Lemma 4.11 is intuitive, when $\mathscr{R}_{0,1}$ is not greater than 1, it implies that the disease fails to spread within the community.

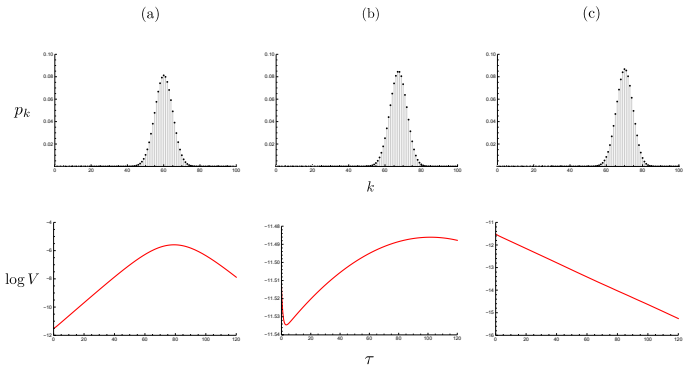

Figure 32: Temporal variation of the total infective subpopulation size. The top row illustrates the class size distribution in terms of q, while the bottom row illustrates the corresponding temporal variation of V. Numerically drawn with (a) $q = 0.6$; (b) $q = 0.673$; (c) $q = 0.7$. $N = 1.0 \times 10^5$; $n = 100$; $p_k = [{}_n\mathrm{C}_k q^k (1-q)^{n-k}]/[1-(1-q)^n]$; $\varepsilon_k = 0.99^{k-1}$; $\gamma_k = 0.998^{k-1}$; $\beta = 2.0 \times 10^{-5}$; $\rho = 0.9$. The initial condition is given by $v_{80}(0) = 1.0 \times 10^{-5}$; $v_i(0) = 0.0$ for $i \neq 80$. $\varepsilon_{80} = 0.452$; $\langle\varepsilon\rangle = (a)\ 0.553$; $(b)\ 0.514$; $(c)\ 0.500$. $(\mathscr{R}_{0,1}, \mathscr{R}_0, \langle\mathscr{R}_{0,i}\rangle, \mathscr{R}_{0,80}) = (a)\ (1.230, 1.093, 1.093, 1.050)$; $(b)\ (1.143, 1.001, 1.001, 0.975)$; $(c)\ (1.112, 0.969, 0.969, 0.949)$. In (b), the early period of V is decreasing, then tends to increase.

4.7.2 *Final epidemic size*

In this subsection, we analyze the sensitivity of the final epidemic size to a small variation in the class size. Suppose $\tilde{p}_i = p_i$ for class $i \notin \{\ell, \ell-1, \ell+1\}$, and

$$\tilde{p}_{\ell-1} = p_{\ell-1} + \alpha\delta p,$$

$$\tilde{p}_\ell = p_\ell - \delta p,$$

$$\tilde{p}_{\ell+1} = p_{\ell+1} + (1-\alpha)\delta p,$$

where $\alpha \in [0,1]$, $\delta p > 0$ and sufficiently small. Initial value of class $i \notin \{\ell, \ell-1, \ell+1\}$ is given by $\tilde{u}_i(0) = u_i(0)$, and those for class $\ell-1$, ℓ, and $\ell+1$ are respectively given by

$$\tilde{u}_{\ell-1}(0) = u_{\ell-1}(0) + \alpha\frac{u_\ell(0)}{p_\ell}\delta p;$$

$$\tilde{u}_\ell(0) = u_\ell(0) - \frac{u_\ell(0)}{p_\ell}\delta p;$$

$$\tilde{u}_{\ell+1}(0) = u_{\ell+1}(0) + (1-\alpha)\frac{u_\ell(0)}{p_\ell}\delta p.$$

Based on the supposition, we derive

$$\begin{aligned} \langle\tilde{\varepsilon}\rangle &= \langle\varepsilon\rangle + \Delta\varepsilon\delta p; \\ \langle\tilde{\varepsilon\gamma}\rangle &= \langle\varepsilon\gamma\rangle + \Delta(\varepsilon\gamma)\delta p; \\ \tilde{\mathscr{R}}_{0,i} &= \mathscr{R}_{0,i} + \mathscr{R}_{0,i}\frac{\Delta\varepsilon}{\langle\varepsilon\rangle}\delta p, \end{aligned} \tag{162}$$

where $\Delta\varepsilon = \alpha\varepsilon_{\ell-1} - \varepsilon_\ell + (1-\alpha)\varepsilon_{\ell+1}$, $\Delta(\varepsilon\gamma) = \alpha\varepsilon_{\ell-1}\gamma_{\ell-1} - \varepsilon_\ell\gamma_\ell + (1-\alpha)\varepsilon_{\ell+1}\gamma_{\ell+1}$.

Let us denote

$$\begin{aligned}\tilde{\mathscr{R}}_0 =& \mathscr{R}_0 + \delta\mathscr{R}_0;\\ \tilde{u}_i^\infty =& u_i^\infty + \delta u_i;\\ \tilde{W}_\infty =& W_\infty + \delta W_\infty.\end{aligned}$$

Then, we derive the following theorems, which respectively characterize the sensitivity of the basic reproduction number and the final epidemic size (Appendix 4.A.11):

Theorem 4.2.

$$\delta\mathscr{R}_0 = \mathscr{R}_0 \frac{\Delta(\varepsilon\gamma)}{\langle\varepsilon\gamma\rangle}\delta p.$$

Theorem 4.3.

$$\delta W_\infty = \frac{D\delta p}{F'(U_\infty)U_\infty}\left\{D_1(\mathscr{R}_{0,k},\alpha) - \frac{u_\ell(0)}{p_\ell}D_2(\mathscr{R}_{0,k},\alpha,U_\infty)\right\} - \frac{u_\ell(0)}{p_\ell}D_3(\alpha,U_\infty)\delta p,$$

where

$$\begin{aligned}D &= \sum_{k=1}^{n}\varepsilon_k u_k(0)U_\infty^{\varepsilon_k},\\ D_1(\mathscr{R}_{0,k},\alpha) &= \alpha(\mathscr{R}_{0,\ell-1}-\mathscr{R}_{0,\ell}) - (1-\alpha)(\mathscr{R}_{0,\ell}-\mathscr{R}_{0,\ell+1}),\\ D_2(\mathscr{R}_{0,k},\alpha,U_\infty) &= \alpha\left\{\mathscr{R}_{0,\ell-1}U_\infty^{\varepsilon_{\ell-1}} - \mathscr{R}_{0,\ell}U_\infty^{\varepsilon_\ell}\right\} - (1-\alpha)\left\{\mathscr{R}_{0,\ell}U_\infty^{\varepsilon_\ell} - \mathscr{R}_{0,\ell+1}U_\infty^{\varepsilon_{\ell+1}}\right\},\\ D_3(\alpha,U_\infty) &= \alpha\left\{U_\infty^{\varepsilon_{\ell-1}} - U_\infty^{\varepsilon_\ell}\right\} - (1-\alpha)\left\{U_\infty^{\varepsilon_\ell} - U_\infty^{\varepsilon_{\ell+1}}\right\}.\end{aligned}$$

Theorem 4.2 indicates that the change in the system basic reproduction number $\mathscr{R}_0$ depends on the α, and distribution of ε_i and γ_i. Increasing the proportion of high caution class could effectively reduce the spread of the transmissible disease. This is because individuals in high caution class exhibit lower susceptibility and infectivity, thereby reducing the potential of transmission. The result given by Theorem 4.3 is more complicated. From (176) in Appendix 4.A.7, and $\varepsilon_{\ell-1} > \varepsilon_\ell > \varepsilon_{\ell+1}$, we can get $U_\infty^{\varepsilon_{\ell+1}} > U_\infty^{\varepsilon_\ell} > U_\infty^{\varepsilon_{\ell-1}}$. Then, we can obtain $\delta W_\infty < 0$ if one of the following conditions is satisfied:

- α is sufficiently small;
- $|\varepsilon_i - \varepsilon_j| \ll 1$ for $\forall i, j$, and

$$\mathscr{R}_{0,\ell} > \alpha\mathscr{R}_{0,\ell-1} + (1-\alpha)\mathscr{R}_{0,\ell+1};$$

- $|\gamma_i - \gamma_j| \ll 1$ for $\forall i, j$, and

$$U_\infty^{\varepsilon_\ell} < U_\infty^{\varepsilon_{\ell-1}} + \frac{1-\alpha}{\alpha}U_\infty^{\varepsilon_{\ell+1}}.$$

The larger value of α indicates a higher proportion of individuals in lower caution classes, leading to a greater final epidemic size. Furthermore, the final epidemic size depends on the distribution of preventive behaviors, characterized by the parameters γ and ε.

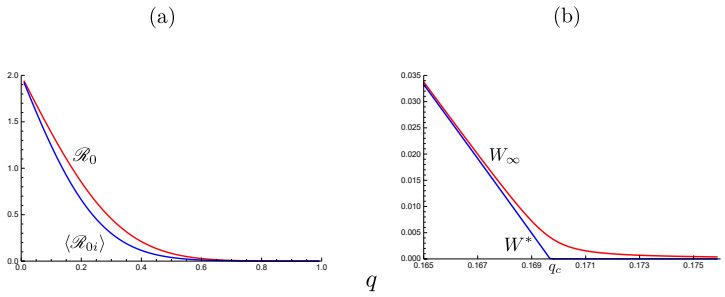

Figure 33: The relation between the class size distribution as defined in (163) and (a) reproduction numbers; (b) final epidemic size. Numerically drawn with $N = 1.0 \times 10^5$; $n = 10$; $b_\varepsilon = 0.5$; $b_\gamma = 0.6$; $\beta = 1.0 \times 10^{-5}$; $\rho = 0.5$. The initial condition is given by $v_1(0) = 1.0 \times 10^{-5}$; $v_i(0) = 0.0$ for $i \neq 1$. The critical value for $W^* = 0$ is given by $q_c = 0.170$.

4.8 MODEL WITH SPECIFIC BEHAVIORAL HETEROGENEITY

4.8.1 *A modified binomial class size distribution*

In this subsection, we consider a specific distribution to illustrate our n class model. Let us consider the following modified binomial distribution $\{p_k\}$, and $\{\varepsilon_k\}$ and $\{\gamma_k\}$:

$$p_k = \frac{{}_n\mathrm{C}_k q^k (1-q)^{n-k}}{1-(1-q)^n}; \quad \varepsilon_k = b_\varepsilon^{k-1}; \quad \gamma_k = b_\gamma^{k-1}, \tag{163}$$

where b_ε in $(0,1)$ and b_γ in $(0,1)$. Then, we can get

$$\begin{aligned}
\langle \varepsilon \rangle &= \sum_{k=1}^{n} \varepsilon_k p_k = \frac{1}{b_\varepsilon} \frac{\{1-q(1-b_\varepsilon)\}^n - (1-q)^n}{1-(1-q)^n}; \\
\langle \gamma \rangle &= \sum_{k=1}^{n} \gamma_k p_k = \frac{1}{b_\gamma} \frac{\{1-q(1-b_\gamma)\}^n - (1-q)^n}{1-(1-q)^n}; \\
\langle \varepsilon\gamma \rangle &= \sum_{k=1}^{n} \varepsilon_k \gamma_k p_k = \frac{1}{\theta} \frac{\{1-q(1-\theta)\}^n - (1-q)^n}{1-(1-q)^n},
\end{aligned}$$

where $\theta = b_\varepsilon b_\gamma$. From the definition of the class-specific basic reproduction number (143) and system basic reproduction number (147), we can get

$$\begin{aligned}
\mathscr{R}_{0i} &= \gamma_i \langle \varepsilon \rangle \mathscr{R}_0^{\sup}; \\
\mathscr{R}_0 &= \langle \varepsilon\gamma \rangle \mathscr{R}_0^{\sup}.
\end{aligned}$$

Following Theorem 4.1, we can derive that $W^* = 0$ if $\langle \varepsilon\gamma \rangle \leq 1/\mathscr{R}_0^{\sup}$, $W^* > 0$ if $\langle \varepsilon\gamma \rangle > 1/\mathscr{R}_0^{\sup}$. The critical condition of $\mathscr{R}_0 = 1$ is given by $\langle \varepsilon\gamma \rangle = 1/\mathscr{R}_0^{\sup}$. Furthermore, the modified binomial distribution p_k is monotonically decreasing for $q < 2/(n+1)$, monotonically increasing for $q > n/(n+1)$, and unimodal for $2/(n+1) < q < n/(n+1)$.

Figure 33 illustrates that increasing the caution level significantly contributes to the reduction of both the system basic reproduction number and the final epidemic size. Figure 34 (a) illustrates that the final epidemic size W_∞ is positive under the condition of small q and large θ. A sufficiently large proportion of individuals with high caution in the community and the significant difference in caution levels can lead to a positive final epidemic

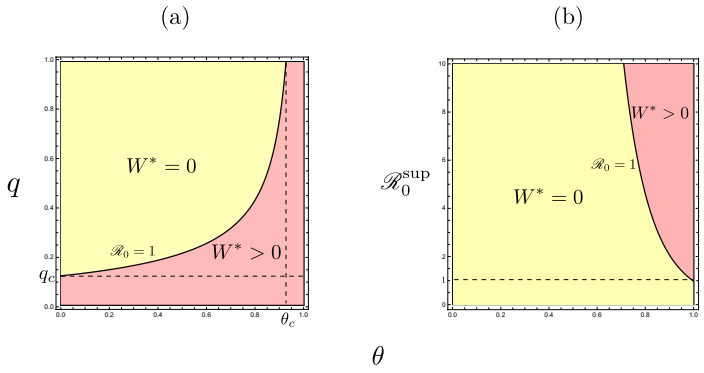

Figure 34: Parameter region of infimum of final epidemic size W^* with the class size distribution as defined in (163). The red region shows $W^* > 0$ for any q in $(0, 1)$, the yellow region shows $W^* = 0$ for any q in $(0, 1)$. The boundary curve is given by $\mathscr{R}_0 = 1$. Numerically with (a) $\mathscr{R}_0^{\sup} = 2.0$; (b) $q = 0.8$. $n = 10$. The critical value $q_c = 0.128$, $\theta_c = 0.926$.

size. As shown in Figure 34 (b), $W^* = 0$ if $\mathscr{R}_0^{\sup} < 1$. Conversely, if $\mathscr{R}_0^{\sup}$ is sufficiently large, the final epidemic size W_∞ is necessarily positive. The formulas for the critical values q_c, θ_c, and $\mathscr{R}_c^{\sup}$ are shown in Appendix 4.A.12.

4.8.2 *Two class model*

We consider the mathematical model (142) with $n = 2$. Here, assume $p_1 = p$, $p_2 = 1 - p$, the class-specific basic reproduction number is given by

$$\mathscr{R}_{0,1} = \gamma_1 \langle \varepsilon \rangle \mathscr{R}_0^{\sup}; \quad \mathscr{R}_{0,2} = \gamma_2 \langle \varepsilon \rangle \mathscr{R}_0^{\sup},$$

where $\langle \varepsilon \rangle = \varepsilon_1 p + \varepsilon_2 (1 - p)$. The basic reproduction number is given by

$$\mathscr{R}_0 = \{\varepsilon_1 \gamma_1 p + \varepsilon_2 \gamma_2 (1 - p)\} \mathscr{R}_0^{\sup}. \tag{164}$$

From equation (155), the final epidemic size is given by

$$W_\infty = 1 - u_1(0) U_\infty^{\varepsilon_1} - u_2(0) U_\infty^{\varepsilon_2}. \tag{165}$$

If all individuals in the community are highly cautious about the epidemic, the risk of infection decreases due to the effectiveness of protective behaviors. According to the definition of the basic reproduction number, $\mathscr{R}_0$ reaches its minimum under this situation. In contrast, $\mathscr{R}_0$ reaches its maximum when all individuals in the community with low caution level. From the above arguments, we can derive that $\mathscr{R}_0$ reaches its minimum if $p = 0$, $\mathscr{R}_0$ reaches its maximum if $p = 1$. Let us define

$$\mathscr{R}_0^{\min} := \varepsilon_2 \gamma_2 \mathscr{R}_0^{\sup}; \quad \mathscr{R}_0^{\max} := \varepsilon_1 \gamma_1 \mathscr{R}_0^{\sup},$$

Under the assumption that $\varepsilon_1 = \gamma_1 = 1$, it follows that $\mathscr{R}_0^{\min} < \mathscr{R}_0^{\max}$. Then, we obtain the following result (Appendix 4.A.13):

1. If $\mathscr{R}_0^{\min} \geq 1$, $W^* > 0$ for any p in $(0, 1)$;
2. If $\mathscr{R}_0^{\max} \leq 1$, $W^* = 0$ for any p in $(0, 1)$;

3. If $\mathscr{R}_0^{\min} < 1 < \mathscr{R}_0^{\max}$, there exists a critical value p_c in $(0,1)$, such that $W^* = 0$ for $p \le p_c$, $W^* > 0$ for $p > p_c$, where

$$p_c = \frac{1}{1 + \left(\mathscr{R}_0^{\max} - 1\right) / \left(1 - \mathscr{R}_0^{\min}\right)}.$$

Furthermore, it is easy to find that the critical value p_c is monotonically decreasing with the ε_2 and γ_2. Smaller values of ε_2 and γ_2 indicate a greater difference of the preventive behavior between these two classes, which leads to a larger p_c and makes the condition $W^* = 0$ easier to satisfy, thereby potentially minimizing the resulting social damage.

4.8.3 *Comparison of two communities*

Suppose that two communities A and B, which have class size distributions given by parameters $p_{\mathrm{A}} \in (0,1)$ and $p_{\mathrm{B}} \in (0,1)$. For mathematical simplification, we assume the following relations between parameters.

$$\begin{aligned}
&\varepsilon_i^{\mathrm{B}} = \omega \varepsilon_i^{\mathrm{A}} \text{ and } \gamma_i^{\mathrm{B}} = \omega \gamma_i^{\mathrm{A}} \text{ for } i = 1,2 \text{ with } \omega > 0;\\
&\varepsilon_2^{\mathrm{A}} = b\varepsilon_1^{\mathrm{A}} \text{ and } \gamma_2^{\mathrm{A}} = b\gamma_1^{\mathrm{A}} \text{ with } b \in (0,1);\\
&\mathscr{R}_0^{\mathrm{sup,B}} = r_0 \mathscr{R}_0^{\mathrm{sup,A}} \text{ with } r_0 > 0.
\end{aligned} \tag{166}$$

Let us suppose that two communities have the same $\mathscr{R}_0 > 1$. Then, since $\mathscr{R}_0 = \langle\varepsilon\gamma\rangle_{\mathrm{A}} \mathscr{R}_0^{\mathrm{sup,A}} = \langle\varepsilon\gamma\rangle_{\mathrm{B}} \mathscr{R}_0^{\mathrm{sup,B}} = r_0 \langle\varepsilon\gamma\rangle_{\mathrm{B}} \mathscr{R}_0^{\mathrm{sup,A}}$, we have $\langle\varepsilon\gamma\rangle_{\mathrm{A}} = r_0 \langle\varepsilon\gamma\rangle_{\mathrm{B}} = \mathscr{R}_0 / \mathscr{R}_0^{\mathrm{sup,A}}$. That is,

$$p_{\mathrm{A}}\varepsilon_1^{\mathrm{A}}\gamma_1^{\mathrm{A}} + (1-p_{\mathrm{A}})\varepsilon_2^{\mathrm{A}}\gamma_2^{\mathrm{A}} = \mathscr{R}_0\{p_{\mathrm{B}}\varepsilon_1^{\mathrm{B}}\gamma_1^{\mathrm{B}} + (1-p_{\mathrm{B}})\varepsilon_2^{\mathrm{B}}\gamma_2^{\mathrm{B}}\} = \frac{\mathscr{R}_0}{\mathscr{R}_0^{\mathrm{sup,A}}}. \tag{167}$$

From (166), the equalities given in (167) lead to

$$p_{\mathrm{A}} + (1-p_{\mathrm{A}})b^2 = r_0\omega^2\{p_{\mathrm{B}} + (1-p_{\mathrm{B}})b^2\} = \kappa := \frac{1}{\varepsilon_1^{\mathrm{A}}\gamma_1^{\mathrm{A}}} \frac{\mathscr{R}_0}{\mathscr{R}_0^{\mathrm{sup,A}}} \in (p_{\mathrm{A}}, 1). \tag{168}$$

From the equalities in (168), we obtain

$$\begin{aligned}
&b = \sqrt{\frac{\kappa - p_{\mathrm{A}}}{1-p_{\mathrm{A}}}} = \sqrt{1 - \frac{1-\kappa}{1-p_{\mathrm{A}}}};\\
&\frac{\kappa}{r_0\omega^2} = p_{\mathrm{B}} + (1-p_{\mathrm{B}})\frac{\kappa - p_{\mathrm{A}}}{1-p_{\mathrm{A}}} = 1 - (1-p_{\mathrm{B}})\frac{1-\kappa}{1-p_{\mathrm{A}}} \in (0,1).
\end{aligned}$$

Furthermore, we can easily get

$$\begin{aligned}
&\langle\varepsilon\rangle_{\mathrm{A}} = p_{\mathrm{A}}\varepsilon_1^{\mathrm{A}} + (1-p_{\mathrm{A}})\varepsilon_2^{\mathrm{A}} = \varepsilon_1^{\mathrm{A}}\{p_{\mathrm{A}} + (1-p_{\mathrm{A}})b\};\\
&\langle\varepsilon\rangle_{\mathrm{B}} = p_{\mathrm{B}}\varepsilon_1^{\mathrm{B}} + (1-p_{\mathrm{B}})\varepsilon_2^{\mathrm{B}} = \omega\varepsilon_1^{A}\{p_{\mathrm{B}} + (1-p_{\mathrm{B}})b\};\\
&\mathscr{R}_{0,2}^{A} = \gamma_2^{\mathrm{A}}\langle\varepsilon\rangle_{\mathrm{A}}\mathscr{R}_0^{\mathrm{sup,A}} = b\gamma_1^{\mathrm{A}}\langle\varepsilon\rangle_{\mathrm{A}}\mathscr{R}_0^{\mathrm{sup,A}} = b\mathscr{R}_{0,1}^{\mathrm{A}};\\
&\mathscr{R}_{0,2}^{\mathrm{B}} = \gamma_2^{\mathrm{B}}\langle\varepsilon\rangle_{\mathrm{B}}\mathscr{R}_0^{\mathrm{sup,B}} = b\gamma_1^{\mathrm{B}}\langle\varepsilon\rangle_{\mathrm{B}}\mathscr{R}_0^{\mathrm{sup,B}} = b\mathscr{R}_{0,1}^{\mathrm{B}};\\
&\mathscr{R}_{0,1}^{\mathrm{A}} = \gamma_1^{\mathrm{A}}\langle\varepsilon\rangle_{\mathrm{A}}\mathscr{R}_0^{\mathrm{sup,A}} = \varphi(p_{\mathrm{A}})\mathscr{R}_0;\\
&\mathscr{R}_{0,1}^{\mathrm{B}} = \gamma_1^{\mathrm{B}}\langle\varepsilon\rangle_{\mathrm{B}}\mathscr{R}_0^{\mathrm{sup,B}} = \varphi(p_{\mathrm{B}})\mathscr{R}_0,
\end{aligned}$$

where

$$\varphi(x) := \frac{x + (1-x)\sqrt{1 - \frac{1-\kappa}{1-p_{\mathrm{A}}}}}{1 - (1-x)\frac{1-\kappa}{1-p_{\mathrm{A}}}}.$$

Thus, we have

$$\varphi(p_{\mathrm{A}}) = \frac{1}{\kappa}\left\{p_{\mathrm{A}} + (1-p_{\mathrm{A}})\sqrt{1 - \frac{1-\kappa}{1-p_{\mathrm{A}}}}\right\};$$
$$\varphi(p_{\mathrm{B}}) = \frac{p_{\mathrm{B}} + (1-p_{\mathrm{B}})\sqrt{1 - \frac{1-\kappa}{1-p_{\mathrm{A}}}}}{1 - (1-p_{\mathrm{B}})\frac{1-\kappa}{1-p_{\mathrm{A}}}}.$$

Therefore, we have $\mathscr{R}^{\mathrm{A}}_{0,2} = b\varphi(p_{\mathrm{A}})\mathscr{R}_0$ and $\mathscr{R}^{\mathrm{B}}_{0,2} = b\varphi(p_{\mathrm{B}})\mathscr{R}_0$. Note that $\varphi(x)$ is monotonically decreasing in terms of $x \in (0,1)$, with $\varphi(0) = 1/b > 1$, and $\varphi(1) = 1$. Hence, $\varphi(x) \in (1, 1/b)$ for $x \in (0,1)$. Therefore, we have $b\varphi(x) < 1 < \varphi(x)$ for $x \in (0,1)$. As a result, the above equalities about the class-specific basic reproduction numbers imply $\mathscr{R}^{\mathrm{A}}_{0,1} > \mathscr{R}_0 > \mathscr{R}^{\mathrm{A}}_{0,2}$ and $\mathscr{R}^{\mathrm{B}}_{0,1} > \mathscr{R}_0 > \mathscr{R}^{\mathrm{B}}_{0,2}$. This result is consistent with the order given in (144) and Lemma 4.2 for the n-class model.

The infima of final epidemic size W^*_{A} and W^*_{B} for communities A and B are determined as

$$W^*_{\mathrm{A}} = 1 - p_{\mathrm{A}}(U^*_{\mathrm{A}})^{\varepsilon^{\mathrm{A}}_1} - (1-p_{\mathrm{A}})(U^*_{\mathrm{A}})^{\varepsilon^{\mathrm{A}}_2} = 1 - p_{\mathrm{A}}(U^*_{\mathrm{A}})^{\varepsilon^{\mathrm{A}}_1} - (1-p_{\mathrm{A}})\{(U^*_{\mathrm{A}})^{\varepsilon^{\mathrm{A}}_1}\}^b;$$
$$W^*_{\mathrm{B}} = 1 - p_{\mathrm{B}}(U^*_{\mathrm{B}})^{\varepsilon^{\mathrm{B}}_1} - (1-p_{\mathrm{B}})(U^*_{\mathrm{B}})^{\varepsilon^{\mathrm{B}}_2} = 1 - p_{\mathrm{B}}\{(U^*_{\mathrm{B}})^{\omega}\}^{\varepsilon^{\mathrm{A}}_1} - (1-p_{\mathrm{B}})[\{(U^*_{\mathrm{B}})^{\omega}\}^{\varepsilon^{\mathrm{A}}_1}]^b,$$

where U^*_{A} and U^*_{B} are given as the roots of $\mathscr{F}_{\mathrm{A}}(U) = 0$ and $\mathscr{F}_{\mathrm{B}}(U) = 0$ in $(0,1)$ with

$$\begin{aligned}
\mathscr{F}_{\mathrm{A}}(U) :=& \log U^{\langle\varepsilon\rangle_{\mathrm{A}}} + \mathscr{R}^{\mathrm{A}}_{0,1}p_{\mathrm{A}}\big(1 - U^{\varepsilon^{\mathrm{A}}_1}\big) + \mathscr{R}^{\mathrm{A}}_{0,2}(1-p_{\mathrm{A}})\big(1 - U^{\varepsilon^{\mathrm{A}}_2}\big)\\
=& \big\{p_{\mathrm{A}} + (1-p_{\mathrm{A}})b\big\}\log U^{\varepsilon^{\mathrm{A}}_1}\\
&+ \mathscr{R}_0\,\varphi(p_{\mathrm{A}})\Big[p_{\mathrm{A}}\big(1 - U^{\varepsilon^{\mathrm{A}}_1}\big) + (1-p_{\mathrm{A}})b\big\{1 - (U^{\varepsilon^{\mathrm{A}}_1})^b\big\}\Big];\\
\mathscr{F}_{\mathrm{B}}(U) :=& \log U^{\langle\varepsilon\rangle_{\mathrm{B}}} + \mathscr{R}^{\mathrm{B}}_{0,1}p_{\mathrm{B}}\big(1 - U^{\varepsilon^{\mathrm{B}}_1}\big) + \mathscr{R}^{\mathrm{B}}_{0,2}(1-p_{\mathrm{B}})\big(1 - U^{\varepsilon^{\mathrm{B}}_2}\big)\\
=& \big\{p_{\mathrm{B}} + (1-p_{\mathrm{B}})b\big\}\log\big(U^{\omega}\big)^{\varepsilon^{\mathrm{A}}_1}\\
&+ \mathscr{R}_0\varphi(p_{\mathrm{B}})\Big(p_{\mathrm{B}}\big\{1 - (U^{\omega})^{\varepsilon^{\mathrm{A}}_1}\big\} + (1-p_{\mathrm{B}})b\big[1 - \big\{(U^{\omega})^{\varepsilon^{\mathrm{A}}_1}\big\}^b\big]\Big).
\end{aligned}$$

Then, let us define

$$\Psi(X,P) := \big\{P + (1-P)b\big\}\log X + \mathscr{R}_0\varphi(P)\big\{P(1-X) + (1-P)b(1-X^b)\big\}.$$

The infima of final epidemic sizes W^*_{A} and W^*_{B} are given by

$$W^*_{\mathrm{A}} = 1 - p_{\mathrm{A}}x^*_{\mathrm{A}} - (1-p_{\mathrm{A}})(x^*_{\mathrm{A}})^b;$$
$$W^*_{\mathrm{B}} = 1 - p_{\mathrm{B}}x^*_{\mathrm{B}} - (1-p_{\mathrm{B}})(x^*_{\mathrm{B}})^b,$$

where $x^*_{\mathrm{A}} \in (0,1)$ and $x^*_{\mathrm{B}} \in (0,1)$ are the root of equations $\Psi(x, p_{\mathrm{A}}) = 0$ and $\Psi(x, p_{\mathrm{B}}) = 0$ respectively.

On the other hand, we have

$$\varphi(P) = \frac{P + (1-P)\sqrt{1 - \frac{1-\kappa}{1-p_{\mathrm{A}}}}}{1 - (1-P)\frac{1-\kappa}{1-p_{\mathrm{A}}}} = \frac{P + (1-P)b}{P + (1-P)b^2}.$$

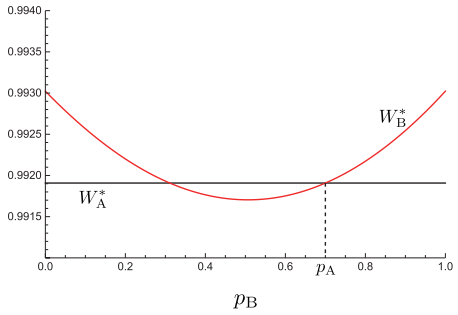

Figure 35: p_{B}-dependence of W^*_{B}. Numerically with $\mathscr{R}_0 = 5.0$; $\kappa = 0.9$, $p_{\mathrm{A}} = 0.7$; $b = 0.816$.

Therefore, the equation $\Psi(x,p) = 0$ is equivalent to

$$\widetilde{\Psi}(x,p) := \{p + (1-p)b^2\}\log x + \mathscr{R}_0\{p(1-x) + (1-p)b(1-x^b)\} = 0.$$

It is easy to find that, when $\mathscr{R}_0 > 1$, the equation $\widetilde{\Psi}(x,p) = 0$ in terms of $x \in (0,1)$ has a unique root $x^*(p) \in (0,1)$, where $\widetilde{\Psi}(x,p) \to -\infty$ as $x \to +0$, and $\widetilde{\Psi}(1,p) = 0$. This result is consistent with Lemma 4.9. Then, we obtain the following results (Appendix 4.A.14):

Lemma 4.12. *If and only if* $r_0\omega^2 = 1$, *it holds that* $p_{\mathrm{B}} = p_{\mathrm{A}}$, *which implies* $x^*_{\mathrm{B}} = x^*_{\mathrm{A}}$, *and consequently* $W^*_{\mathrm{A}} = W^*_{\mathrm{B}}$.

Lemma 4.13. *If and only if* $r_0\omega^2 > 1$, *it holds that* $p_{\mathrm{B}} < p_{\mathrm{A}}$, *which implies* $x^*_{\mathrm{B}} < x^*_{\mathrm{A}}$.

Lemma 4.12 demonstrates that two communities with different qualities of caution level could have the same final epidemic size. The larger community may have the same final epidemic size if it has a higher quality of preventive behavior, that is, smaller ω. Lemma 4.13 implies that the final epidemic sizes of two communities are generally different from each other even if they have the common $\mathscr{R}_0$. It should be noted that Lemma 4.13 does not directly imply that the final epidemic size W^*_{B} would be larger than W^*_{A}, since the two communities have different size distributions represented by p_{A} and p_{B} with $p_{\mathrm{B}} < p_{\mathrm{A}}$ for $r_0\omega^2 > 1$. These findings are illustrated numerically in Figure 35. Furthermore, from equation (168), it is easy to find that ω is monotonically decreasing in terms of p_{B} for given values of κ, r_0 and b. Therefore, even though community B has a larger population of high caution individuals, its lower quality of preventive behavior, that is, larger ω, may lead to a larger final epidemic size than that of community A. Alternatively, when community B has a larger proportion of low caution individuals, its final epidemic size would be larger than that of community A, even with higher quality of preventive behavior.

4.9 DISCUSSION

In this work, we consider a mathematical model for the epidemic dynamics with the heterogeneity of preventive behavior among individuals about a disease transmission, focusing on the relation of the distribution of preventive behavior to the final epidemic consequence in a community.

To clarify the heterogeneity, we divided the total population into n classes, each class representing a different level of caution against a transmissible disease. We focused on the distribution of class size and preventive behavior, that is the variations in both susceptibility and infectivity in the population. The class structure is assumed to reflect educational background, individuals of higher education exhibiting higher levels of caution and more effective preventive behaviors.

We defined two types of basic reproduction numbers: the class-specific basic reproduction number, which reflects the transmission potential within each class, and the system-level basic reproduction number, which reflects the overall transmission potential in the population.

Based on the time-independent equality, we derived the final epidemic size. Our results showed that the final epidemic size and system basic reproduction number strongly depends on the class size distribution. There exists a criticality for the distribution of caution level that determines the severity of social damage by the disease spread. In particular, a large proportion of individuals in low caution classes increases the system reproduction number and results in a larger final epidemic size. Conversely, when the population is majority composed of high caution individuals, the damage due to the disease spread is significantly suppressed. These findings emphasize the importance of promoting preventive awareness, especially in more vulnerable or less-informed groups, and highlight the potential benefits of increasing people's caution through education or public health interventions. We also investigated the initial change of the total infected population size, and obtain mathematical conditions for the outbreak, revival, and unsuccessful spread of the disease. Our analysis revealed how the class size distribution influence initial epidemic dynamics.

This work aims to provide a theoretical understanding of epidemic dynamics by introducing a structured SIR model that investigates how individual preventive heterogeneity influences the epidemic consequence. The results demonstrate that the distribution of caution levels in the population plays a crucial role in determining both the initial progression and the final size of disease spread.

APPENDIX FOR CHAPTER 4

APPENDIX 4.A.1: PROOF OF LEMMA 4.1

From the equations in (142), we can derive

$$u_i(\tau) = u_i(0) \exp\left[-\frac{\varepsilon_i}{\langle\varepsilon\rangle}\int_0^\tau \sum_{k=1}^n \mathscr{R}_{0,k} v_k(\nu) d\nu\right] > 0$$

with $u_i(0) > 0$ for any $\tau > 0$. Then consider the case of $v_i(0) > 0$ for all i. We have

$$\frac{dv_i}{d\tau} > u_i \frac{\varepsilon_i}{\langle\varepsilon\rangle}\mathscr{R}_{0,i} v_i - v_i \tag{169}$$

for all i. Making the integration for the right-hand side of (169), we can derive it by

$$v_i(0) \exp\left[\int_0^\tau u_i(\nu)\frac{\varepsilon_i}{\langle\varepsilon\rangle}\mathscr{R}_{0,i} d\nu - \tau\right] > 0 \tag{170}$$

with $v_i(0) > 0$ for all i. From (169) and (170), we can derive $v_i(\tau) > 0$ for any $\tau > 0$ with $v_i(0) > 0$ for all i. Next, consider the case $v_j(0) = 0$ for all j, and there exists $v_i(0) > 0$ for $i \neq j$, we can derive

$$\frac{dv_j}{d\tau}\Big|_{\tau=0} = u_j \frac{\varepsilon_j}{\langle\varepsilon\rangle}\sum_{k=1,\neq j}^n \mathscr{R}_{0,k} v_k > 0 \tag{171}$$

at the initial moment $\tau_1 > 0$ and $\tau_1 \ll 1$. Hence, we can get $v_j(\tau_1) > 0$. For $\tau \geq \tau_1$, we can solve the equation (171), and is given by

$$v_j(\tau) = v_j(\tau_1) \exp\left[\int_{\tau_1}^\tau \frac{u_i(\nu)}{v_i(\nu)}\frac{\varepsilon_i}{\langle\varepsilon\rangle}\sum_{k=1}^n \mathscr{R}_{0,k} v_k(\nu) d\nu - \tau\right] > 0.$$

From the above arguments, we can derive $v_j(\tau) > 0$ for any $\tau > 0$. Since $w_i(\tau) = p_i - u_i(\tau) - v_i(\tau)$, we can get $w_i(\tau) > 0$ for any $\tau > 0$, and obtain the lemma.

APPENDIX 4.A.2: DERIVATION OF REPRODUCTION NUMBERS

From system (141), we can derive

$$\begin{aligned}\frac{d}{dt}\sum_{i=1}^n I_i &= \sum_{i=1}^n \left\{\varepsilon_i \beta \sum_{k=1}^n \gamma_k I_k S_i\right\} - \sum_{i=1}^n \rho I_i \\ &= \sum_{k=1}^n \left\{\sum_{i=1}^n \varepsilon_i \beta S_i \gamma_k I_k\right\} - \sum_{i=1}^n \rho I_i.\end{aligned}$$

From the above equation, the amount of new infections by a single infected individual of caution level i during the time interval $[t, t+\Delta t]$ is given by $\sum_{k=1}^n \varepsilon_k \beta S_k \gamma_i \Delta t$. At the time t, the effective basic reproduction number of caution level i is given by

$$\sum_{k=1}^n \frac{1}{\rho}\varepsilon_k \beta S_k \gamma_i.$$

Since the basic reproduction number of caution level i is the supremum of the effective basic reproduction number, we can derive it as shown in (143).

APPENDIX 4.A.3: DERIVATION OF SYSTEM REPRODUCTION NUMBER

In order to derive the system basic reproduction number $\mathscr{R}_0$, we use the next generation matrix method and decompose the system (141) into the recruitment terms of new infections and the other terms as follows:

$$\frac{d\mathbf{X}}{dt} = \mathfrak{F}(\mathbf{X}) - \mathfrak{V}(\mathbf{X}),$$

where $\mathbf{X} = (I_1(t), \ldots, I_n(t), S_i(t), \ldots, S_n(t))^{\mathrm{T}}$. $\mathfrak{F}$ represents the recruitment rate of new infections, and $\mathfrak{V}$ represents the other factors related to the epidemic dynamics, where

$$\mathfrak{F} := \begin{pmatrix} \varepsilon_1\beta\sum_{k=1}^{n}\gamma_k I_k S_1 \\ \vdots \\ \varepsilon_n\beta\sum_{k=1}^{n}\gamma_k I_k S_n \\ 0 \\ \vdots \\ 0 \end{pmatrix}; \quad \mathfrak{V} := \begin{pmatrix} \rho I_1 \\ \vdots \\ \rho I_n \\ \varepsilon_1\beta\sum_{k=1}^{n}\gamma_k I_k S_1 \\ \vdots \\ \varepsilon_n\beta\sum_{k=1}^{n}\gamma_k I_k S_n \end{pmatrix}.$$

Then, we have the Jacobian matrices of $\mathfrak{F}$ and $\mathfrak{V}$ about $\mathbf{X}$:

$$D\mathfrak{F}(\mathbf{X}) := \begin{pmatrix} \mathfrak{F}_1 & \mathfrak{F}_2 \\ \mathbf{0} & \mathbf{0} \end{pmatrix}; D\mathfrak{V}(\mathbf{X}) := \begin{pmatrix} \mathfrak{V}_1 & \mathbf{0} \\ \mathfrak{F}_1 & \mathfrak{F}_2 \end{pmatrix},$$

where

$$\mathfrak{F}_1 = \begin{pmatrix} \varepsilon_1\beta\gamma_1 S_1 & \cdots & \varepsilon_1\beta\gamma_n S_1 \\ \vdots & \ddots & \vdots \\ \varepsilon_1\beta\gamma_1 S_n & \cdots & \varepsilon_1\beta\gamma_n S_n \end{pmatrix};$$

$$\mathfrak{F}_2 = \begin{pmatrix} \varepsilon_1\beta\sum_{k=1}^{n}\gamma_k I_k & 0 & \cdots & 0 \\ 0 & \varepsilon_2\beta\sum_{k=1}^{n}\gamma_k I_k & \cdots & 0 \\ \vdots & \vdots & \ddots & \vdots \\ 0 & 0 & \cdots & \varepsilon_n\beta\sum_{k=1}^{n}\gamma_k I_k \end{pmatrix};$$

$\mathfrak{V}_1 = \rho \times I_n$, an $n \times n$ diagonal matrix with all diagonal elements equal to ρ. At the disease-free state $\mathrm{X}_0 := (0, \ldots, 0, S_1, \ldots, S_n)$, we have

$$D\mathfrak{F}(\mathbf{X_0}) := \begin{pmatrix} \mathfrak{F}_1^* & \mathbf{0} \\ \mathbf{0} & \mathbf{0} \end{pmatrix}; D\mathfrak{V}(\mathbf{X_0}) := \begin{pmatrix} \mathfrak{V}_1 & \mathbf{0} \\ \mathfrak{F}_1^* & \mathbf{0} \end{pmatrix},$$

where

$$\mathfrak{F}_1^* := \begin{pmatrix} \varepsilon_1\beta\gamma_1 S_1 & \cdots & \varepsilon_1\beta\gamma_n S_1 \\ \vdots & \ddots & \vdots \\ \varepsilon_1\beta\gamma_1 S_n & \cdots & \varepsilon_1\beta\gamma_n S_n \end{pmatrix}.$$

Taking the top left hand corner $n \times n$ matrices in each of the two matrices, we have

$$\mathcal{F} := \mathfrak{F}_i^* \qquad \mathcal{V} := \mathfrak{V}_1.$$

The next generation matrix (NGM) is obtained by

$$\mathcal{K} = \mathcal{F}\mathcal{V}^{-1} = \rho^{-1} \begin{pmatrix} \varepsilon_1\beta\gamma_1 S_1 & \cdots & \varepsilon_1\beta\gamma_n S_1 \\ \vdots & \ddots & \vdots \\ \varepsilon_1\beta\gamma_1 S_n & \cdots & \varepsilon_1\beta\gamma_n S_n \end{pmatrix}. \tag{172}$$

The eigenvalues of (172) are given by

$$\lambda_1 = \frac{1}{\rho}\sum_{k=1}^{n} \beta\gamma_k\varepsilon_k S_k, \qquad \lambda_2 = \cdots = \lambda_n = 0. \tag{173}$$

The maximum absolute value of the eigenvalues of (173) is λ_1. From the definition of the basic reproduction number $\mathscr{R}_0$, taking the supremum of λ_1 with respect to S_i, we have

$$\mathscr{R}_0 = \sup_{\{S_i\}} \frac{1}{\rho}\sum_{i=1}^{n} \varepsilon_i\beta S_i\gamma_i = \frac{1}{\rho}\sum_{i=1}^{n} \varepsilon_i\beta p_i N\gamma_i = \frac{\langle\varepsilon\gamma\rangle\beta N}{\rho}.$$

APPENDIX 4.A.4: PROOF OF LEMMA 4.2

From the meaning of the ε_k and γ_k, a smaller value of ε_k indicates that individuals of class k have a higher level of caution and contribute less to the spread of the epidemic. Then, the covariance between ε_k and γ_k is positive. Since

$$\langle\varepsilon\gamma\rangle = \langle\varepsilon\rangle\langle\gamma\rangle + \mathrm{Cov}(\varepsilon,\gamma),$$

we can obtain $\langle\varepsilon c\rangle > \langle\varepsilon\rangle\langle\gamma\rangle$. Then we have $\mathscr{R}_0 > \langle\mathscr{R}_{0,i}\rangle$. From the definition of the system basic reproduction number,

$$\mathscr{R}_0 := \sup_{\{S_i\}} \frac{1}{\rho}\sum_{i=1}^{n} \varepsilon_i\beta S_i\gamma_i = \frac{1}{\rho}\sum_{i=1}^{n} \varepsilon_i\beta p_i N\gamma_i < \frac{1}{\rho}\sum_{i=1}^{n} \varepsilon_i\beta p_i N\gamma_1,$$

we can obtain $\mathscr{R}_0 < \mathscr{R}_{0,1}$. Lemma 4.2 is proved.

APPENDIX 4.A.5: DERIVATION OF TIME-INDEPENDENT QUANTITIES

From equation $du_i/d\tau$ in (142), we can derive the following differential equation:

$$\frac{du_i}{du_j} = \frac{u_i\varepsilon_i}{u_j\varepsilon_j}. \tag{174}$$

We can solve equation (174), and find equation (148) with $u_i(0) > 0$ for all i. Next, from the definition of $X(\tau) := \sum_{k=1}^{n} \mathscr{R}_{0,k} v_k(\tau)$, we can get the following closed system:

$$\begin{aligned} \frac{dX}{d\tau} &= X \sum_{k=1}^{n} u_k \mathscr{R}_{0,k} \frac{\varepsilon_k}{\langle \varepsilon \rangle} - X; \\ \frac{du_i}{d\tau} &= -X u_i \frac{\varepsilon_i}{\langle \varepsilon \rangle}. \end{aligned} \tag{175}$$

We can derive the following differential equation from (175):

$$\frac{dX}{du_i} = -\sum_{k=1}^{n} \mathscr{R}_{0,k} \frac{u_k \varepsilon_k}{u_i \varepsilon_i} + \frac{\langle \varepsilon \rangle}{u_i \varepsilon_i}.$$

Then, using equation (148), we position the differential du_i on the right-hand side and integrate both sides with respect to u_i, we can obtain

$$\begin{aligned} X(\tau) - X(0) &= -\int_0^\tau \sum_{k=1}^{n} \mathscr{R}_{0,k} \frac{u_k(\tau)\varepsilon_k}{u_i(\tau)\varepsilon_i} du_i + \int_0^\tau \frac{\langle \varepsilon \rangle}{u_i(\tau)\varepsilon_i} du_i \\ X(\tau) &= \sum_{k=1}^{n} \mathscr{R}_{0,k}(p_k - u_k(0)) - \int_0^\tau \sum_{k=1}^{n} \mathscr{R}_{0,k} \left(\frac{u_i(\tau)}{u_i(0)} \right)^{\varepsilon_k/\varepsilon_i} \frac{u_k(0)\varepsilon_k}{u_i(\tau)\varepsilon_i} du_i \\ &\quad + \frac{\langle \varepsilon \rangle}{\varepsilon_i} \log \frac{u_i(\tau)}{u_i(0)} \\ &= \sum_{k=1}^{n} \mathscr{R}_{0,k}(p_k - u_k(0)) - \sum_{k=1}^{n} \mathscr{R}_{0,k} u_k(0) \frac{u_i(\tau)^{\varepsilon_k/\varepsilon_i} - u_i(0)^{\varepsilon_k/\varepsilon_i}}{u_i(0)^{\varepsilon_k/\varepsilon_i}} \\ &\quad + \log \{U(\tau)\}^{\langle \varepsilon \rangle} \\ &= \sum_{k=1}^{n} \mathscr{R}_{0,k} p_k - \sum_{k=1}^{n} \mathscr{R}_{0,k} u_k(0) \{U(\tau)\}^{\varepsilon_k} + \log \{U(\tau)\}^{\langle \varepsilon \rangle}. \end{aligned}$$

Then, we can derive the time-independent equality (149).

APPENDIX 4.A.6: PROOF OF LEMMA 4.5 AND 4.6

From the equation $du_i/d\tau$ in (142), we can get $u_i(\tau)$ is monotonically decreasing for any i. Suppose $u_i(\tau) \to u_i^\infty > 0$ as $\tau \to \infty$ for some i. We have $du_i/d\tau \to 0$ as $\tau \to \infty$ with the supposition $u_i(\tau) \to u_i^\infty > 0$. Therefore, it is necessary that $X(\tau) \to 0$ as $\tau \to \infty$. With the definition of X, and $v_i(\tau) > 0$ for any $\tau > 0$ in Lemma 4.1, we can get that $v_i(\tau) \to 0$ as $\tau \to \infty$ for all i. At the same time, since $v_i(\tau) > 0$ for any $\tau > 0$, from the equation $dw_i/d\tau$ in (142), we can get $w_i(\tau) \to w_i^\infty > 0$ as $\tau \to \infty$ for all i. Next, suppose $u_i(\tau) \to 0$ as $\tau \to \infty$ for all i, we can get $\sum_{k=1}^{n} u_k(\tau) \mathscr{R}_{0,k} \varepsilon_k / \langle \varepsilon \rangle - 1 < 0$ for sufficiently large τ. Then, we can get $dX/d\tau < 0$ in (175) with positive $X(\tau)$ for sufficiently large τ. If $X(\tau) > 0$ for any $\tau > 0$, it is necessary that $\sum_{k=1}^{n} u_k(\tau) \mathscr{R}_{0,k} \varepsilon_k / \langle \varepsilon \rangle - 1 = 0$ as $\tau \to \infty$, there is a contradiction for our supposition that $u_i(\tau) \to 0$ as $\tau \to \infty$. Therefore, it is necessary that $X(\tau) \to 0$ as $\tau \to \infty$. With the definition of X, and $v_i(\tau) > 0$ for any $\tau > 0$ in Lemma 4.1, we can get that $v_i(\tau) \to 0$ as $\tau \to \infty$ for all i. Since $u_i(\tau) + v_i(\tau) + w_i(\tau) = p_i$ for any τ, we can get $w_i(\tau) \to w_i^\infty > 0$ as $\tau \to \infty$ for all i. Based on the above arguments, Lemma 4.5 is proved.

From (152), denote $F(U) = f_1(U) - f_2(U)$, where $f_1(U) = \sum_{k=1}^{n} \mathscr{R}_{0,k}(p_k - u_k(0) U^{\varepsilon_k})$, $f_2(U) = -\log U^{\langle \varepsilon \rangle}$. We can get that $f_1(0) = \sum_{k=1}^{n} \mathscr{R}_{0,k} p_k > 0$,

$f_1(1) = \sum_{k=1}^{n} \mathscr{R}_{0,k}(p_k - u_k(0)) > 0$, $f_2(U)|_{U\to+0} = +\infty$, and $f_2(1) = 0$. It indicates that there exists at least one intersection for the curve $f_1(U)$ and $f_2(U)$. Then we can get that $f_1'(U) = -\sum_{k=1}^{n} \mathscr{R}_{0,k} u_k(0)\varepsilon_k U^{\varepsilon_k - 1} < 0$, $f_1''(U) = \sum_{k=1}^{n} \mathscr{R}_{0,k} u_k(0)\varepsilon_k(1-\varepsilon_k)U^{\varepsilon_k - 2} > 0$, $f_2'(U) = -\langle\varepsilon\rangle/U < 0$, and $f_2''(U) = \langle\varepsilon\rangle/U^2 > 0$, these two curves are both monotonically decreasing with convex shape. It indicates that there is a unique intersection between these two curves for $U \in (0,1)$. Hence there is unique root of $F(U) = f_1(U) - f_2(U) = 0$ for $U \in (0,1)$. Since $U \to U_\infty$ and $X \to 0$ as $\tau \to \infty$, $F(U_\infty) = 0$ satisfied for $U_\infty \in (0,1)$. Therefore, Lemma 4.6 is proved.

APPENDIX 4.A.7: PROOF OF LEMMA 4.7

Making partial derivative in terms of $u_j(0)$ for equation $F(U_\infty) = 0$, we can get

$$F'(U_\infty)\frac{\partial U_\infty}{\partial u_j(0)} - \frac{\gamma_j}{\langle\varepsilon\rangle}U_\infty^{\varepsilon_j} = 0$$

for any j. From the nature of $F(U)$ in Lemma 4.6, we can get

$$F'(U_\infty) = f_1'(U_\infty) - f_2'(U_\infty) > 0. \tag{176}$$

We can get

$$\frac{\partial U_\infty}{\partial u_j(0)} = \frac{\gamma_j U_\infty^{\varepsilon_j}}{\langle\varepsilon\rangle F'(U_\infty)} > 0$$

for any j. Then we can get

$$\frac{\partial u_i^\infty}{\partial u_j(0)} = \frac{\partial}{\partial u_j(0)}\{u_i(0)U_\infty^{\varepsilon_i}\} = u_i(0)\varepsilon_i U_\infty^{\varepsilon_i - 1}\frac{\partial U_\infty}{\partial u_j(0)} > 0$$

for any j. Since $u_i(0) + v_i(0) = p_i$ for all i, the large value of $u_i(0)$ indicates the small value of $v_i(0)$, we can get $\dfrac{\partial u_i^\infty}{\partial v_j(0)} < 0$ for any j. Lemma 4.7 is proved.

APPENDIX 4.A.8: PROOF OF LEMMA 4.8, 4.9, AND THEOREM 4.1

For $i \neq j$, we can get that

$$\frac{\partial}{\partial u_j(0)}\left(\frac{u_i^\infty}{u_i(0)}\right) = \frac{1}{u_i(0)}\frac{\partial u_i^\infty}{\partial u_j(0)} > 0.$$

For $i = j$, we can get

$$\begin{aligned}
\frac{\partial}{\partial u_i(0)}\left(\frac{u_i^\infty}{u_i(0)}\right) =& \frac{1}{u_i^2(0)}\left\{u_i(0)\frac{\partial u_i^\infty}{\partial u_i(0)} - u_i^\infty\right\} \\
=& \frac{1}{u_i^2(0)}\left\{u_i(0)\frac{\partial u_i^\infty}{\partial u_i(0)} - u_i(0)U_\infty^{\varepsilon_i}\right\} \\
=& \frac{1}{u_i(0)}\left\{\frac{\partial}{\partial u_i(0)}(u_i(0)U_\infty^{\varepsilon_i}) - U_\infty^{\varepsilon_i}\right\} \\
=& \varepsilon_i U_\infty^{\varepsilon_i - 1}\frac{\partial U_\infty}{\partial u_i(0)} > 0.
\end{aligned}$$

Hence Lemma 4.8 is proved.

Denote $\mathscr{F}(U) = g_1(U) - g_2(U)$, where $g_1(U) = \sum_{k=1}^{n} \mathscr{R}_{0,k} p_k \{1 - U^{\varepsilon_k}\}$, $g_2(U) = -\log U^{\langle \varepsilon \rangle}$. We can get $g_1(0) = \sum_{k=1}^{n} \mathscr{R}_{0,k} p_k > 0$, $g_1(1) = 0$, $g_2(U)|_{U \to +0} = +\infty$, and $g_2(1) = 0$. There exists at least one root of $\mathscr{F}(U) = 0$ for $U \in (0, 1]$. Then we can get $g_1'(U) = -\sum_{k=1}^{n} \mathscr{R}_{0,k} p_k \varepsilon_k U^{\varepsilon_k - 1} < 0$, $g_1''(U) = \sum_{k=1}^{n} \mathscr{R}_{0,k} p_k \varepsilon_k (1 - \varepsilon_k) U^{\varepsilon_k - 1} > 0$, $g_2'(U) = -\langle \varepsilon \rangle / U < 0$, and $g_2''(U) = \langle \varepsilon \rangle / U^2 > 0$. There exists unique root of $\mathscr{F}(U) = 0$ for $U \in (0, 1]$ because $g_1(U)$ and $g_2(U)$ are both convex curve. In addition, $\mathscr{F}(U) = 0$ has an unique root $U = 1$ if the following condition holds:

$$g_1'(1) \geq g_2'(1). \tag{177}$$

The condition (177) is equivalent to

$$\mathscr{R}_0 \leq 1.$$

Hence Lemma 4.9 is proved. Similarly, $\mathscr{F}(U) = 0$ has an unique root in $(0, 1)$ if the following condition holds:

$$g_1'(1) < g_2'(1). \tag{178}$$

The condition (178) is equivalent to

$$\mathscr{R}_0 > 1.$$

Next, let us prove U^* is the unique root of equation $\mathscr{F}(U) = 0$ for $\mathscr{R}_0 > 1$. From (152), we can find that there exists U_c for $\mathscr{R}_0 > 1$, where $U_\infty < U_c < 1$, and

$$F'(U_c) = \frac{1}{U_c} \left\{ \langle \varepsilon \rangle - \sum_{k=1}^{n} \mathscr{R}_{0,k} \varepsilon_k u_k(0) U_c^{\varepsilon_k} \right\} = 0.$$

Then, take the limit $u_k(0) \to p_k$, we can derive

$$\mathscr{F}'(U_c) = \frac{1}{U_c} \left\{ \langle \varepsilon \rangle - \sum_{k=1}^{n} \mathscr{R}_{0,k} \varepsilon_k p_k U_c^{\varepsilon_k} \right\} < 0.$$

Since $F'(1) = \langle \varepsilon \rangle - \sum_{k=1}^{n} \mathscr{R}_{0,k} \varepsilon_k u_k(0) < 0$ for $\mathscr{R}_0 > 1$, we can derive $\mathscr{F}'(1) = \langle \varepsilon \rangle - \sum_{k=1}^{n} \mathscr{R}_{0,k} \varepsilon_k p_k < 0$. It is easy to find that $\mathscr{F}'(1) < \mathscr{F}'(U_c)$. There exists $U_c^* < U_c < 1$, where $\mathscr{F}'(U_c^*) = 0$. Thus, when take the limit $u_k(0) \to p_k$, we can derive that $U_\infty \to U^* \in (0, 1)$.

APPENDIX 4.A.9: PROOF OF LEMMA 4.10

Suppose the initial condition for system (142) is given by $v_\ell(0) = v_0 > 0$, and $v_k(0) = 0$ for any $k \neq \ell$. We can get

$$V(0) = \sum_{i=1}^{n} v_i(0) = v_0, \qquad \sum_{k=1}^{n} \mathscr{R}_{0,k} v_k(0) = \mathscr{R}_{0,\ell} v_0.$$

At $\tau = 0$, we can get

$$\begin{aligned}
\left.\frac{dV(\tau)}{d\tau}\right|_{\tau=0} &= \sum_{i=1}^{n} u_i(0)\frac{\varepsilon_i}{\langle\varepsilon\rangle}\sum_{k=1}^{n}\mathscr{R}_{0,k}v_k(0) - V(0); \\
&= \mathscr{R}_{0,\ell}v_0\sum_{i=1}^{n} u_i(0)\frac{\varepsilon_i}{\langle\varepsilon\rangle} - v_0 \\
&= \left\{\mathscr{R}_{0,\ell}\left(\sum_{i=1,i\neq\ell}^{n} u_i(0)\frac{\varepsilon_i}{\langle\varepsilon\rangle} + u_\ell(0)\frac{\varepsilon_\ell}{\langle\varepsilon\rangle}\right) - 1\right\}v_0 \\
&= \left\{\mathscr{R}_{0,\ell}\left(\sum_{i=1,i\neq\ell}^{n} p_i\frac{\varepsilon_i}{\langle\varepsilon\rangle} + (p_\ell - v_0)\frac{\varepsilon_\ell}{\langle\varepsilon\rangle}\right) - 1\right\}v_0 \\
&= \left\{\mathscr{R}_{0,\ell}\left(\sum_{i=1}^{n} p_i\frac{\varepsilon_i}{\langle\varepsilon\rangle} - v_0\frac{\varepsilon_\ell}{\langle\varepsilon\rangle}\right) - 1\right\}v_0 \\
&= \left\{\mathscr{R}_{0,\ell}\left(1 - v_0\frac{\varepsilon_\ell}{\langle\varepsilon\rangle}\right) - 1\right\}v_0.
\end{aligned}$$

Since $\langle\varepsilon\rangle > p_\ell\varepsilon_\ell > v_0\varepsilon_\ell$, it is easy to obtain $1 - v_0\varepsilon_\ell/\langle\varepsilon\rangle > 0$. With $v_0 > 0$, the sign of $dV(\tau)/d\tau|_{\tau=0}$ depends on the sign of $\mathscr{R}_{0,\ell}\left(1 - v_0\varepsilon_\ell/\langle\varepsilon\rangle\right) - 1$. Then, we can get $dV(\tau)/d\tau|_{\tau=0} < 0$ if the following condition satisfied:

$$\mathscr{R}_{0,\ell}\left(1 - v_0\frac{\varepsilon_\ell}{\langle\varepsilon\rangle}\right) - 1 < 0.$$

By simplification, we can get

$$\langle\varepsilon\rangle(\mathscr{R}_{0,\ell} - 1) < \mathscr{R}_{0,\ell}v_0\varepsilon_\ell.$$

When $\mathscr{R}_{0,\ell} \leq 1$, the above inequality holds, indicating that V initially decreases. Since $\mathscr{R}_{0,1} > \cdots > \mathscr{R}_{0,n}$, we can get that V initially decreases if $\mathscr{R}_{0,1} \leq 1$. Similarly, $dV(\tau)/d\tau|_{\tau=0} > 0$ if

$$\langle\varepsilon\rangle(\mathscr{R}_{0,\ell} - 1) > \mathscr{R}_{0,\ell}v_0\varepsilon_\ell.$$

Then, let us consider the situation that

$$\left.\frac{dV(\tau)}{d\tau}\right|_{\tau=0} = 0,$$

meaning that

$$\mathscr{R}_{0,\ell} = \frac{\langle\varepsilon\rangle}{\langle\varepsilon\rangle - v_0\varepsilon_\ell}. \tag{179}$$

During a very short time interval $\Delta\tau$, we obtain

$$V(\Delta\tau) - V(0) = \left.\frac{dV(\tau)}{d\tau}\right|_{\tau=0}\Delta\tau + \frac{1}{2}\left.\frac{d^2V(\tau)}{d\tau^2}\right|_{\tau=0}(\Delta\tau)^2 + o((\Delta\tau)^2).$$

To determine the sign of $d^2V(\tau)/d\tau^2\big|_{\tau=0}$, the following calculation is required:

$$\left.\frac{dv_i(\tau)}{d\tau}\right|_{\tau=0} = \begin{cases} p_i\dfrac{\varepsilon_i}{\langle\varepsilon\rangle}\mathscr{R}_{0,\ell}v_0, & \text{for } i \neq \ell; \\ (p_\ell - v_0)\dfrac{\varepsilon_\ell}{\langle\varepsilon\rangle}\mathscr{R}_{0,\ell}v_0 - v_0, & \text{for } i = \ell. \end{cases}$$

$$\left.\frac{d^2 v_i(\tau)}{d\tau^2}\right|_{\tau=0} = \begin{cases} p_i \dfrac{\varepsilon_i}{\langle\varepsilon\rangle}\mathscr{R}_{0,\ell} v_0 \Bigg\{ -\dfrac{\varepsilon_i}{\langle\varepsilon\rangle}\mathscr{R}_{0,\ell} v_0 - \dfrac{\varepsilon_\ell}{\langle\varepsilon\rangle}\mathscr{R}_{0,\ell} v_0 \\ \qquad\qquad + \displaystyle\sum_{k=1}^{n} \mathscr{R}_{0,k} p_k \frac{\varepsilon_k}{\langle\varepsilon\rangle} - 2 \Bigg\}, & \text{for } i \neq \ell; \\ (p_\ell - v_0)\dfrac{\varepsilon_\ell}{\langle\varepsilon\rangle}\mathscr{R}_{0,\ell} v_0 \Bigg\{ -2\dfrac{\varepsilon_\ell}{\langle\varepsilon\rangle}\mathscr{R}_{0,\ell} v_0 \\ \qquad\qquad + \displaystyle\sum_{k=1}^{n} \mathscr{R}_{0,k} p_k \frac{\varepsilon_k}{\langle\varepsilon\rangle} - 2 \Bigg\} + v_\ell, & \text{for } i = \ell. \end{cases}$$

Then, we can get

$$\begin{aligned} \left.\frac{d^2 V(\tau)}{d\tau^2}\right|_{\tau=0} &= \sum_{i=1}^{n} \left.\frac{d^2 v_i(\tau)}{d\tau^2}\right|_{\tau=0} \\ &= \sum_{i=1, i\neq\ell}^{n} p_i \frac{\varepsilon_i}{\langle\varepsilon\rangle}\mathscr{R}_{0,\ell} v_0 \left\{ -\frac{\varepsilon_i}{\langle\varepsilon\rangle}\mathscr{R}_{0,\ell} v_0 - \frac{\varepsilon_\ell}{\langle\varepsilon\rangle}\mathscr{R}_{0,\ell} v_0 + \sum_{k=1}^{n} \mathscr{R}_{0,k} p_k \frac{\varepsilon_k}{\langle\varepsilon\rangle} - 2 \right\} \\ &\quad + (p_\ell - v_0)\frac{\varepsilon_\ell}{\langle\varepsilon\rangle}\mathscr{R}_{0,\ell} v_0 \left\{ -2\frac{\varepsilon_\ell}{\langle\varepsilon\rangle}\mathscr{R}_{0,\ell} v_0 + \sum_{k=1}^{n} \mathscr{R}_{0,k} p_k \frac{\varepsilon_k}{\langle\varepsilon\rangle} - 2 \right\} + v_\ell \\ &= \left\{ \sum_{i=1}^{n} -p_i \frac{\varepsilon_i}{\langle\varepsilon\rangle}\frac{\varepsilon_i}{\langle\varepsilon\rangle} + 2v_0 \frac{\varepsilon_\ell}{\langle\varepsilon\rangle}\frac{\varepsilon_\ell}{\langle\varepsilon\rangle} - \sum_{i=1}^{n} p_i \frac{\varepsilon_i}{\langle\varepsilon\rangle}\frac{\varepsilon_\ell}{\langle\varepsilon\rangle} \right\} (\mathscr{R}_{0,\ell} v_0)^2 \\ &\quad + \left\{ \sum_{i=1}^{n} p_i \frac{\varepsilon_i}{\langle\varepsilon\rangle} - v_0 \frac{\varepsilon_\ell}{\langle\varepsilon\rangle} \right\} \sum_{i=1}^{n} \mathscr{R}_{0,k} p_k \frac{\varepsilon_k}{\langle\varepsilon\rangle}\mathscr{R}_{0,\ell} v_0 \\ &\quad + 2\left\{ -\sum_{i=1}^{n} pi \frac{\varepsilon_i}{\langle\varepsilon\rangle} + v_0 \frac{\varepsilon_\ell}{\langle\varepsilon\rangle} \right\} \mathscr{R}_{0,\ell} v_0 + v_0 \\ &= \left\{ \sum_{i=1}^{n} -p_i \frac{\varepsilon_i}{\langle\varepsilon\rangle}\frac{\varepsilon_i}{\langle\varepsilon\rangle} + 2v_0 \frac{\varepsilon_\ell}{\langle\varepsilon\rangle}\frac{\varepsilon_\ell}{\langle\varepsilon\rangle} - \frac{\varepsilon_\ell}{\langle\varepsilon\rangle} \right\} (\mathscr{R}_{0,\ell} v_0)^2 \\ &\quad + \left\{ 1 - v_0 \frac{\varepsilon_\ell}{\langle\varepsilon\rangle} \right\} \left\{ \sum_{i=1}^{n} \mathscr{R}_{0,k} p_k \frac{\varepsilon_k}{\langle\varepsilon\rangle} - 2 \right\} \mathscr{R}_{0,\ell} v_0 + v_0. \end{aligned} \tag{180}$$

By making use of the equality (179) into (180), we can obtain

$$\left.\frac{d^2 V(\tau)}{d\tau^2}\right|_{\tau=0} = M_1 v_0^3 + M_2 v_0^2 + M_3 v_0, \tag{181}$$

where

$$\begin{aligned} M_1 &= \left(\frac{\varepsilon_\ell}{\langle\varepsilon\rangle}\mathscr{R}_{0,\ell} \right)^2; \\ M_2 &= -\sum_{i=1}^{n} p_i \frac{\varepsilon_i}{\langle\varepsilon\rangle}\frac{\varepsilon_i}{\langle\varepsilon\rangle}\mathscr{R}_{0,\ell}^2 - \frac{\varepsilon_\ell}{\langle\varepsilon\rangle}\mathscr{R}_{0,\ell}; \\ M_3 &= \sum_{k=1}^{n} \mathscr{R}_{0,k} p_k \frac{\varepsilon_k}{\langle\varepsilon\rangle} - 1. \end{aligned}$$

Since v_0 is sufficiently small, the sign of equation (181) is governed by the sign of M_3 when $M_3 \neq 0$. From (143), we can get

$$M_3 = \sum_{k=1}^{n} \frac{\gamma_k \langle\varepsilon\rangle \beta N}{\rho} p_k \frac{\varepsilon_k}{\langle\varepsilon\rangle} - 1 = \sum_{k=1}^{n} \frac{\gamma_k \varepsilon_k p_k \beta N}{\rho} - 1 = \frac{\langle\varepsilon\gamma\rangle \beta N}{\rho} - 1 = \mathscr{R}_0 - 1.$$

Then, $d^2V(\tau)/d\tau^2|_{\tau=0} > 0$ if $\mathscr{R}_0 > 1$, $d^2V(\tau)/d\tau^2|_{\tau=0} < 0$ if $\mathscr{R}_0 < 1$. When $\mathscr{R}_0 = 1$, the sign of $d^2V(\tau)/d\tau^2|_{\tau=0}$ is determined by M_2, which is negative. Hence when $dV(\tau)/d\tau|_{\tau=0} = 0$, V initially decreases if $\mathscr{R}_0 \leq 1$ and initially increases if $\mathscr{R}_0 > 1$.

APPENDIX 4.A.10: PROOF OF LEMMA 4.11

Suppose the initial condition for system (142) is given by $v_\ell(0) = v_0 > 0$, and $v_k(0) = 0$ for any $k \neq \ell$. We can get

$$\begin{aligned}\frac{dV(\tau)}{d\tau} &= \sum_{i=1}^{n} u_i(\tau)\frac{\varepsilon_i}{\langle\varepsilon\rangle}\sum_{k=1}^{n}\mathscr{R}_{0,k}v_k(\tau) - V(\tau)\\ &< \sum_{i=1}^{n} p_i\frac{\varepsilon_i}{\langle\varepsilon\rangle}\sum_{k=1}^{n}\mathscr{R}_{0,k}v_k(\tau) - V(\tau) = \sum_{k=1}^{n}\mathscr{R}_{0,k}v_k(\tau) - V(\tau). \quad (182)\end{aligned}$$

Since $\mathscr{R}_{0,1} > \mathscr{R}_{0,i}$ holds for $i \neq 1$, we can get when $\mathscr{R}_{0,1} \leq 1$,

$$\sum_{k=1}^{n}\mathscr{R}_{0,k}v_k(\tau) - V(\tau) < 0.$$

Therefore, if $\mathscr{R}_{0,1} \leq 1$, $\dfrac{dV(\tau)}{d\tau} < 0$ for any τ.

APPENDIX 4.A.11: DERIVATION OF THEOREM 4.2 AND 4.3

First, from the definition of system basic reproduction number (147) and (162), we can easily derive

$$\tilde{\mathscr{R}}_0 = \frac{\langle\tilde{\varepsilon\gamma}\rangle\beta N}{\rho} = \frac{\langle\varepsilon\gamma\rangle\beta N}{\rho} + \frac{\beta N}{\rho}\Delta(\varepsilon\gamma)\delta p = \mathscr{R}_0 + \frac{\mathscr{R}_0}{\langle\varepsilon\gamma\rangle}\Delta(\varepsilon\gamma)\delta p.$$

Theorem 4.2 is proved. From (154), we can get

$$\delta W_\infty = -\sum_{i=1}^{n}\delta u_i.$$

Assume $\delta u_i = A_i\delta p$ for $\forall i$, we have

$$\delta W_\infty = -\sum_{i=1}^{n} A_i\delta p.$$

From (151), $\tilde{U}_\infty$ is defined by

$$\tilde{U}_\infty := \left(\frac{\tilde{u}_i^\infty}{u_i(0)}\right)^{1/\varepsilon_i} = \left(\frac{\tilde{u}_{\ell-1}^\infty}{\tilde{u}_{\ell-1}(0)}\right)^{1/\varepsilon_{\ell-1}} = \left(\frac{\tilde{u}_\ell^\infty}{\tilde{u}_\ell(0)}\right)^{1/\varepsilon_\ell} = \left(\frac{\tilde{u}_{\ell+1}^\infty}{\tilde{u}_{\ell+1}(0)}\right)^{1/\varepsilon_{\ell+1}} \quad (183)$$

for $\forall i \neq \ell-1, \ell, \ell+1$. Then we can denote

$$\tilde{U}_\infty = U_\infty + \delta U_\infty.$$

From (152), let us define

$$\begin{aligned}\tilde{F}(\tilde{U}) := \log\tilde{U}^{\langle\tilde{\varepsilon}\rangle} &+ \sum_{k=1,\neq\ell-1,\ell,\ell+1}^{n}\tilde{\mathscr{R}}_{0,k}\left\{p_k - u_k(0)\tilde{U}^{\varepsilon_k}\right\}\\ &+ \sum_{k=\ell-1}^{\ell+1}\tilde{\mathscr{R}}_{0,k}\left\{\tilde{p}_k - \tilde{u}_k(0)\tilde{U}^{\varepsilon_k}\right\}.\end{aligned}$$

From Lemma 4.6, we can get $\tilde{U}_\infty$ is the unique root of $\tilde{F}(\tilde{U}) = 0$ in $(0, 1)$. By using Taylor expansion for (183), we can get

$$\delta U_\infty = N_i M_i \delta p \tag{184}$$

for $i \neq \ell - 1, \ell, \ell + 1$, where $N_i = U_\infty/(\varepsilon_i u_i(0))$, $M_i = A_i/U_\infty^{\varepsilon_i}$. For $i = \ell - 1, \ell, \ell + 1$, we can get

$$\delta U_\infty = \begin{cases} N_{\ell-1}\left(M_{\ell-1} - \alpha\dfrac{u_\ell(0)}{p_\ell}\right)\delta p; \\ N_\ell\left(M_\ell + \dfrac{u_\ell(0)}{p_\ell}\right)\delta p; \\ N_{\ell+1}\left(M_{\ell+1} - (1-\alpha)\dfrac{u_\ell(0)}{p_\ell}\right)\delta p. \end{cases}$$

Making use of Taylor expansion for the equation $\tilde{F}(\tilde{U}_\infty) = 0$, we can get

$$\begin{aligned} \tilde{F}(\tilde{U}_\infty) = \left(1 + \frac{\Delta\varepsilon}{\langle\varepsilon\rangle}\delta p\right)\Bigg\{ & F(U_\infty) + F'(U_\infty)\delta U_\infty \\ & + \alpha\mathscr{R}_{0,\ell-1}\left(1 - \frac{u_\ell(0)}{p_\ell}U_\infty^{\varepsilon_{\ell-1}}\right)\delta p \\ & - \mathscr{R}_{0,\ell}\left(1 - \frac{u_\ell(0)}{p_\ell}U_\infty^{\varepsilon_\ell}\right)\delta p \\ & + (1-\alpha)\mathscr{R}_{0,\ell+1}\left(1 - \frac{u_\ell(0)}{p_\ell}U_\infty^{\varepsilon_{\ell+1}}\right)\delta p\Bigg\} = 0. \end{aligned} \tag{185}$$

Since $F(U_\infty) = 0$, from (184) and (185), we can get

$$\begin{aligned} M_\ell + \frac{u_\ell(0)}{p_\ell} = \frac{1}{F'(U_\infty)N_\ell}\Bigg\{ & -\alpha\mathscr{R}_{0,\ell-1}\left(1 - \frac{u_\ell(0)}{p_\ell}U_\infty^{\varepsilon_{\ell-1}}\right) \\ & + \mathscr{R}_{0,\ell}\left(1 - \frac{u_\ell(0)}{p_\ell}U_\infty^{\varepsilon_\ell}\right) \\ & - \mathscr{R}_{0,\ell+1}(1-\alpha)\left(1 - \frac{u_\ell(0)}{p_\ell}U_\infty^{\varepsilon_{\ell+1}}\right)\Bigg\}. \end{aligned}$$

Then we have

$$\begin{aligned} \delta W_\infty =& -\sum_{i=1}^n A_i\delta p \\ =& -\sum_{k=1}^n\left\{\frac{N_\ell}{N_k}\left(M_\ell + \frac{u_\ell(0)}{p_\ell}\right)\right\} + \frac{u_\ell(0)}{p_\ell}\left\{U_\infty^{\varepsilon_\ell} - \alpha U_\infty^{\varepsilon_{\ell-1}} - (1-\alpha)U_\infty^{\varepsilon_{\ell+1}}\right\} \\ =& \frac{D\delta p}{F'(U_\infty)U_\infty}\left\{D_1(\mathscr{R}_{0,k},\alpha) - \frac{u_\ell(0)}{p_\ell}D_2(\mathscr{R}_{0,k},\alpha,U_\infty)\right\} \\ & - \frac{u_\ell(0)}{p_\ell}D_3(\alpha,U_\infty)\delta p, \end{aligned}$$

where

$$\begin{aligned} D &= \sum_{k=1}^{n} \varepsilon_k u_k(0) U_\infty^{\varepsilon_k}, \\ D_1(\mathscr{R}_{0,k}, \alpha) &= \alpha(\mathscr{R}_{0,\ell-1} - \mathscr{R}_{0,\ell}) - (1-\alpha)(\mathscr{R}_{0,\ell} - \mathscr{R}_{0,\ell+1}), \\ D_2(\mathscr{R}_{0,k}, \alpha, U_\infty) &= \alpha \left\{ \mathscr{R}_{0,\ell-1} U_\infty^{\varepsilon_{\ell-1}} - \mathscr{R}_{0,\ell} U_\infty^{\varepsilon_\ell} \right\} - (1-\alpha) \left\{ \mathscr{R}_{0,\ell} U_\infty^{\varepsilon_\ell} - \mathscr{R}_{0,\ell+1} U_\infty^{\varepsilon_{\ell+1}} \right\}, \\ D_3(\alpha, U_\infty) &= \alpha \left\{ U_\infty^{\varepsilon_{\ell-1}} - U_\infty^{\varepsilon_\ell} \right\} - (1-\alpha) \left\{ U_\infty^{\varepsilon_\ell} - U_\infty^{\varepsilon_{\ell+1}} \right\}. \end{aligned}$$

APPENDIX 4.A.12: DERIVATION OF q_c, θ_c, AND $\mathscr{R}_c^{\sup}$

From Theorem 4.1 and equation (164), the condition $\mathscr{R}_0 = 1$ represents the threshold at which $W^* = 0$, and it can be rewritten as

$$\mathscr{R}_0^{\sup} \frac{1}{\theta} \frac{\{1 - q(1-\theta)\}^n - (1-q)^n}{1 - (1-q)^n} = 1.$$

Let us define

$$f(\theta, q, \mathscr{R}_0^{\sup}) = \mathscr{R}_0^{\sup} \frac{1}{\theta} \frac{\{1 - q(1-\theta)\}^n - (1-q)^n}{1 - (1-q)^n}.$$

Then, making use of Taylor expansion at $\theta = 0$ for $f(\theta, q)$, we derive

$$\begin{aligned} f(\theta, q, \mathscr{R}_0^{\sup})\big|_{\theta \to 0+} &= \mathscr{R}_0^{\sup} \frac{1}{\theta} \frac{(1-q)^n + \theta n q (1-q)^{n-1} - (1-q)^n}{1 - (1-q)^n} \\ &= \mathscr{R}_0^{\sup} \frac{nq(1-q)^{n-1}}{1 - (1-q)^n}. \end{aligned}$$

Then, given $\mathscr{R}_0^{\sup}$, the critical value q_c can be determined as the root of

$$\sum_{k=1}^{n} {}_n\mathrm{C}_k (-1)^k q_c^k \left\{ (1-\theta)^k + (1 - \frac{\theta}{\mathscr{R}^{\sup}}) \right\} = 0. \tag{186}$$

Similarly, given q, the critical value $\mathscr{R}_c^{\sup}$ is given by

$$\mathscr{R}_c^{\sup} = \frac{1 - (1-q)^n}{nq(1-q)^{n-1}}.$$

Next, consider the case of $q \to 1$, we can get

$$f(\theta, q, \mathscr{R}_0^{\sup})\big|_{q=1} = \mathscr{R}_0^{\sup} \theta^{n-1},$$

the critical value θ_c is given by

$$\theta_c = \left(\mathscr{R}_0^{\sup}\right)^{-1/(n-1)}. \tag{187}$$

APPENDIX 4.A.13: DERIVATION OF CONDITIONS FOR $W^* = 0$

From Theorem 4.1 and equation (164) , we can derive that $W^* = 0$ if

$$\mathscr{R}_0 = p\mathscr{R}_0^{\max} + (1-p)\mathscr{R}_0^{\min} < 1. \tag{188}$$

We can solve the inequality (188) and derive:

$$p < \frac{1 - \mathscr{R}_0^{\min}}{\mathscr{R}_0^{\max} - \mathscr{R}_0^{\min}}, \tag{189}$$

From the definition, $\mathscr{R}_0^{\max} > \mathscr{R}_0^{\min}$. If $\mathscr{R}_0^{\min} > 1$, the right hand side of (189) is negative, and $W^* > 0$ for any p in $(0,1)$. If $\mathscr{R}_0^{\max} < 1$, (189) holds for any p in $(0,1)$. If $\mathscr{R}_0^{\min} < 1 < \mathscr{R}_0^{\max}$, we can find the critical value q_c satisfied

$$p_c = \frac{1 - \mathscr{R}_0^{\min}}{\mathscr{R}_0^{\max} - \mathscr{R}_0^{\min}},$$

and shown in Subsection 4.8.2.

APPENDIX 4.A.14: PROOF OF LEMMA 4.12 AND 4.13

Let us suppose that $x_{\mathrm{B}}^* < x_{\mathrm{A}}^*$. From the feature of $\widetilde{\Psi}(x,p)$ and the definition of x_{A}^*, we have $\widetilde{\Psi}(x_{\mathrm{A}}^*, p_{\mathrm{A}}) = 0$, $\widetilde{\Psi}(x, p_{\mathrm{A}}) < 0$ for $x \in (0, x_{\mathrm{A}}^*)$, and $\widetilde{\Psi}(x, p_{\mathrm{A}}) > 0$ for $x \in (x_{\mathrm{A}}^*, 1)$. Hence, it holds that $\widetilde{\Psi}(x_{\mathrm{B}}^*, p_{\mathrm{A}}) < 0$, that is,

$$\left\{p_{\mathrm{A}} + (1-p_{\mathrm{A}})b^2\right\} \log x_{\mathrm{B}}^* + \mathscr{R}_0 \left\{p_{\mathrm{A}}(1 - x_{\mathrm{B}}^*) + (1-p_{\mathrm{A}})b\{1 - (x_{\mathrm{B}}^*)^b\}\right\} < 0. \tag{190}$$

On the other hand, from the definition of x_{B}^*, we have $\widetilde{\Psi}(x_{\mathrm{B}}^*, p_{\mathrm{B}}) = 0$, that is,

$$\left\{p_{\mathrm{B}} + (1-p_{\mathrm{B}})b^2\right\} \log x_{\mathrm{B}}^* + \mathscr{R}_0 \left\{p_{\mathrm{B}}(1 - x_{\mathrm{B}}^*) + (1-p_{\mathrm{B}})b\{1 - (x_{\mathrm{B}}^*)^b\}\right\} = 0.$$

This equation leads to

$$\frac{1}{\mathscr{R}_0} \log x_{\mathrm{B}}^* = -\frac{p_{\mathrm{B}}(1 - x_{\mathrm{B}}^*) + (1-p_{\mathrm{B}})b\{1 - (x_{\mathrm{B}}^*)^b\}}{p_{\mathrm{B}} + (1-p_{\mathrm{B}})b^2}. \tag{191}$$

Substituting equation (191) for inequality (190), we have

$$(p_{\mathrm{A}} - p_{\mathrm{B}})[b(1 - x_{\mathrm{B}}^*) - \{1 - (x_{\mathrm{B}}^*)^b\}] < 0. \tag{192}$$

Since $b(1-x) - (1-x^b) < 0$ for $x \in (0,1)$ and $b \in (0,1)$, the inequality (192) holds if and only if $p_{\mathrm{B}} < p_{\mathrm{A}}$. Consequently, $x_{\mathrm{B}}^* < x_{\mathrm{A}}^*$ only if $p_{\mathrm{B}} < p_{\mathrm{A}}$. In the same way, we can demonstrate that $x_{\mathrm{B}}^* > x_{\mathrm{A}}^*$ only if $p_{\mathrm{B}} > p_{\mathrm{A}}$. Furthermore, we can prove that $x_{\mathrm{B}}^* = x_{\mathrm{A}}^*$ only if $p_{\mathrm{B}} = p_{\mathrm{A}}$. We can easily find that the inverses of these propositions are true.

On the other hand, from equation (168), we note that $r_0\omega^2 = 1$ if and only if $p_{\mathrm{B}} = p_{\mathrm{A}}$, while $r_0\omega^2 > 1$ if and only if $p_{\mathrm{B}} < p_{\mathrm{A}}$. Therefore, Lemma 4.12 and 4.13 have been proved.

5

CONCLUDING REMARKS

In this dissertation, we aimed to investigate how structural factors associated with social vulnerability influence epidemic consequence and the effectiveness of public health measures. Social vulnerability refers to the limited resilience of certain populations when facing disasters, including the outbreak of transmissible diseases, and is influenced by medical access, population distribution, cultural differences, and other societal constraints[122]. Understanding these factors is crucial since they determine whether an epidemic can be effectively controlled and how severe the social damage will be after the pandemic.

To address this question, we developed mathematical models to investigate the roles of mobility restrictions, limitations in isolation capacity, and behavioral heterogeneity in shaping epidemic consequences. Our purpose was to provide theoretical insights to help design equitable and adaptive strategies for epidemic control.

In Chapter 2, we investigated the impact of regional lockdown policies on the epidemic consequence. The purpose of this analysis was to determine which type of mobility restriction policy minimizes epidemic size. The model considers a community composed of two regions with different healthcare conditions. Our findings revealed that both complete and strong lockdowns lead to the same and smaller endemic sizes compared to the weak lockdown, which indicates that strong lockdown without additional restrictions on hospital use could be more favorable in terms of maintaining economic activity. Moreover, we compared two types of the weak lockdown, and found that those permitting restricted movement from high to low density areas were the most effective in suppressing disease spread. Interestingly, when the isolation period in the central region is sufficiently longer than in the peripheral area, the number of free infectives under a strong lockdown may be even lower than under a complete lockdown. These results underscore the importance of considering both population distribution and healthcare conditions when considering the effective mobility restriction policies.

In Chapter 3, we investigated the influence of limited isolation capacity on epidemic dynamics. We considered three situations based on assumptions: non-reinfectious diseases, reinfectious diseases, and reinfectious diseases with discharge mechanisms incorporated into the isolation strategy. Our results revealed that a larger isolation capacity could enhance the feasibility of effective quarantine management as a controllable public health measure to minimize the social damage caused by disease transmission. When the isolation strategy breaks down due to limited capacity, it may lead to unexpectedly severe epidemic consequences, such as the revival of outbreak in the case of reinfectious diseases, or bistability when discharge mechanisms are considered. In particular, a sufficiently large isolation capacity is required to avoid severe consequences of the epidemic dynamics with a reinfectious disease since recovered individuals may become susceptible again and contribute to further transmission. Furthermore, a higher discharge rate and a lower quarantine rate make it more feasible to maintain sufficient isolation capacity, as they reduce the occupancy level and help avoid saturation. Naturally the quarantine/isolation could not be necessarily the principal factor

for the public health policy against the spread of an infectious disease, while it must be important and could have a significant contribution to the suppression of the epidemic size, accompanied with the other measures against the epidemic. These findings emphasize the importance of maintaining adequate public health infrastructure as indicated by Unruh *et al.*[160] on the social response to the COVID-19 pandemic. However, such infrastructure requires sufficient social investment, which implies that the management of effective quarantine policies may bring substantial challenges in controlling the spread of an infectious disease within a community.

In Chapter 4, we proposed a structured SIR model to analyze the impact of behavioral heterogeneity on epidemic dynamics. The purpose of this analysis was to clarify how differences in preventive behaviors across groups affect the final epidemic size. Our findings revealed that the final epidemic size strongly depends on the distribution of caution level among individuals in the community. In particular, the larger proportion of low cautious individuals in the community not only accelerates the spread of a transmissible disease in the early stage but also contributes to the greater final epidemic size, thereby resulting in more severe social damage. Our findings also emphasize the importance of public health efforts, such as health education in schools and awareness programs in the community, which aim to encourage the adoption of preventive practices, including hand hygiene, mask-wearing, and vaccination.

Through the studies conducted by these chapters, we obtained a deeper understanding of the complex phenomena associated with differences in mobility structure, limitations in medical resources, and heterogeneity in social structure. These factors significantly influence not only the dynamics of disease transmission but also the feasibility and effectiveness of public health interventions.

This dissertation underscores the necessity of incorporating social vulnerability into the design of equitable and adaptive public health strategies. The findings suggest that public health measures must be evaluated not only by the effectiveness in reducing disease transmission but also by taking into account structural diversity and societal constraints. In particular, a balanced strategy is required. Short-term measures such as lockdowns and quarantines should be combined with long-term structural interventions, including education programs to improve individual caution levels. In addition, preparing satisfactory public health infrastructure in advance requires substantial social investment, and establishing well-functioning epidemic monitoring systems that can adjust measures in time remains a major challenge. Moreover, enhancing people's awareness of infectious disease risks could reduce social vulnerability and increase the effectiveness of other interventions. By presenting mathematical models for the epidemics, this dissertation aims to provide theoretical insights for designing satisfactory public strategies in the face of epidemics in the future.

[1] Abdelrazec A., Bélair J., Shan C., and Zhu H., (2016) Modeling the spread and control of dengue with limited public health resources, *Mathematical Biosciences* 271: 136–145.

[2] Acemoglu D., Chernozhukov V., Werning I., and Whinston M. D., (2021) Optimal targeted lockdowns in a multigroup SIR model, *American Economic Review: Insights* 3 (4): 487–502.

[3] Agusto F. B., (2017) Mathematical model of Ebola transmission dynamics with relapse and reinfection, *Mathematical Biosciences* 283: 48–59.

[4] Ahmad I. and Seno H., (2023) An epidemic dynamics model with limited isolation capacity, *Theory Biosci.* 142: 259–273.

[5] Aleta A., Martín-Corral D., Pastore y Piontti A., et al., (2020) Modelling the impact of testing, contact tracing and household quarantine on second waves of COVID-19, *Nature Human Behaviour* 4: 964–971.

[6] Alfano V. and Ercolano S., (2020) The efficacy of lockdown against COVID-19: a cross-country panel analysis, *Applied Health Economics and Health Policy* 18 (4): 509–517.

[7] Almeida L., Bliman P. A., Nadin G., Perthame B., and Vauchelet N., (2021) Final size and convergence rate for an epidemic in heterogeneous populations, *Mathematical Models and Methods in Applied Sciences* 31 (5): 1021–1051.

[8] Althouse B. M., Wenger E. A., Miller J. C., Scarpino S. V., Allard A., Hébert-Dufresne L., and Hu H., (2020) Superspreading events in the transmission dynamics of SARS-CoV-2: Opportunities for interventions and control, *PLoS Biology* 18 (11): e3000897.

[9] Amador J. and Gómez-Corral A., (2020) A stochastic epidemic model with two quarantine states and limited carrying capacity for quarantine, *Physica A: Statistical Mechanics and its Applications* 544: 121899.

[10] Anderson R. M., Fraser C., Ghani A. C., Donnelly C. A., Riley S., Ferguson N. M., *et al.*, (2004) Epidemiology, transmission dynamics and control of SARS: the 2002–2003 epidemic, *Philosophical Transactions of the Royal Society of London. Series B: Biological Sciences* 359 (1447): 1091–1105.

[11] Antali M. and Stepan G., (2018) Sliding and crossing dynamics in extended Filippov systems, *SIAM Journal on Applied Dynamical Systems* 17: 823–858.

[12] Baker M. G., Durrheim D., Hsu L. Y., and Wilson N., (2023) COVID-19 and other pandemics require a coherent response strategy, *The Lancet* 401 (10373): 265–266.

[13] Bambra C., Riordan R., Ford J., and Matthews F., (2020) The COVID-19 pandemic and health inequalities, *Journal of Epidemiology and Community Health* 74 (11): 964–968.

[14] Bell D., Nicoll A., Fukuda K., and others, (2006) Non-pharmaceutical interventions for pandemic influenza: national and community measures, *Emerging Infectious Diseases* 12 (1): 88–94.

[15] Belykh I., Kuske R., Porfiri M., and Simpson D. J., (2023) Beyond the Bristol book: advances and perspectives in non-smooth dynamics and applications, *Chaos: An Interdisciplinary Journal of Nonlinear Science* 33 (1): 010402.

[16] Benedictow O. J., (2004) The Black Death 1346–1353: The Complete History, *Boydell Press*.

[17] Bonaccorsi S. and Ottaviano S., (2016) Epidemics on networks with heterogeneous population and stochastic infection rates, *Mathematical Biosciences* 279: 43–52.

[18] Brauer F. and Castillo-Chavez C., (2012) Mathematical Models in Population Biology and Epidemiology, Second Edition, *Springer*, New York.

[19] Brauer F., van den Driessche P., and Wu J., (2008) Mathematical Epidemiology, *Springer*, Berlin, Heidelberg.

[20] Brauer F., Castillo-Chavez C., and Feng Z., (2019) Mathematical Models in Epidemiology, Springer, New York.

[21] Brauer F., (2008) Epidemic models with heterogeneous mixing and treatment, *Bulletin of Mathematical Biology* 70: 1869–1885.

[22] Brauer F., (2017) Mathematical epidemiology: past, present, and future, *Infectious Disease Modelling* 2 (2): 113–127.

[23] Britton T., Ball F., and Trapman P., (2020) A mathematical model reveals the influence of population heterogeneity on herd immunity to SARS-CoV-2, *Science* 369 (6505): 846–849.

[24] Brodeur A., Gray D., Islam A., and Bhuiyan S., (2021) A literature review of the economics of COVID–19, *Journal of Economic Surveys* 35 (4): 1007–1044.

[25] Brooks S. K., Webster R. K., Smith L. E., Woodland L., Wessely S., Greenberg N., and Rubin G. J., (2020) The psychological impact of quarantine and how to reduce it: rapid review of the evidence, *The Lancet* 395 (10227): 912–920.

[26] Buonomo B., (2020) Effects of information-dependent vaccination behavior on coronavirus outbreak: insights from a SIRI model, *Ricerche di Matematica* 69: 483–499.

[27] Cantor N. F., (2014) In the wake of the plague: The Black Death and the world it made, *Simon and Schuster*.

[28] Centre for Disease Control and Prevention (CDC), (2025) COVID-19, *CDC Official Website* (accessed on 30 April 2025).

[29] Chandra S., Kassens-Noor E., Kuljanin G., and Vertalka J., (2012) A geographic analysis of population density thresholds in the 1918 influenza pandemic in India, *International Journal of Health Geographics* 11: 7.

[30] Chang S., Pierson E., Koh P. W., et al., (2021) Mobility network models of COVID-19 explain inequities and inform reopening, *Nature* 589: 82–87.

[31] Chau S. W., Wong O. W., Ramakrishnan R., Chan S. S., Wong E. K., Li P. Y., *et al.*, (2021) History for some or lesson for all? A systematic review and meta-analysis on the immediate and long-term mental health impact of the 2002–2003 Severe Acute Respiratory Syndrome (SARS) outbreak, *BMC Public Health* 21 (1): 670.

[32] Cherry J. D. and Krogstad P., (2004) SARS: the first pandemic of the 21st century, *Pediatric Research* 56 (1): 1–5.

[33] Chowell D., Safan M., and Castillo-Chavez C., (2016) Modeling the case of early detection of Ebola virus disease, *Mathematical and Statistical Modeling for Emerging and Re-emerging Infectious Diseases* 57–70.

[34] Ciotti M., Ciccozzi M., Terrinoni A., Jiang W. C., Wang C. B., and Bernardini S., (2020) The COVID-19 pandemic, *Critical Reviews in Clinical Laboratory Sciences* 57 (6): 365–388.

[35] Coccia M., (2021) The relation between length of lockdown, numbers of infected people and deaths of COVID-19, and economic growth of countries: Lessons learned to cope with future pandemics similar to COVID-19 and to constrain the deterioration of economic system, *Sci. Total Environ.* 775: 145801.

[36] Cohn Jr, S. K., (2018) Epidemics: Hate and Compassion from the Plague of Athens to AIDS, Oxford University Press.

[37] Cutter S.L. and Finch C., (2003) Temporal and spatial changes in social vulnerability to natural hazards, *Proceedings of the National Academy of Sciences* 105 (7): 2301–2306.

[38] Davies J. R., Grilli E. A., and Smith A. J., (1984) Influenza A: infection and reinfection, *Epidemiology and Infection* 92 (1): 125–127.

[39] de Oliveira R.B., Rubio F.A., and Anderle R., (2022) Incorporating social determinants of health into the mathematical modeling of HIV/AIDS, *Scientific Reports* 12: 20541.

[40] Dechsupa S., Assawakosri S., Phakham S., and Honsawek S., (2020) Positive impact of lockdown on COVID-19 outbreak in Thailand, *Travel Medicine and Infectious Disease* 36: 101802.

[41] Deighton J., Lereya S. T., Casey P., Patalay P., Humphrey N., and Wolpert M., (2019) Prevalence of mental health problems in schools: poverty and other risk factors among 28 000 adolescents in England, *The British Journal of Psychiatry* 215 (3): 565–567.

[42] del Rio-Chanona R. M., Mealy P., Pichler A., Lafond F., and Farmer J. D., (2020) Supply and demand shocks in the COVID-19 pandemic: An industry and occupation perspective, *Oxford Review of Economic Policy* 36 (Supplement): S94–S137.

[43] Delamater P. L., Street E. J., Leslie T. F., Yang Y. T., and Jacobsen K. H., (2019) Complexity of the basic reproduction number (R_0), *Emerging Infectious Diseases* 25 (1): 1–4.

[44] Delardas O., Kechagias K. S., Pontikos P. N., and Giannos P., (2022) Socio-economic impacts and challenges of the coronavirus pandemic (COVID-19): an updated review, *Sustainability* 14 (15): 9699.

[45] di Bernardo M. and Hogan S. J., (2010) Discontinuity-induced bifurcations of piecewise smooth dynamical systems, *Philosophical Transactions of the Royal Society A* 368 (1930): 4915–4935.

[46] di Bernardo M., Budd C., Champneys A. R., and Kowalczyk P., (2008) Piecewise-smooth Dynamical Systems: Theory and Applications, Springer, London.

[47] Diekmann O., Heesterbeek H., and Britton T., (2013) Mathematical Tools for Understanding Infectious Disease Dynamics, Princeton Series in Theoretical and Computational Biology, Princeton University Press, Princeton.

[48] Dimarco G., Perthame B., Toscani G., et al., (2021) Kinetic models for epidemic dynamics with social heterogeneity, *Journal of Mathematical Biology* 83: 4.

[49] Dolbeault J. and Turinici G., (2020) Heterogeneous social interactions and the COVID-19 lockdown outcome in a multi-group SEIR model, *Mathematical Modelling of Natural Phenomena* 15 (36).

[50] Du Z., Wang C., Liu C., Bai Y., Pei S., Adam D. C., Wang L., Wu P., Lau E. H. Y., and Cowling B. J., (2022) Systematic review and meta-analyses of superspreading of SARS-CoV-2 infections, *Transboundary and Emerging Diseases* 69 (5): e3007–e3014.

[51] Dwyer G., Elkinton J. S., and Buonaccorsi J. P., (1997) Host heterogeneity in susceptibility and disease dynamics: tests of a mathematical model, *American Naturalist* 150: 685–707.

[52] Dwyer G., Dushoff J., Elkinton J. S., and Levin S. A., (2000) Pathogen-driven outbreaks in forest defoliators revisited: building models from experimental data, *American Naturalist* 156: 105–120.

[53] Earn D. J., Dushoff J., and Levin S. A., (2002) Ecology and evolution of the flu, *Trends in Ecology & Evolution* 17 (7): 334–340.

[54] European Centre for Disease Prevention and Control (ECDC), (2025) COVID-19, *ECDC Official Website*. (accessed on 30 April 2025).

[55] Eisenberg M. and Mordechai L., (2019) The Justinianic Plague: an interdisciplinary review, *Byzantine and Modern Greek Studies* 43 (2): 156–180.

[56] Elbasha E. H. and Gumel A. B., (2021) Vaccination and herd immunity thresholds in heterogeneous populations, *Journal of Mathematical Biology* 83: 73.

[57] Erdem M., Safan M., and Castillo-Chavez C., (2017) Mathematical analysis of an SIQR influenza model with imperfect quarantine, *Bulletin of Mathematical Biology* 79 (7): 1612–1636.

[58] Farrell N. M., Hayes B. D., and Linden J. A., (2020) Critical medication shortages further dwindling hospital resources during COVID-19, *The American Journal of Emergency Medicine* 40: 202.

[59] Feng Z. and Thieme H. R., (1995) Recurrent outbreaks of childhood diseases revisited: the impact of isolation, *Mathematical Biosciences* 128 (1–2): 93–130.

[60] Filippov A. F., (1988) Differential Equations with Discontinuous Right-hand Sides: Control Systems, Springer, Dordrecht.

[61] Flanagan B. E., Gregory E. W., Hallisey E. J., Heitgerd J. L., and Lewis B., (2011) A social vulnerability index for disaster management, *Journal of Homeland Security and Emergency Management* 8 (1).

[62] Ganesan B., Al-Jumaily A., Fong K.N., Prasad P., Meena S.K., Tong R.K.Y., (2021) Impact of coronavirus disease 2019 (COVID-19) outbreak quarantine, isolation, and lockdown policies on mental health and suicide, *Front. Psychiatry* 12: 565190.

[63] Garnett G. P. and Anderson R. M., (1996) Antiviral therapy and the transmission dynamics of HIV-1, *The Journal of Antimicrobial Chemotherapy* 37 (Suppl B): 135–150.

[64] Gavrilova N. S. and Gavrilov L. A., (2020) Patterns of mortality during pandemic: An example of Spanish flu pandemic of 1918, *Population and Economics* 4 (2): 56.

[65] Georgescu P. and Zhang H., (2013) A Lyapunov functional for a SIRI model with nonlinear incidence of infection and relapse, *Applied Mathematics and Computation* 219 (16): 8496–8507.

[66] Ghosh M., Olaniyi S., and Obabiyi O. S., (2020) Mathematical analysis of reinfection and relapse in malaria dynamics, *Applied Mathematics and Computation* 373: 125044.

[67] Gomes M. G., White L. J., and Medley G. F., (2004) Infection, reinfection, and vaccination under suboptimal immune protection: epidemiological perspectives, *Journal of Theoretical Biology* 228 (4): 539–549.

[68] Gomes M. G., White L. J., and Medley G. F., (2005) The reinfection threshold, *Journal of Theoretical Biology* 236 (1): 111–113.

[69] Guo P., Yang X., and Yang Z., (2014) Dynamical behaviors of an SIRI epidemic model with nonlinear incidence and latent period, *Advances in Difference Equations* 2014: 164.

[70] Gökaydin D., Oliveira-Martins J. B., Gordo I., and Gomes M. G., (2007) The reinfection threshold regulates pathogen diversity: the case of influenza, *Journal of the Royal Society Interface* 4 (12): 137–142.

[71] Hao R., Zhang Y., Cao Z., and others, (2021) Control strategies and their effects on the COVID-19 pandemic in 2020 in representative countries, *Journal of Biosafety and Biosecurity* 3 (2): 76–81.

[72] Hay A. J., Gregory V., Douglas A. R., and Lin Y. P., (2001) The evolution of human influenza viruses, *Philosophical Transactions of the Royal Society of London B: Biological Sciences* 356 (1416): 1861–1870.

[73] Heymann D. L. and Rodier G. R., (2004) SARS: Lessons from a new disease, *Microbes and Infection* 6 (3): 311–318.

[74] Heymann D., (2005) Social, behavioural and environmental factors and their impact on infectious disease outbreaks, *Journal of Public Health Policy* 26: 133–139.

[75] Heymann D. L., (2015) *Control of Communicable Diseases Manual*, 20th ed., APHA Press, Washington, DC.

[76] Hickson R. I. and Roberts M. G., (2014) How population heterogeneity in susceptibility and infectivity influences epidemic dynamics, *Journal of Theoretical Biology* 350: 70–80.

[77] Hill A. N., Glasser J. W., and Feng Z., (2023) Implications for infectious disease models of heterogeneous mixing on control thresholds, *Journal of Mathematical Biology* 86: 53.

[78] Huang X., Shao X., Xing L., Hu Y., Sin D. D., and Zhang X., (2021) The impact of lockdown timing on COVID-19 transmission across US counties, *EClinicalMedicine* 38: 100945.

[79] Huber C., Finelli L., and Stevens W., (2018) The economic and social burden of the 2014 Ebola outbreak in West Africa, *The Journal of Infectious Diseases* 218 (Supplement_5): S698–S704.

[80] Huremović D. (ed.), (2019) Psychiatry of Pandemics: A Mental Health Response to Infection Outbreak, *Springer*.

[81] Iannelli M., Pugliese A., (2014) An Introduction to Mathematical Population Dynamics: Along the Trail of Volterra and Lotka, *Springer, Cham, Switzerland*.

[82] Izhar R. and Ben-Ami F., (2015) Host age modulates parasite infectivity, virulence and reproduction, *Journal of Animal Ecology* 84: 1018–1028.

[83] Jentsch P. C., Anand M., and Bauch C. T., (2021) Prioritising COVID-19 vaccination in changing social and epidemiological landscapes: A mathematical modelling study, *The Lancet Infectious Diseases* 21 (8): 1097–1106.

[84] Johnson N. P. and Mueller J., (2002) Updating the accounts: global mortality of the 1918–1920 "Spanish" influenza pandemic, *Bulletin of the History of Medicine* 76 (1): 105–115.

[85] Japan Institute for Health Security (JIHS), (2025) The Infectious Disease Information Website, *JIHS Official Website* (accessed on 30 April 2025).

[86] Jiloha R. C., (2020) COVID-19 and mental health, *Epidemiology International* 5 (1): 7–9.

[87] Jones S. and Walter M., (2023) Shortages of care and medical devices affecting the pediatric patient population, *Canadian Journal of Health Technologies* 3 (8).

[88] Kantamneni N., (2020) The impact of the COVID-19 pandemic on marginalized populations in the United States: A research agenda, *Journal of Vocational Behavior* 119: 103439.

[89] Karaye I.M. and Horney J.A., (2020) The impact of social vulnerability on COVID-19 in the U.S.: An analysis of spatially varying relationships, *American Journal of Preventive Medicine* 59 (3): 317–325.

[90] Kaur H., Garg S., Joshi H., Ayaz S., Sharma S., and Bhandari M., (2020) A review: Epidemics and pandemics in human history, *International Journal of Pharma Research and Health Sciences* 8 (2): 3139–3142.

[91] Kazanjian P., (2014) The AIDS Pandemic in Historic Perspective, *Journal of the History of Medicine and Allied Sciences* 69 (3): 351–382.

[92] Kermack W. O. and McKendrick A. G., (1927) A contribution to the mathematical theory of epidemics, *Proceedings of the Royal Society A* 115: 700–721.

[93] Kermack W. O. and McKendrick A. G., (1932) Contributions to the mathematical theory of epidemics, Part II, *Proceedings of the Royal Society of London. Series A* 138: 55–83.

[94] King J. G., Souto-Maior C., Sartori L. M., de Freitas R. M., and Gomes M. G. M., (2018) Variation in Wolbachia effects on *Aedes* mosquitoes as a determinant of invasiveness and vectorial capacity, *Nature Communications* 9: 1483.

[95] Kumar A., Srivastava P. K., Dong Y., and Takeuchi Y., (2020) Optimal control of infectious disease: information-induced vaccination and limited treatment, *Physica A* 542: 123196.

[96] Kuylen E. J., Torneri A., Willem L., Libin P. J. K., Abrams S., Coletti P., et al., (2022) Different forms of superspreading lead to different outcomes: Heterogeneity in infectiousness and contact behavior relevant for the case of SARS-CoV-2, *PLoS Computational Biology* 18 (8): e1009980.

[97] Kuznetsov Y. A., Rinaldi S., and Gragnani A., (2003) One-parameter bifurcations in planar Filippov systems, *International Journal of Bifurcation and Chaos* 13 (8): 2157–2188.

[98] Lai S., Ruktanonchai N. W., Zhou L., and others, (2020) Effect of non-pharmaceutical interventions to contain COVID-19 in China, *Nature* 585 (7825): 410–413.

[99] Lau H., Khosrawipour V., Kocbach P., Mikolajczyk A., Schubert J., Bania J., and Khosrawipour T., (2020) The positive impact of lockdown in Wuhan on containing the COVID-19 outbreak in China, *Journal of Travel Medicine* 27 (3): taaa037.

[100] Levin B. R., Bull J. J., and Stewart F. M., (2001) Epidemiology, Evolution, and Future of the HIV/AIDS Pandemic, *Emerging Infectious Diseases* 7 (7): 505–511.

[101] Lewis M. A., Shuai Z., and van den Driessche P., (2019) A general theory for target reproduction numbers with applications to ecology and epidemiology, *Journal of Mathematical Biology* 78: 2317–2339.

[102] Liu Y., Eggo R. M., and Kucharski A. J., (2020) Secondary attack rate and superspreading events for SARS-CoV-2, *The Lancet* 395 (10227): e47.

[103] Lloyd-Smith J., Schreiber S., Kopp P., and Getz W. M., (2005) Superspreading and the effect of individual variation on disease emergence, *Nature* 438: 355–359.

[104] Lu L., Peng J., Wu J., Lu Y., (2021) Perceived impact of the COVID-19 crisis on SMEs in different industry sectors: Evidence from Sichuan, China, *Int. J. Disaster Risk Reduct.* 55: 102085.

[105] Lytras T. and Tsiodras S., (2021) Lockdowns and the COVID-19 pandemic: What is the endgame?, *Scand. J. Public Health* 49 (1): 37–40.

[106] MacIntyre C. R. and Chughtai A. A., (2016) Recurrence and reinfection: a new paradigm for the management of Ebola virus disease, *International Journal of Infectious Diseases* 43: 58–61.

[107] Mamelund S.-E., Dimka J., and Aaby P., (2021) Social inequalities in infectious disease outcomes, *Annual Review of Sociology* 47: 155–173.

[108] Marks S., (2002) An Epidemic Waiting to Happen? The Spread of HIV/AIDS in South Africa in Social and Historical Perspective, *African Studies* 61 (1): 13–26.

[109] Markwalter C. F., Lapp Z., Abel L., et al., (2024) Plasmodium falciparum infection in humans and mosquitoes influence natural Anopheline biting behavior and transmission, *Nature Communications* 15: 4626.

[110] Martcheva M., (2015) An Introduction to Mathematical Epidemiology, *Springer*, New York.

[111] Martins J., Pinto A., and Stollenwerk N., (2009) A scaling analysis in the SIRI epidemiological model, *Journal of Biological Dynamics* 3 (5): 479–496.

[112] McGillen J. B., Anderson S. J., Dybul M. R., and Hallett T. B., (2016)Optimum resource allocation to reduce HIV incidence across sub-Saharan Africa: A mathematical modelling study,*The Lancet HIV*3(9):e441–e448.

[113] McMahon D. E., Peters G. A., Ivers L. C., and Freeman E. E., (2020) Global resource shortages during COVID-19: Bad news for low-income countries, *PLoS Neglected Tropical Diseases* 14 (7): e0008412.

[114] Mendez-Brito A., El Bcheraoui C., and Pozo-Martin F., (2021) Systematic review of empirical studies comparing the effectiveness of non-pharmaceutical interventions against COVID-19, *Journal of Infection* 83 (3): 281–293.

[115] Meo S. A., Abukhalaf A. A., Alomar A. A., AlMutairi F. J., Usmani A. M., and Klonoff D. C., (2020) Impact of lockdown on COVID-19 prevalence and mortality during 2020 pandemic: observational analysis of 27 countries, *European Journal of Medical Research* 25 (1): 56.

[116] Mills C. E., Robins J. M., and Lipsitch M., (2004) Transmissibility of 1918 pandemic influenza, *Nature* 432 (7019): 904–906.

[117] Milne G. J., Xie S., Poklepovich D., O' Halloran D., Yap M., and Whyatt D., (2021) A modelling analysis of the effectiveness of second wave COVID-19 response strategies in Australia, *Scientific Reports* 11 (1): 11958.

[118] Moris D. and Schizas D., (2020) Lockdown during COVID-19: the Greek success, *In Vivo* 34 (3 suppl): 1695–1699.

[119] Mu R., Wei A., and Yang Y., (2019) Global dynamics and sliding motion in A(H7N9) epidemic models with limited resources and Filippov control, *Journal of Mathematical Analysis and Applications* 477 (2): 1296–1317.

[120] Munday J. D., van Hoek A. J., Edmunds W. J., and Atkins K. E., (2018) Quantifying the impact of social groups and vaccination on inequalities in infectious diseases using a mathematical model, *BMC Medicine* 16 (1): 162.

[121] Musa S. S., Wang X., Zhao S., Li S., Hussaini N., Wang W., and He D., (2022) The heterogeneous severity of COVID-19 in African countries: A modeling approach, *Bulletin of Mathematical Biology* 84 (3): 32.

[122] Naidoo M., Shephard W., Kambewe I., et al., (2024) Incorporating social vulnerability in infectious disease mathematical modelling: a scoping review, *BMC Medicine* 22: 125.

[123] Naidoo M., Shephard W., Mtshali N., Kambewe I., Muthien B., Abuelezam N. N., and Rasella D., (2025) How to incorporate social vulnerability into epidemic mathematical modelling: Recommendations from an international Delphi, *Social Science & Medicine* 118352.

[124] Ngonghala C. N., Iboi E., Eikenberry S., and others, (2020) Mathematical assessment of the impact of non-pharmaceutical interventions on curtailing the 2019 novel Coronavirus, *Mathematical Biosciences* 325: 108364.

[125] Nicola M., Alsafi Z., Sohrabi C., Kerwan A., Al-Jabir A., Iosifidis C., Agha M., Agha R., (2020) The socio-economic implications of the coronavirus pandemic (COVID-19): A review, *Int. J. Surg.* 78: 185–193.

[126] Olson P. E., Hames C. S., Benenson A. S., Genovese E. N., (1996) The Thucydides syndrome: Ebola Déjà vu? (or Ebola Reemergent?), *Emerging Infectious Diseases* 2(2): 155–156.

[127] Onyeaka H., Anumudu C. K., Al-Sharify Z. T., Egele-Godswill E., and Mbaegbu P., (2021) COVID-19 pandemic: A review of the global lockdown and its far-reaching effects, *Science Progress* 104 (2): 00368504211019854.

[128] Oraby T., Tyshenko M.G., Maldonado J.C., Vatcheva K., Elsaadany S., Alali W.Q., Longenecker J.C., Al-Zoughool M., (2021) Modeling the effect of lockdown timing as a COVID-19 control measure in countries with differing social contacts, *Sci. Rep.* 11 (1): 1–13.

[129] Oum T. H. and Wang K., (2020) Socially optimal lockdown and travel restrictions for fighting communicable virus including COVID-19, *Transport Policy* 96: 94–100.

[130] Pagliara R., Dey B., and Leonard N. E., (2018) Bistability and resurgent epidemics in reinfection models, *IEEE Control Systems Letters* 2 (2): 290–295.

[131] Parzonka K., Ndayishimiye C., and Domagala A., (2023) Methods and tools used to estimate the shortages of medical staff in European countries: scoping review, *International Journal of Environmental Research and Public Health* 20 (4): 2945.

[132] Pearce N., Lawlor D. A., and Brickley E. B., (2020) Comparisons between countries are essential for the control of COVID-19, *International Journal of Epidemiology* 49 (4): 1059–1062.

[133] Pinto A., Aguiar M., Martins J., and Stollenwerk N., (2010) Dynamics of epidemiological models, *Acta Biotheoretica* 58: 381–389.

[134] Price O., Birrell F., Mifsud E., and Sullivan S., (2022) Epidemiology of repeat influenza infection in Queensland, Australia, 2005–2017, *Epidemiology and Infection* 150: e144.

[135] Qin W., Tang S., Xiang C., and Yang Y., (2016) Effects of limited medical resource on a Filippov infectious disease model induced by selection pressure, *Applied Mathematics and Computation* 283: 339–354.

[136] Richards P., Amara J., Ferme M.C., et al., (2015) Social pathways for Ebola virus disease in rural Sierra Leone, and some implications for containment, *PLoS Neglected Tropical Diseases* 9 (4): e0003567.

[137] Ridley E. J., Freeman-Sanderson A., and Haines K. J., (2021) Surge capacity for critical care specialised allied health professionals in Australia during COVID-19, *Australian Critical Care* 34 (2): 191–193.

[138] Rocha R., Atun R., Massuda A., Rache B., Spinola P., Nunes L., and Castro M. C., (2021) Effect of socioeconomic inequalities and vulnerabilities on health-system preparedness and response to COVID-19 in Brazil: A comprehensive analysis, *The Lancet Global Health* 9 (6): e782–e792.

[139] Rose C., Medford A. J., Goldsmith C. F., Vegge T., Weitz J. S., and Peterson A. A., (2021) Heterogeneity in susceptibility dictates the order of epidemic models, *Journal of Theoretical Biology* 528: 110839.

[140] Sabbatani S., Fiorino S., (2009) The Antonine plague and the decline of the Roman Empire, *Infez Med* 17(4): 261–275.

[141] Saha S. and Samanta G. P., (2019) Modelling and optimal control of HIV/AIDS prevention through PrEP and limited treatment, *Physica A* 516: 280–307.

[142] Sattenspiel L. and Dietz K., (1995) A structured epidemic model incorporating geographic mobility among regions, *Mathematical Biosciences* 128 (1–2): 71–91.

[143] Sen-Crowe B., Sutherland M., McKenney M., and Elkbuli A., (2021) A closer look into global hospital beds capacity and resource shortages during the COVID-19 pandemic, *Journal of Surgical Research* 260: 56–63.

[144] Seno H., (2022) A Primer on Population Dynamics Modeling: Basic Ideas for Mathematical Formulation, Springer, Singapore.

[145] Sepulaveda-Salcedo L. S., Vasilieva O., and Svinin M., (2020) Optimal control of dengue epidemic outbreaks under limited resources, *Studies in Applied Mathematics* 144 (2): 185–212.

[146] Shahverdi B., Miller-Hooks E., Tariverdi M., Ghayoomi H., Prentiss D., and Kirsch T. D., (2023) Models for assessing strategies for improving hospital capacity for handling patients during a pandemic, *Disaster Medicine and Public Health Preparedness* 17: e110.

[147] Sharp P. M. and Hahn B. H., (2011) Origins of HIV and the AIDS pandemic, *Cold Spring Harbor Perspectives in Medicine* 1 (1): a006841.

[148] Singh S. R., Eghdami M. R., and Singh S., (2014) The concept of social vulnerability: A review from disasters perspectives, *International Journal of Interdisciplinary and Multidisciplinary Studies* 1 (6): 71–82.

[149] Sivaramakrishnan K., (2020) Endemic risks: Influenza pandemics, public health, and making self-reliant Indian citizens, *Journal of Global History* 15 (3): 459–477.

[150] Smith D. L., Dushoff J., Snow R. W., and Hay S. I., (2005) The entomological inoculation rate and *Plasmodium falciparum* infection in African children, *Nature* 438: 492–495.

[151] Song L. P., Jin Z., and Sun G. Q., (2011) Reinfection induced disease in a spatial SIRI model, *Journal of Biological Physics* 37: 133–140.

[152] Spinney L., (2017) Pale Rider: The Spanish Flu of 1918 and How It Changed the World, Hachette UK.

[153] Srivastava A., Sonu, and Srivastava P. K., (2022) Nonlinear dynamics of a SIRI model incorporating the impact of information and saturated treatment with optimal control, *European Physical Journal Plus* 137 (9): 1028.

[154] Stanturf J. A., Goodrick S. L., Warren Jr M. L., Charnley S., and Stegall C. M., (2015) Social vulnerability and Ebola virus disease in rural Liberia, *PLOS ONE* 10 (9): e0137208.

[155] Stollenwerk N., Martins J., and Pinto A., (2007) The phase transition lines in pair approximation for the basic reinfection model SIRI, *Physics Letters A* 371 (5–6): 379–388.

[156] Suryasa I. W., Rodríguez-Gámez M., and Koldoris T., (2021) The COVID-19 pandemic, *International Journal of Health Sciences* 5 (2): 572194.

[157] Taubenberger J. K. and Morens D. M., (2006) 1918 Influenza: The mother of all pandemics, *Emerging Infectious Diseases* 12 (1): 15–22.

[158] Tonnoir A., Ciotir I., Scutariu A.L., Dospinescu O., (2021) A model for the optimal investment strategy in the context of pandemic regional lockdown, *Mathematics* 9 (9): 1058.

[159] Trilla A., Trilla G., and Daer C., (2008) The 1918 "Spanish flu" in Spain, *Clinical Infectious Diseases* 47 (5): 668–673.

[160] Unruh L., Allin S., Marchildon G., Burke S., Barry S., Siersbaek R., Thomas S., Rajan S., Koval A., Alexander M., and Merkur S., (2022) A comparison of 2020 health policy responses to the COVID-19 pandemic in Canada, Ireland, the United Kingdom and the United States of America, *Health Policy* 126 (5): 427–437.

[161] Velavan T. P. and Meyer C. G., (2020) The COVID-19 epidemic, *Tropical Medicine & International Health* 25 (3): 278.

[162] Wagner D. M., Klunk J., Harbeck M., Devault A., Waglechner N., Sahl J. W., *et al.*, (2014) Yersinia pestis and the Plague of Justinian 541–543 AD: a genomic analysis, *The Lancet Infectious Diseases* 14 (4): 319–326.

[163] Wang A., Xiao Y., and Zhu H., (2018) Dynamics of Filippov epidemic model with limited hospital beds, *Math. Biosci. Eng* 15 (3): 739.

[164] Wang G., Zhang Y., Zhao J., Zhang J., and Jiang F., (2020) Mitigate the effects of home confinement on children during the COVID-19 outbreak, *The Lancet* 395 (10228): 945–947.

[165] Wang J., Jiang L., Xu Y., He W., Zhang C., Bi F., Tan Y., and Ning C., (2022) Epidemiology of influenza virus reinfection in Guangxi, China: a

retrospective analysis of a nine-year influenza surveillance data: characteristics of influenza virus reinfection, *International Journal of Infectious Diseases* 120: 135–141.

[166] Wang S., (2021) Dynamic assessment of population by using SIRI model, *Proceedings of the 4th International Conference on Biometric Engineering and Applications*, May 25, 93–97.

[167] Wei W., Xu W., Song Y., and Liu J., (2021) Bifurcation and basin stability of an SIR epidemic model with limited medical resources and switching noise, *Chaos, Solitons & Fractals* 152: 111423.

[168] World Health Organization, (2019) Non-pharmaceutical public health measures for mitigating the risk and impact of epidemic and pandemic influenza, *WHO Guidelines*.

[169] World Health Organization, (2020) Modes of transmission of virus causing COVID-19: implications for IPC precaution recommendations, *WHO Scientific Brief*, 29 March 2020.

[170] World Health Organization (WHO), (2025) Coronavirus disease (COVID-19) pandemic, *WHO Official Website* (accessed on 30 April 2025).

[171] Wilder-Smith A., (2006) The severe acute respiratory syndrome: Impact on travel and tourism, *Travel Med. Infect. Dis.* 4 (2): 53–60.

[172] Wong F. and Collins J. J., (2020) Evidence that coronavirus superspreading is fat-tailed, *Proceedings of the National Academy of Sciences* 117: 29416–29418.

[173] Yapijakis C., (2009) Hippocrates of Kos, the father of clinical medicine, and Asclepiades of Bithynia, the father of molecular medicine, *In Vivo*, 23(4): 507–514.

[174] Yum H.-K., Park I.-N., Shin B.-M., and Choi S.-J., (2014) Recurrent *Pseudomonas aeruginosa* infection in chronic lung diseases: relapse or reinfection?, *Tuberculosis and Respiratory Diseases* 77 (4): 172–177.

[175] Zahran S., Peek L., Snodgrass J. G., Weiler S., and Hempel L., (2011) Economics of disaster risk, social vulnerability, and mental health resilience, *Risk Analysis: An International Journal* 31 (7): 1107–1119.

[176] Zhang Q., Zhou M., Yang Y., You E., Wu J., Zhang W., Jin J., and Huang F., (2019) Short-term effects of extreme meteorological factors on childhood hand, foot, and mouth disease reinfection in Hefei, China: a distributed lag non-linear analysis, *Science of The Total Environment* 653: 839–848.

[177] Zhao H., Wang L., Oliva S. M., and Zhu H., (2020) Modeling and dynamics analysis of Zika transmission with limited medical resources, *Bulletin of Mathematical Biology* 82: 1–50.